

General Disclaimer

One or more of the Following Statements may affect this Document

- This document has been reproduced from the best copy furnished by the organizational source. It is being released in the interest of making available as much information as possible.
- This document may contain data, which exceeds the sheet parameters. It was furnished in this condition by the organizational source and is the best copy available.
- This document may contain tone-on-tone or color graphs, charts and/or pictures, which have been reproduced in black and white.
- This document is paginated as submitted by the original source.
- Portions of this document are not fully legible due to the historical nature of some of the material. However, it is the best reproduction available from the original submission.

(NASA-CR-167960) WIND TUNNEL EVALUATION OF
AIR-FOIL PERFORMANCE USING SIMULATED ICE
SHAPES Final Report (Ohio State Univ.,
Columbus.) 172 p HC A08/MF A01 CSCL 01A

N83-15265

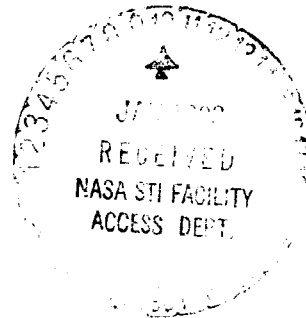
G3/02 Unclass
02349

NASA Contractor Report 167960

WIND TUNNEL EVALUATION OF AIRFOIL PERFORMANCE USING
SIMULATED ICE SHAPES

M. B. Bragg, R. J. Zaguli, and G. M. Gregorek

The Ohio State University
Columbus, Ohio



November 1982

Prepared for

NATIONAL AERONAUTICS AND SPACE ADMINISTRATION
Lewis Research Center
Under Grant NAG 3-28

CONTENTS

	Page
NOMENCLATURE	iii
INTRODUCTION	1
Background	1
EXPERIMENTAL METHOD	3
Equipment	3
Data Reduction	4
RESULTS & DISCUSSION	6
IRT Operation	6
Simulated Ice Results	8
SUMMARY & CONCLUSIONS	10
APPENDIX	12
Run Summary	12
Cumulative Plots	17
C_l vs α Plots	17
C_l vs C_d Plots	24
C_m vs C_l Plots	30
C_p Distributions	36
REFERENCES	158
FIGURES	159

NOMENCLATURE

**ORIGINAL PAGE IS
OF POOR QUALITY**

c	Airfoil chord length, m
C_d	Drag coefficient, $D/q_\infty c$
C_l	Lift coefficient, $L/q_\infty c$
C_m	Moment coefficient about the quarter chord, $M/q_\infty c^2$
C_p	Pressure coefficient, $(P - P_\infty)/q_\infty$
LWC	Liquid water content, g/m^3
P	Local static pressure, N/m^2
P_∞	Free stream static pressure, N/m^2
q_∞	Free stream dynamic pressure, N/m^2
T	Temperature, $^\circ C$
t	Time, minutes
U	Free stream velocity, m/sec
α	Angle of attack, degrees
δ	Particle diameter, microns
ρ	Air density, Kg/m^3
ρ_{ice}	Ice density, g/cm^3

PRECEDING PAGE BLANK NOT FILMED

INTRODUCTION

Until recently very little experimental data has been available on the performance degradation of airfoil sections resulting from rime or glaze ice accretions. The test program described in this report provides some of this needed information. It's primary objectives were:

- 1) To examine a method of simulating ice accretions with wood shapes which were instrumented with surface pressure taps to obtain detailed aerodynamic data.
- 2) To study the complex flowfield in the area of the ice accretion through these pressure distributions.
- 3) To evaluate the accuracy of the theoretical analysis methods presently utilized¹.

This paper is primarily a data report and presents information taken on the 63A415 airfoil. Further analysis on other classes of airfoils is required to fully analyze the icing problem and to refine conclusions drawn from the results of this test.

Background

The first tunnel entry, conducted May 4-15, 1981, was an ice accretion study. Rime and glaze ice shapes were grown on a NACA 63₂-A415 airfoil with a 1.36 m chord. The resultant section drag coefficients were measured using a drag wake survey probe positioned approximately one chord length downstream of the model. Tests were conducted at free stream conditions to simulate typical aircraft cruise (high velocity, low angle of attack) and climb (low velocity, high angle of attack) conditions. In order to generate glaze ice a total temperature of -4°C was chosen while -26°C was used to yield rime shapes.

ORIGINAL PAGE IS
OF POOR QUALITY.

Two methods were used to record the characteristics of the accreted shapes. The first involved fitting a template to the leading edge of the wing after a small section of the ice near the centerline had been removed. A tracing of the shape could then be made onto the template. The second method, typically used for longer icing times, involved removing a section of the accretion by spraying steam inside the model near the area to be removed. The ice section could then be lifted out and dipped into a container of beeswax which hardened around the ice. After the ice has melted, plaster was poured inside and the casts were then available for careful tracings².

From the shapes generated in the first entry, 2 rime and 2 glaze shapes were chosen to represent typical climb and cruise conditions. These were then modelled for the second tunnel entry. Table I gives a summary of the test parameters which produced these shapes.

TABLE I
TEST PARAMETERS

TYPE	T	α	U	δ	LWC	t	ρ_{ice}
Rime	-26	2.6	51	15	1.5	15	0.421
Rime	-26	6.6	40	15	1.5	15	0.534
Glaze	- 4	2.6	51	15	1.5	15	-
Glaze	- 4	6.6	40	20	2.9	15	-

Equipment

The testing was performed in the NASA Lewis 6' x 9' Icing Research Tunnel. Tracings of the shapes generated during the first tunnel entry were used to make the simulated ice shapes for the second test. The shapes were formed from mahogany and extended full span with filletting at the ends for attachment to the model. The inside of each of the four shapes, two rime and two glaze, was hollowed out to provide clearance for the 1/16" ID tubing required for tapping the ice shape. In an effort to obtain as much data as possible in the critical region around the leading edge, the number of taps on the shape was concentrated in this area (see Figures 1A-1D). The airfoil was instrumented to obtain surface pressure measurements, using 1/8" OD strip-a-tube attached to the airfoil surface (Figure 2). In order to add surface roughness to the ice shapes, aluminum oxide grit with a $K/C = .00058$ was attached using a spray acrylic adhesive to the glaze shapes while for the rime cases a grit with $K/C = .0012$ was used.

Data acquisition and on-line reduction was accomplished using the Digital Data Acquisition and Reduction System (DDARS)³, designed at The Ohio State University's Aeronautical and Astronautical Research Laboratory. The DDARS package is illustrated in Figure 3. The heart of the system is the central processing unit (CPU), which is a Digital Equipment Corporation (DEC) LSI-11 microcomputer. The analog data signals from the various transducers and the wake probe slidewire are routed to the computer

through the analog front-end, consisting of the various analog and signal conditioning equipment. Input and output is accomplished through a teletype terminal and data storage is achieved through a dual-drive single head double-density floppy disc system.

In order to obtain pressures on the airfoil surface a Scanivalve transducer set-up was used (Figure 4). Connected through an analog box to the LSI-11 microcomputer were wake total, static, tunnel velocity, and tunnel static transducers taps. Drag data were taken using the wake momentum deficit technique. While the drag data obtained during the first tunnel entry were obtained using the IRT wake probe, for the aerodynamic testing an airfoil mounted probe was used. It was attached to the model on centerline and 0.413m back from the trailing edge, and measured both wake total and wake static pressure.

Data Reduction

On-line reduction is a key feature of the OSU DDARS. A quick-look C_p distribution is made available to the engineer as well as integrated values of C_l , C_m , and C_d . This permits immediate evaluation of the progress of the test and thus maximum use can be made of tunnel time.

Final reduction was performed on the OSU Harris/6 Computer System. The raw data obtained during testing in the IRT were copied onto the Harris System from the LSI-11. Pressure coefficient distributions, as well as lift and moment coefficients were obtained in the same manner as the on-line reduction, however a provision in the program permitted omitting from the final results any blocked taps on the model.

**ORIGINAL PAGE IS
OF POOR QUALITY**

The drag coefficient reduction program displayed the wake on a graphics terminal. This allows the operator to choose the integration limits required by the Jones Equation⁴. If it was clear from the displayed wake trace that the extent of the probe's traverse was not sufficient to capture the entire wake, that reduction was bypassed. This limitation was observed at the higher angles of attack and is represented in the run summary tables by a dashed line in the drag coefficient column.

RESULTS AND DISCUSSION

During the course of the wind tunnel test program a few observations were made which merit discussion and are pertinent to further operation of the Icing Research Tunnel. These comments will be made first. Following, a brief summary of the data collected is presented. The tabulated Run Summary and plots of C_p 's and integrated results are given in the appendices.

IRT Operation

The initial aerodynamic tests were conducted with the model installed in the wind tunnel with a 0.06m (2 inch) gap between the end of the wing and the tunnel ceiling. This gap, at high lift coefficients, can influence the quality of the desired two-dimensional data; therefore, any clearances between two-dimensional airfoil model ends and the tunnel walls must be minimized.

The early tests (runs 2 to 13) with the gap present can be compared with test conducted on the model, Figure 2, with sealed ends in Figure 5, 6 and 7. These figures present the lift coefficient vs. angle of attack, drag polar, and moment coefficient vs. lift, respectively at Reynolds number near 5×10^6 . The solid line shows on the figures represents earlier NACA data of the 632-415 airfoil at Reynolds number of 6×10^6 with NACA standard roughness applied to the leading edge.

Data scatter in the C_l vs. α plot of Figure 5 is attributed to difficulty with angle of attack measurements, but at high angles the lift coefficients of the gap tests appear below those of the sealed gap. Unfortunately, angles above 11° were not examined for the gap case. Figure 6, the drag polar, removes the

**ORIGINAL PAGE IS
OF POOR QUALITY.**

angle of attack discrepancies and clearly illustrates the deviations between the gap and sealed gap tests. The open symbols, representing the sealed gap, track the early two dimensional NACA data⁵, while the gap data at high lift appear to have low drag coefficients. The anomalous behavior is caused by the relative locations of the pressure belt used to determine lift coefficient and the wake probe that measured the drag coefficient. The probe was near the tunnel centerline, while the belt was inboard 0.2 m further from the gap. The effect of the gap is to alter the spanwise angle of attack, producing a lift coefficient at the belt location greater than the lift coefficient at the probe station, and in turn generating the drag polar of Figure 6. A truly two dimensional test would, of course, have a constant spanwise angle of attack. The moment coefficient curves of Figure 7 illustrate a similar disagreement at high lift coefficients.

A second observation made during the test program was the need for more accurate angle of attack setting and monitoring. The scatter in the C_l vs. α plot is largely due to the inability to set the angle of the turntable to better than ± 0.1 degree.

As a result of these comparisons, the need to ensure that the model spans the entire tunnel has been demonstrated. Only the data obtained with the gap sealed will be used for later comparisons. Also, the problem with the tunnel turntable in setting and measuring the angle of attack has been discussed. The purpose of the test program was in part to evaluate and demonstrate the use of the IRT as an aerodynamic tunnel. The problem with the turntable has been identified and can hopefully

be improved. Other possible problems such as tunnel flow quality are still being studied. It is important then to note when using these data, that the IRT is still being improved, and is under evaluation as an aerodynamic facility.

Simulated Ice Results

Comparisons were made between the drag measured on the actual iced airfoil and the simulated shapes in order to determine the accuracy of the model. In addition, experimental values of C_l and C_m as well as pressure distributions were compared with theoretical results¹.

Data were taken on the four smooth and rough simulated configurations, as well as the clean airfoil for lift coefficients of zero up to $C_{l_{max}}$. The glaze ice C_p distributions show very clearly the adverse pressure gradient in the region around the leading edge. Prominent pressure spikes can be seen on the distribution where the flow is forced around the horns of the ice shapes. These severe adverse gradients will promote separation and lower the $C_{l_{max}}$, as well as increasing the drag of the wing. This problem was also seen in the rime cases, however, it was not as severe.

Interestingly enough, even though the simulated shapes do show a reduction in $C_{l_{max}}$, it was not as large as expected. In general, the rime cases failed to show a reduction and actually increased $C_{l_{max}}$ by 0.2 in the climb case, essentially forming a leading edge flap. The glaze shapes reduced $C_{l_{max}}$ by approximately 0.2.

The drag results for the Rime 3 case show the importance of the addition of the surface roughness. The comparison between

ORIGINAL PAGE IS
OF POOR QUALITY

the actual ice and simulated ice was very good when the roughness was added. However, the Rime 7 case did not agree as favorably and at present no explanation is available for this problem. The drag increase was much higher for the glaze cases when compared to those for the rime shapes, however the effect of surface roughness did not appear to be as crucial.

For the climb cases at the lower lift coefficients, the rime case shows a more negative pitching moment while at the higher C_L 's the trend was reversed. For the glaze cases, however, more positive C_m 's were found at the lower lift coefficients and more negative at higher C_L 's. The change in C_m is almost negligible for the cruise case at low C_L 's.

A run summary has been included at the end of this report. It is arranged by configuration; 1) clean, 2) rime 3, 3) glaze 3, 4) rime 7, and 5) glaze 7. These tables are further subdivided into rough and smooth. Following these are the cumulative C_L vs. α , C_D vs. C_L and C_m vs. C_L plots. Lastly, the C_p distributions are included and are organized in the same order as the run summary tables.

SUMMARY AND CONCLUSIONS

An experimental program was conducted in which ice accretions on airfoils were measured, and simulated shapes tested, to determine the degradation in airfoil section performance. The research was conducted in the NASA Icing Research Tunnel on a full-scale general aviation airfoil of construction and surface conditions typical of that found in industry. The airfoil model and simulated ice accretions were instrumented to obtain surface pressures which provided additional insight into the flowfield behavior.

As a result of this work some important observations can be made:

- 1) The model must span the entire tunnel to obtain accurate 2-D results. Data accuracy could be improved by increased accuracy in the angle of attack measurement.
- 2) The approximate ice shape modelling technique of a smooth shape with roughness added accurately simulated the ice in most cases^{1,2}. The addition of surface roughness was particularly important in the rime ice simulation.
- 3) Measured C_p distributions on the ice shapes showed extremely severe adverse gradients.
- 4) The data showed a significant increase in drag for all ice shapes tested. However, the maximum lift coefficient actually increased in one case and in all cases was higher with the simulated ice than expected. A zero lift angle of attack shift was also noted.

This test demonstrated the capability of the IRT and the present ice simulation methods to generate aerodynamic data. While the comparisons of the aerodynamic performance of simulated and actual ice in the IRT appear good, an external check

**ORIGINAL PAGE IS
OF POOR QUALITY**

on the quality of these data are still needed. The results presented here represent a first step in generating the needed data base on the effect of ice accretion on airfoil performance. Combined with future results, these data will provide a means by which current analysis methods can be validated, as well as provide much needed guidance in the development of new methods.

APPENDIX

ORIGINAL PAGE IS
OF POOR QUALITY

Run Summary

CLEAN CONFIGURATION

RUN	AOA ¹	VEL ²	TEMP ³	PALT ⁴	C _l	C _d	C _m
2	2.6	99.25	58.0	1297.3	0.6288	0.0112	-0.0848
3	2.6	99.50	60.0	1304.4	0.6540	0.0126	-0.0868
4	-0.4	96.55	60.0	1278.0	0.2677	0.0116	-0.0726
5	-3.4	98.95	49.0	1295.2	-0.0463	0.0104	-0.0675
6	1.6	99.90	58.0	1303.4	0.4313	0.0120	-0.0667
7	3.6	98.75	62.0	1285.9	0.7572	0.0126	-0.0909
8	5.6	103.25	51.0	1319.2	0.9228	0.0139	-0.0819
9	7.6	99.80	55.0	1289.3	1.1485	0.0149	-0.0855
10	8.6	97.35	49.0	1260.6	1.1701	0.0156	-0.0778
11	9.6	100.00	58.0	1280.1	1.1889	0.0165	-0.0711
12	10.6	98.85	52.0	1269.1	1.2751	0.0180	-0.0783
13	11.6	98.75	59.0	1263.4	1.3638	0.0183	-0.0942
14	2.6	98.15	79.0	1179.1	0.5894	0.0130	-0.0707
15	7.6	102.20	71.0	1218.6	1.0544	0.0177	-0.0507
16	-0.4	100.15	34.0	1202.3	0.2900	0.0113	-0.0685
17	11.6	99.50	49.0	1196.9	1.3699	0.0250	-0.0915
18	12.6	98.95	53.0	1188.1	1.4232	0.0265	-0.1044
19	13.6	98.05	51.0	1170.2	1.3910	0.0344	-0.0958
20	14.6	100.70	52.0	1194.5	1.3963	0.0387	-0.1239
21	2.6	108.25	53.0	1275.6	0.6606	0.0118	-0.0746
22	2.6	122.15	54.0	1429.1	0.6312	0.0122	-0.0673
56	2.6	100.05	60.0	1232.5	0.6609	0.0122	-0.0758
57	7.6	99.15	58.0	1224.3	1.2974	0.0190	-0.0809
58	-3.4	81.90	56.0	1079.4	0.0086	0.0122	-0.0835
59	-3.4	82.45	54.0	1074.1	0.0015	0.0114	-0.0822
60	-0.4	-----	54.0	-----	0.3447	0.0113	-0.0864
61	2.6	84.30	54.0	1089.5	0.6363	0.0121	-0.0751
62	4.6	82.40	54.0	1073.6	0.9467	0.0129	-0.0979
63	6.6	80.35	54.0	1059.3	1.0343	0.0166	-0.0668
64	8.6	83.35	57.0	1076.8	1.1823	0.0218	-0.0576
65	10.6	82.15	57.0	1077.3	1.3309	0.0263	-0.0595
66	11.6	81.50	57.0	1078.7	1.4416	0.0324	-0.0529

1Degrees
2Knots
3of
4Ft

ORIGINAL PAGE IS
OF POOR QUALITY

RIME 3 SMOOTH CONFIGURATION

RUN	AOA	VEL	TEMP	PALT	C_l	C_d	C_m
114	-3.4	111.65	45.0	1362.1	-0.1004	0.0233	-0.0851
115	-0.4	112.90	53.0	1373.7	0.2792	0.0131	-0.0862
116	2.6	113.40	50.0	1387.5	0.6182	0.0122	-0.0669
117	4.6	113.25	50.0	1380.8	0.8742	0.0141	-0.0725
118	6.6	113.40	48.0	1380.3	1.1129	0.0179	-0.0630
119	8.6	111.35	49.0	1499.4	1.2627	0.0220	-0.0439
120	9.6	113.65	48.0	1512.4	1.4184	0.0252	-0.0497
121	10.6	112.00	48.0	1491.7	1.5428	0.0290	-0.0534
122	11.6	112.65	49.0	1495.1	1.5689	0.0347	-0.0386
123	12.6	112.65	50.0	1491.1	1.6200	-----	-0.0453
124	13.6	111.25	50.0	1477.0	1.6669	-----	-0.0598

RIME 3 ROUGH CONFIGURATION

91	-3.4	113.75	63.0	1448.1	-0.0705	0.0210	-0.0875
92	-0.4	114.25	51.0	1451.1	0.2780	0.0149	-0.0765
93	2.6	113.40	49.0	1437.2	0.6161	0.0156	-0.0656
94	-0.4	113.10	47.0	1379.6	0.3008	0.0148	-0.0800
95	4.6	112.10	48.0	1355.2	0.9274	0.0190	-0.0673
96	6.6	111.60	49.0	1348.6	1.0707	0.0265	-0.0578
97	8.6	111.90	48.0	1337.6	1.1951	0.0348	-0.0372
98	9.6	112.65	48.0	1343.8	1.2996	0.0432	-0.0419
99	10.6	115.10	48.0	1376.6	1.3705	0.0517	-0.0328
100	11.6	114.00	48.0	1366.1	1.4113	0.0714	-0.0380
101	12.6	112.75	48.0	1346.3	1.4463	-----	-0.0315
102	13.6	112.30	49.0	1340.4	1.4043	-----	-0.0458

GLAZE 3 SMOOTH CONFIGURATION

RUN	AOA	VEL	TEMP	PALT	C_l	C_d	C_m
37	2.6	107.60	74.0	1297.5	0.6681	0.0190	-0.0738
38	-0.4	106.90	57.0	1286.9	0.3148	0.0157	-0.0738
39	7.6	108.00	57.0	1299.6	1.0679	-----	-0.0287
40	7.6	108.50	57.0	1307.6	1.1208	-----	-0.0383
41	7.6	109.00	57.0	1307.4	1.0983	0.0668	-0.0430
42	8.6	108.15	58.0	1309.5	1.2054	-----	-0.0301
43	10.6	108.70	57.0	1314.7	1.1935	-----	-0.0356
44	11.6	109.65	57.0	1321.6	1.1526	-----	-0.0433
45	5.6	108.15	55.0	1312.4	1.0114	0.0385	-0.0487
46	-3.4	107.65	55.0	1300.7	-0.0427	0.0248	-0.0911

GLAZE 3 ROUGH CONFIGURATION

23	2.6	108.45	62.0	1283.5	0.5998	0.0161	-0.0653
24	2.6	108.80	62.0	1287.5	0.5993	0.0180	-0.0650
25	-3.4	108.45	59.0	1283.5	-0.0492	-----	-0.0798
26	-3.4	108.15	56.0	1280.0	-0.0445	0.0247	-0.0907
27	-0.4	107.90	58.0	1277.6	0.2617	0.0177	-0.0762
28	4.6	108.25	58.0	1278.1	0.8034	0.0271	-0.0530
29	5.6	108.85	62.0	1274.7	0.9575	0.0343	-0.0536
30	6.6	107.55	57.0	1254.0	1.0038	-----	-0.0357
31	7.6	107.20	57.0	1238.2	1.1051	-----	-0.0371
32	8.6	108.70	55.0	1247.2	1.1070	-----	-0.0213
33	9.6	109.70	52.0	1266.3	1.1771	-----	-0.0287
34	10.6	107.25	48.0	1239.8	1.2723	-----	-0.0426
35	3.6	110.25	57.0	1272.6	0.8242	0.0214	-0.0663
36	1.6	107.45	48.0	1245.9	0.5542	0.0181	-0.0703

RIME 7 SMOOTH CONFIGURATION

ORIGINAL PAGE IS
OF POOR QUALITY

RUN	AOA	VEL	TEMP	PALT	C_L	C_D	C_M
79	-3.4	83.80	58.0	1163.3	-0.0533	-----	-0.0813
80	-3.4	83.45	55.0	1176.2	-0.0890	0.0262	-0.0799
81	-0.4	87.85	53.0	1209.3	0.2907	0.0140	-0.0911
82	2.6	87.05	50.0	1202.9	0.6596	0.0125	-0.0842
83	4.6	87.15	47.0	1206.7	0.9115	0.0141	-0.0983
84	6.6	85.45	47.0	1190.8	1.0771	-----	-0.0846
85	8.6	87.10	45.0	1201.1	1.3015	0.0225	-0.0828
86	8.6	87.85	49.0	1205.4	1.3150	0.0219	-0.0785
87	10.6	86.75	46.0	1195.9	1.5177	0.0275	-0.0770
88	12.6	87.25	44.0	1196.8	1.7316	0.0428	-0.0735
89	14.6	86.80	43.0	1196.3	1.6831	-----	-0.0495
90	13.6	86.65	44.0	1199.6	1.6046	0.0714	-0.0399

RIME 7 ROUGH CONFIGURATION

103	-3.4	86.65	49.0	1125.4	-0.0421	0.0249	-0.0912
104	-0.4	86.75	50.0	1136.6	0.3304	0.0160	-0.0917
105	2.6	85.45	50.0	1121.4	0.6531	0.0143	-0.0846
106	4.6	88.50	50.0	1143.1	0.8990	0.0163	-0.0829
107	6.6	87.85	50.0	1138.6	0.9751	0.0196	-0.0615
108	8.6	86.75	50.0	1135.1	1.1610	0.0245	-0.0548
109	9.6	87.60	50.0	1139.3	1.2821	0.0280	-0.0494
110	10.6	87.20	50.0	1138.6	1.4624	-----	-0.0699
111	11.6	87.60	50.0	1137.2	1.5794	-----	-0.0794
112	12.6	88.25	49.0	1133.6	1.5198	-----	-0.0693
113	13.6	86.55	46.0	1121.6	1.4914	-----	-0.0767

ORIGINAL PAGE IS
OF POOR QUALITY

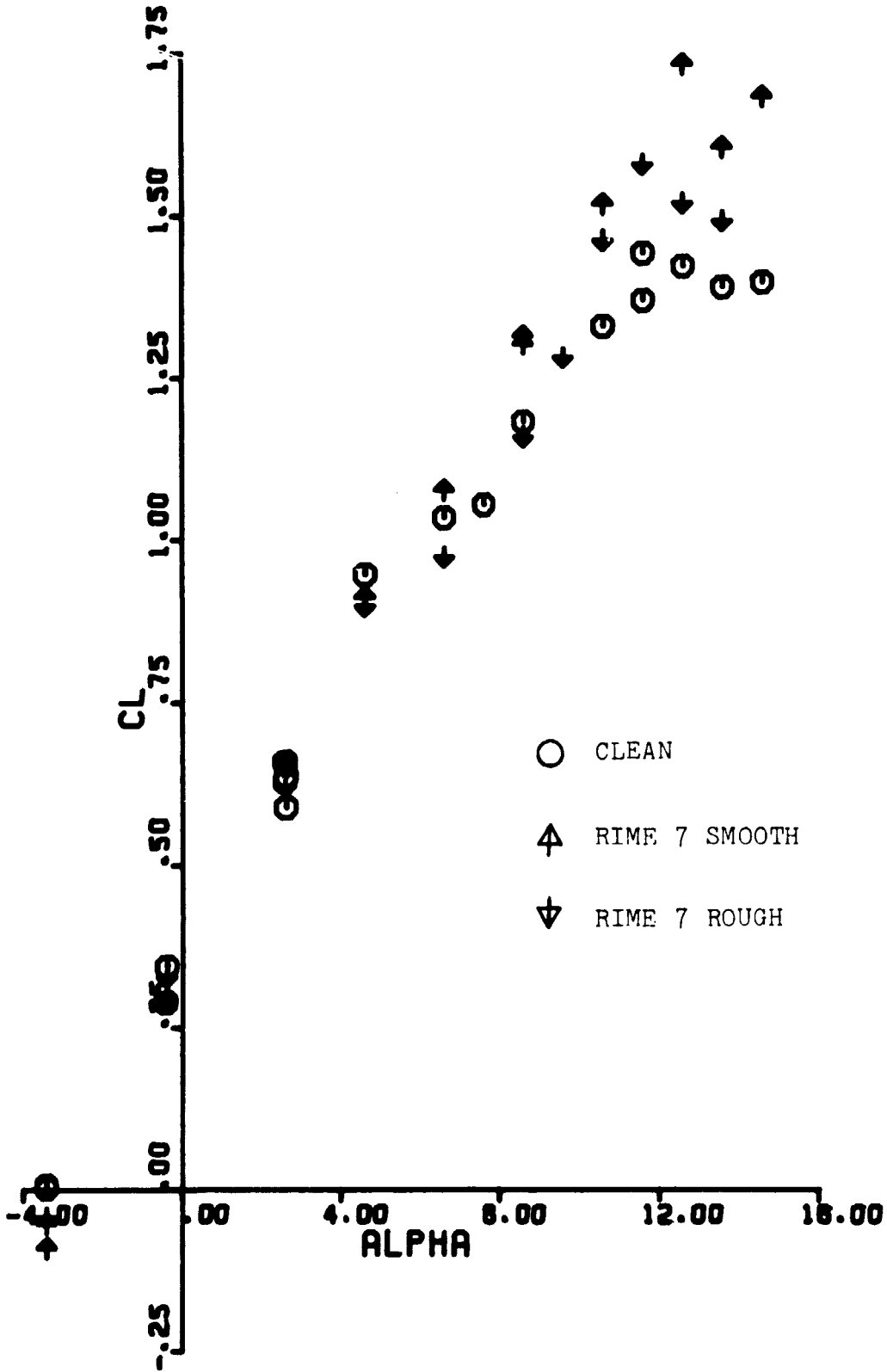
GLAZE 7 SMOOTH CONFIGURATION

RUN	AOA	VEL	TEMP	PALT	C_l	C_d	C_m
47	6.6	77.80	62.0	1055.8	1.0544	0.0280	-0.0700
48	6.6	81.60	62.0	1080.7	1.0976	0.0311	-0.0719
49	8.6	82.05	60.0	1083.7	1.2997	0.0505	-0.0626
50	9.6	82.25	58.0	1086.9	1.2890	0.0611	-0.0504
51	10.6	81.75	58.0	1078.2	1.3259	-----	-0.0411
52	11.6	82.60	56.0	1086.4	1.3102	-----	-0.0279
53	4.6	81.75	56.0	1072.4	0.9008	0.0229	-0.0621
54	2.6	81.20	56.0	1069.4	0.7032	0.0169	-0.0758
55	-0.4	81.35	56.0	1074.3	0.3618	0.0170	-0.0857

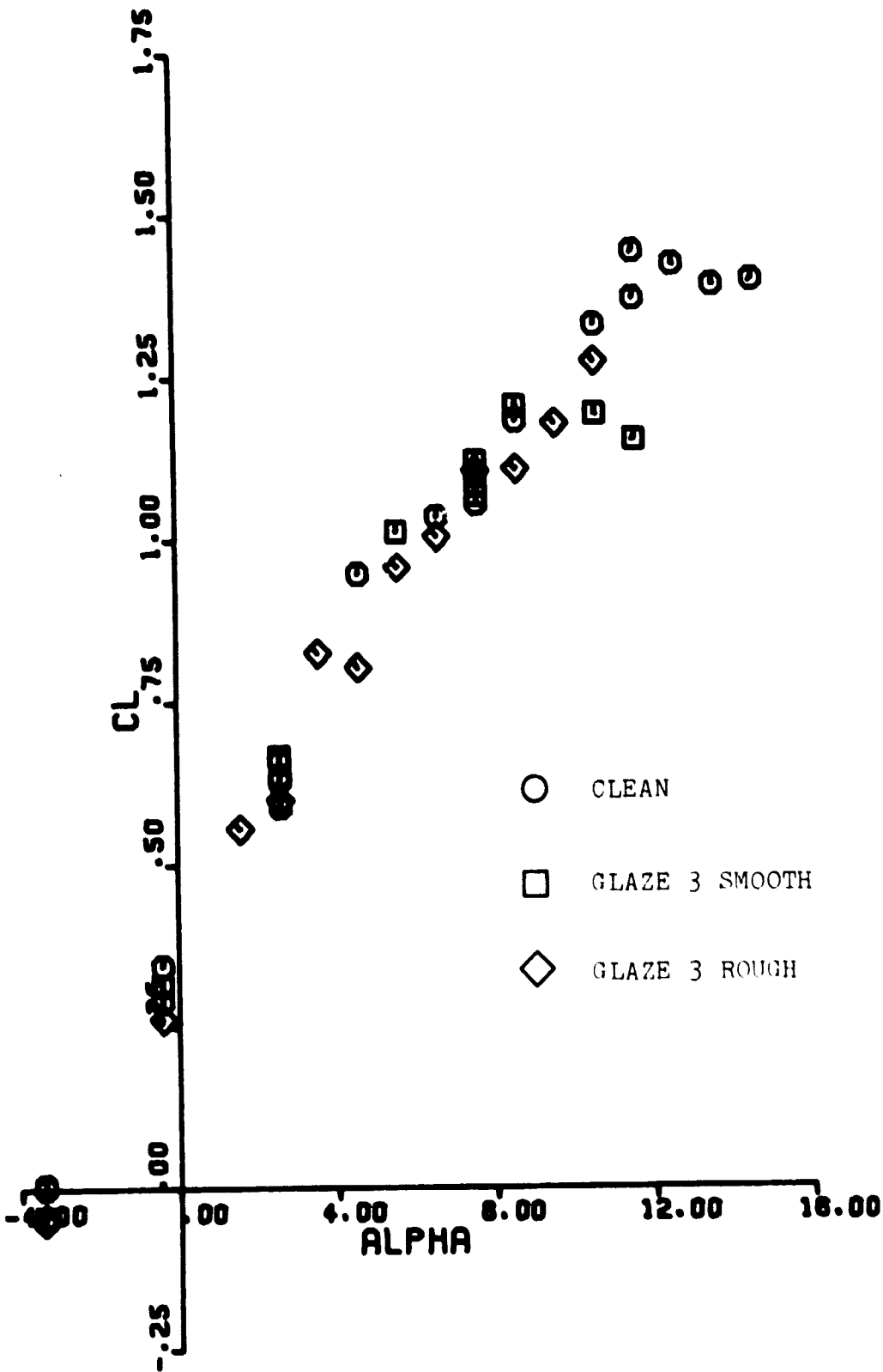
GLAZE 7 ROUGH CONFIGURATION

67	-3.4	80.05	47.0	1180.9	-0.0311	-----	-0.0693
69	-0.4	80.70	47.0	1175.1	0.2667	0.0177	-0.0568
70	-3.4	79.60	44.0	1165.3	-0.0262	0.0280	-0.0828
71	2.6	79.30	44.0	1162.4	0.5997	0.0175	-0.0665
72	4.6	82.10	43.0	1182.5	0.8541	0.0211	-0.0751
73	6.6	81.30	44.0	1181.4	1.0842	0.0296	-0.0880
74	8.6	79.80	43.0	1165.6	1.2246	0.0476	-0.0775
75	9.6	80.05	44.0	1160.6	1.2967	0.0613	-0.0579
76	10.6	80.70	48.0	1172.9	1.3196	-----	-0.0412
77	11.6	80.65	45.0	1159.9	1.3557	-----	-0.0594
78	12.6	79.80	44.0	1149.1	1.2287	-----	-0.0368

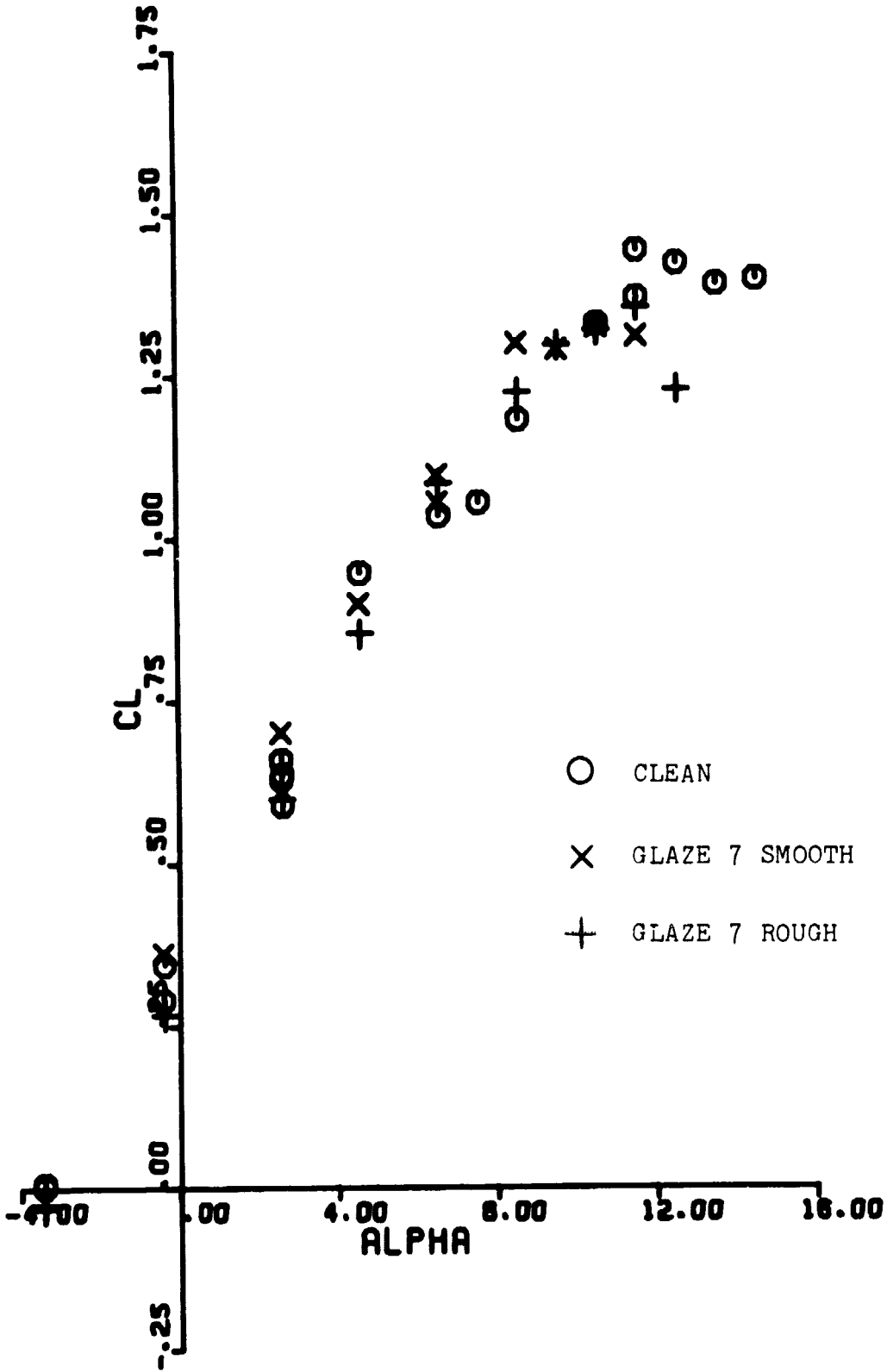
ORIGINAL PAGE IS
OF POOR QUALITY



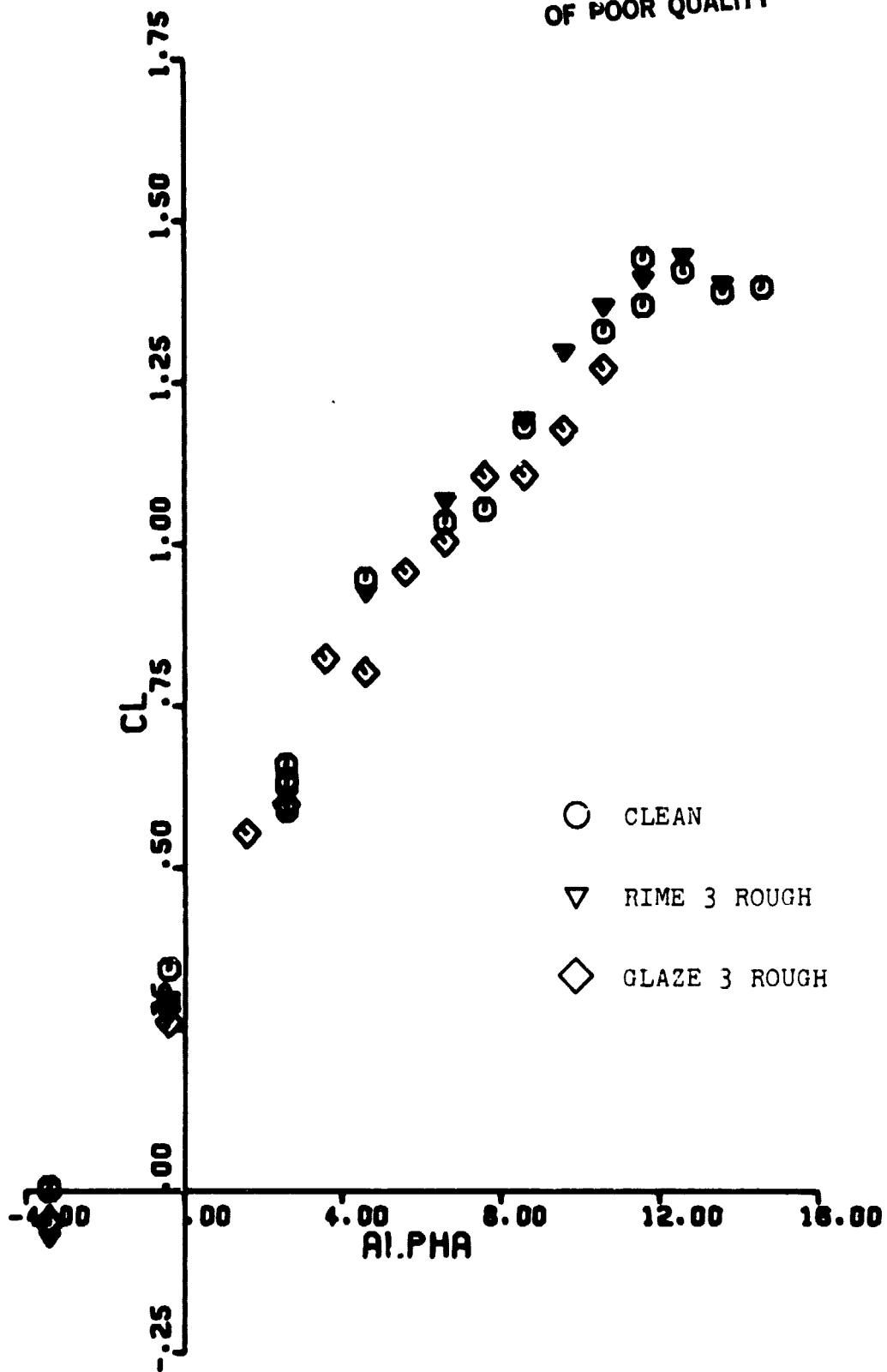
ORIGINAL PAGE IS
OF POOR QUALITY



ORIGINAL PAGE 13
OF POOR QUALITY

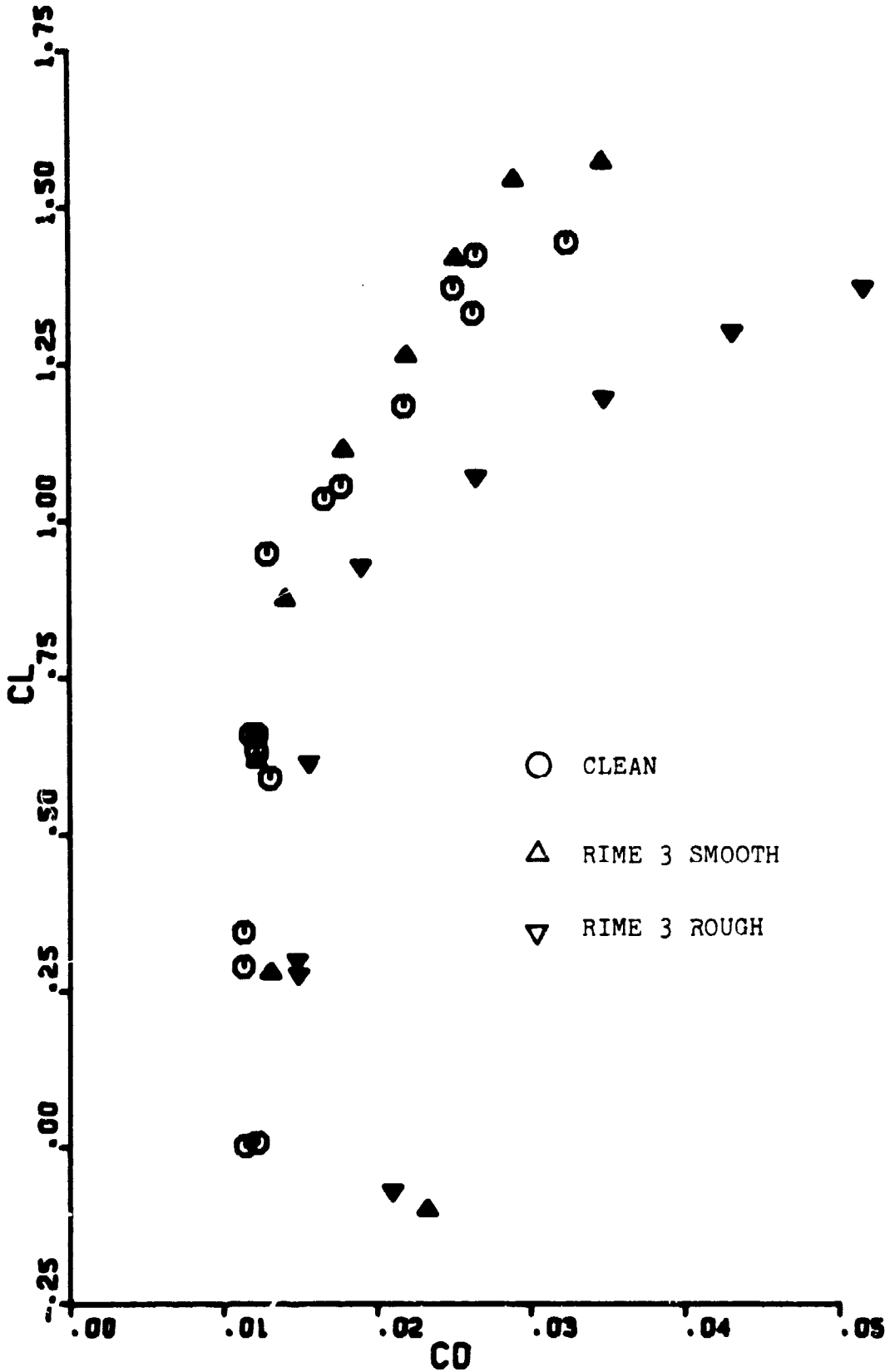


ORIGINAL PAGE 13
OF POOR QUALITY

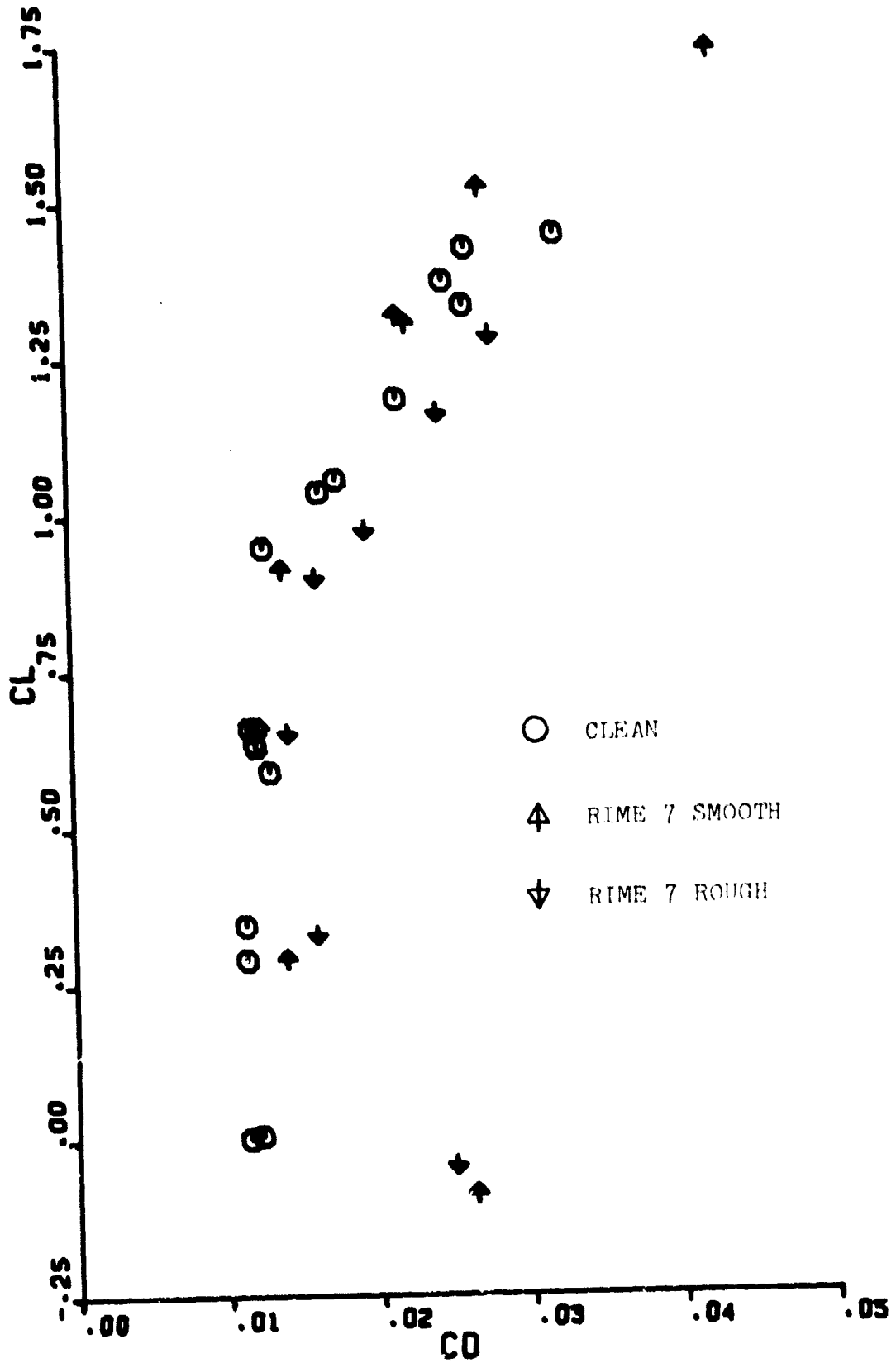


C_l vs C_d Plots

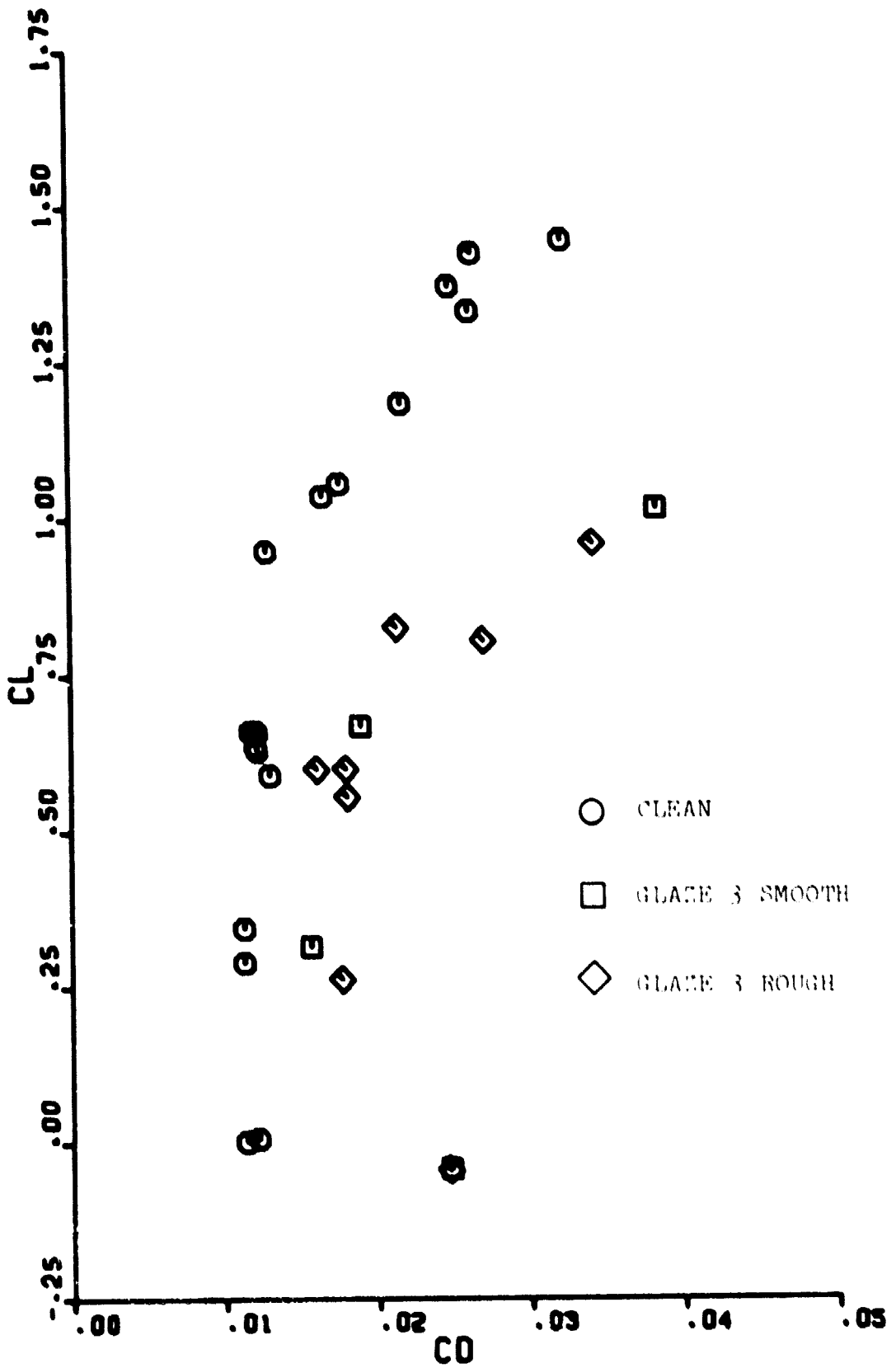
ORIGINAL PAGE IS
OF POOR QUALITY



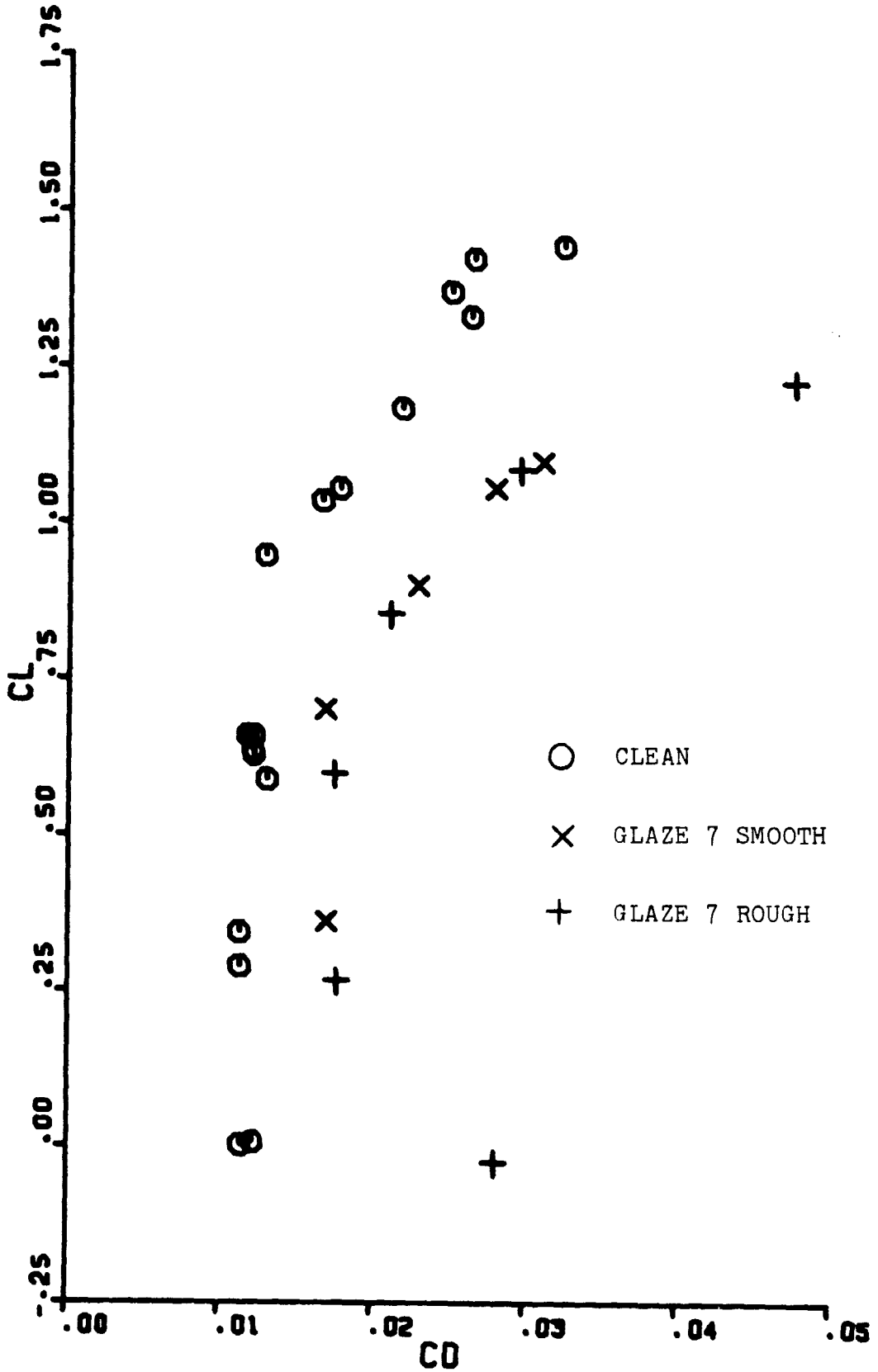
ORIGINAL PAGE 13
OF POOR QUALITY



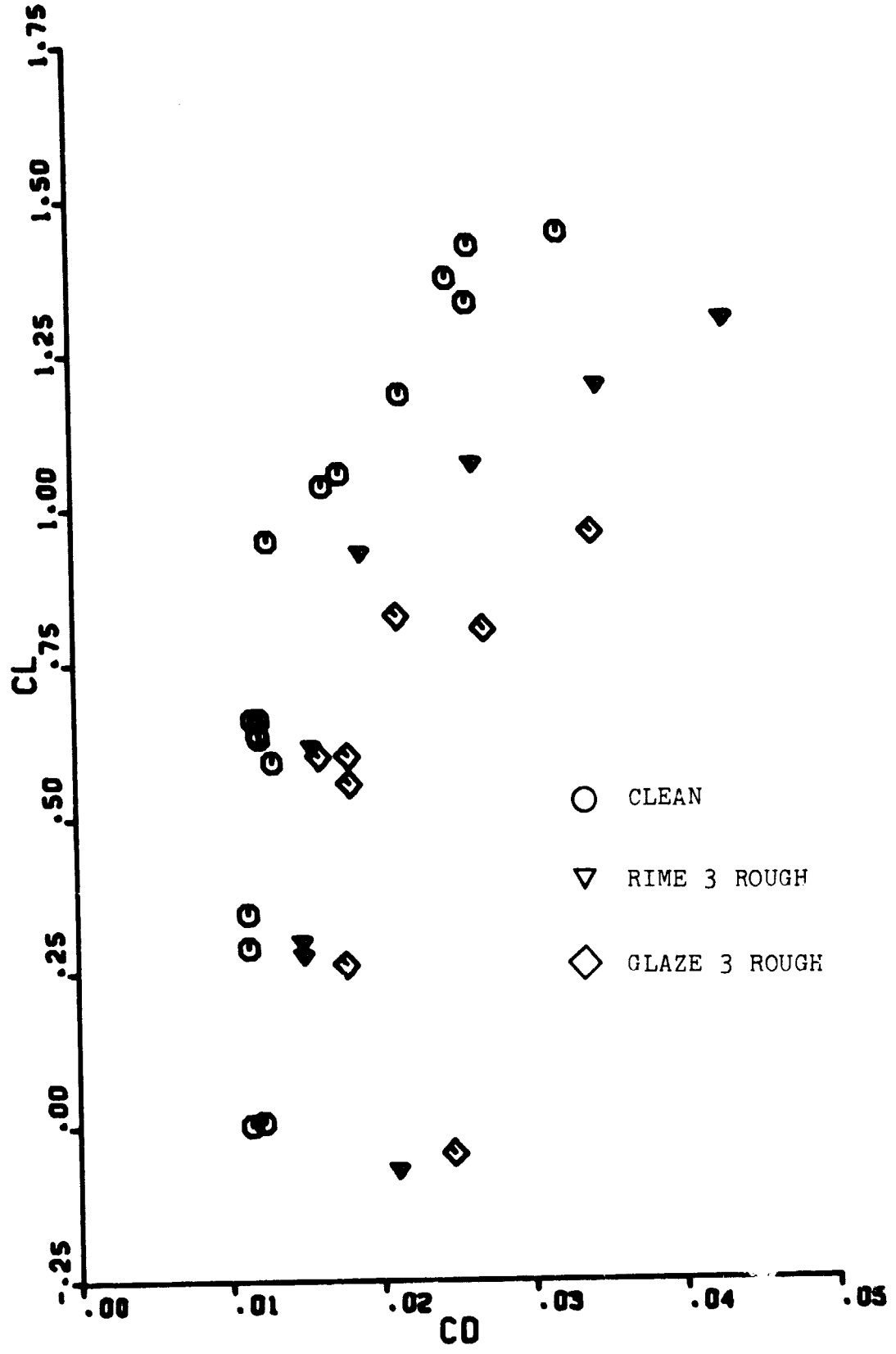
ORIGINAL PAGE IS
OF POOR QUALITY



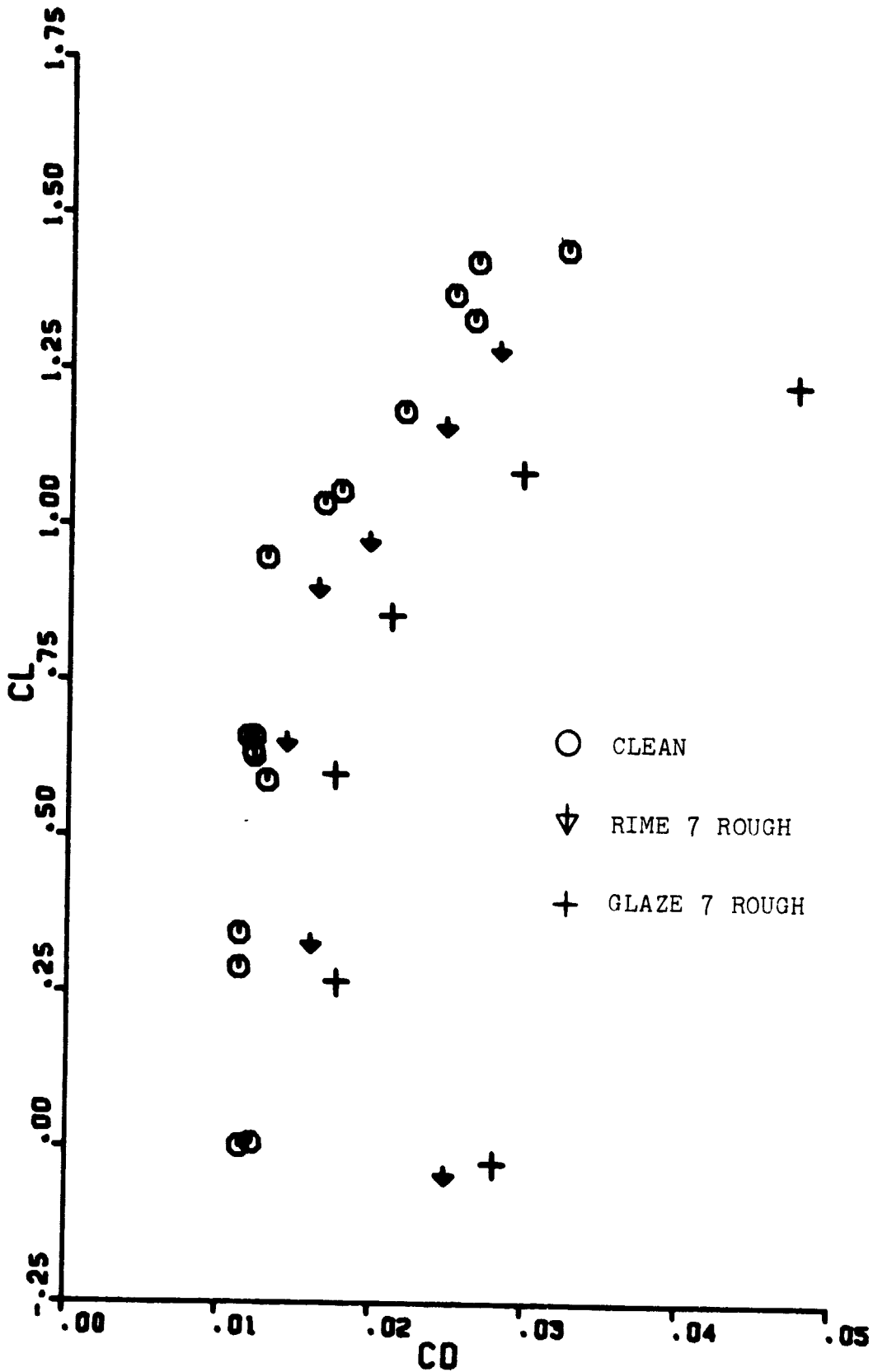
ORIGINAL PAGE IS
OF POOR QUALITY



ORIGINAL PAGE IS
OF POOR QUALITY

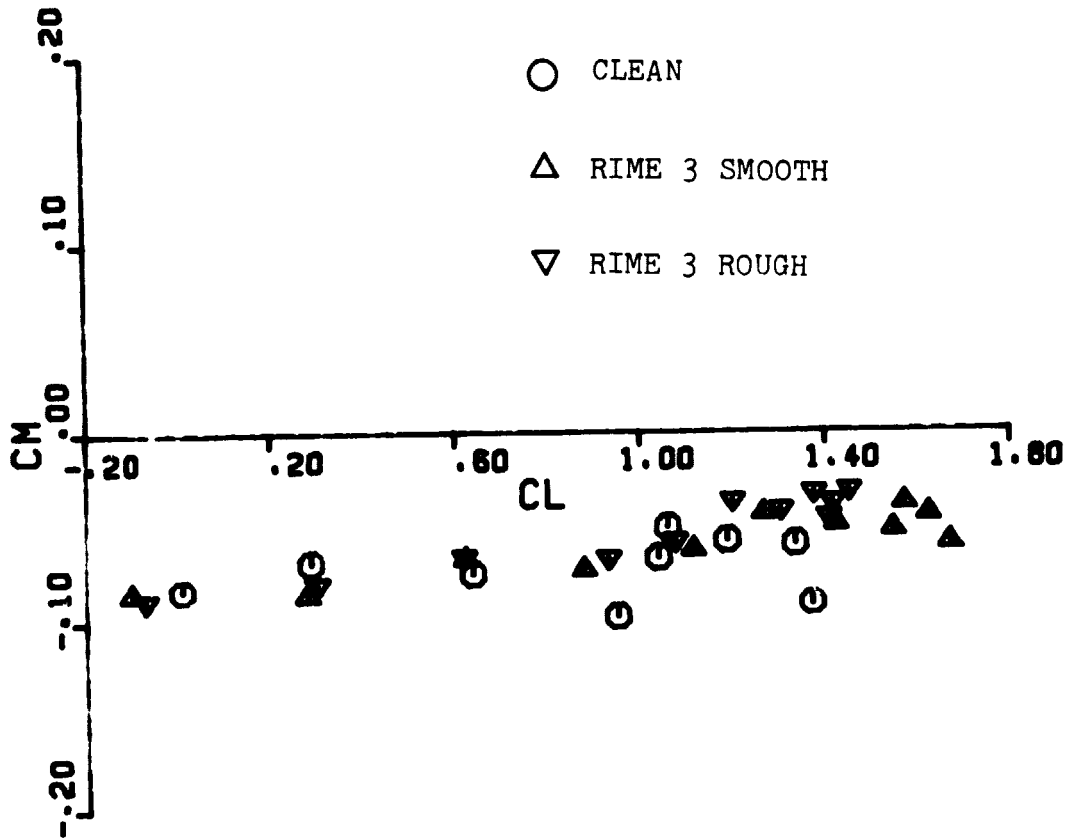


ORIGINAL PAGE IS
OF POOR QUALITY

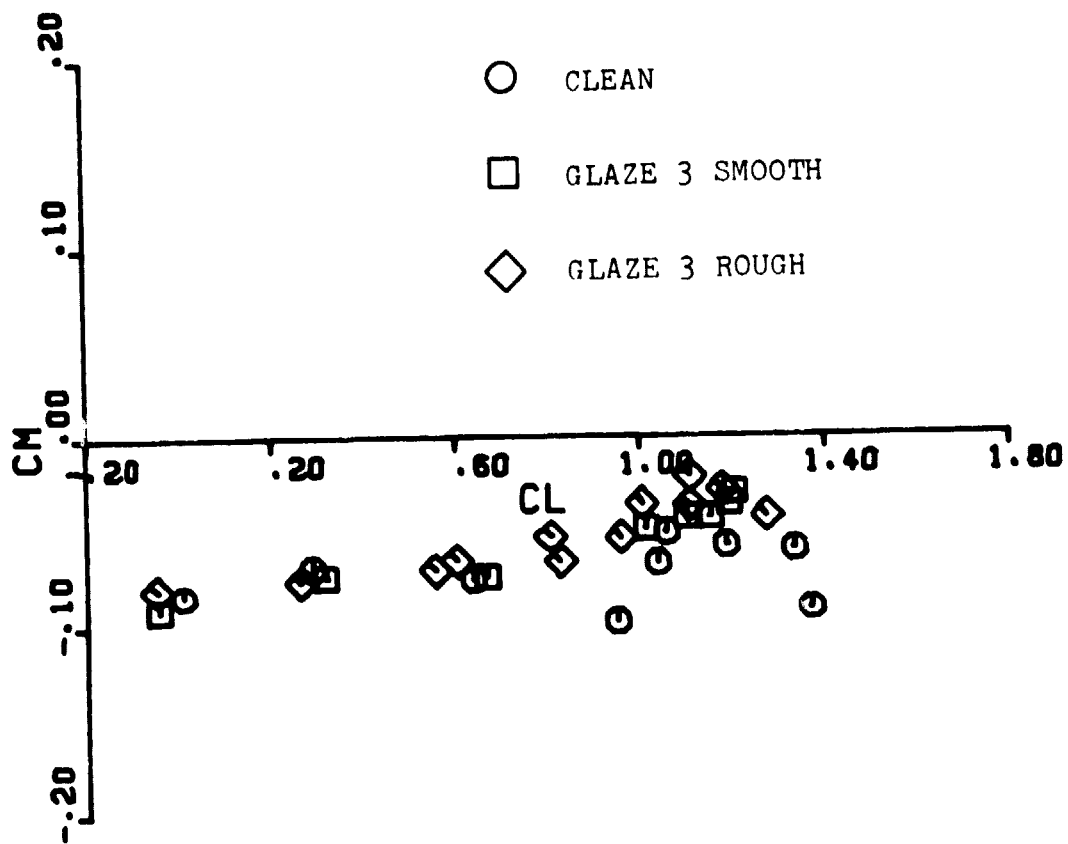


ORIGINAL FROM
OF POOR QUALITY

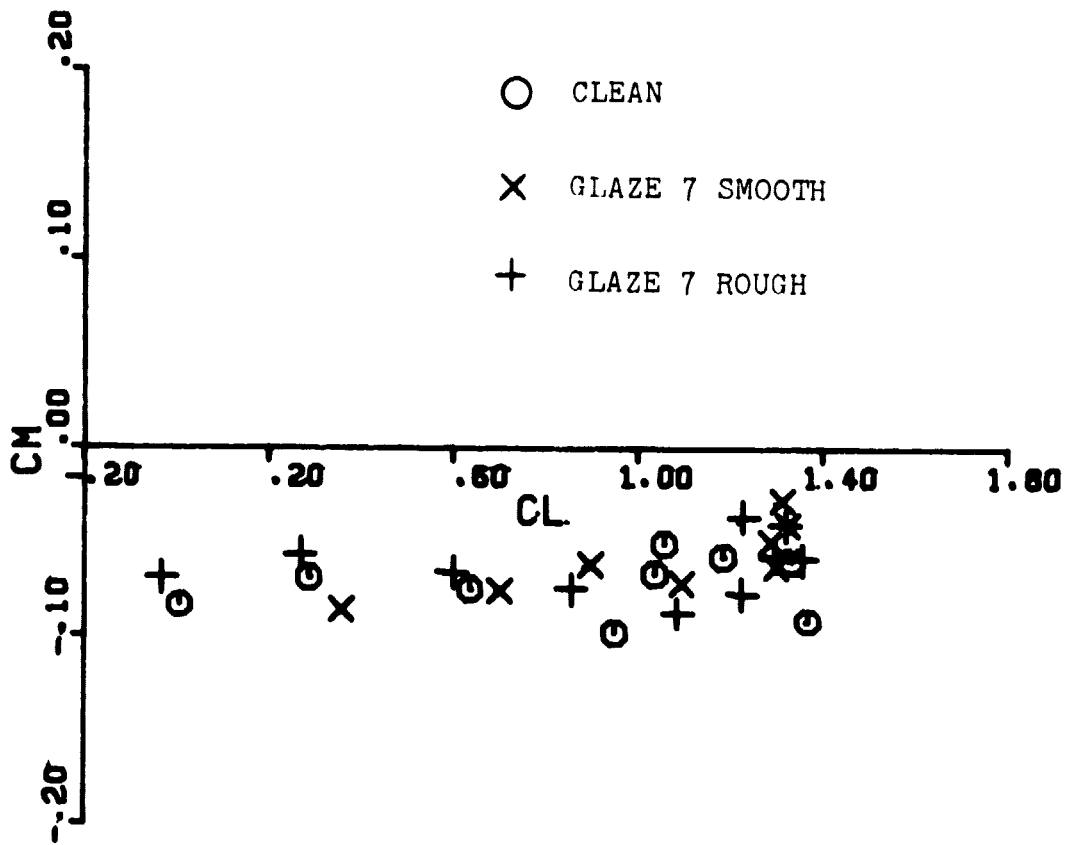
C_m vs C_l Plots



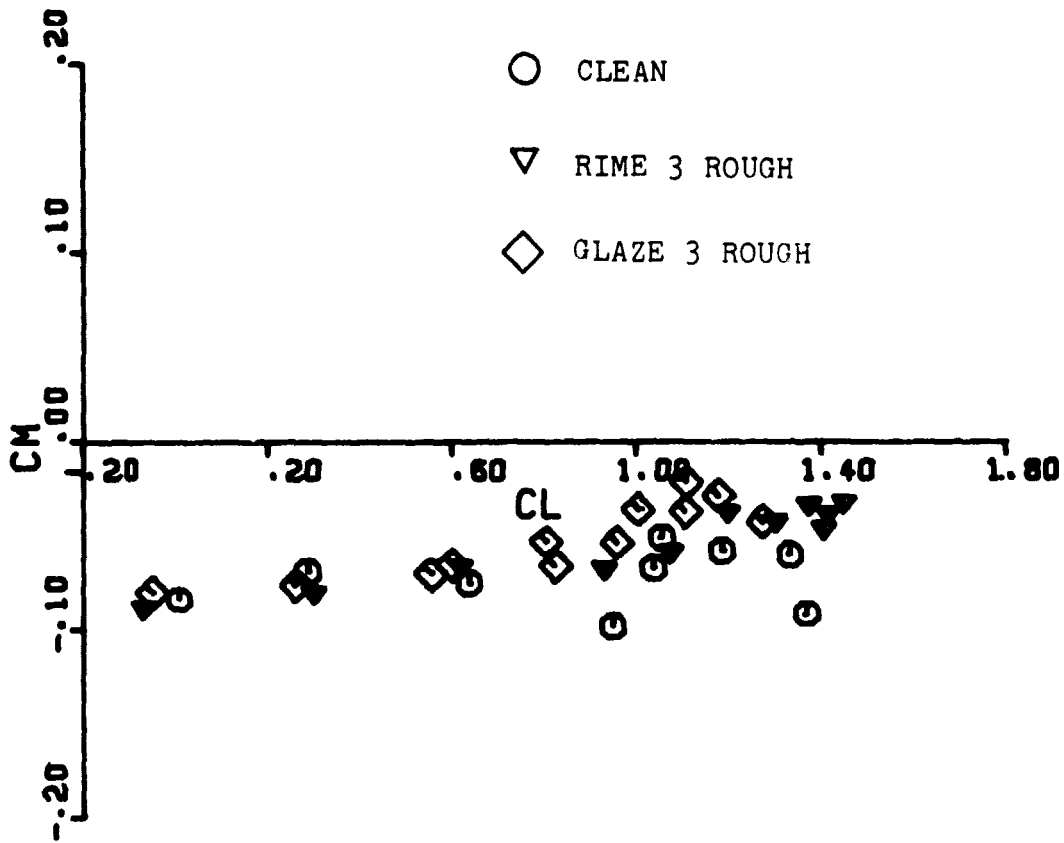
ORIGINAL PAGE IS
OF POOR QUALITY



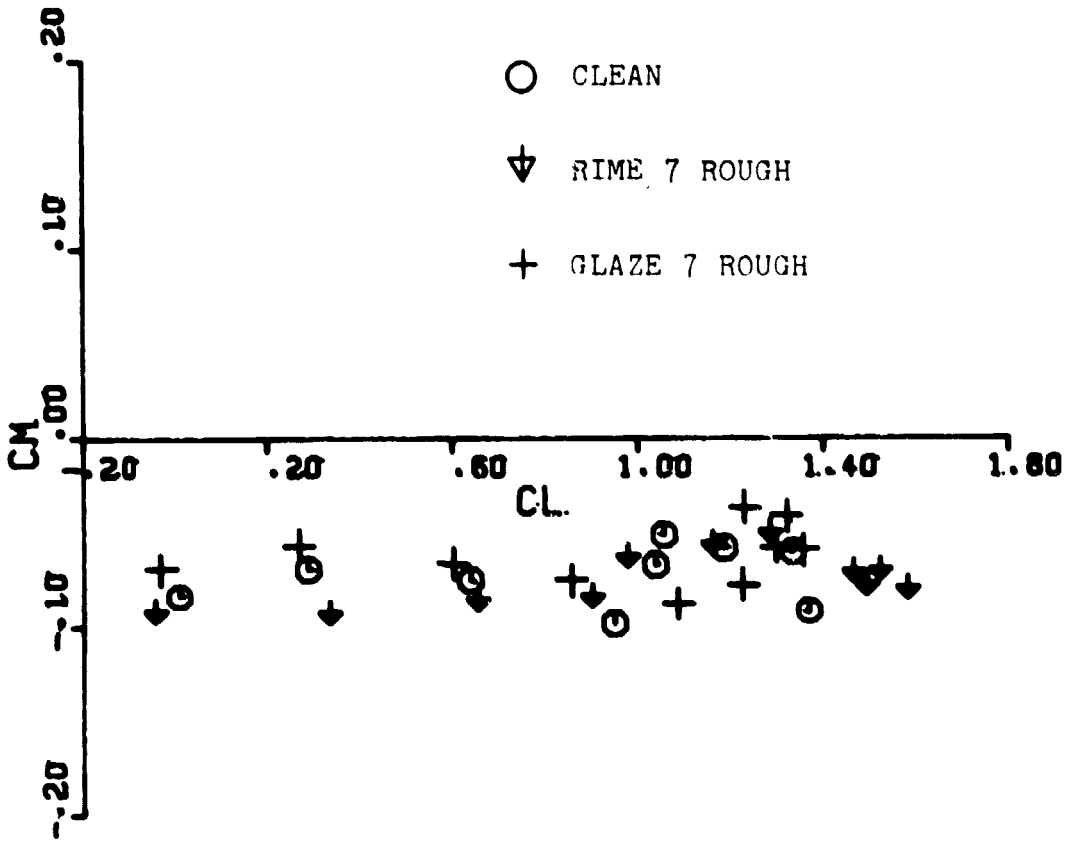
ORIGINAL PAGE IS
OF POOR QUALITY



ORIGINAL PAGE NO
OF POOR QUALITY

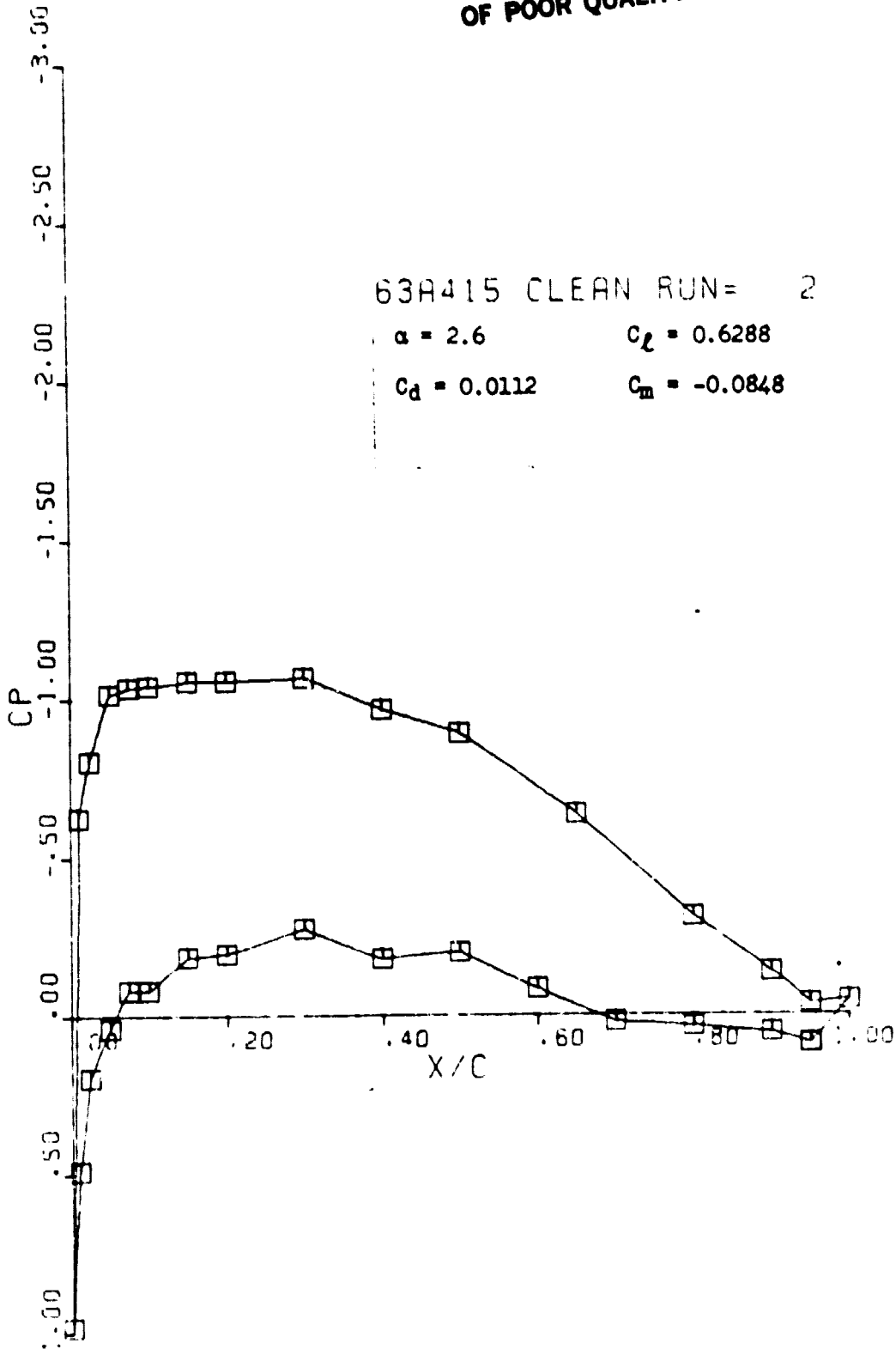


ORIGINAL PAGE IS
OF POOR QUALITY

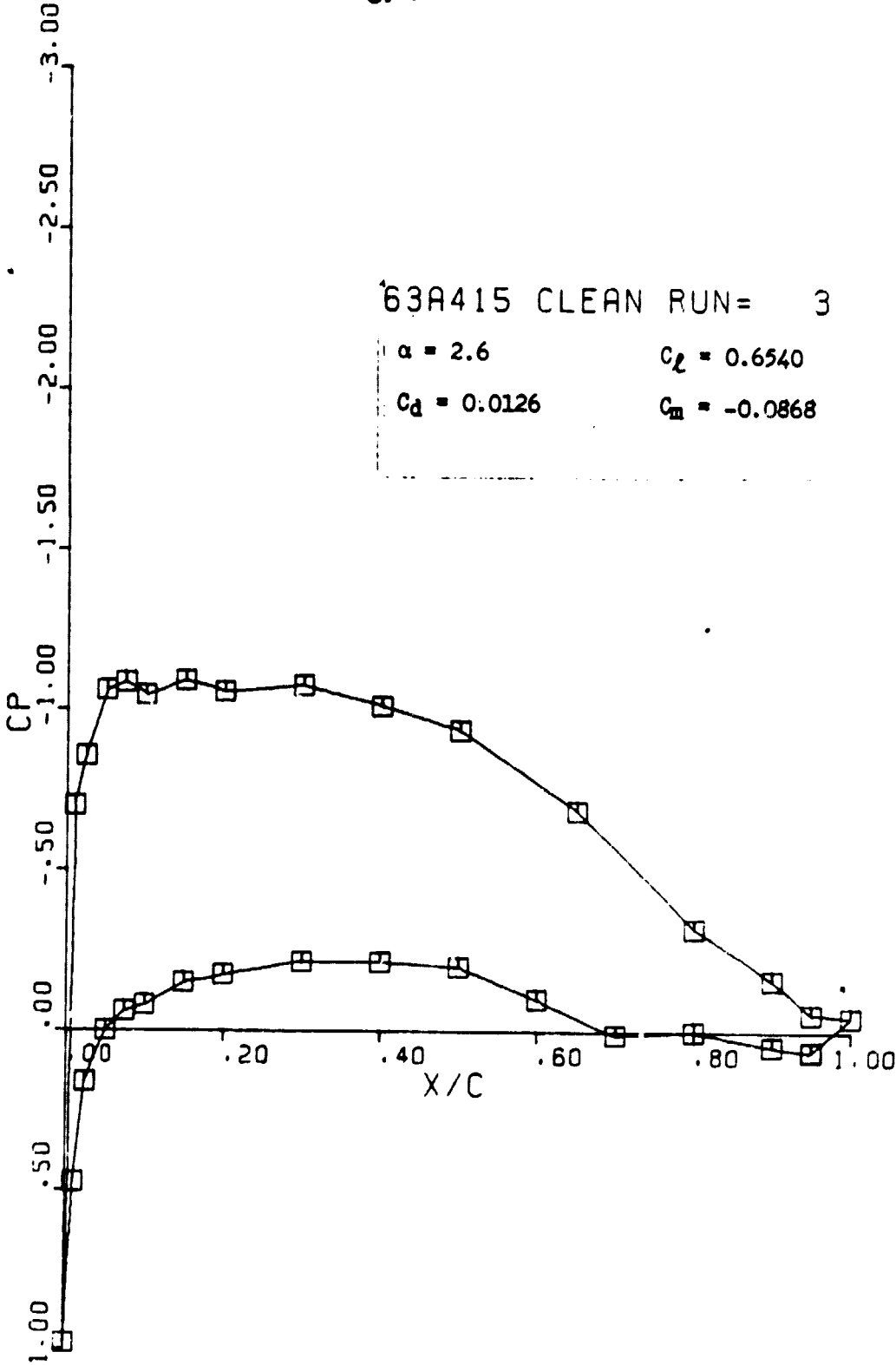


C_p Distributions

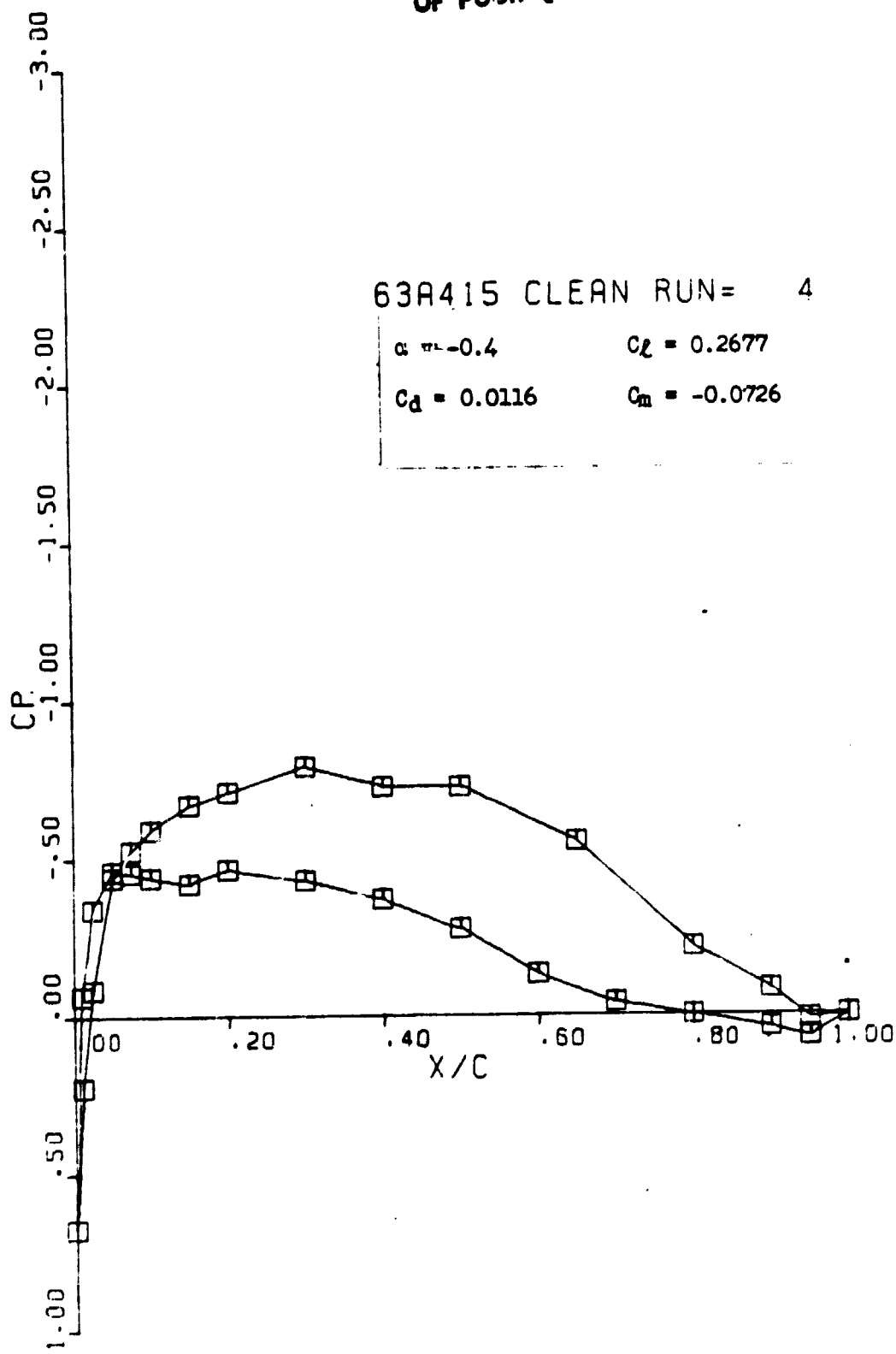
ORIGINAL PAGE IS
OF POOR QUALITY



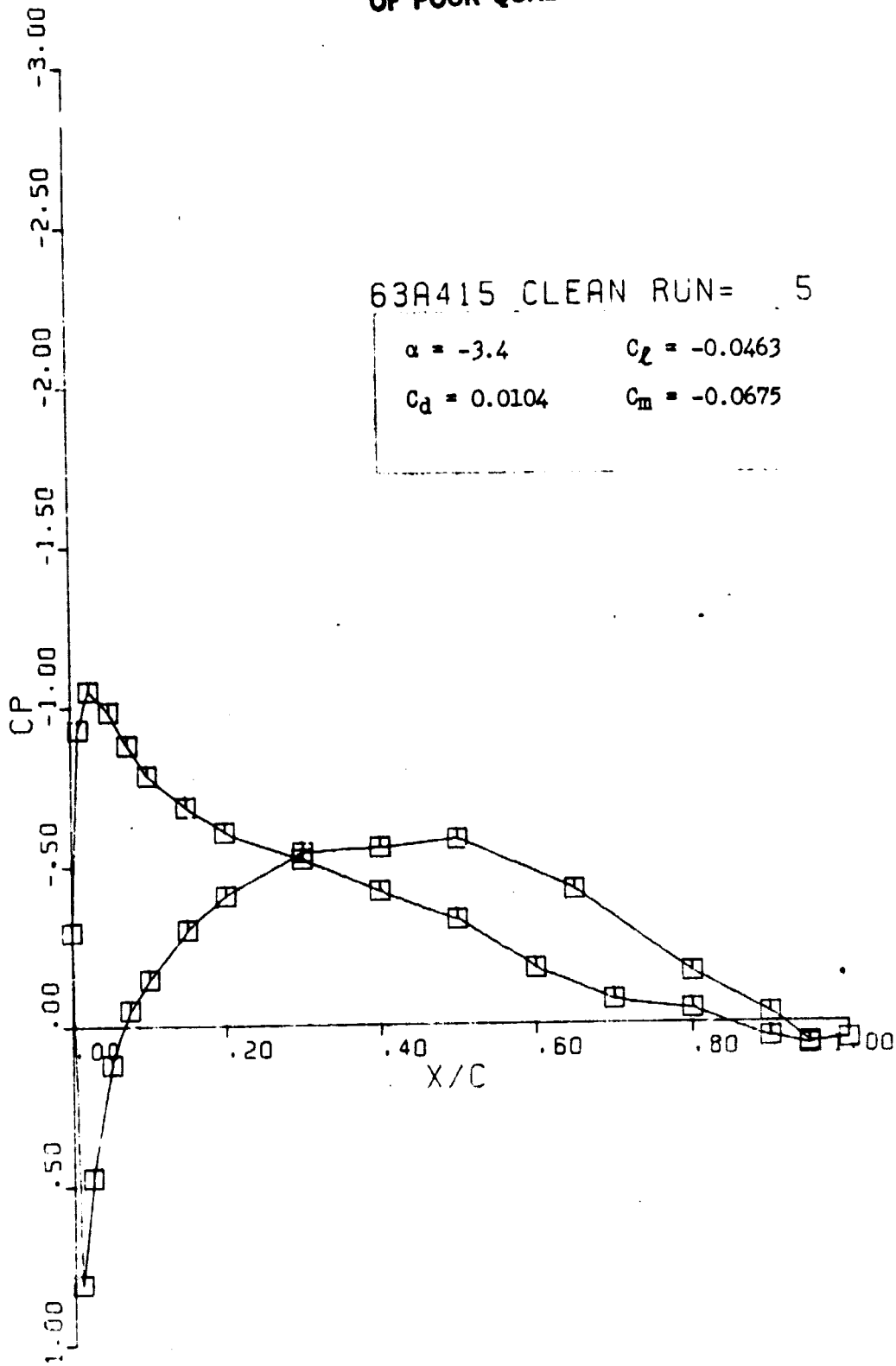
ORIGINAL PAGE IS
OF POOR QUALITY



ORIGINAL PAGE IS
OF POOR QUALITY



ORIGINAL PAGE IS
OF POOR QUALITY



ORIGINAL PAGE IS
OF POOR QUALITY

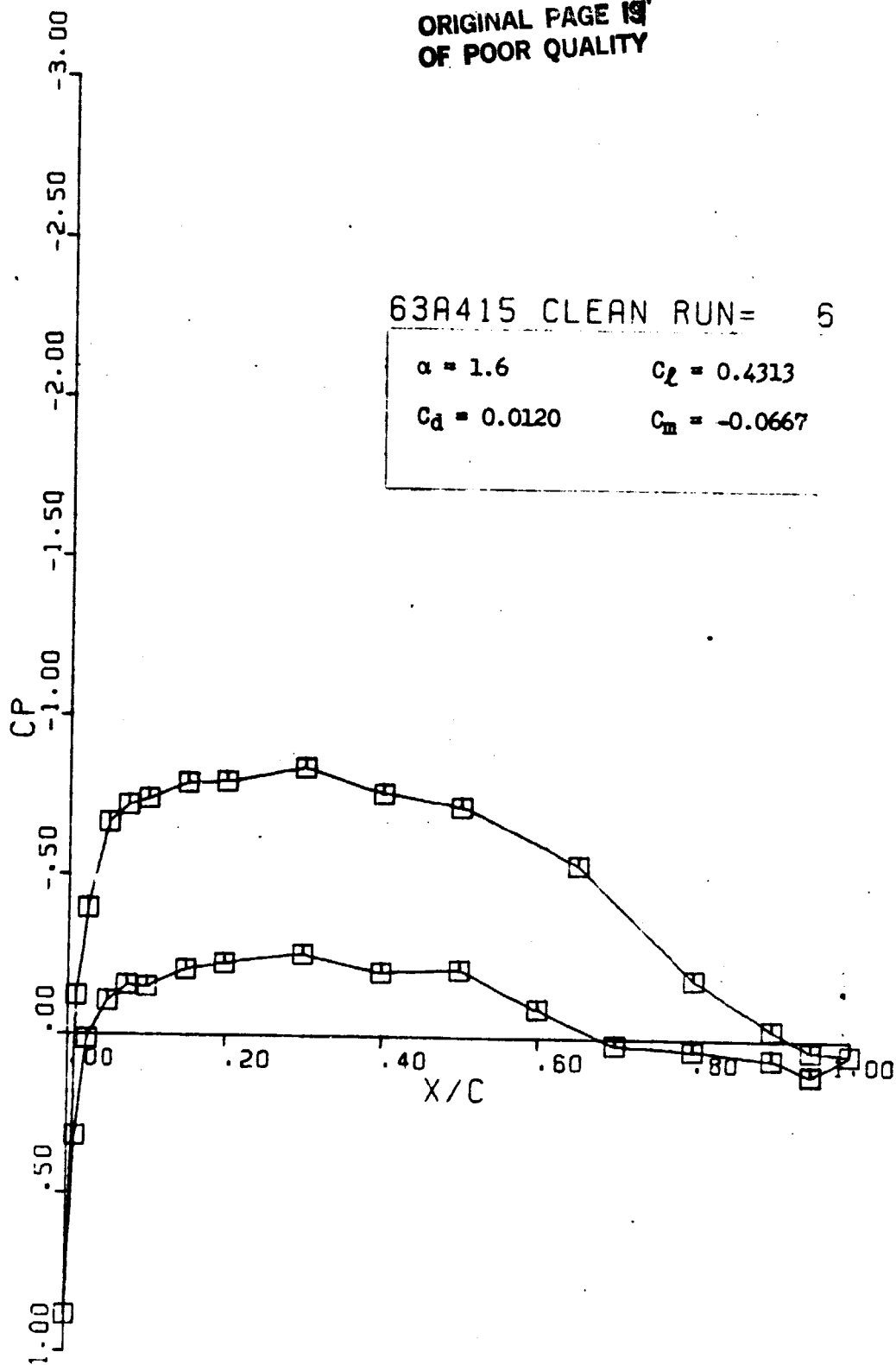
63A415 CLEAN RUN= 5

$\alpha = 1.6$

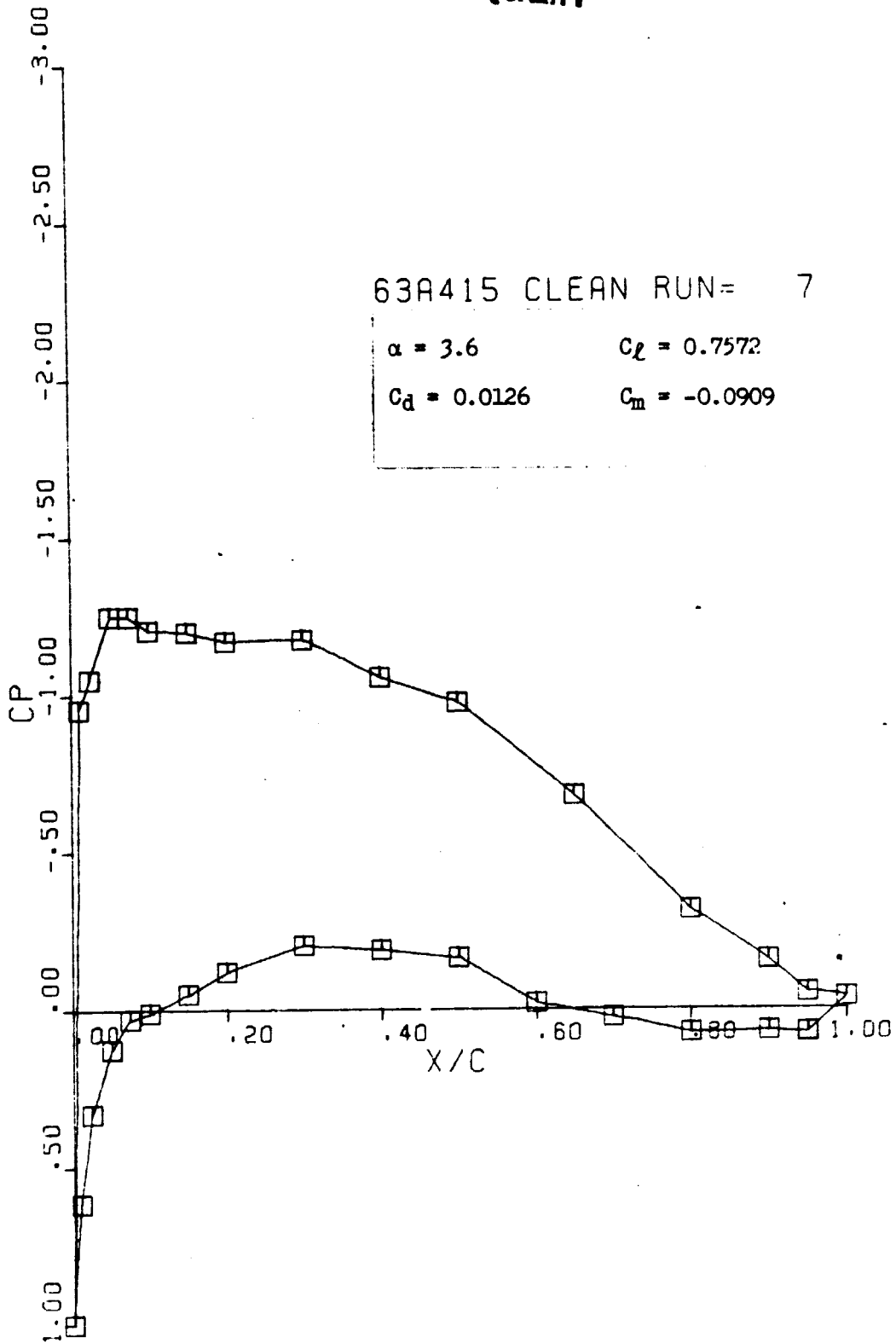
$C_L = 0.4313$

$C_d = 0.0120$

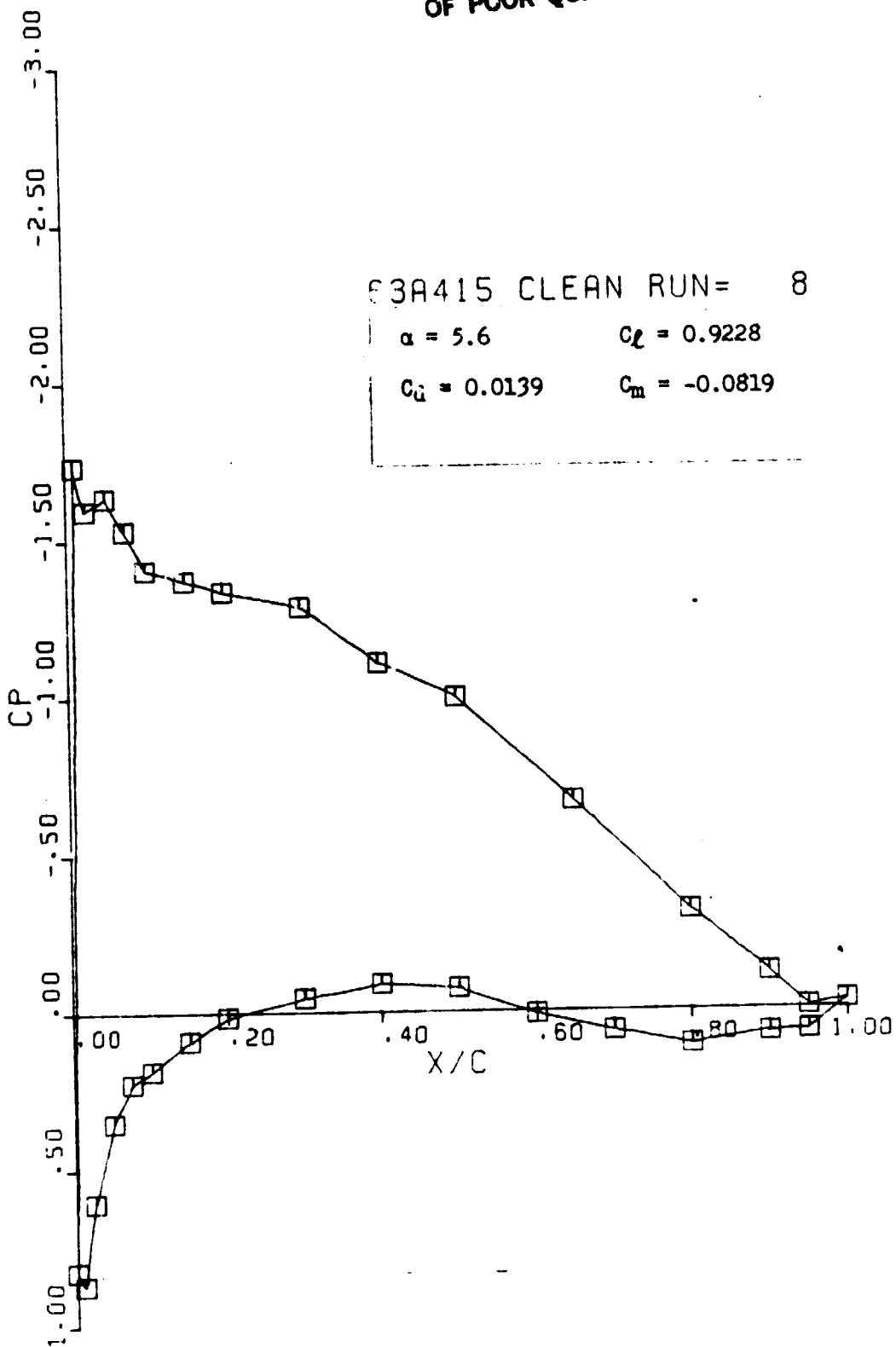
$C_m = -0.0667$



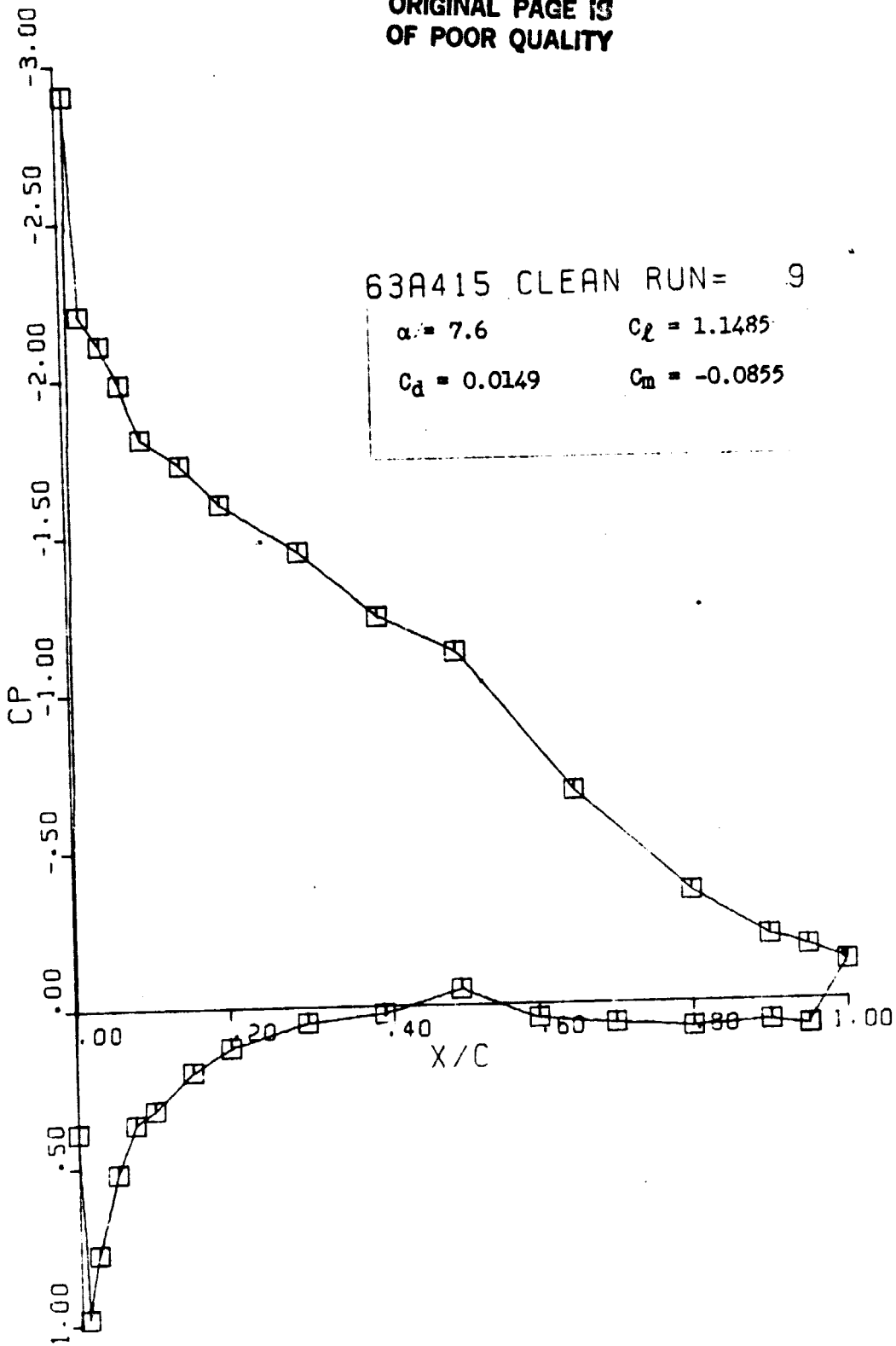
ORIGINAL PAGE IS
OF POOR QUALITY



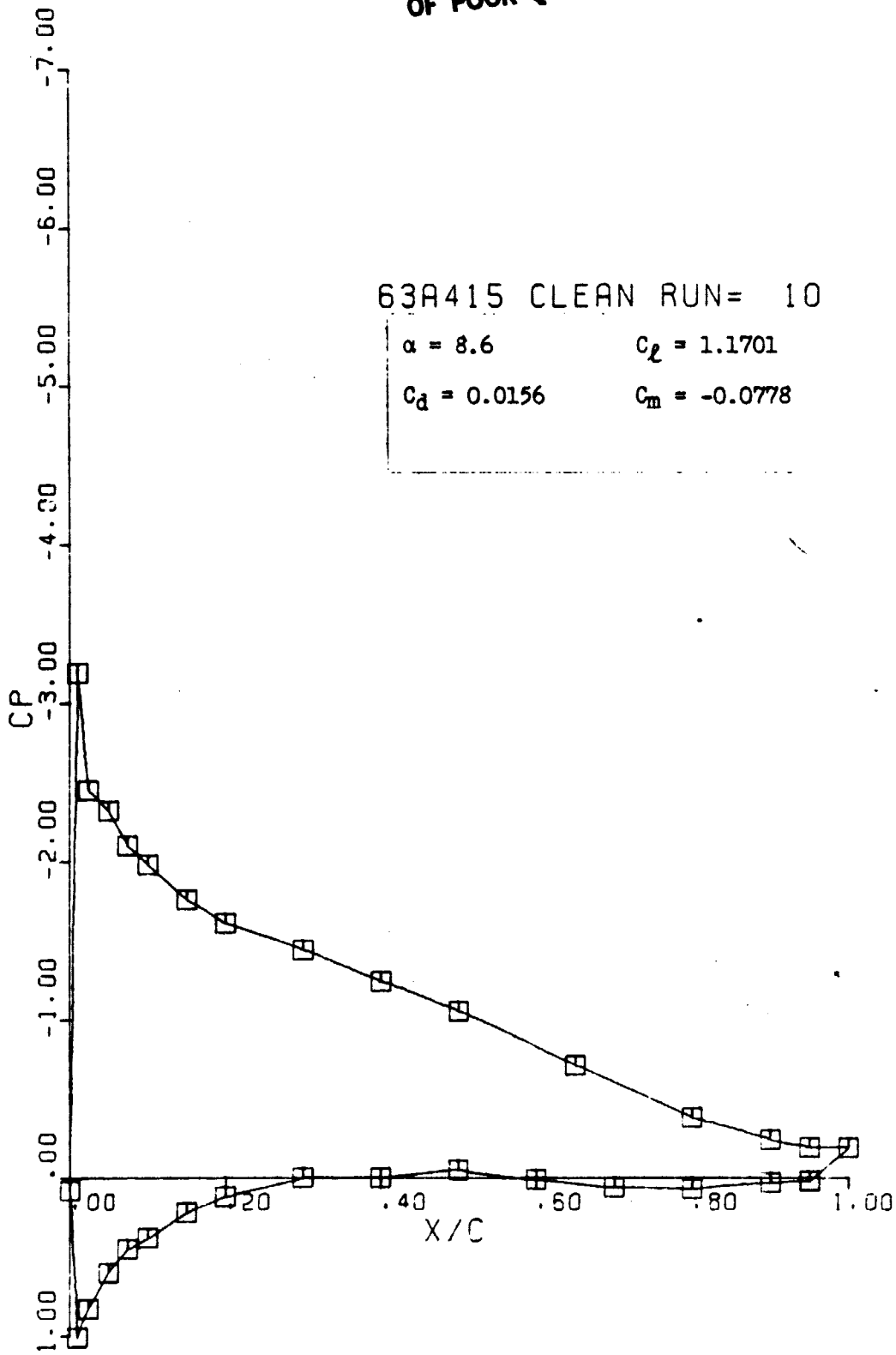
ORIGINAL PAGE IS
OF POOR QUALITY



ORIGINAL PAGE IS
OF POOR QUALITY



ORIGINAL PAGE IS
OF POOR QUALITY



ORIGINAL PAGE IS
OF POOR QUALITY

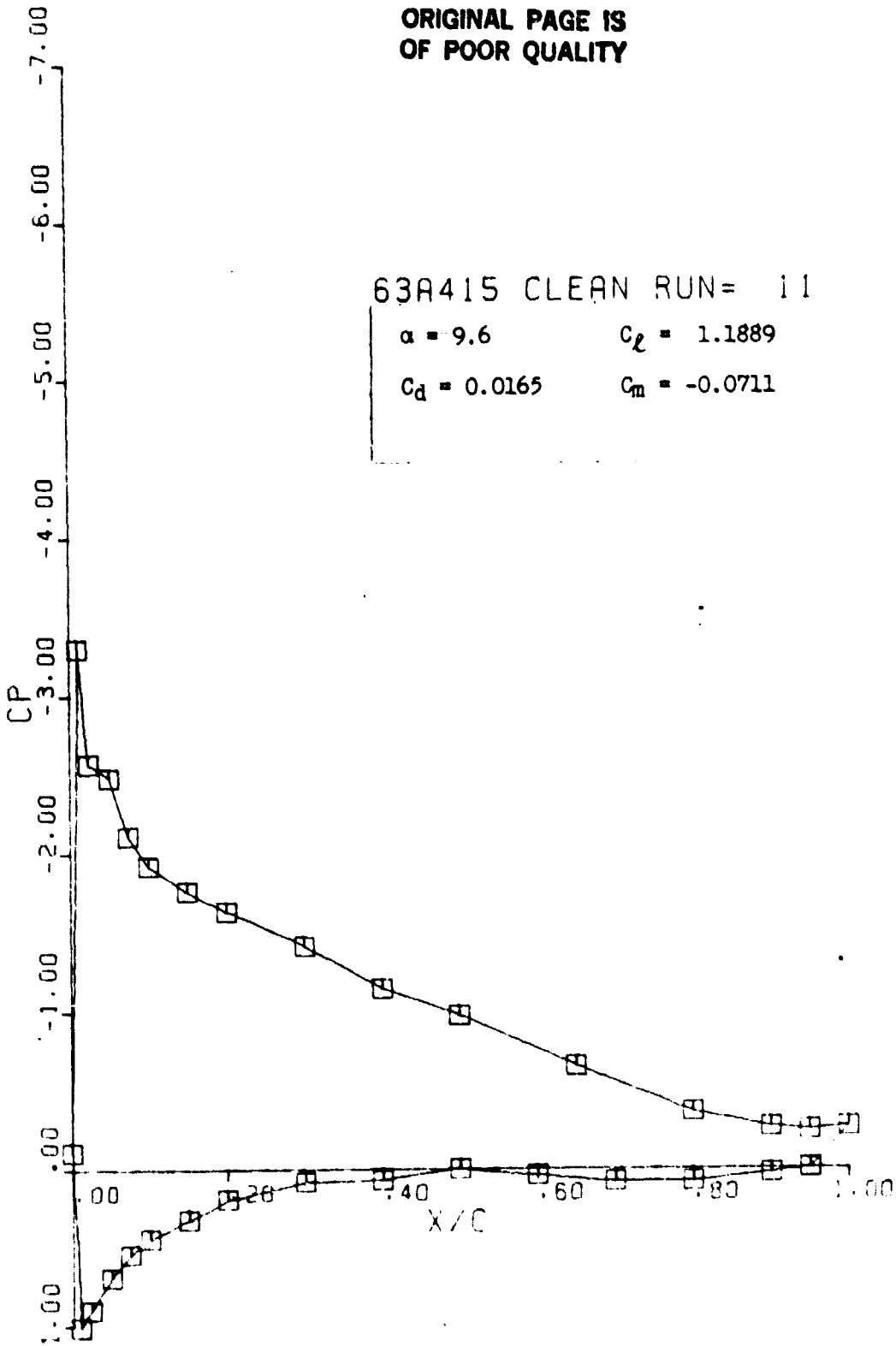
63A415 CLEAN RUN= 11

$$\alpha = 9.6$$

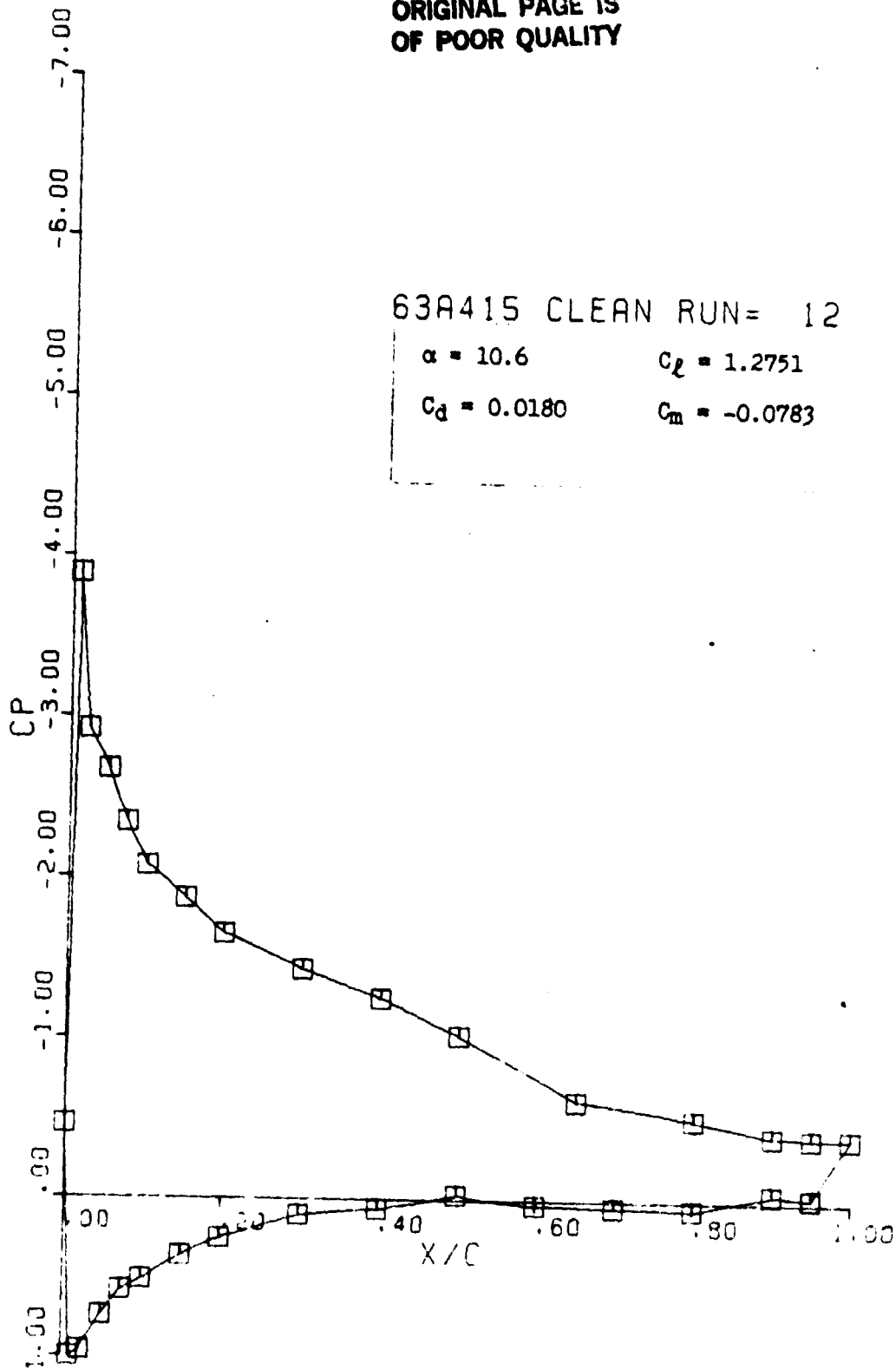
$$C_l = 1.1889$$

$$C_d = 0.0165$$

$$C_m = -0.0711$$



ORIGINAL PAGE IS
OF POOR QUALITY



ORIGINAL PAGE IS
OF POOR QUALITY

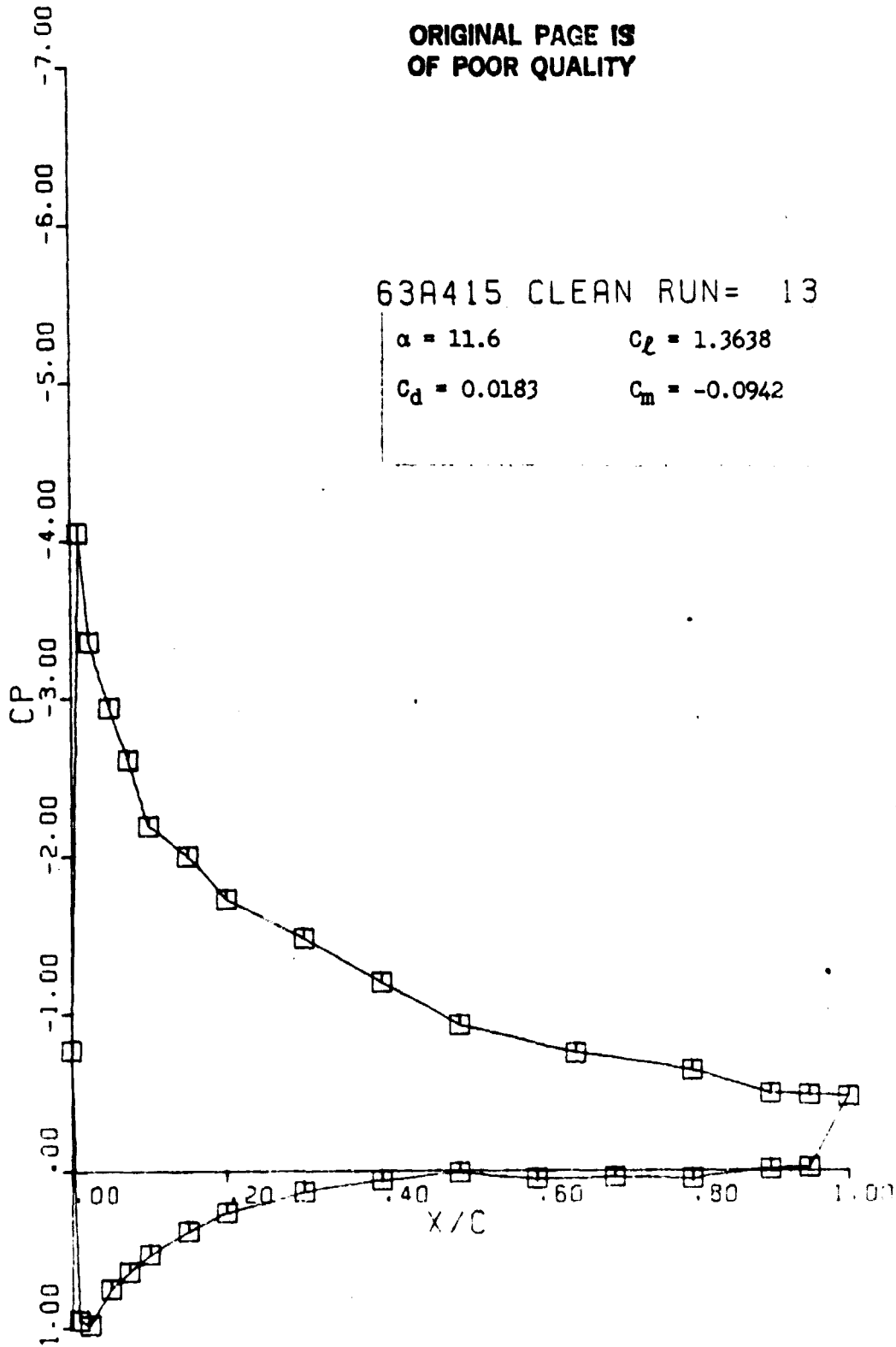
63R415 CLEAN RUN= 13

$\alpha = 11.6$

$C_L = 1.3638$

$C_d = 0.0183$

$C_m = -0.0942$



ORIGINAL PAGE IS
OF POOR QUALITY

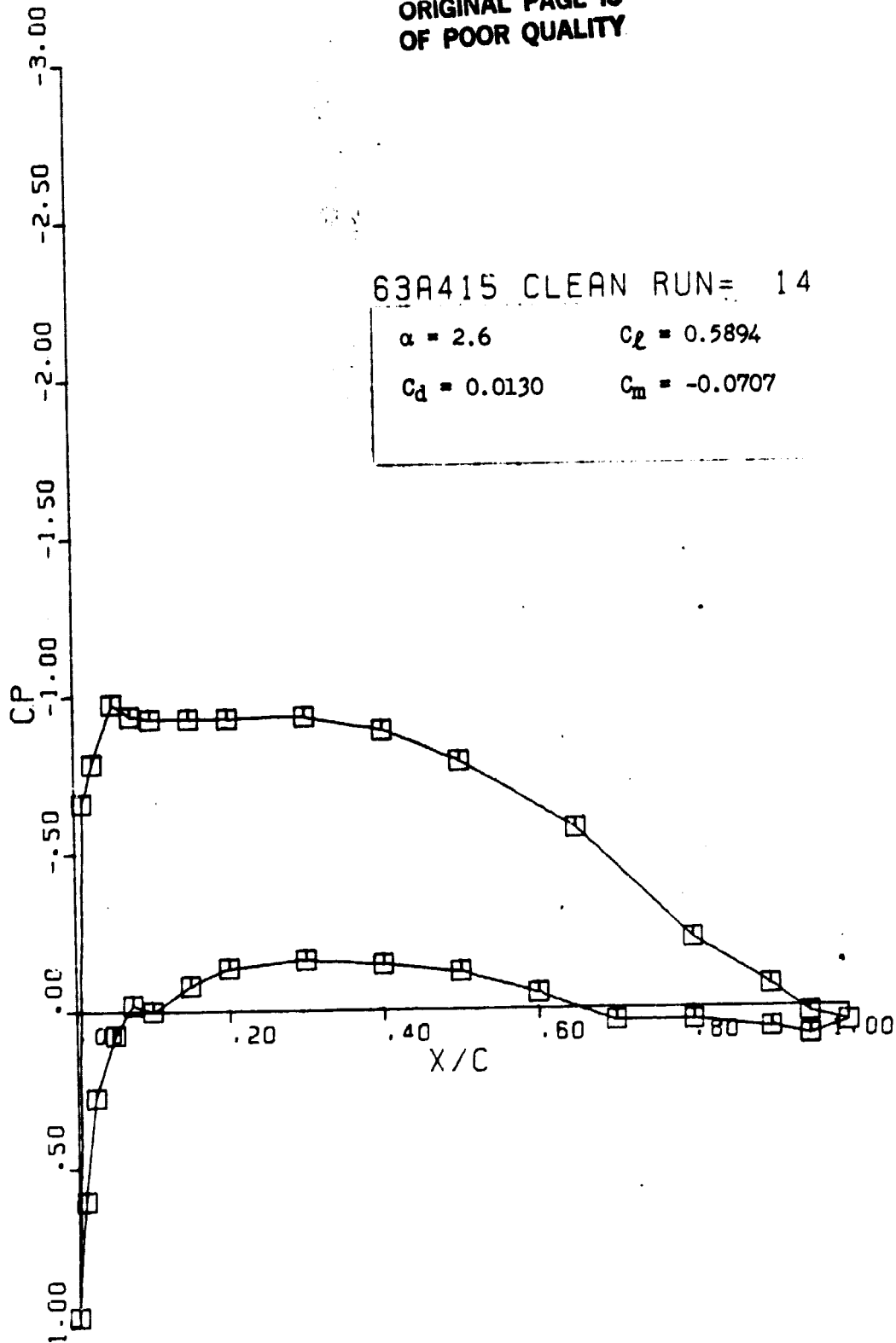
63A415 CLEAN RUN= 14

$$\alpha = 2.6$$

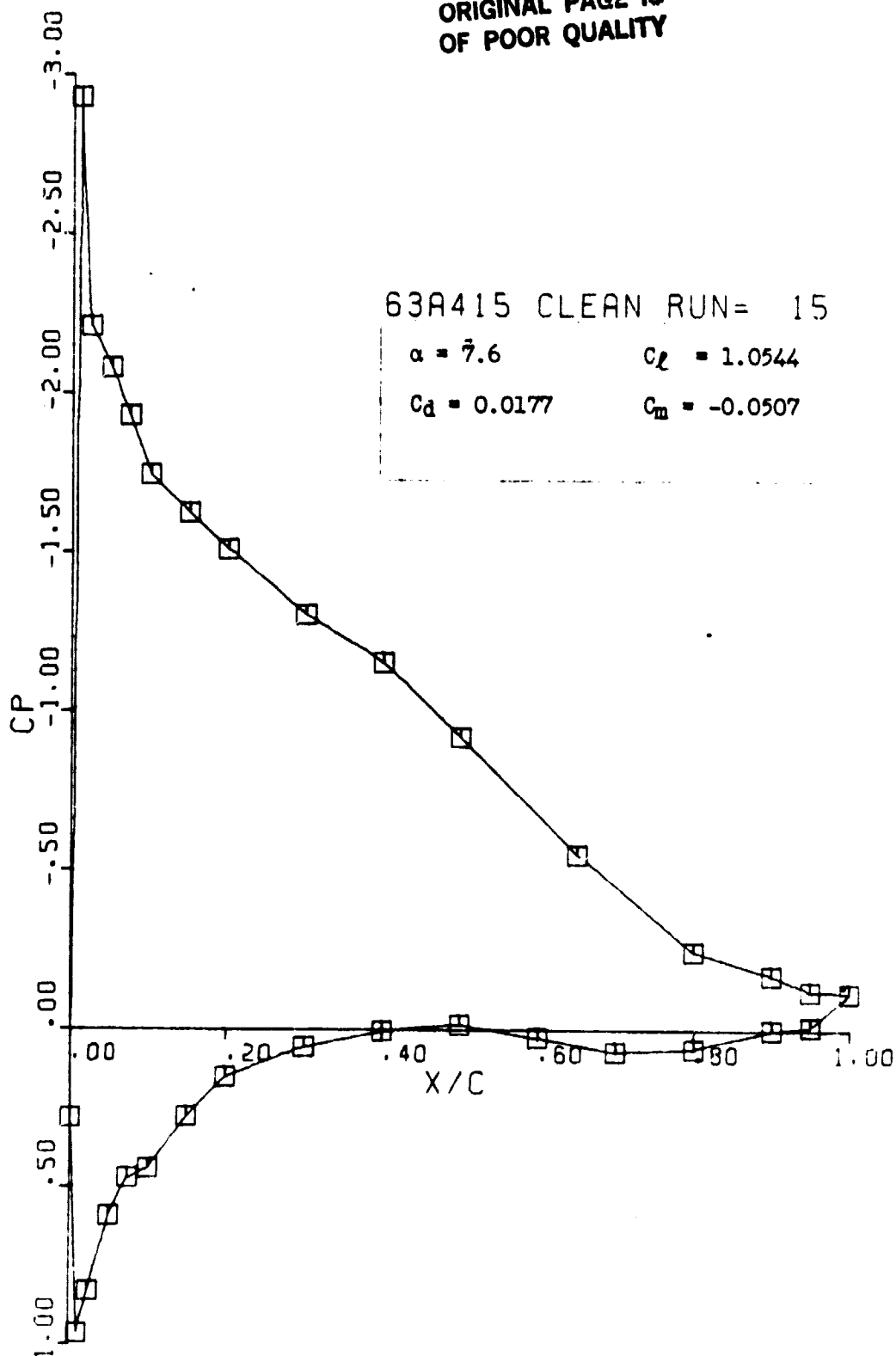
$$C_l = 0.5894$$

$$C_d = 0.0130$$

$$C_m = -0.0707$$



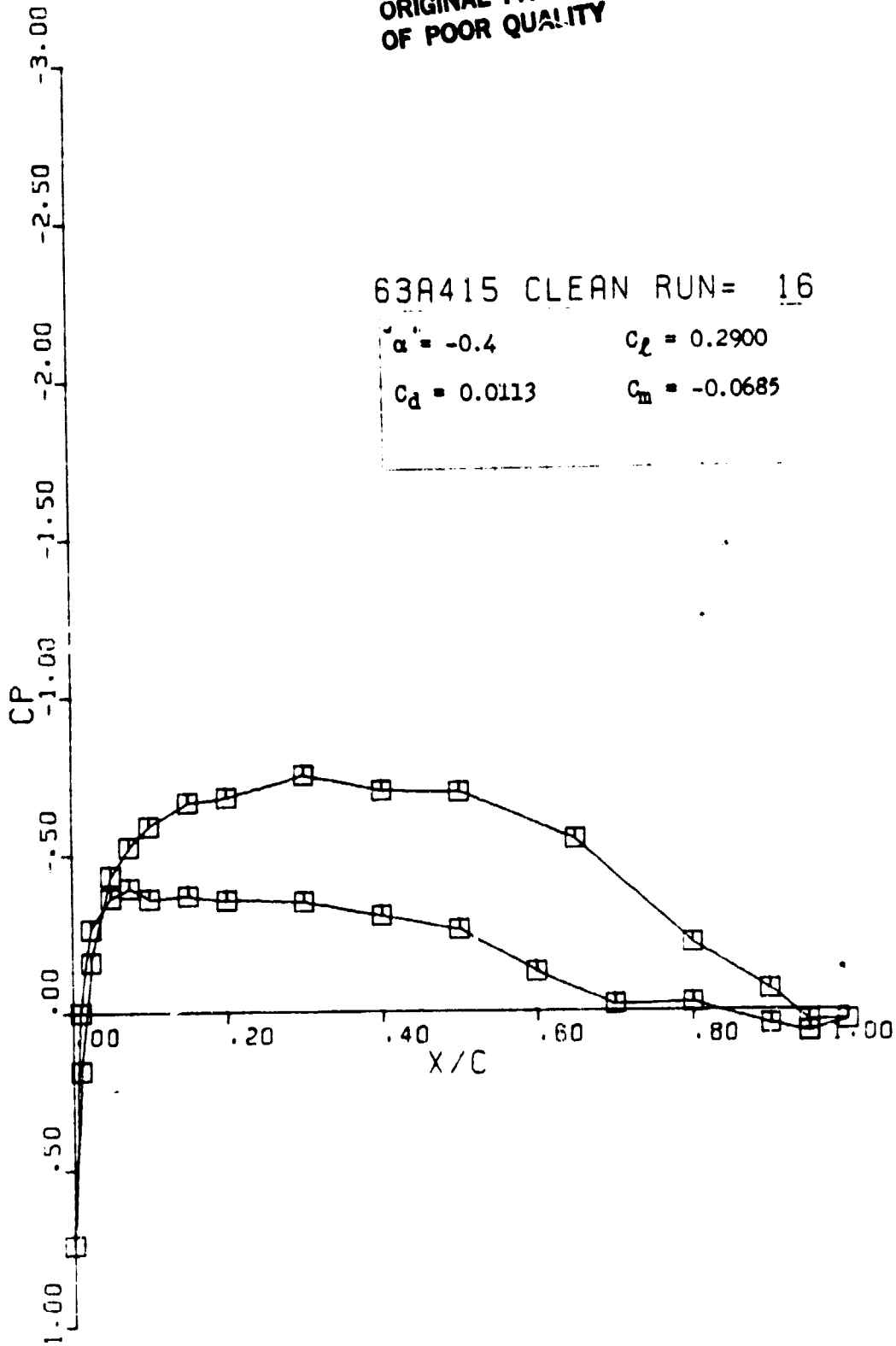
ORIGINAL PAGE IS
OF POOR QUALITY



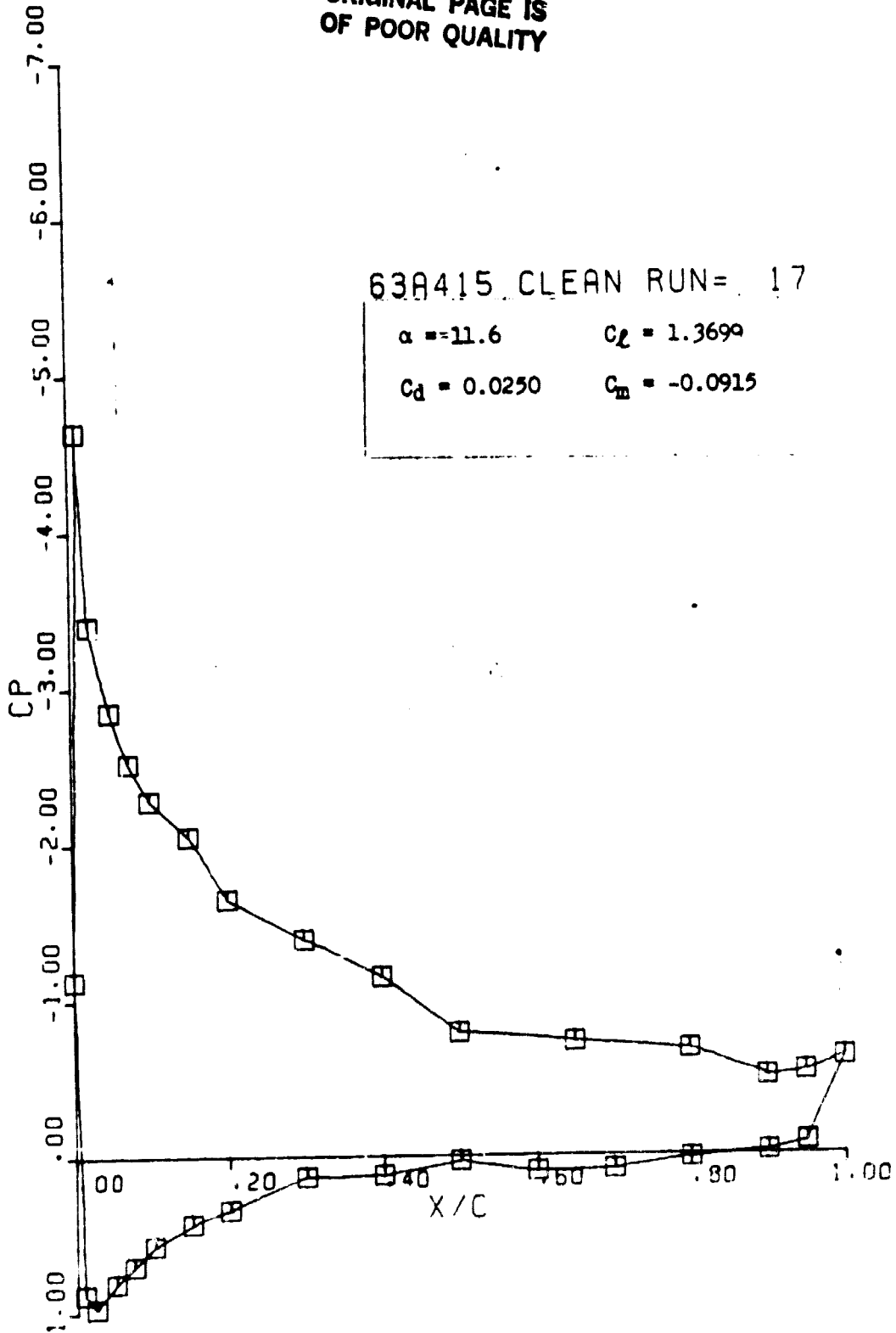
ORIGINAL PAGE IS
OF POOR QUALITY

63A415 CLEAN RUN= 16

$\alpha^* = -0.4$ $C_L = 0.2900$
 $C_d = 0.0113$ $C_m = -0.0685$



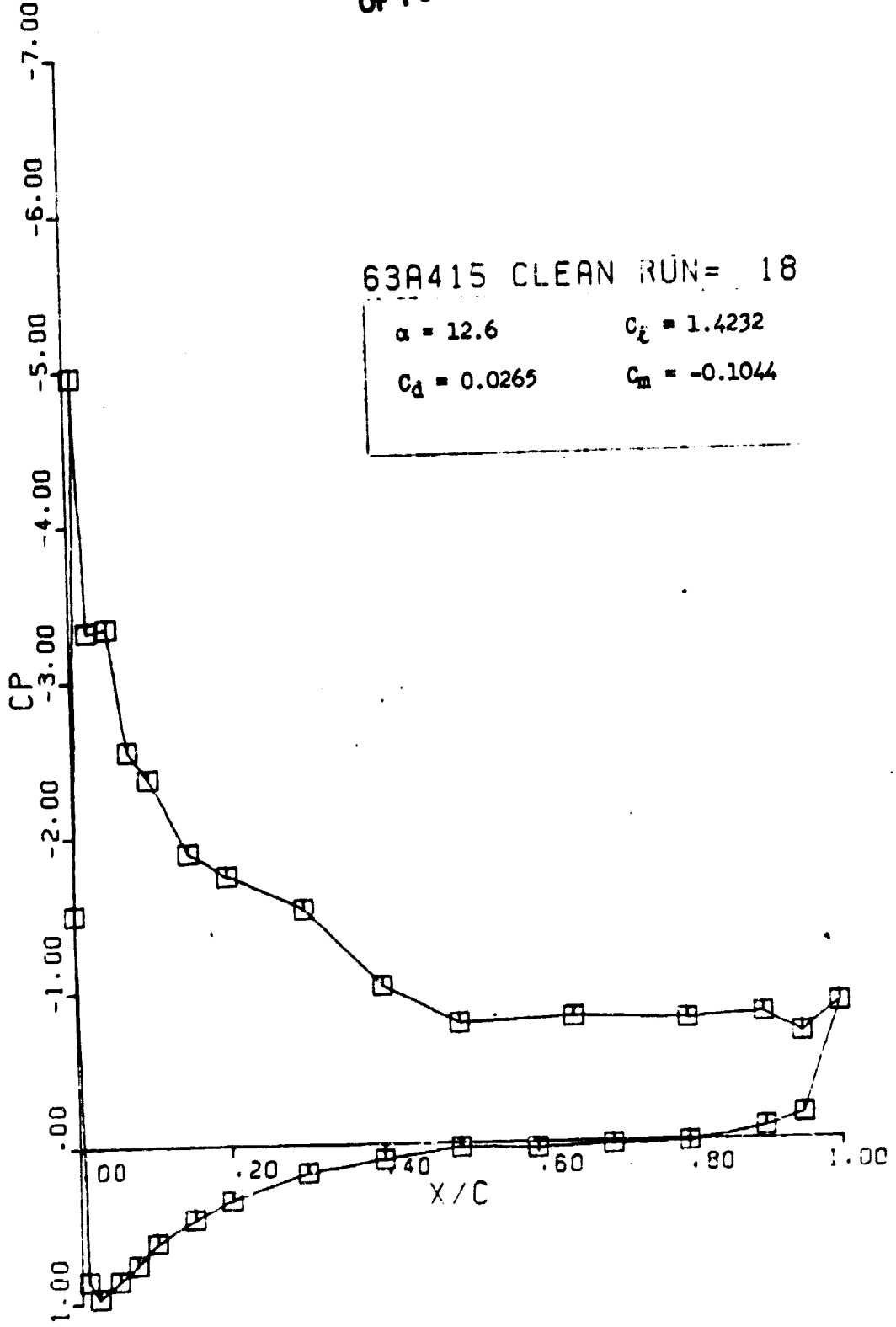
ORIGINAL PAGE IS
OF POOR QUALITY



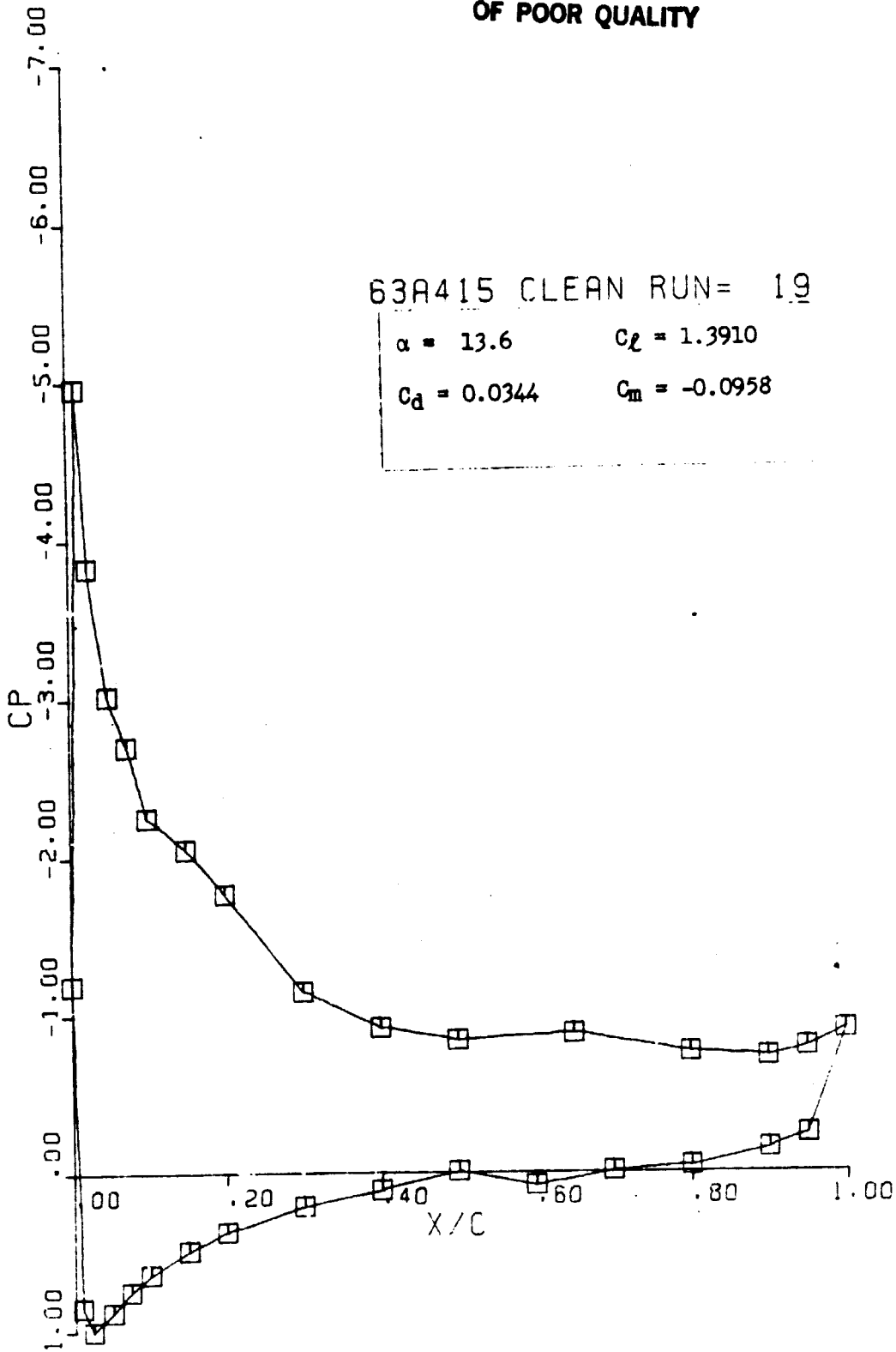
ORIGINAL PAGE IS
OF POOR QUALITY

63A415 CLEAN RUN= 18

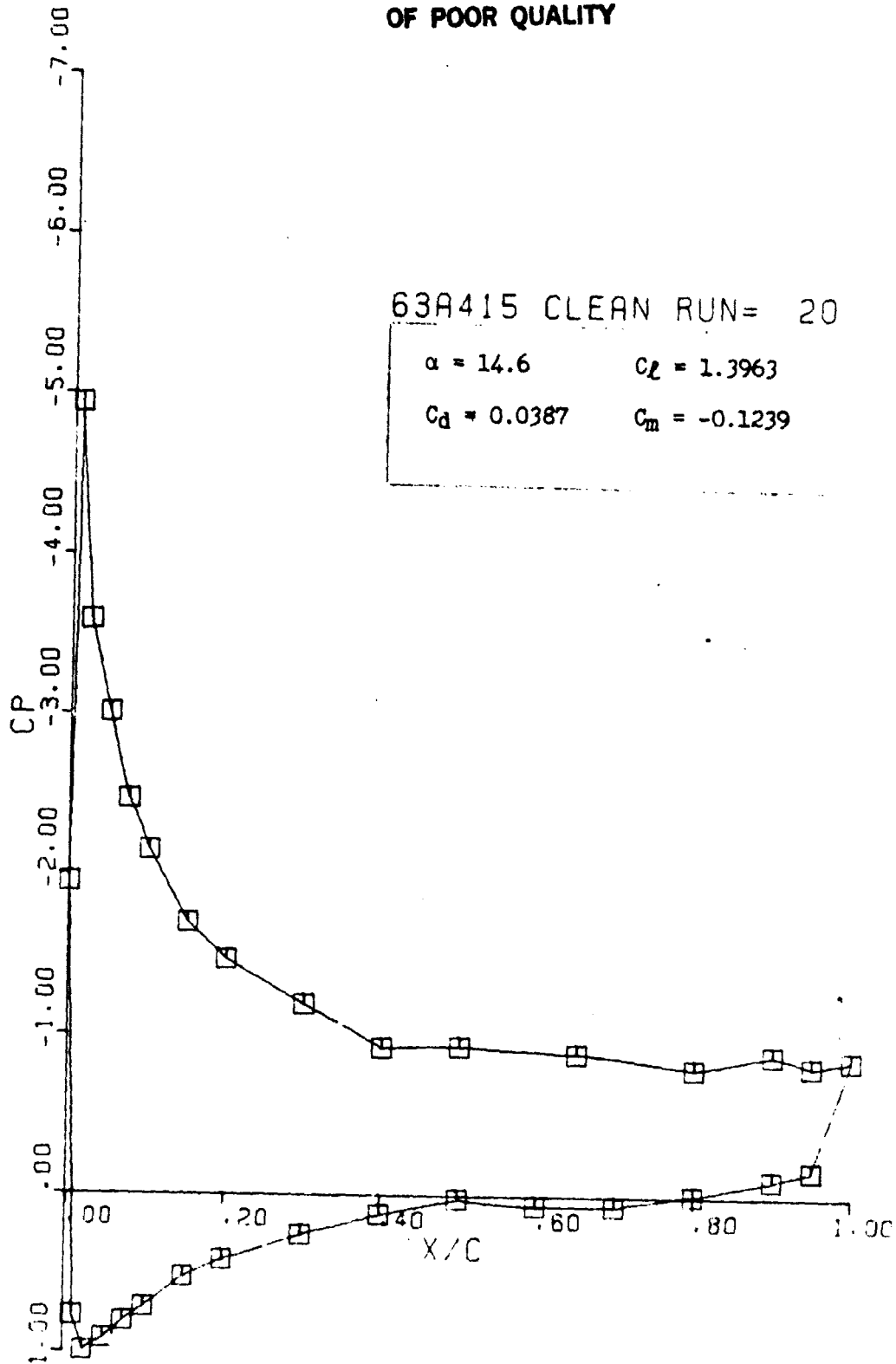
$\alpha = 12.6$	$C_L = 1.4232$
$C_d = 0.0265$	$C_m = -0.1044$



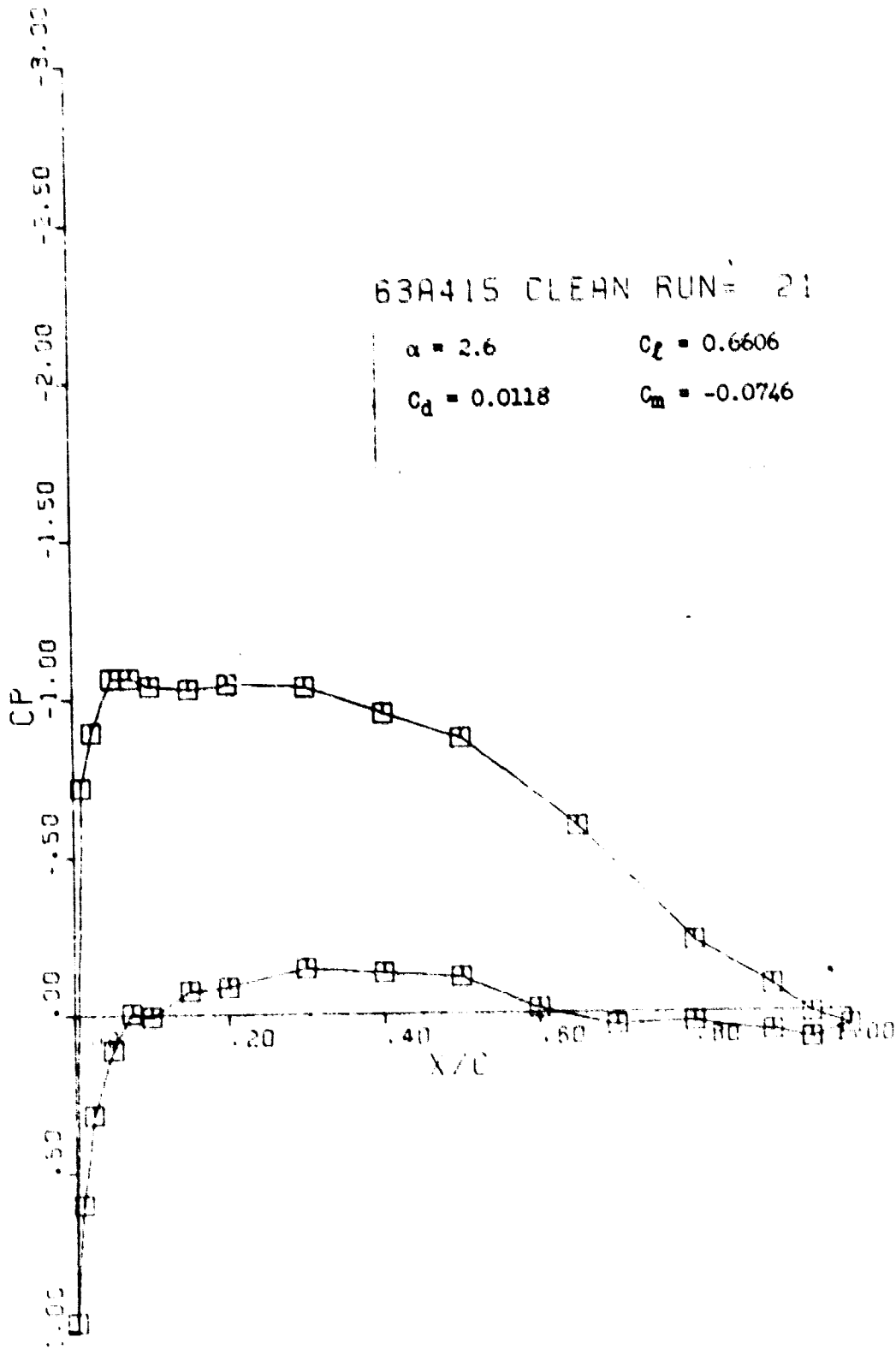
ORIGINAL PAGE IS
OF POOR QUALITY



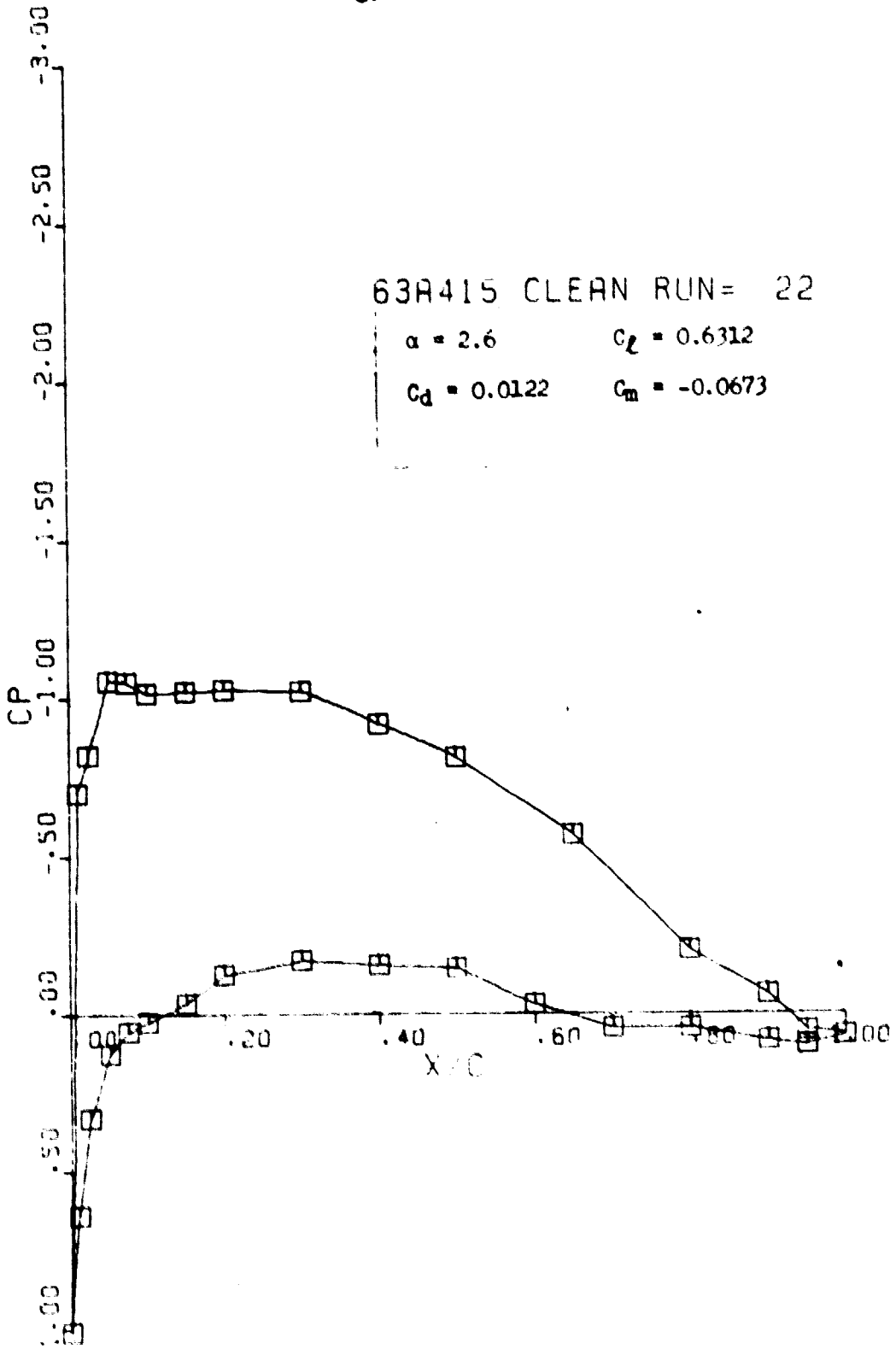
ORIGINAL PAGE IS
OF POOR QUALITY



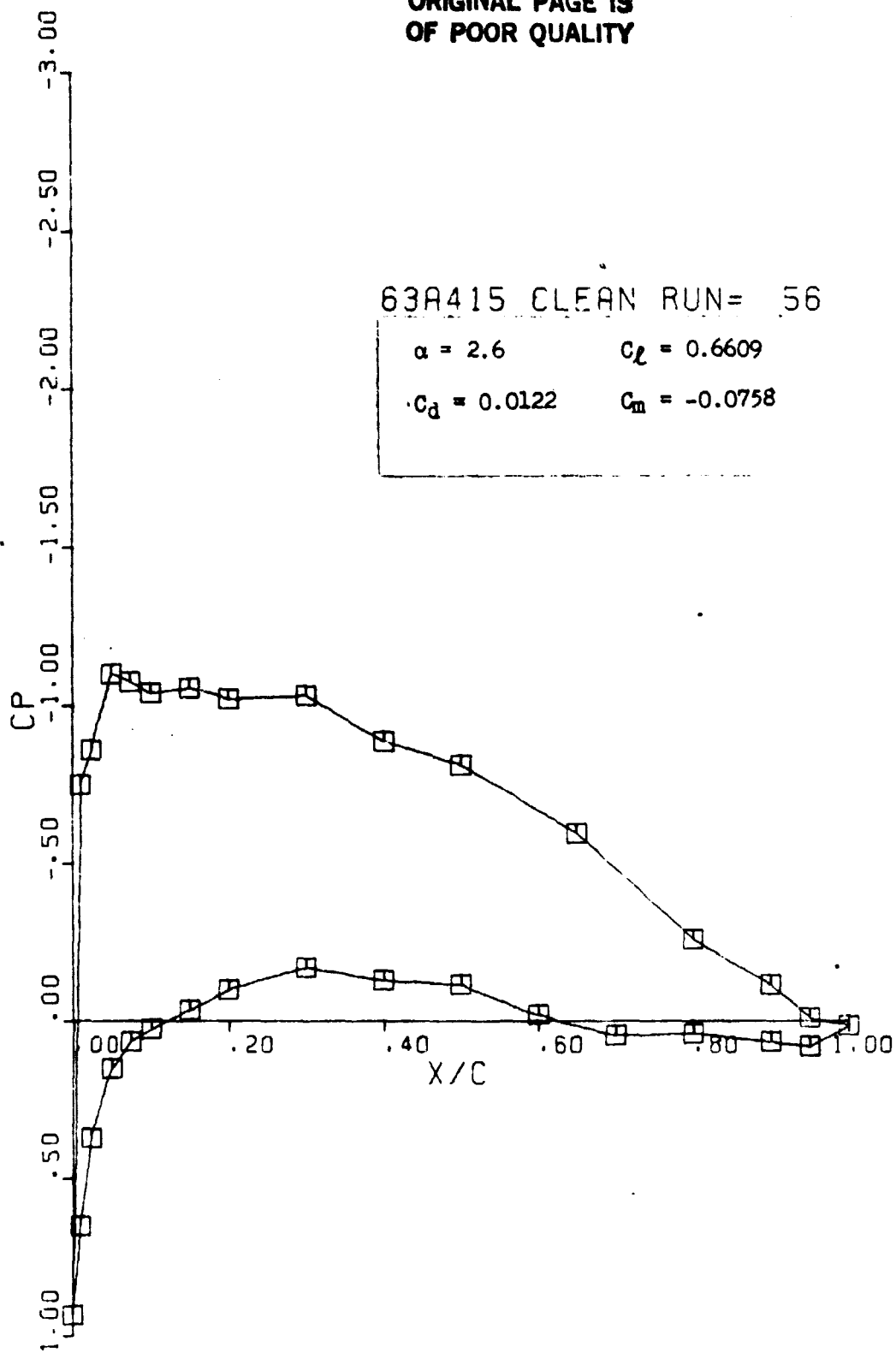
ORIGINAL PAGE IS
OF POOR QUALITY



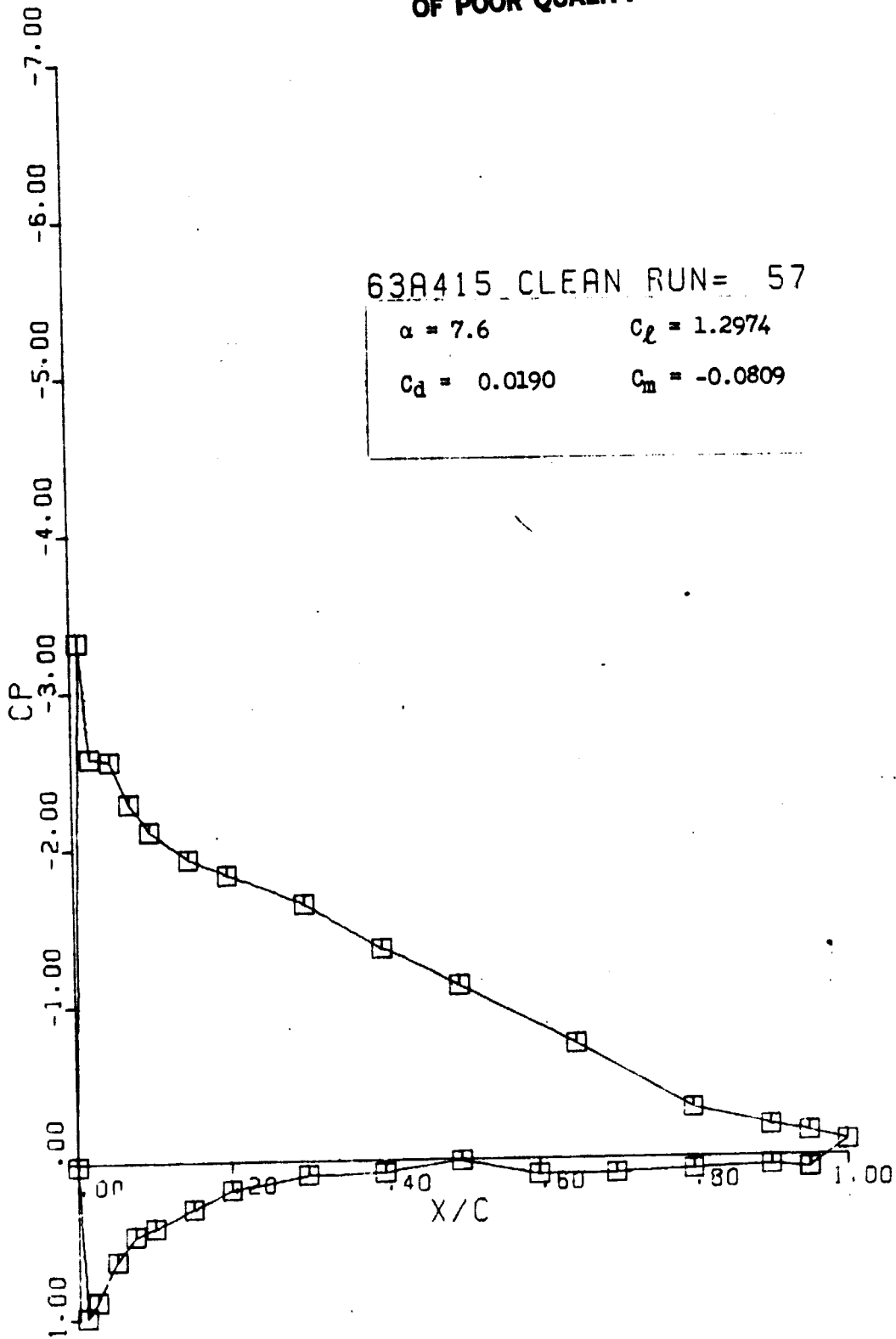
ORIGINAL PAGE IS
OF POOR QUALITY



ORIGINAL PAGE IS
OF POOR QUALITY



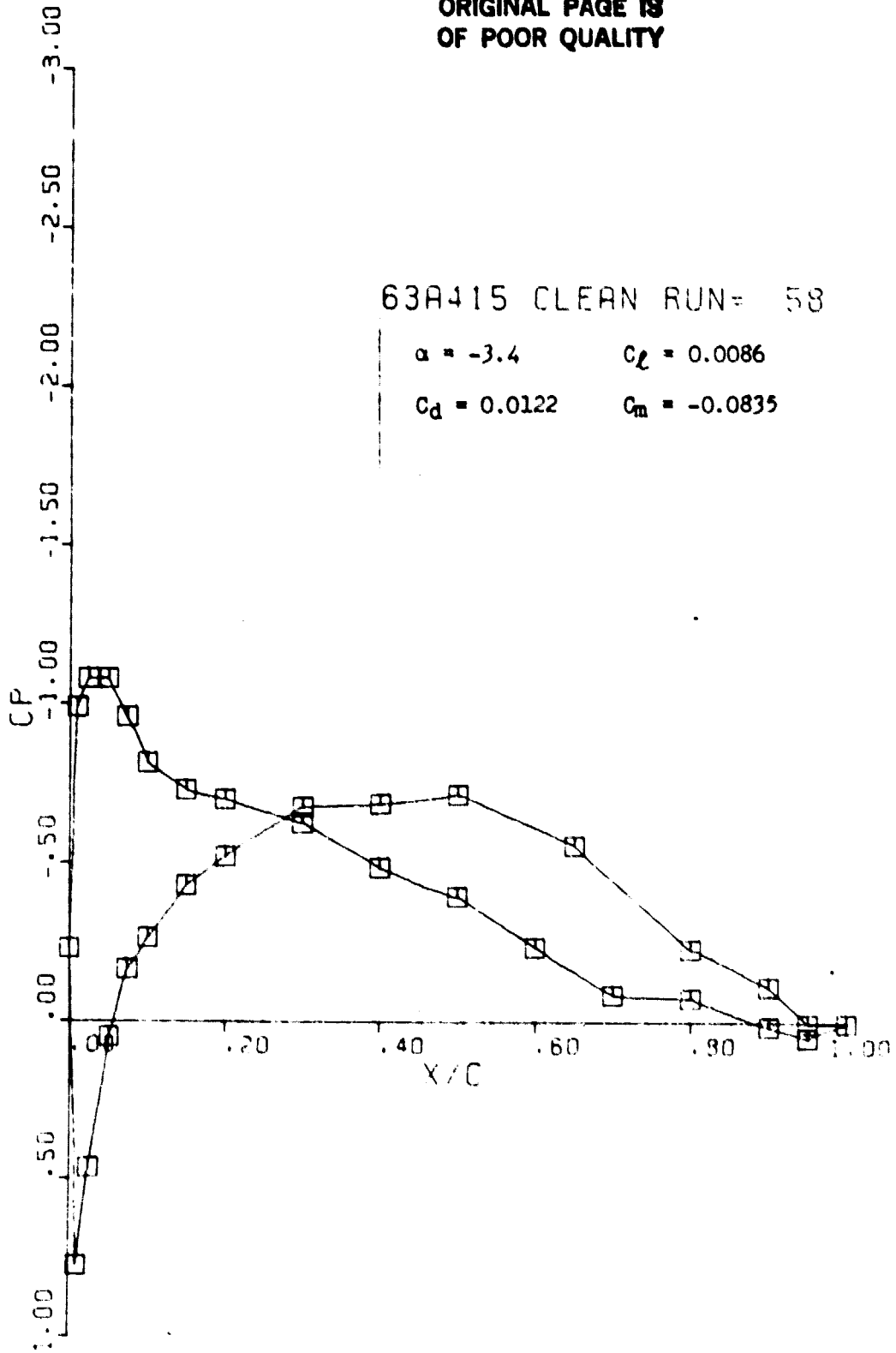
ORIGINAL PAGE IS
OF POOR QUALITY



ORIGINAL PAGE IS
OF POOR QUALITY

63A415 CLEAN RUN= 58

$\alpha = -3.4$ $C_l = 0.0086$
 $C_d = 0.0122$ $C_m = -0.0835$



ORIGINAL PAGE IS
OF POOR QUALITY

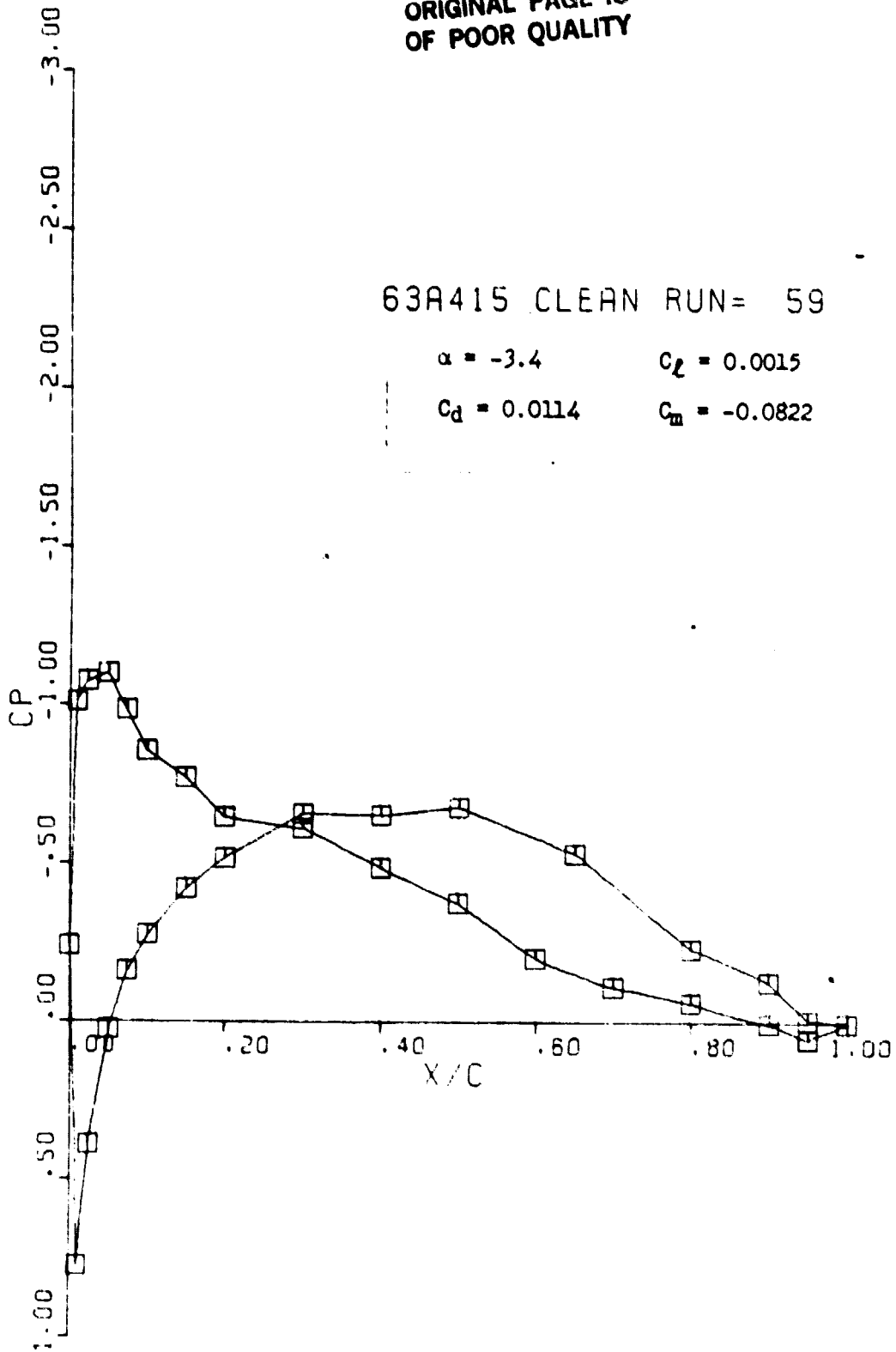
63A415 CLEAN RUN= 59

$\alpha = -3.4$

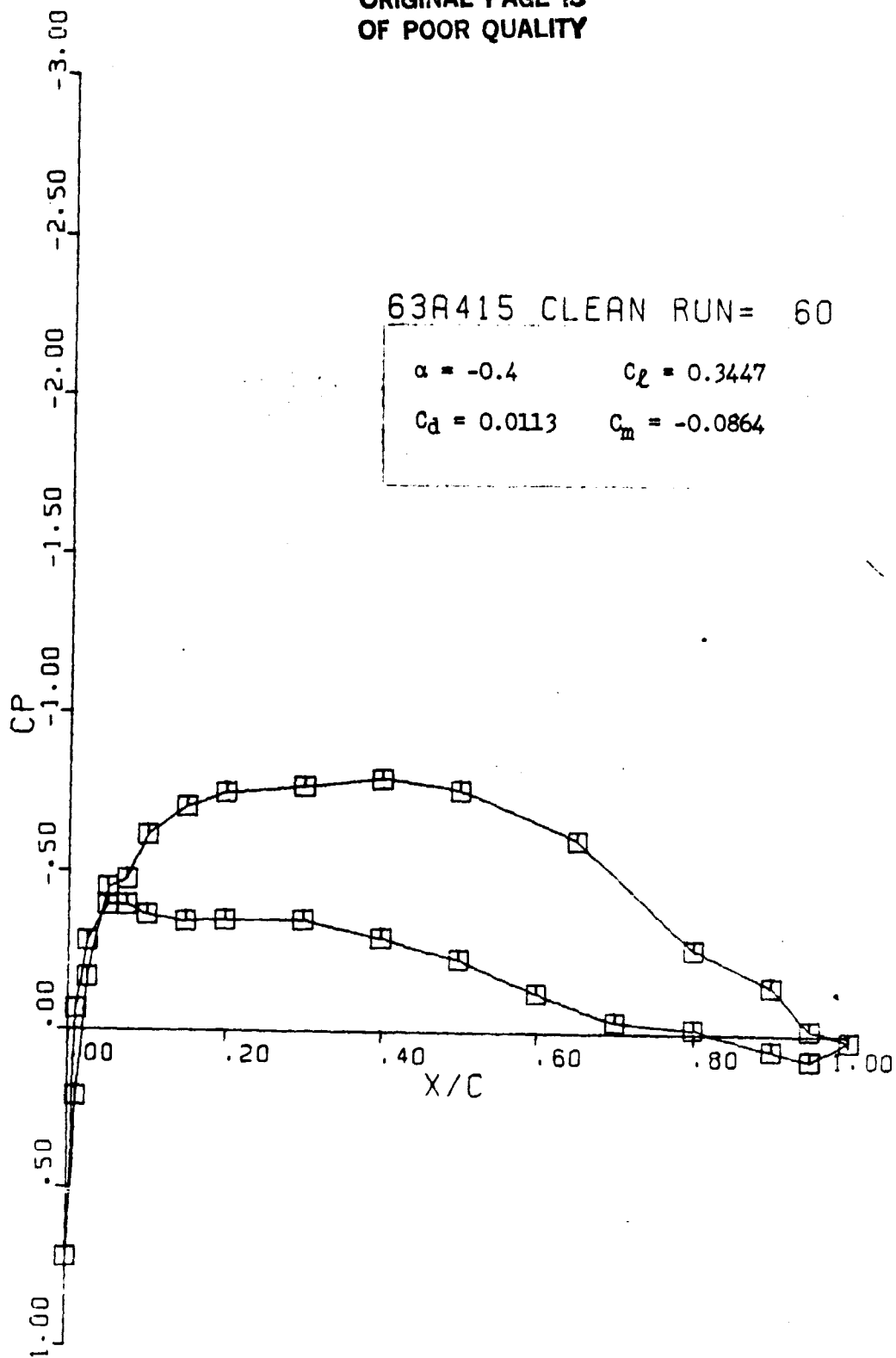
$C_L = 0.0015$

$C_d = 0.0114$

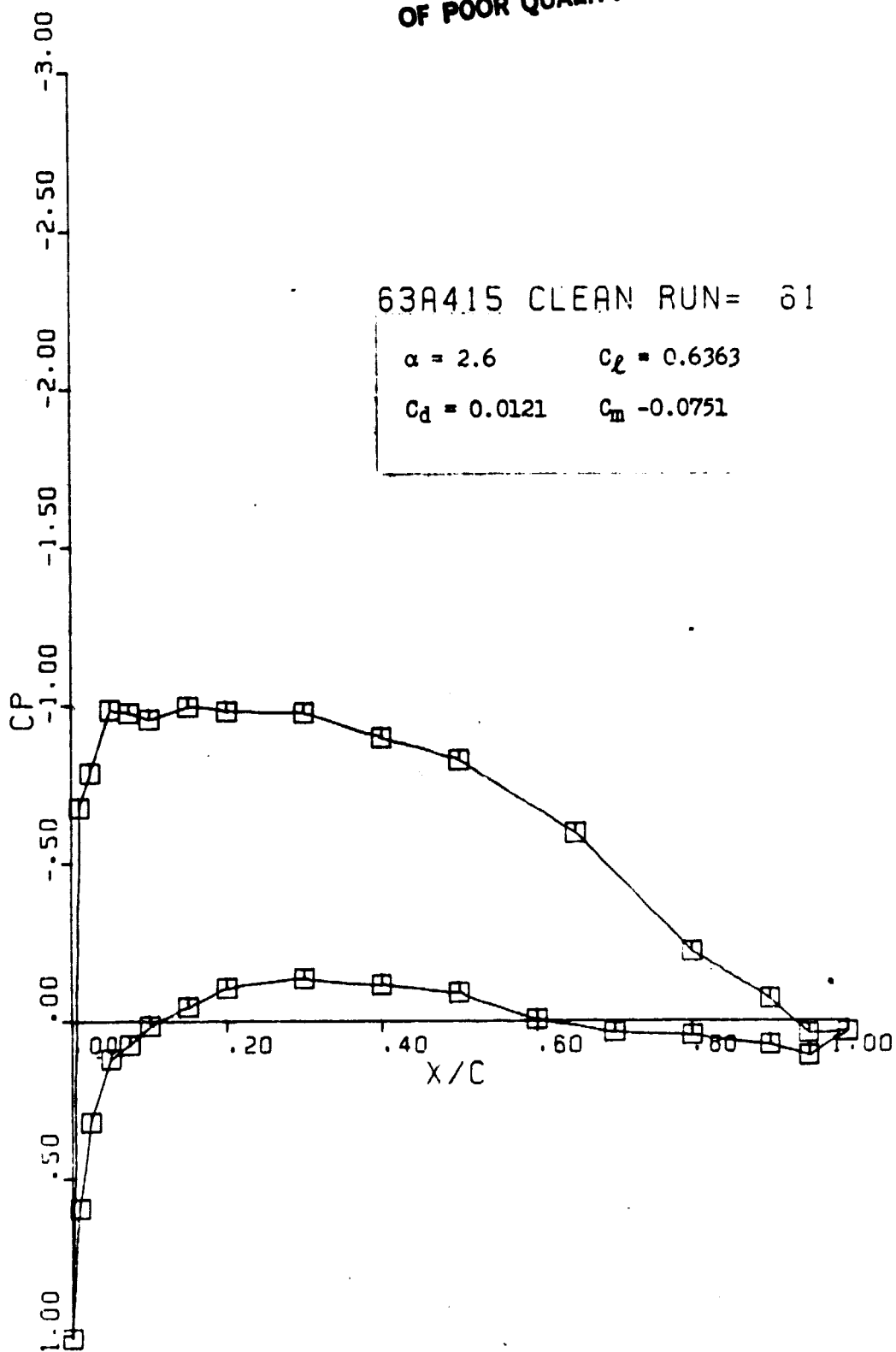
$C_m = -0.0822$



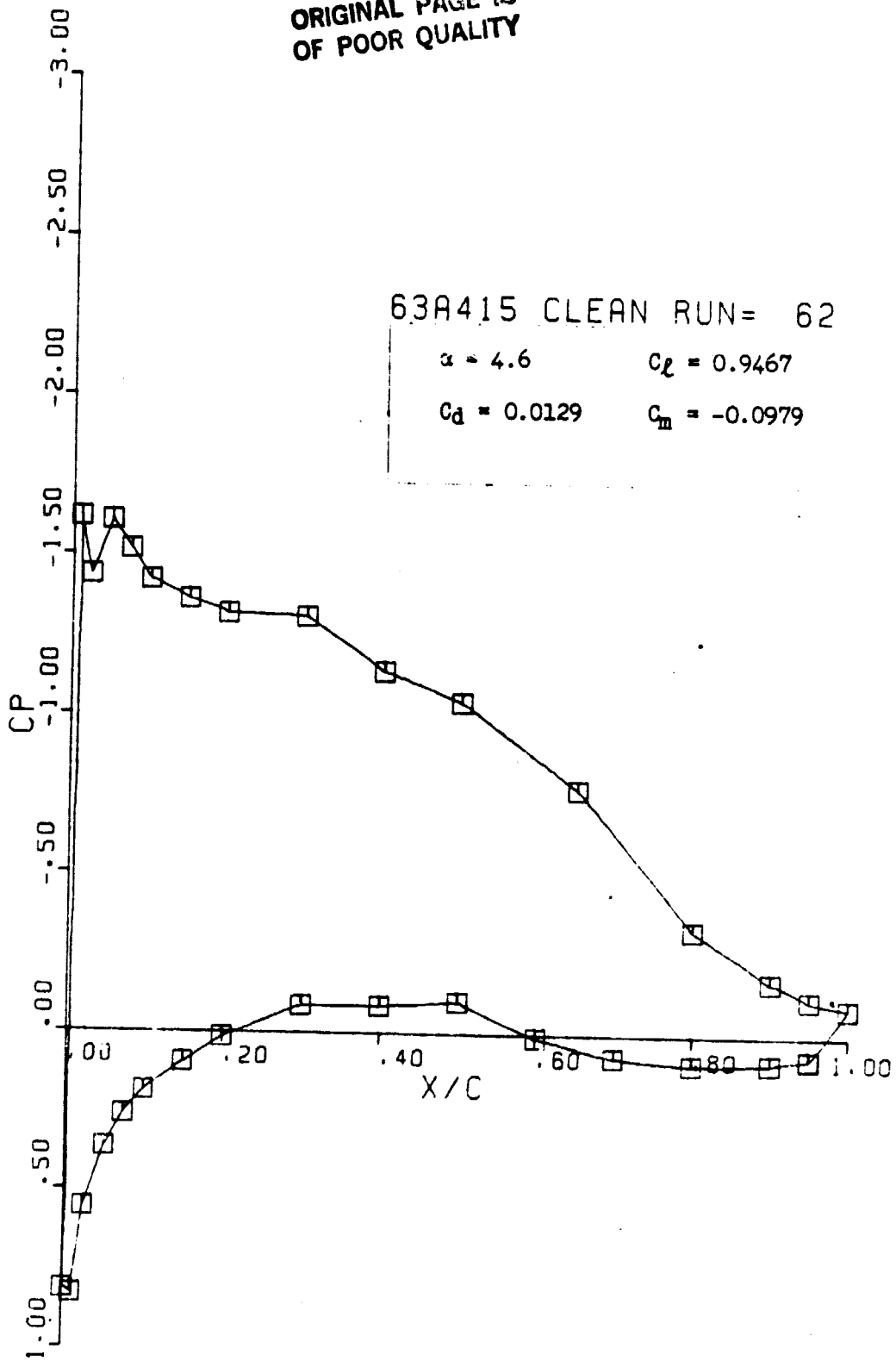
ORIGINAL PAGE IS
OF POOR QUALITY



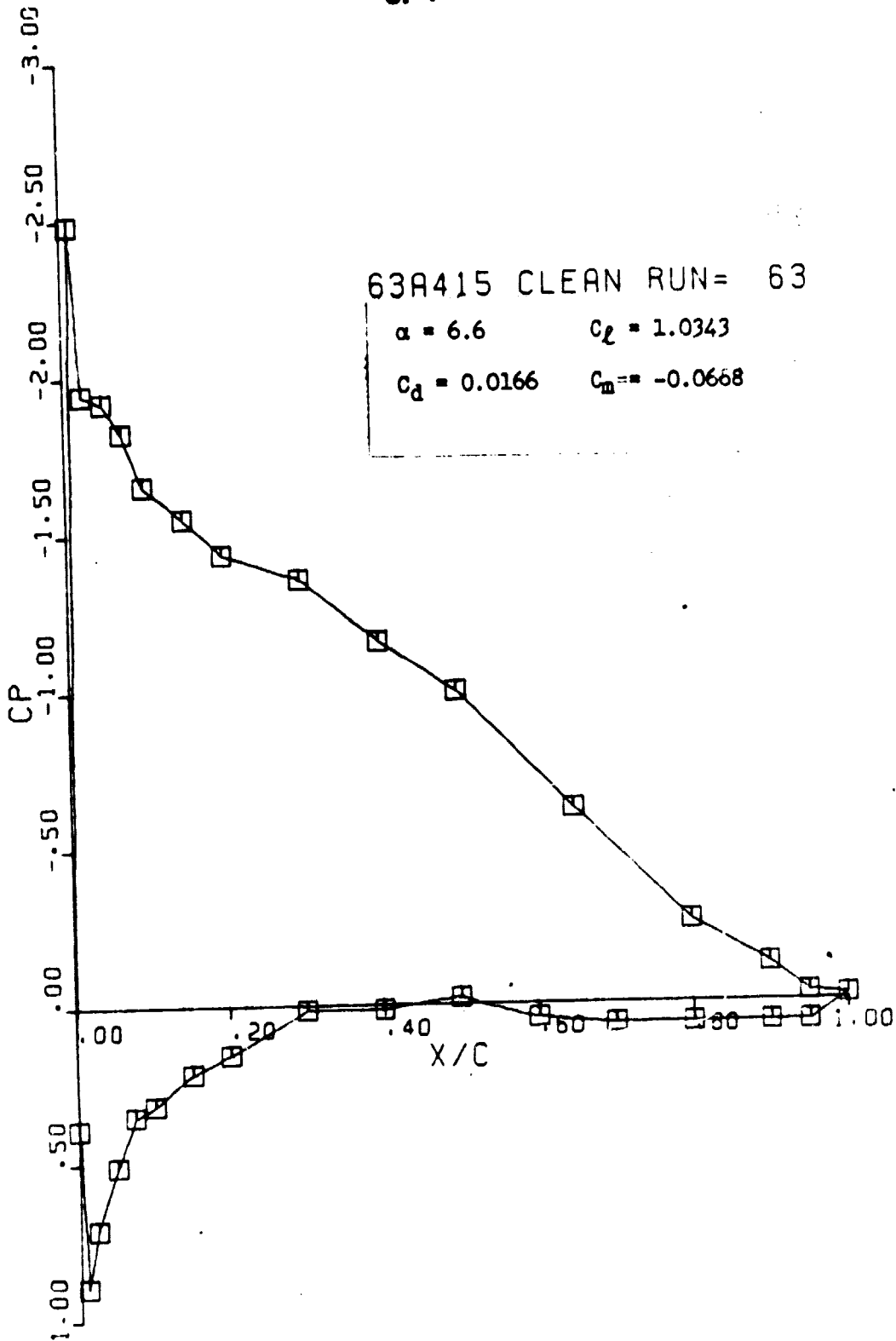
ORIGINAL PAGE IS
OF POOR QUALITY



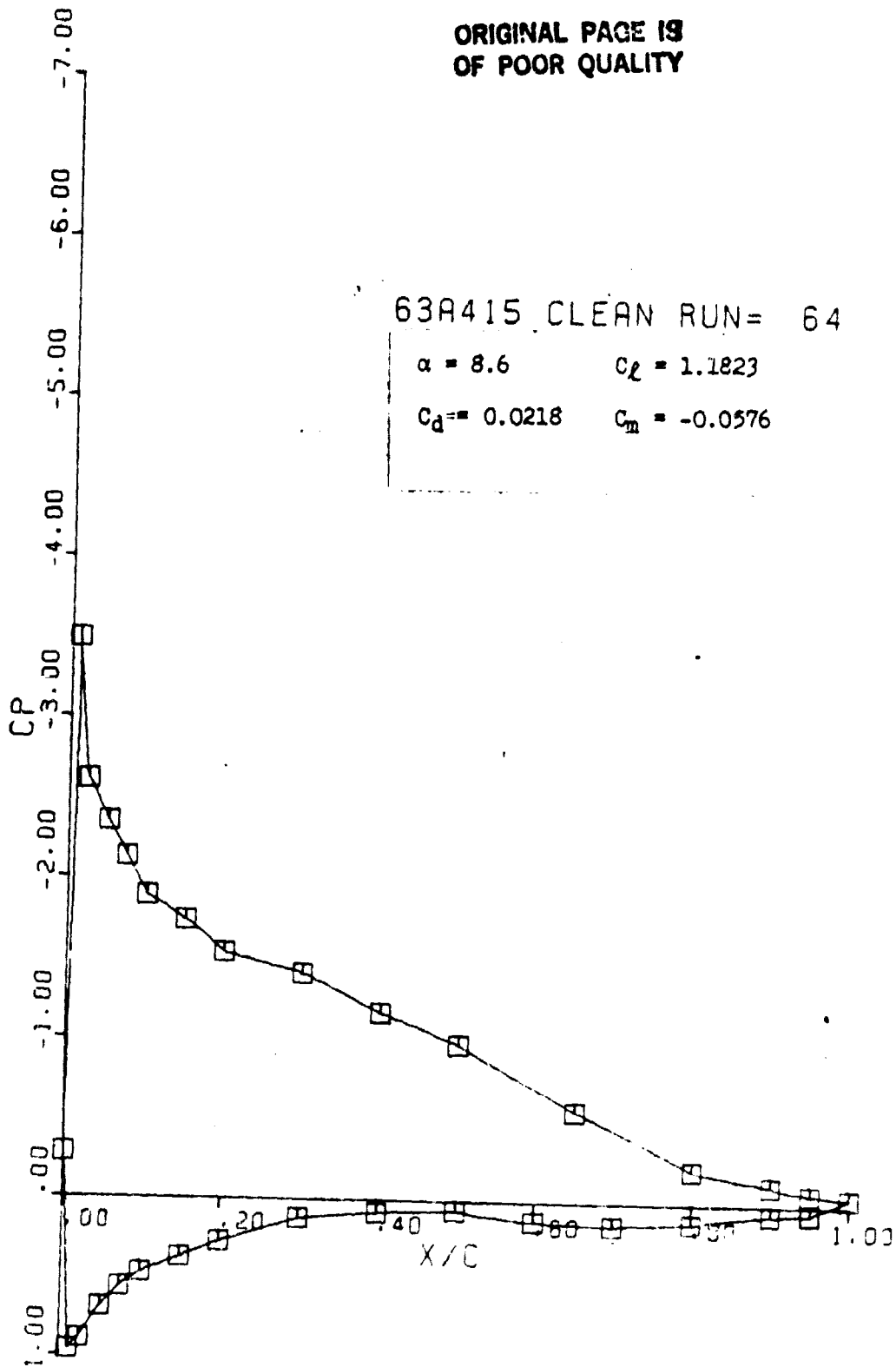
ORIGINAL PAGE 13
OF POOR QUALITY



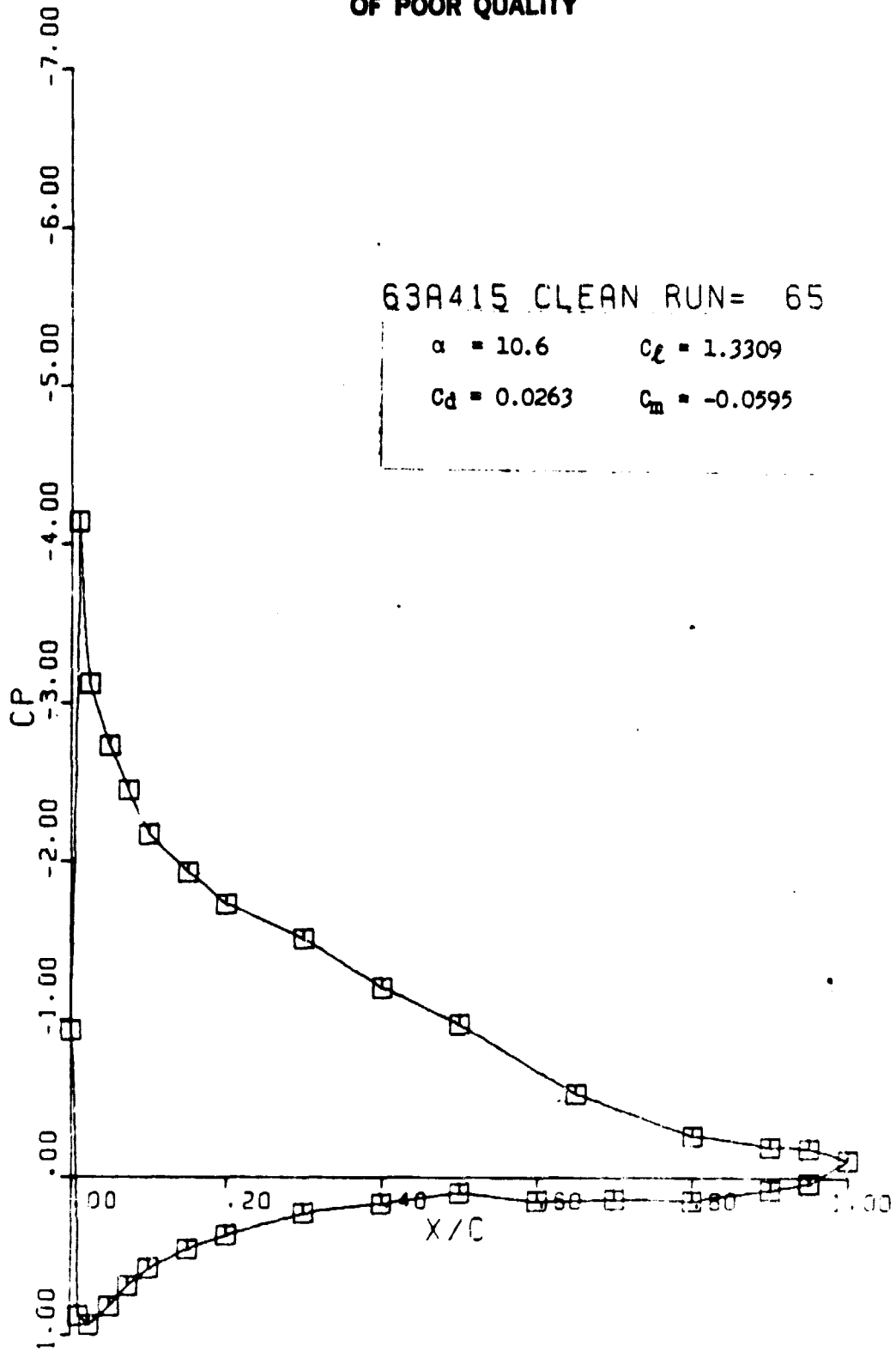
ORIGINAL PAGE IS
OF POOR QUALITY



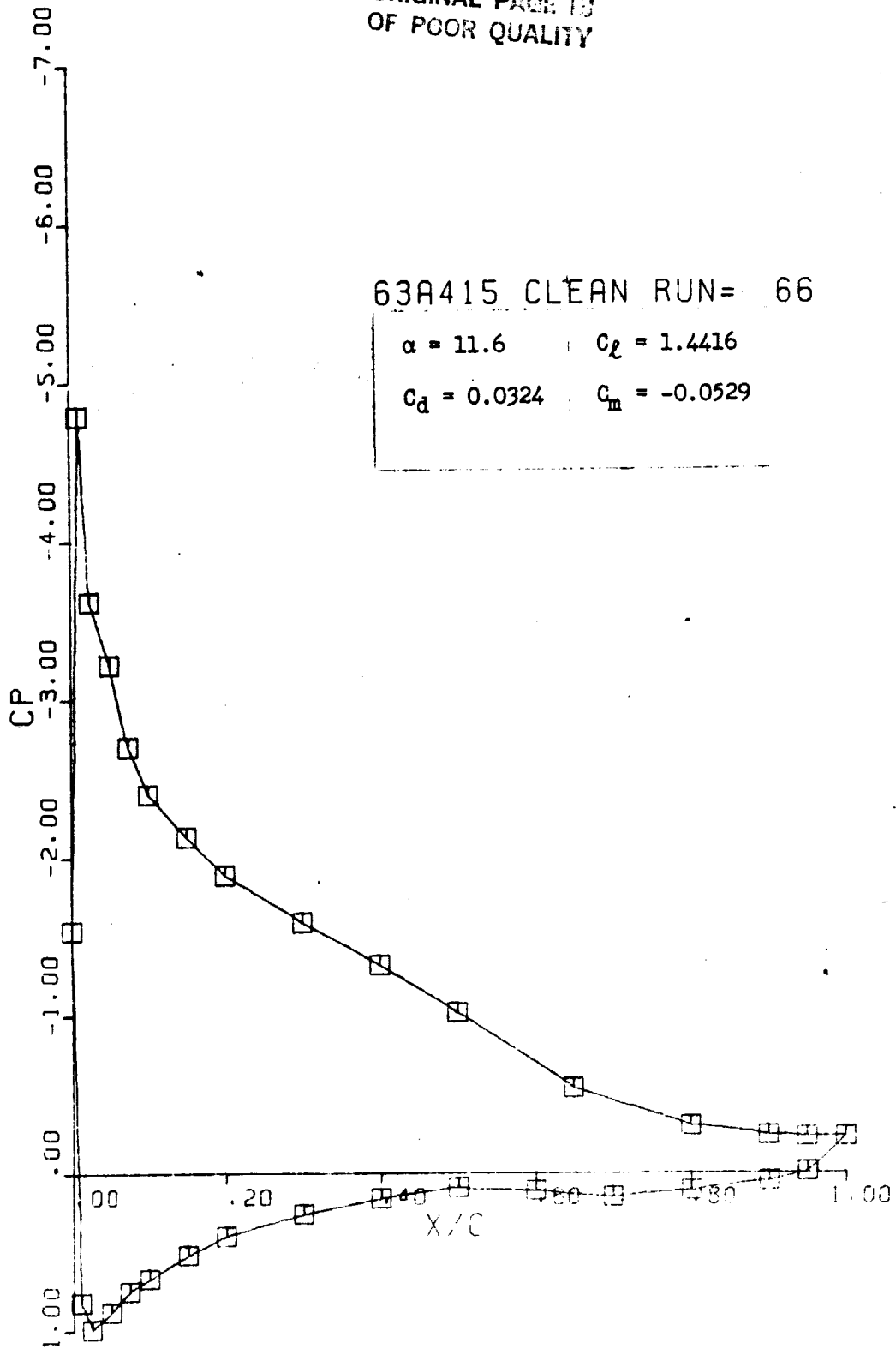
ORIGINAL PAGE IS
OF POOR QUALITY



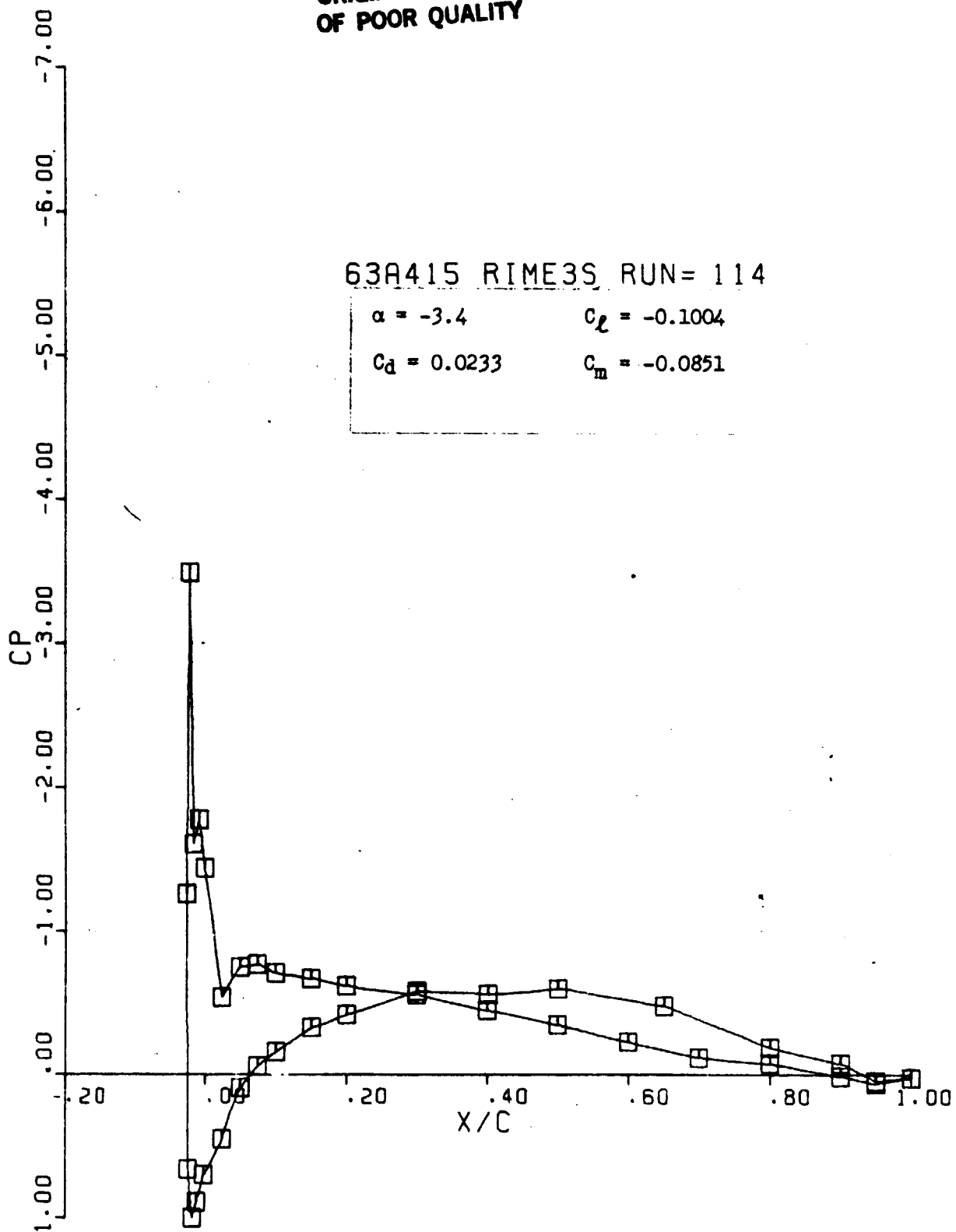
ORIGINAL PAGE IS
OF POOR QUALITY



ORIGINAL PAGE IS
OF POOR QUALITY



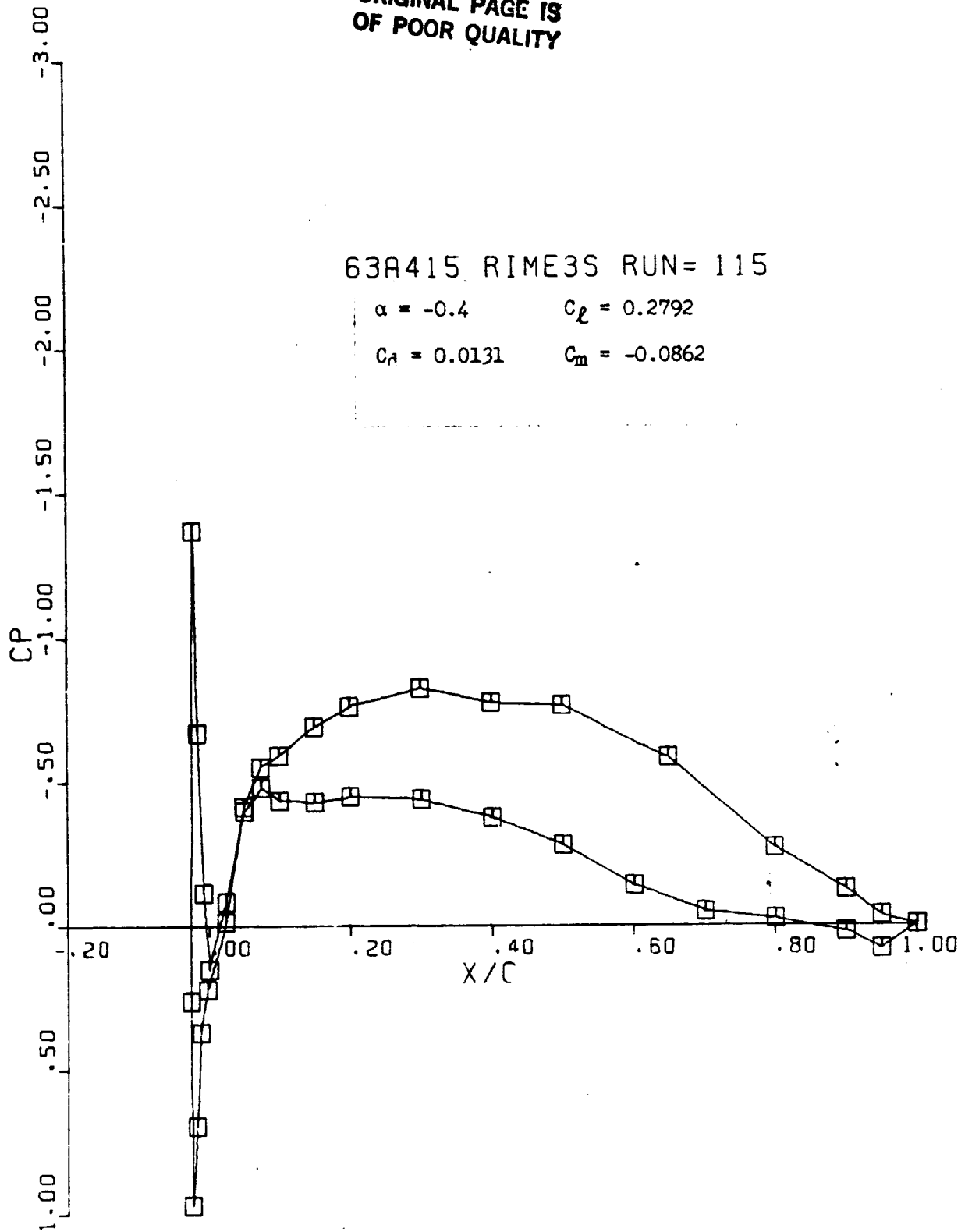
ORIGINAL PAGE IS
OF POOR QUALITY



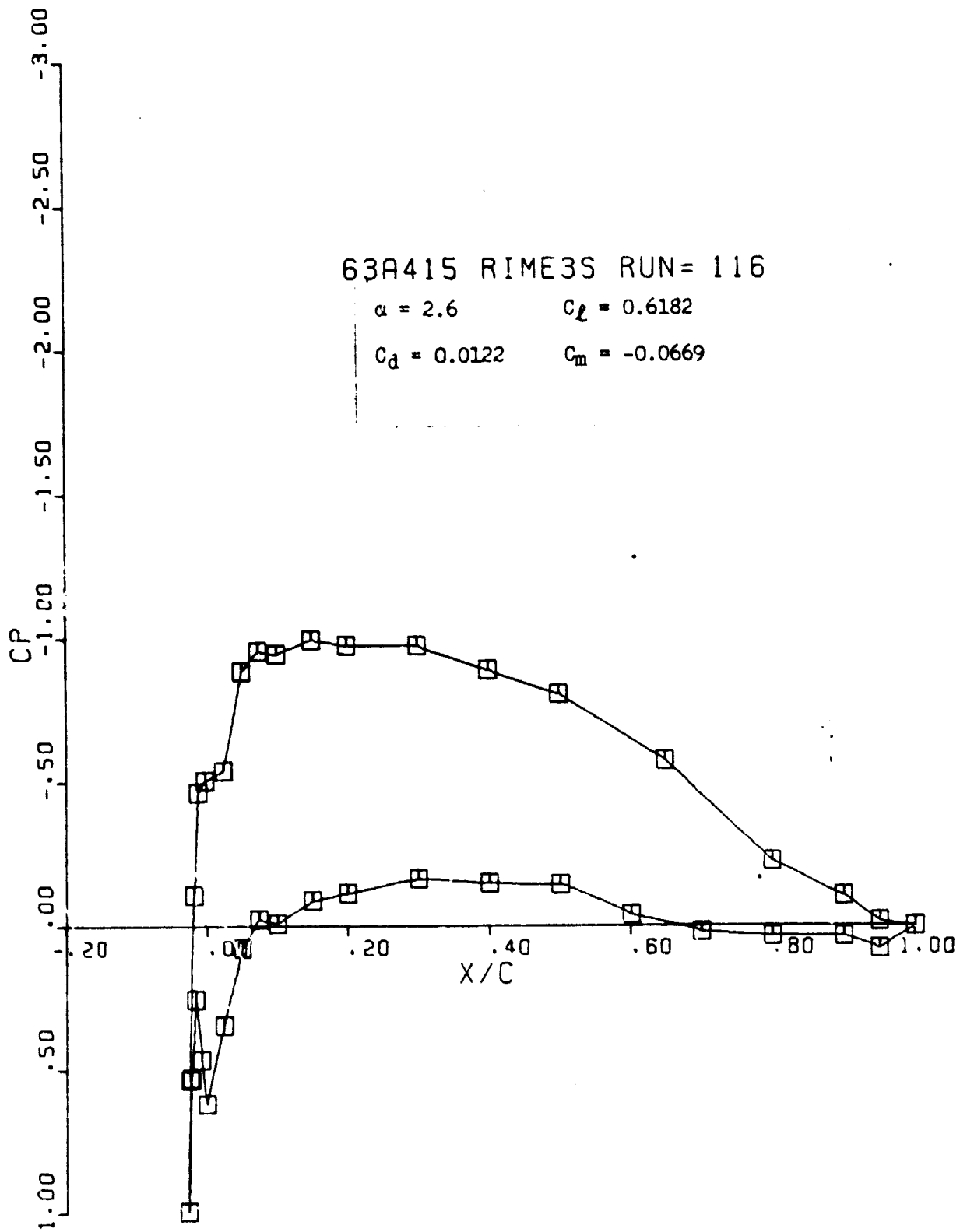
ORIGINAL PAGE IS
OF POOR QUALITY

63A415 RIME3S RUN= 115

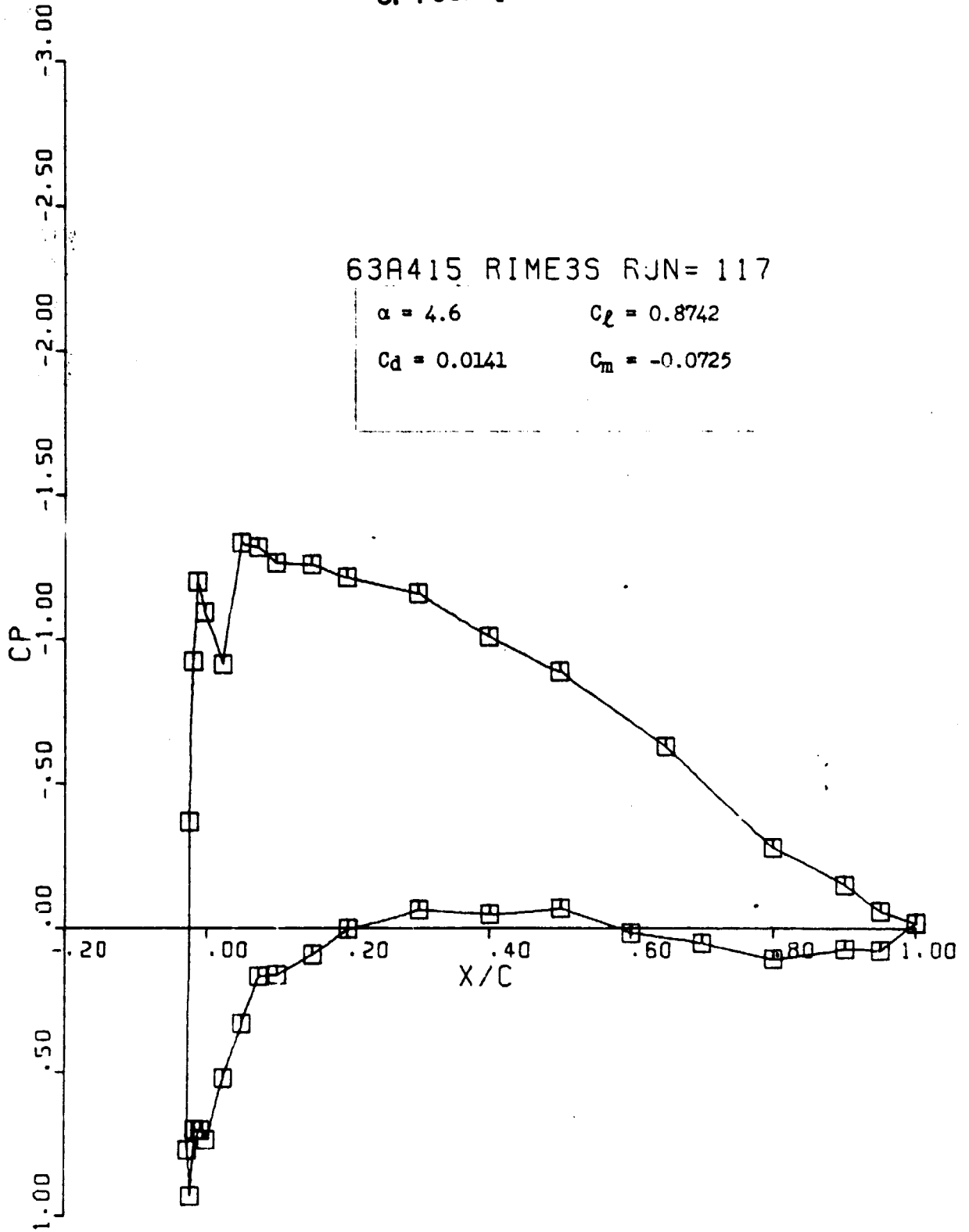
$\alpha = -0.4$ $C_l = 0.2792$
 $C_d = 0.0131$ $C_m = -0.0862$



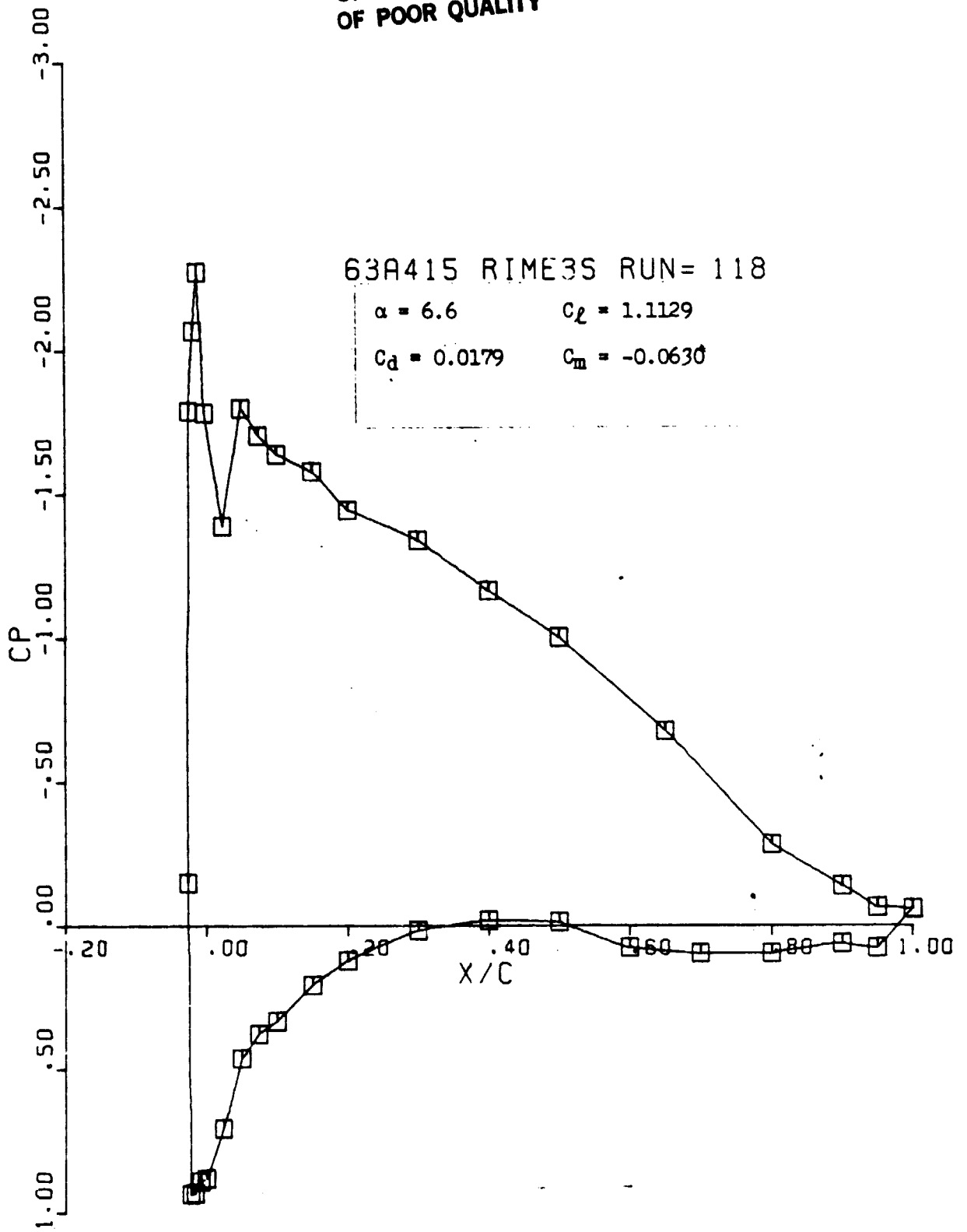
ORIGINAL PAGE IS
OF POOR QUALITY



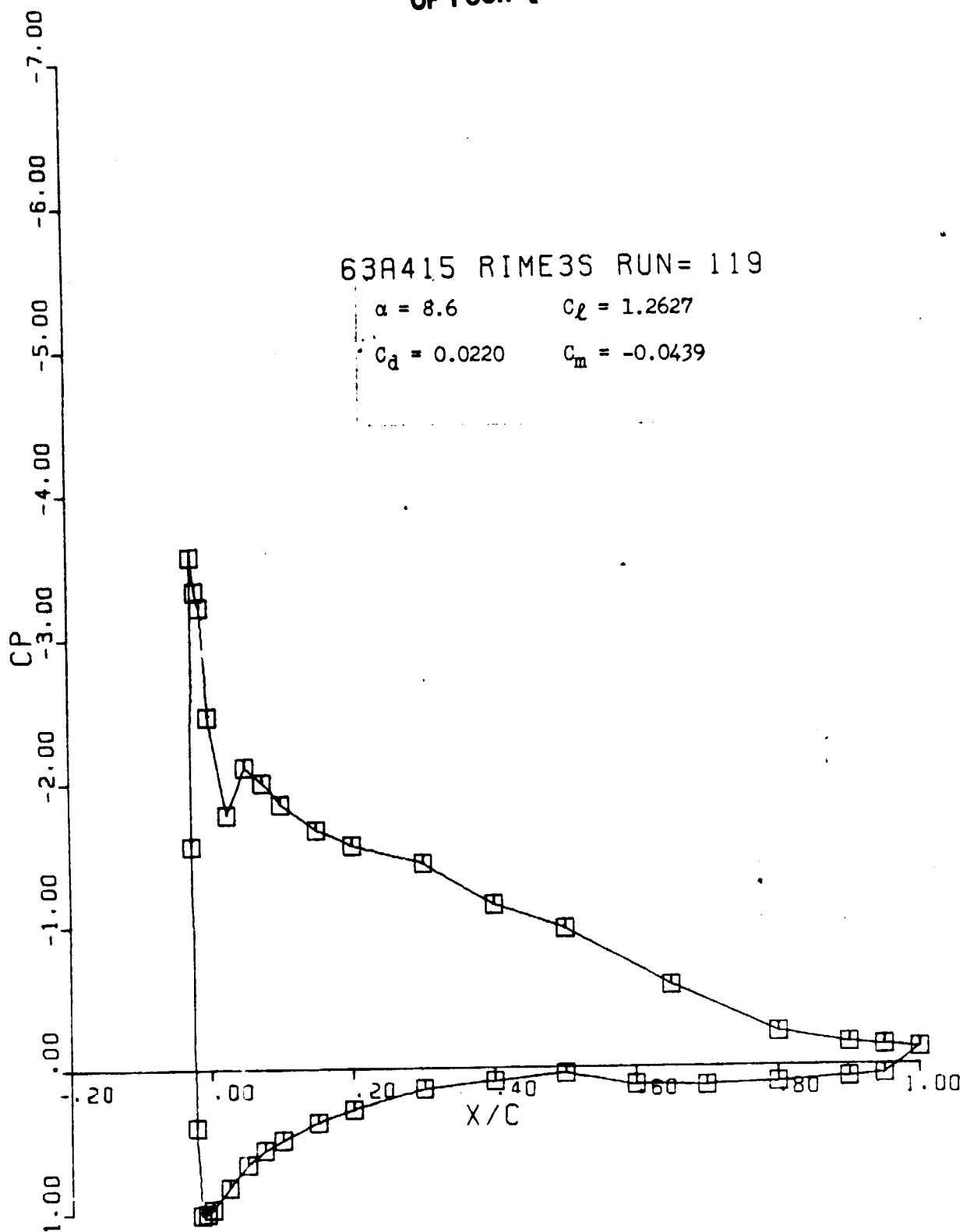
ORIGINAL PAGE IS
OF POOR QUALITY



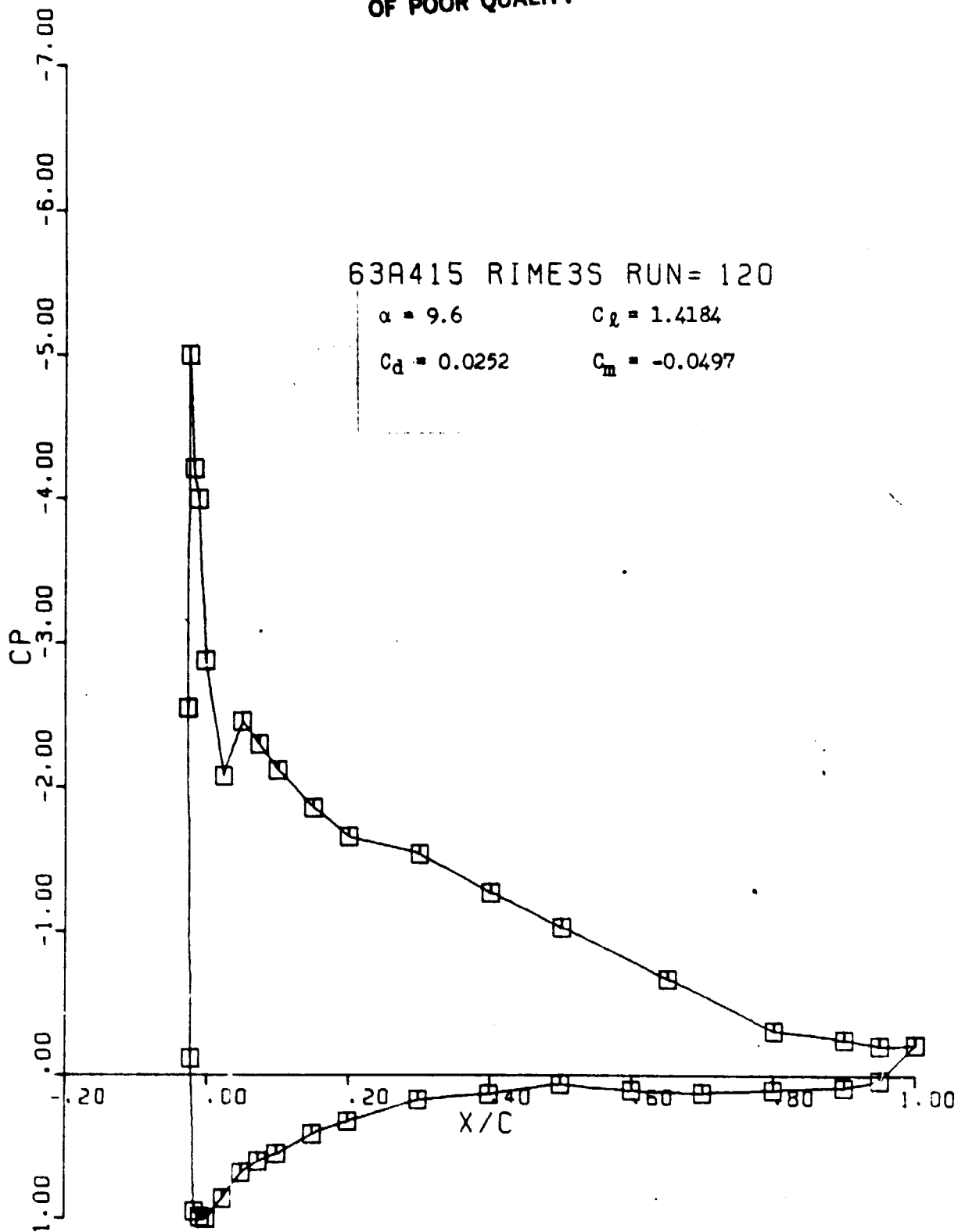
ORIGINAL PAGE IS
OF POOR QUALITY



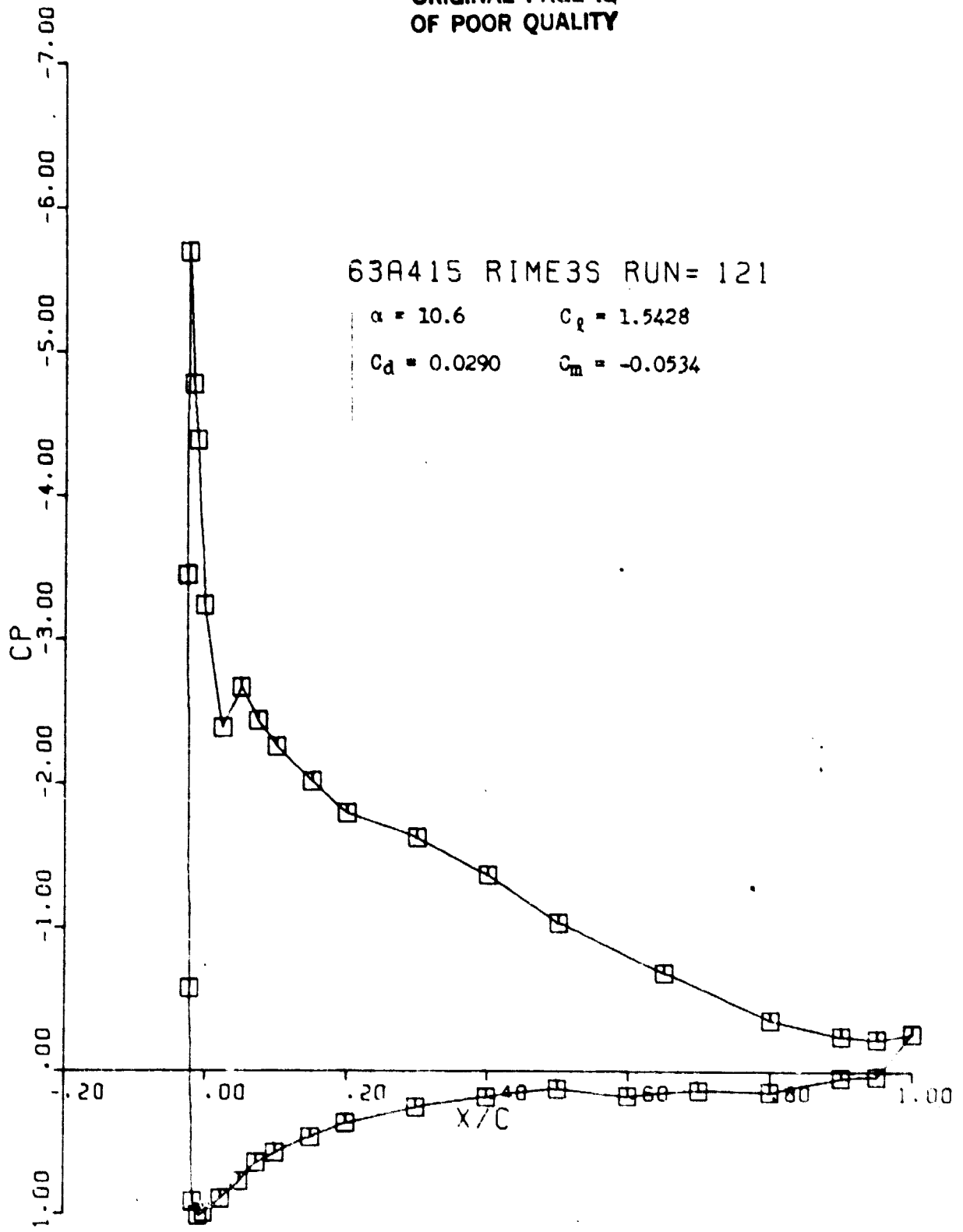
ORIGINAL PAGE IS
OF POOR QUALITY



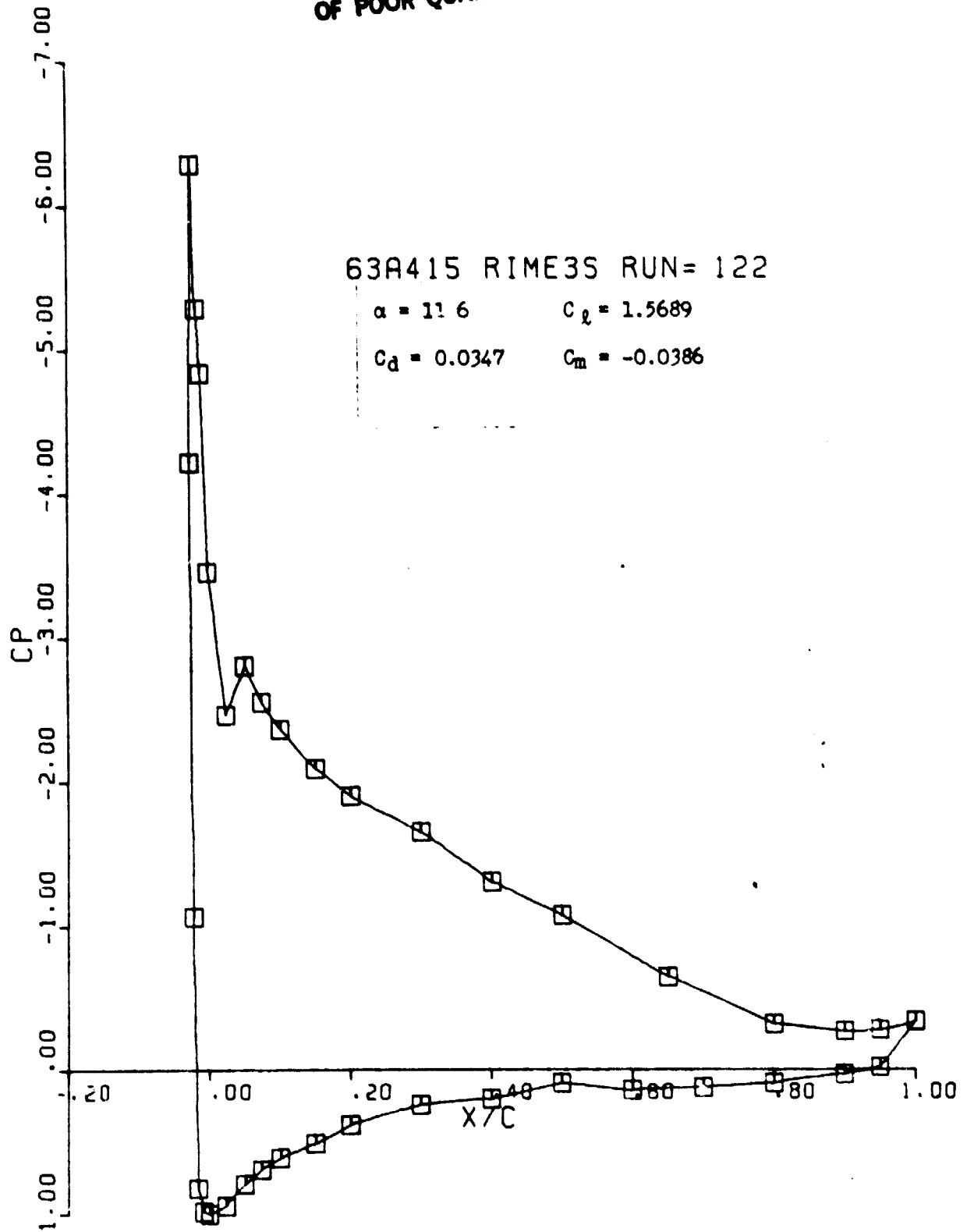
ORIGINAL PAGE IS
OF POOR QUALITY



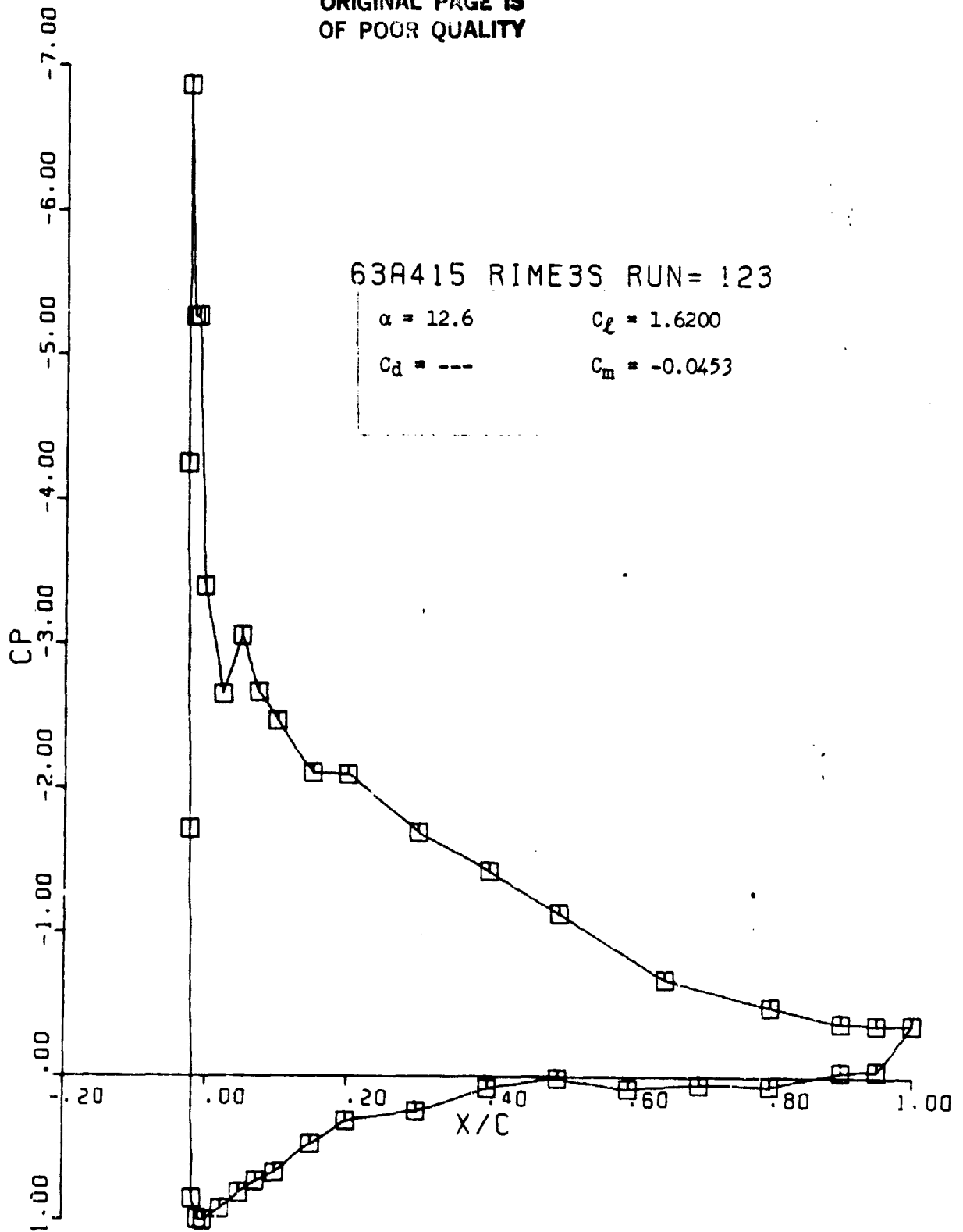
ORIGINAL PAGE IS
OF POOR QUALITY



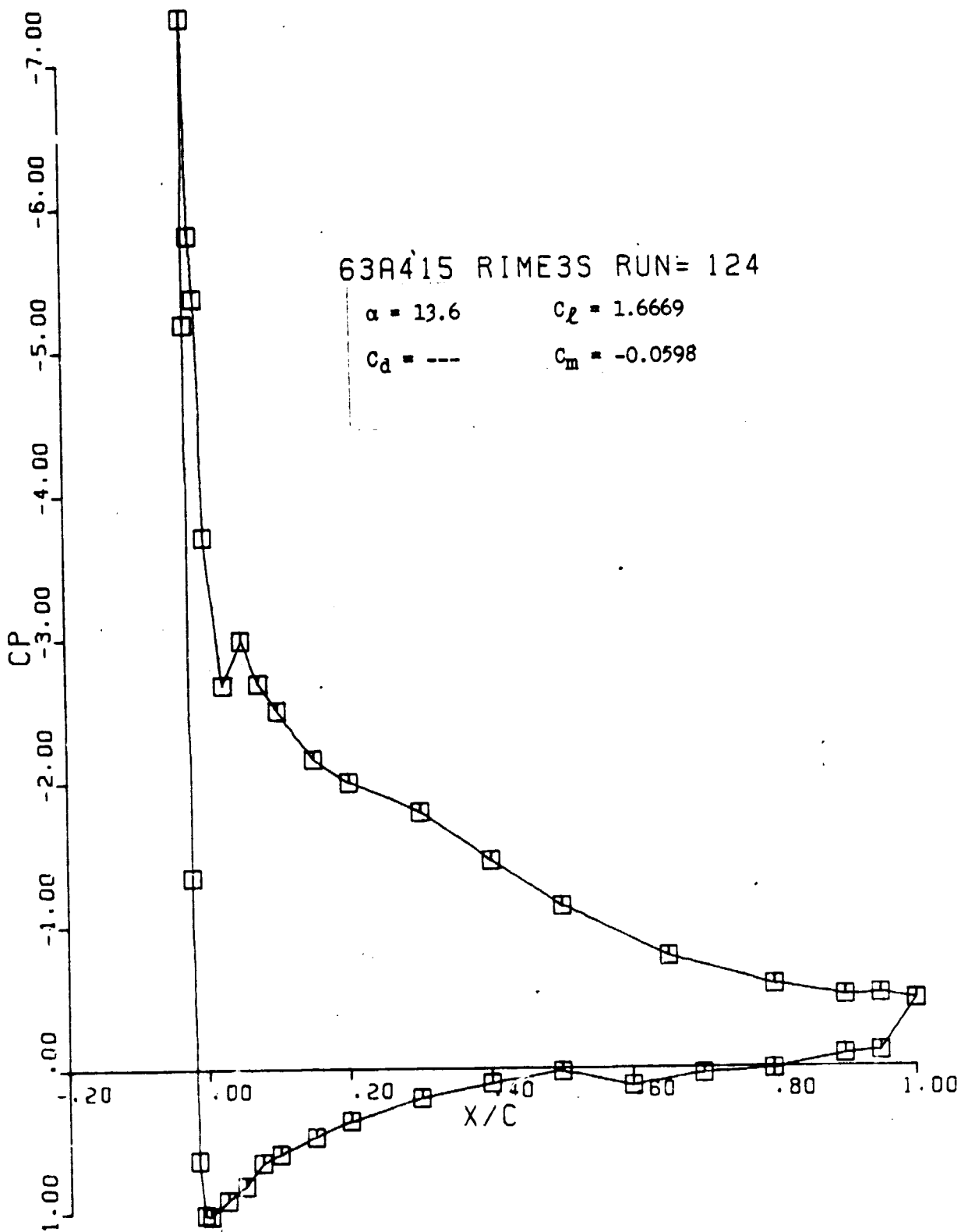
ORIGINAL PAGE IS
OF POOR QUALITY



ORIGINAL PAGE IS
OF POOR QUALITY



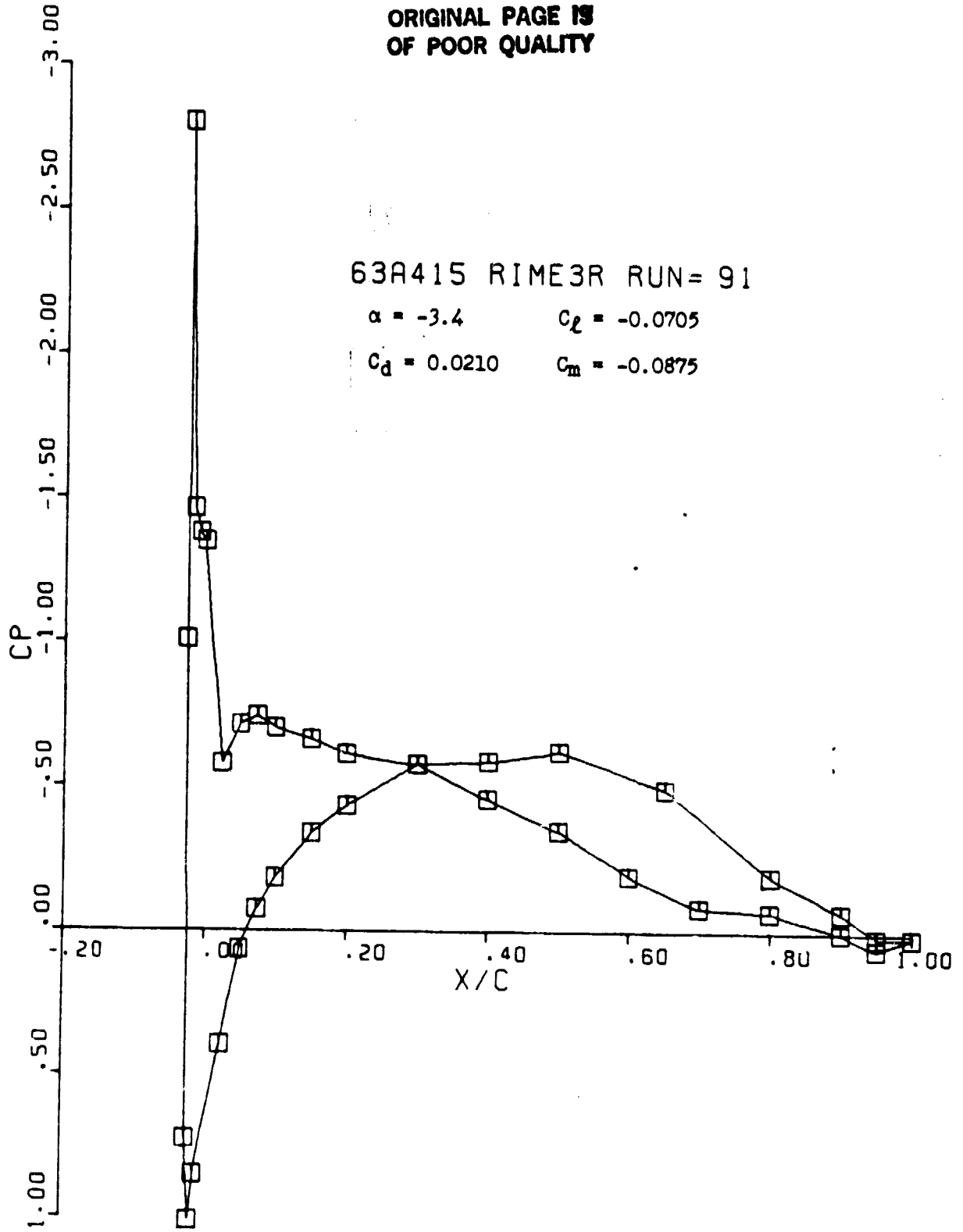
ORIGINAL PAGE IS
OF POOR QUALITY



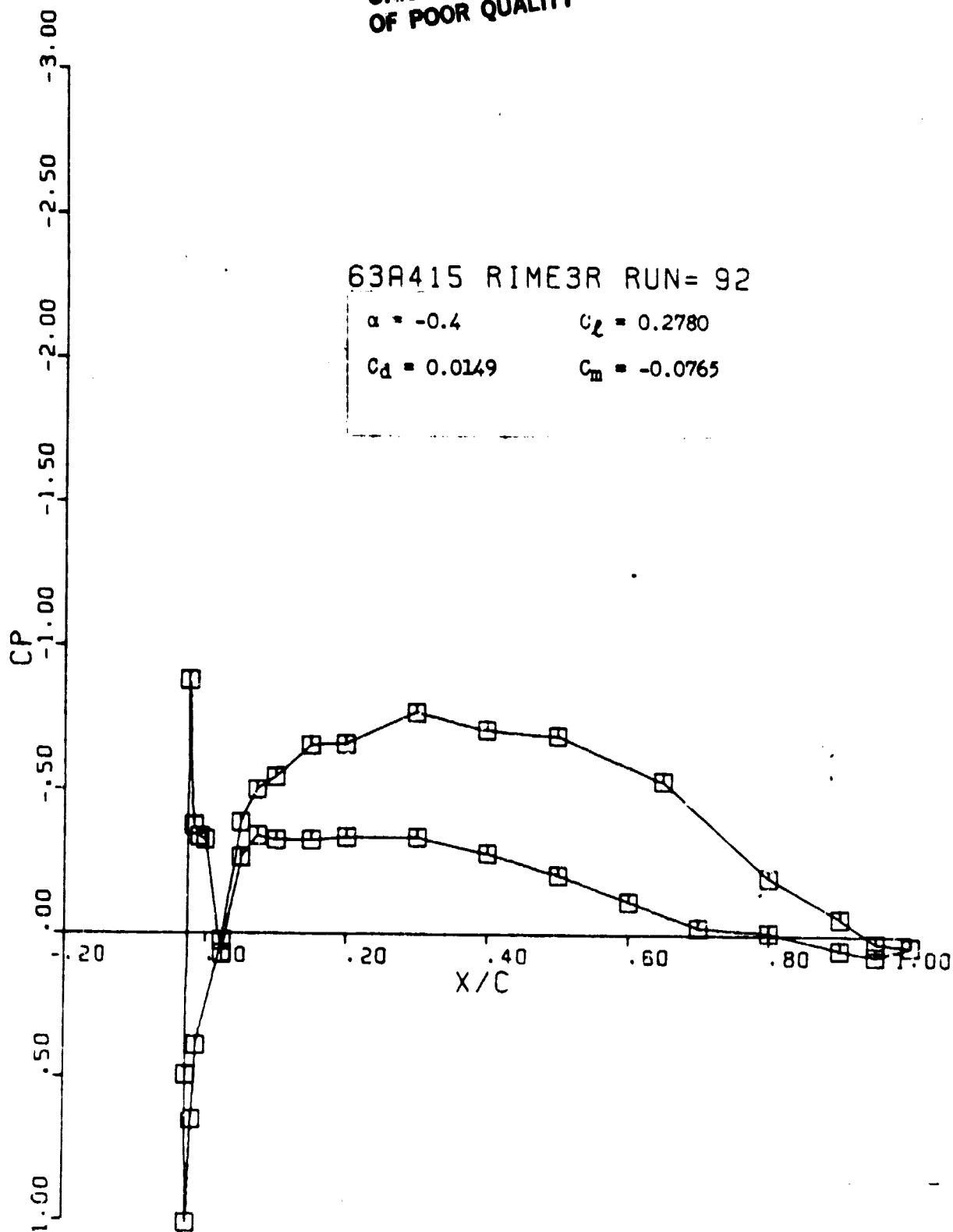
ORIGINAL PAGE IS
OF POOR QUALITY

63A415 RIME3R RUN = 91

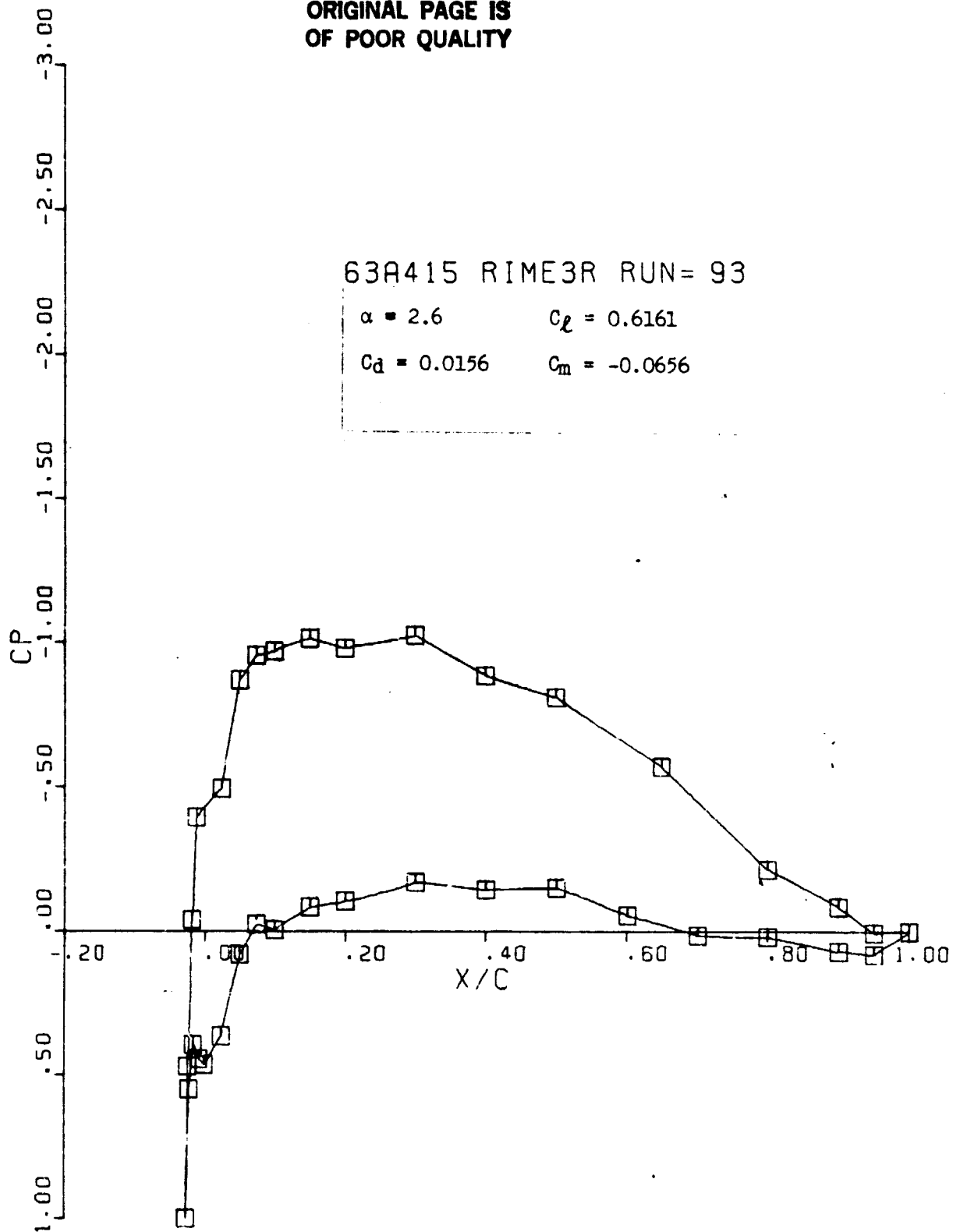
$\alpha = -3.4$ $C_l = -0.0705$
 $C_d = 0.0210$ $C_m = -0.0875$



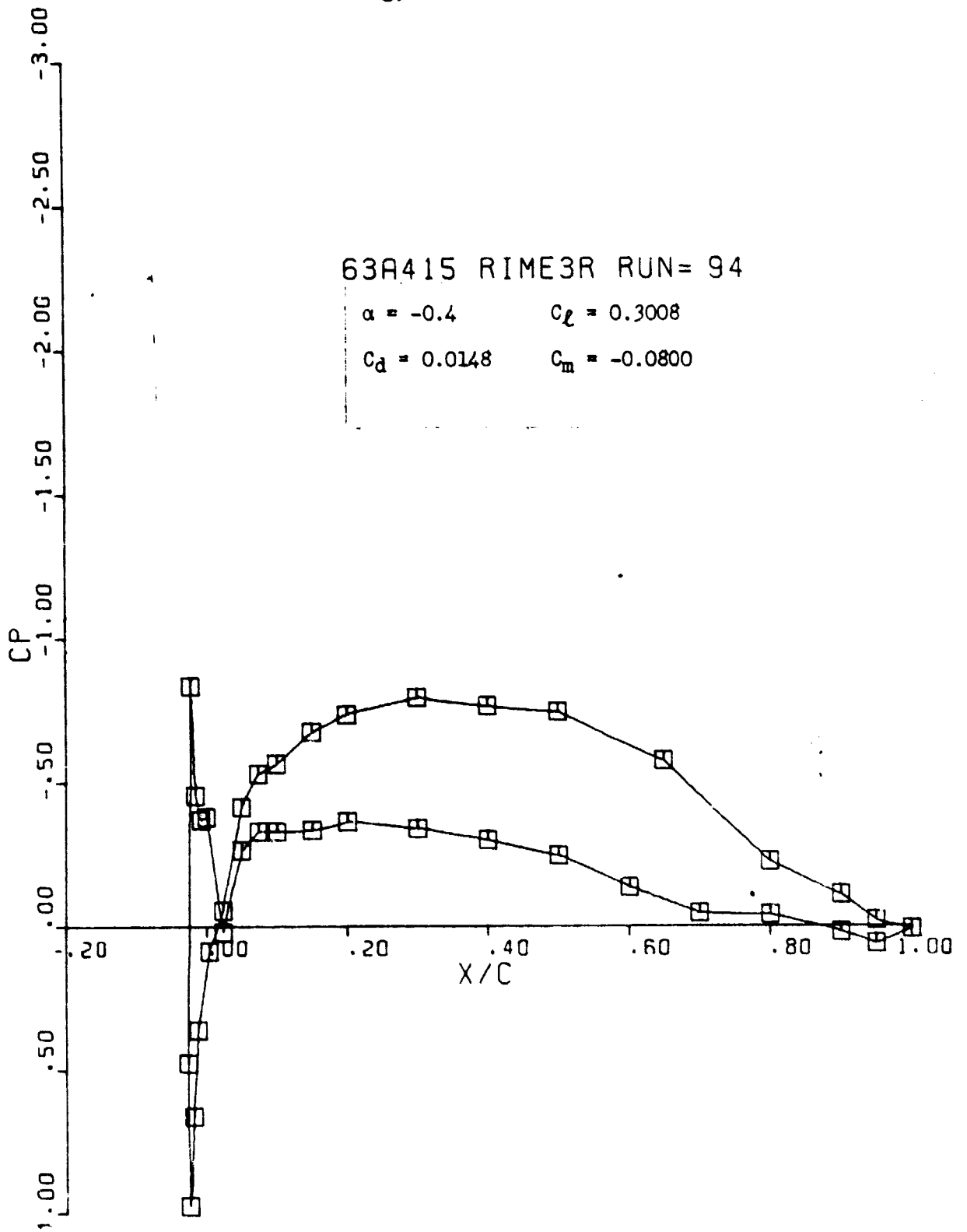
ORIGINAL PAGE IS
OF POOR QUALITY



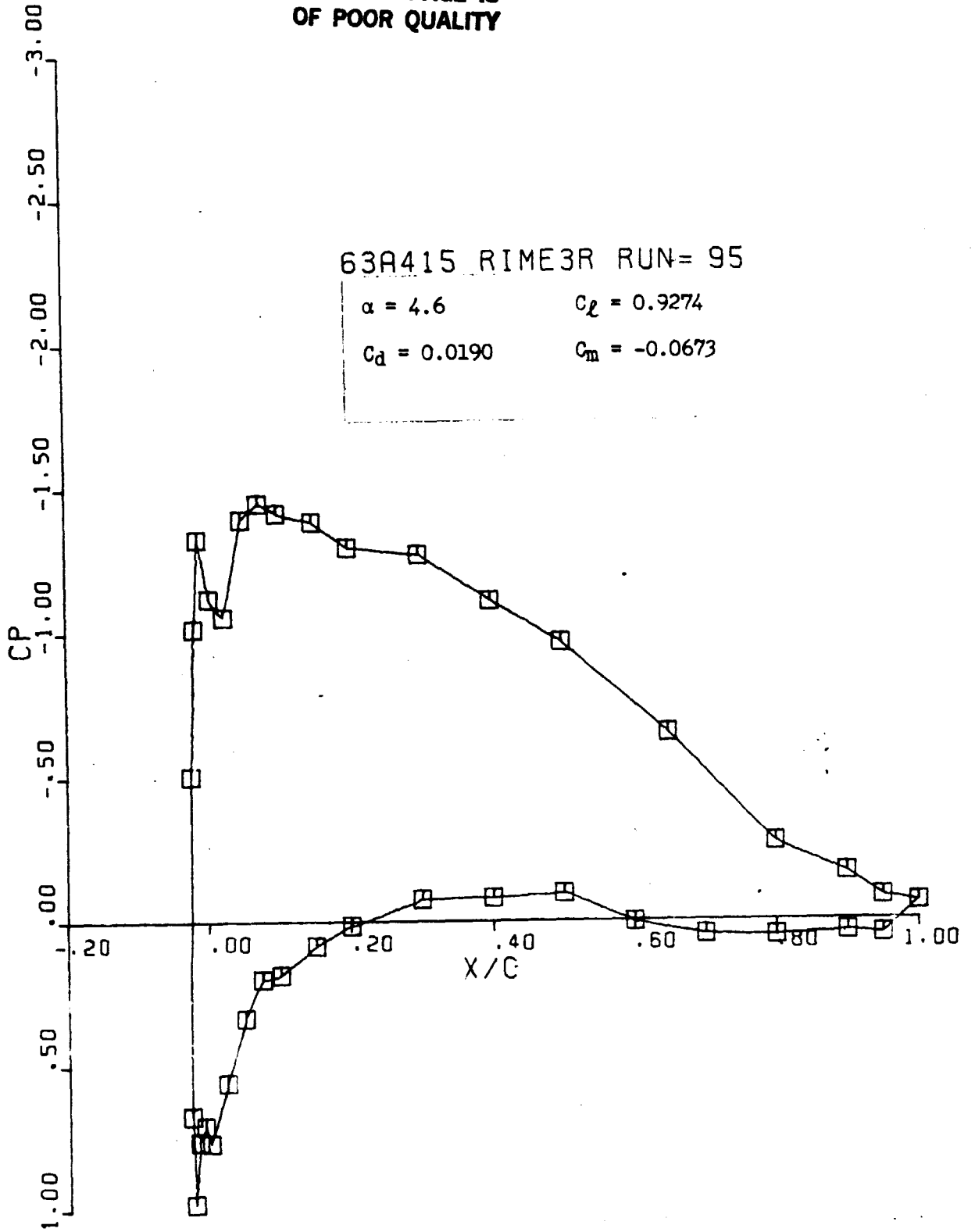
ORIGINAL PAGE IS
OF POOR QUALITY



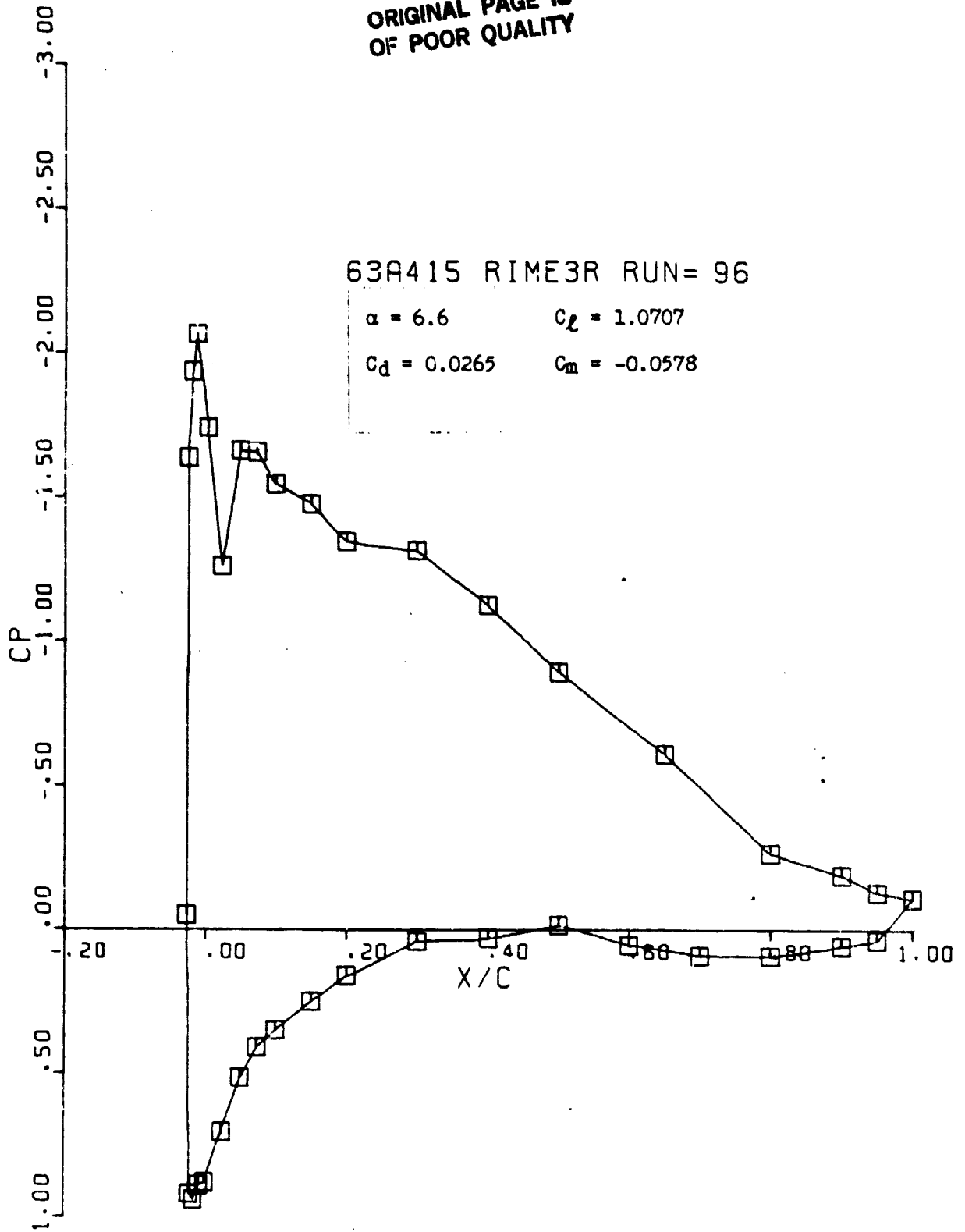
ORIGINAL PAGE IS
OF POOR QUALITY



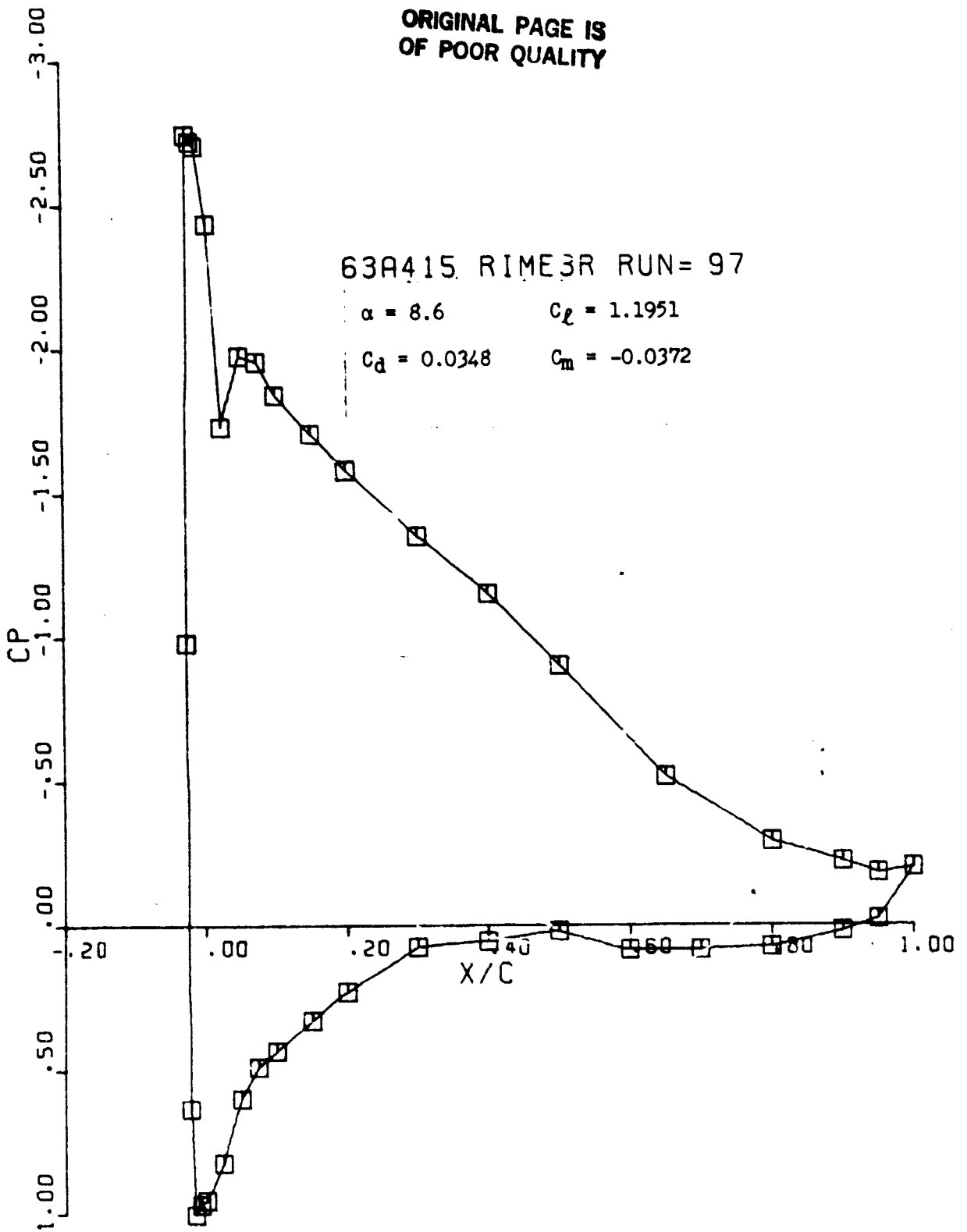
ORIGINAL PAGE IS
OF POOR QUALITY



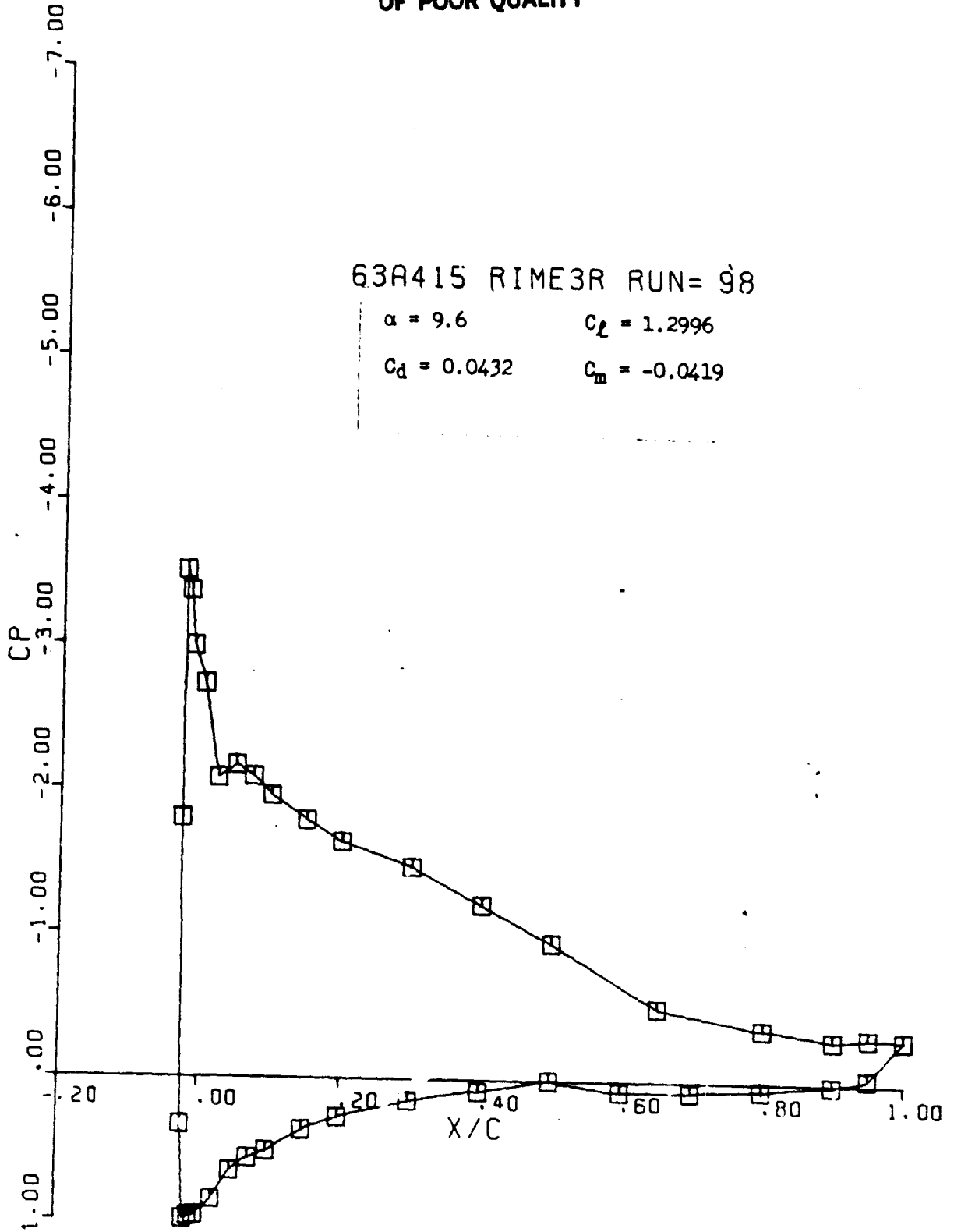
ORIGINAL PAGE IS
OF POOR QUALITY



ORIGINAL PAGE IS
OF POOR QUALITY



ORIGINAL PAGE IS
OF POOR QUALITY



ORIGINAL PAGE IS
OF POOR QUALITY

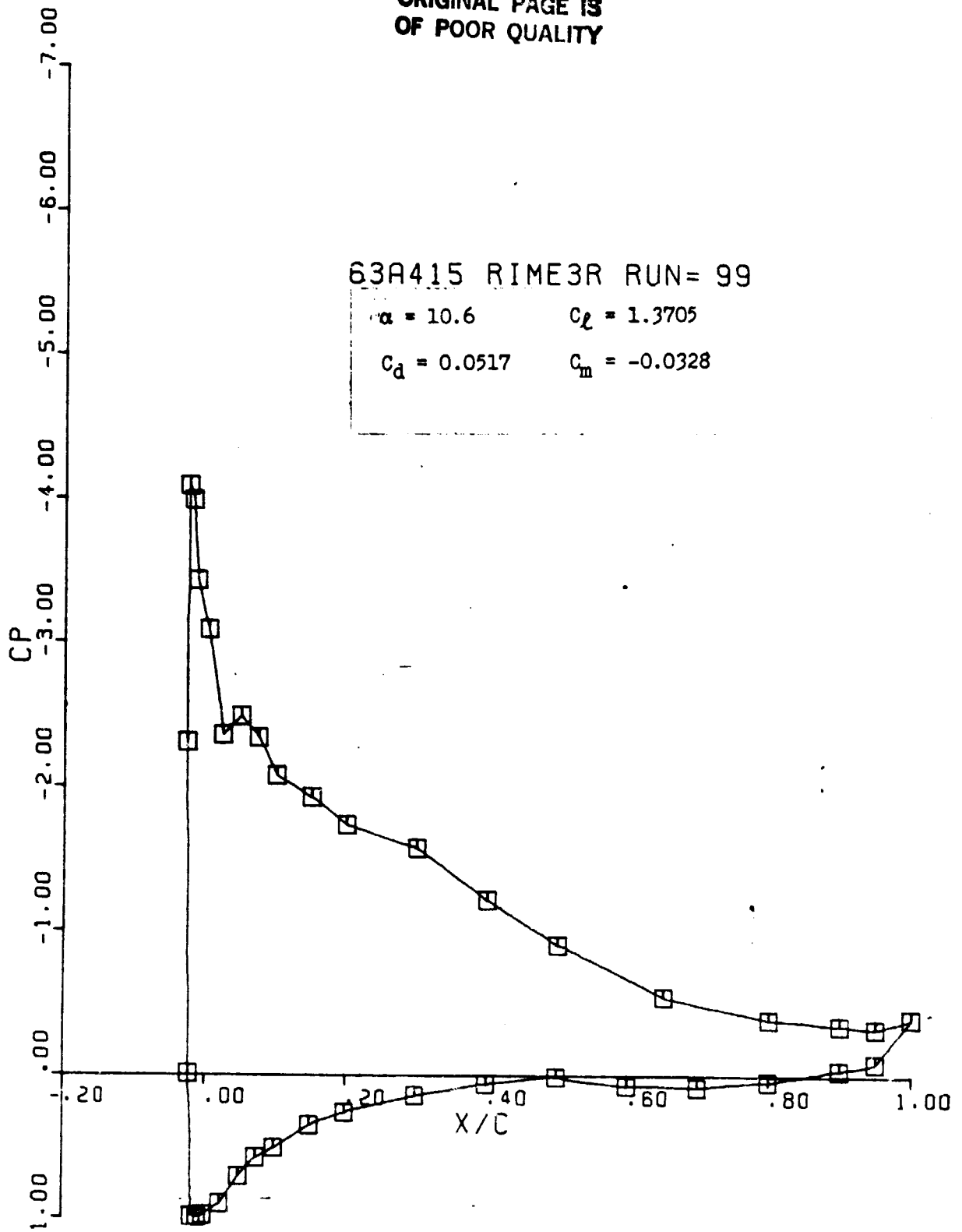
63A415 RIME3R RUN= 99

$\alpha = 10.6$

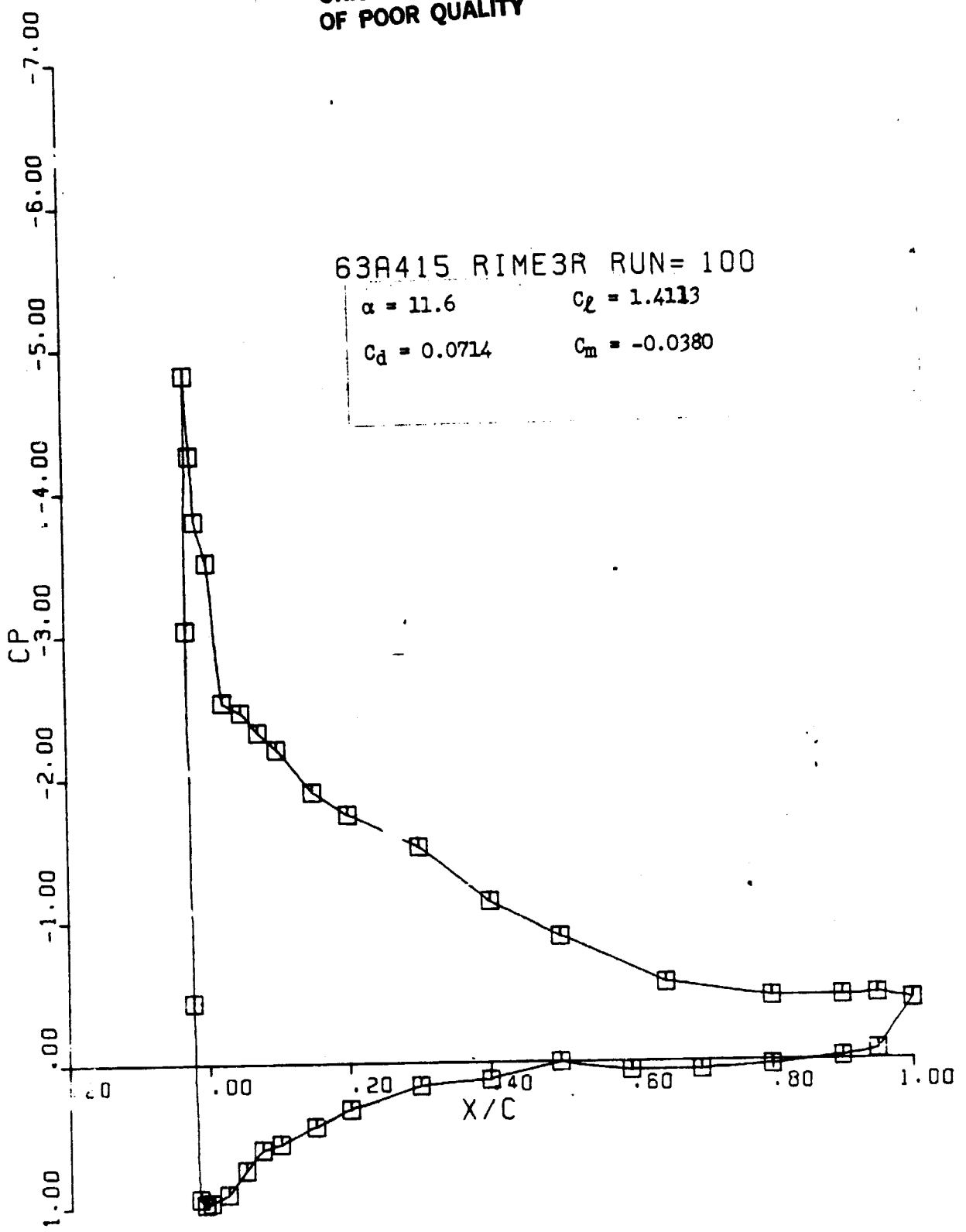
$C_l = 1.3705$

$C_d = 0.0517$

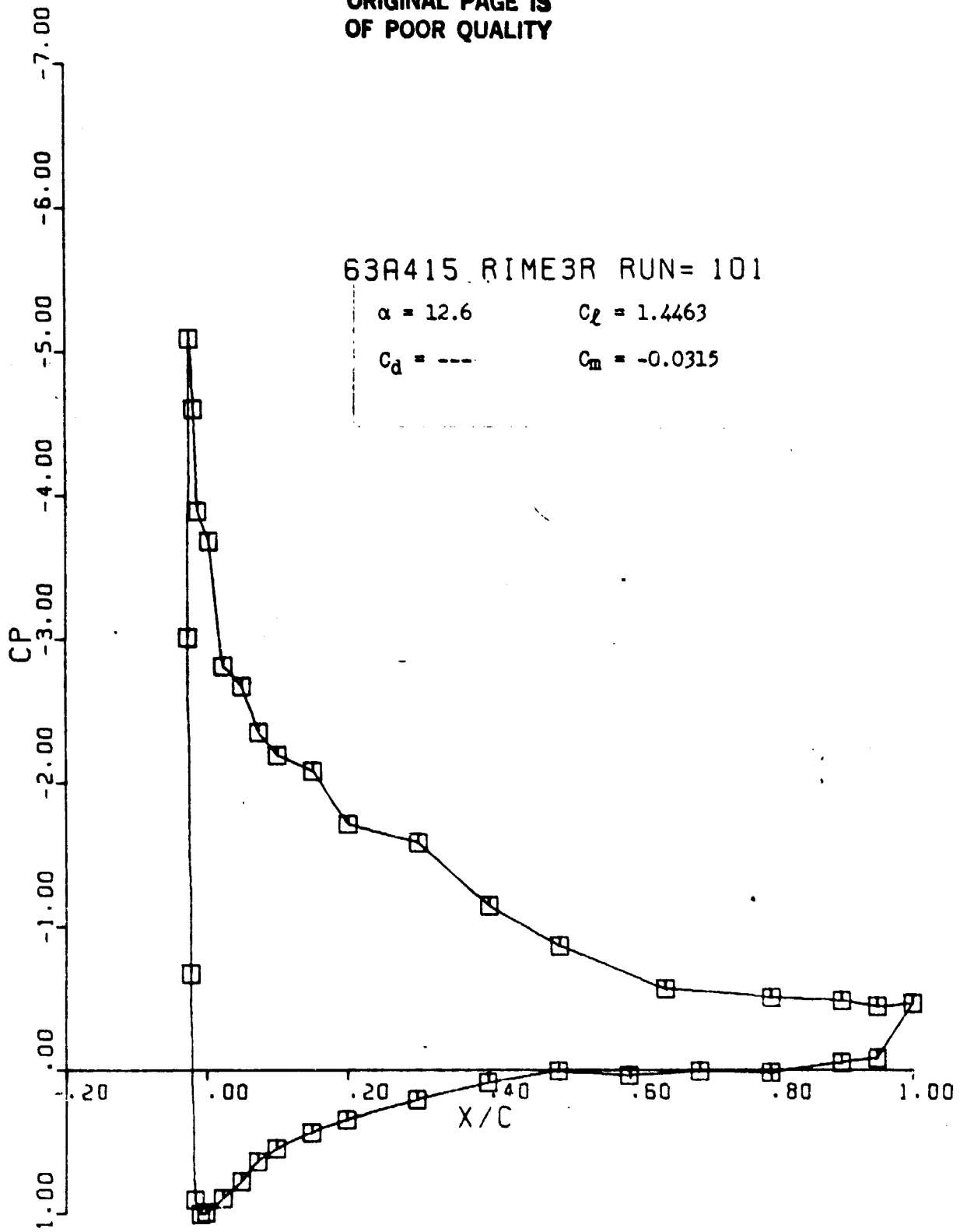
$C_m = -0.0328$



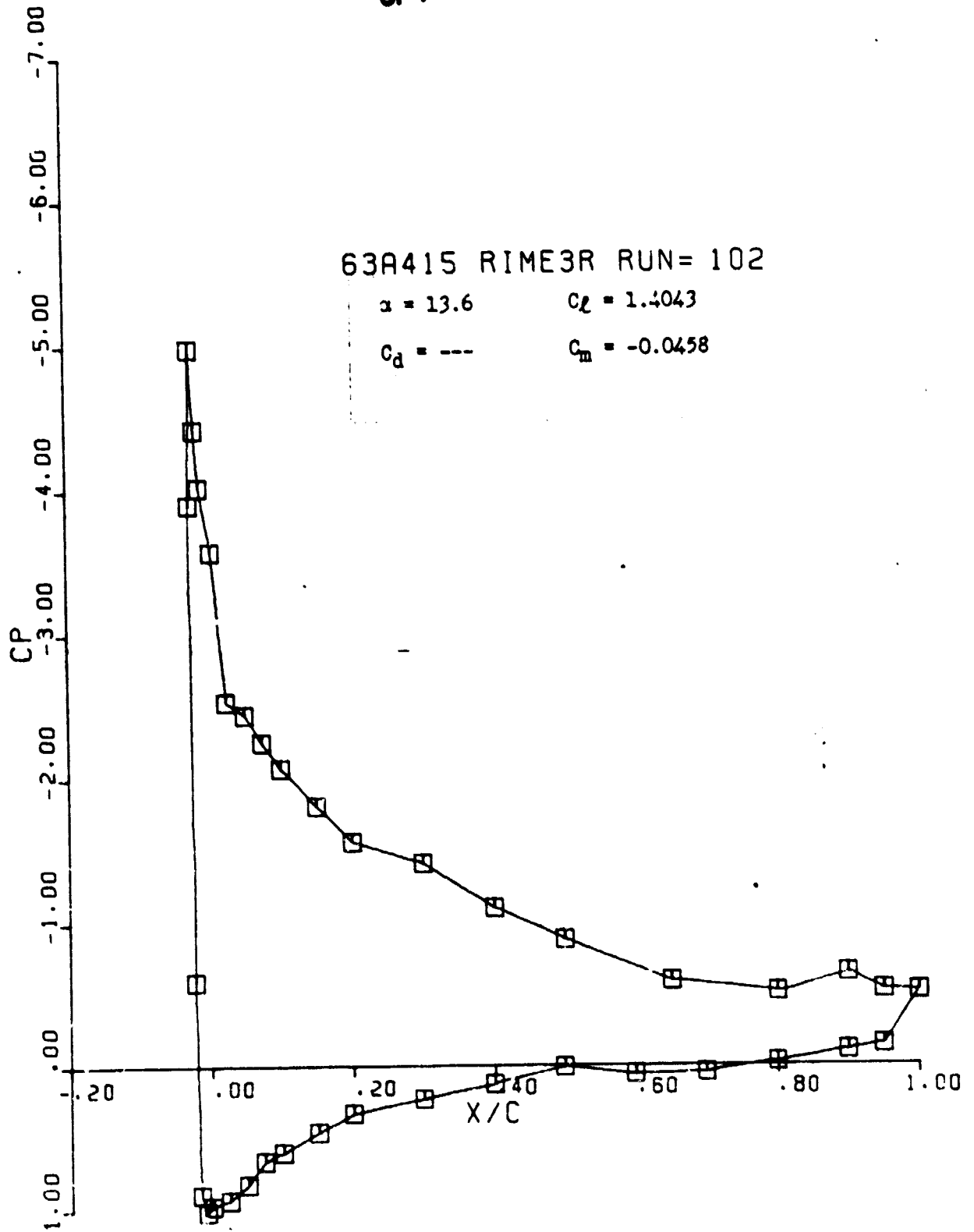
ORIGINAL PAGE IS
OF POOR QUALITY



ORIGINAL PAGE IS
OF POOR QUALITY



ORIGINAL PAGE IS
OF POOR QUALITY



ORIGINAL PAGE IS
OF POOR QUALITY

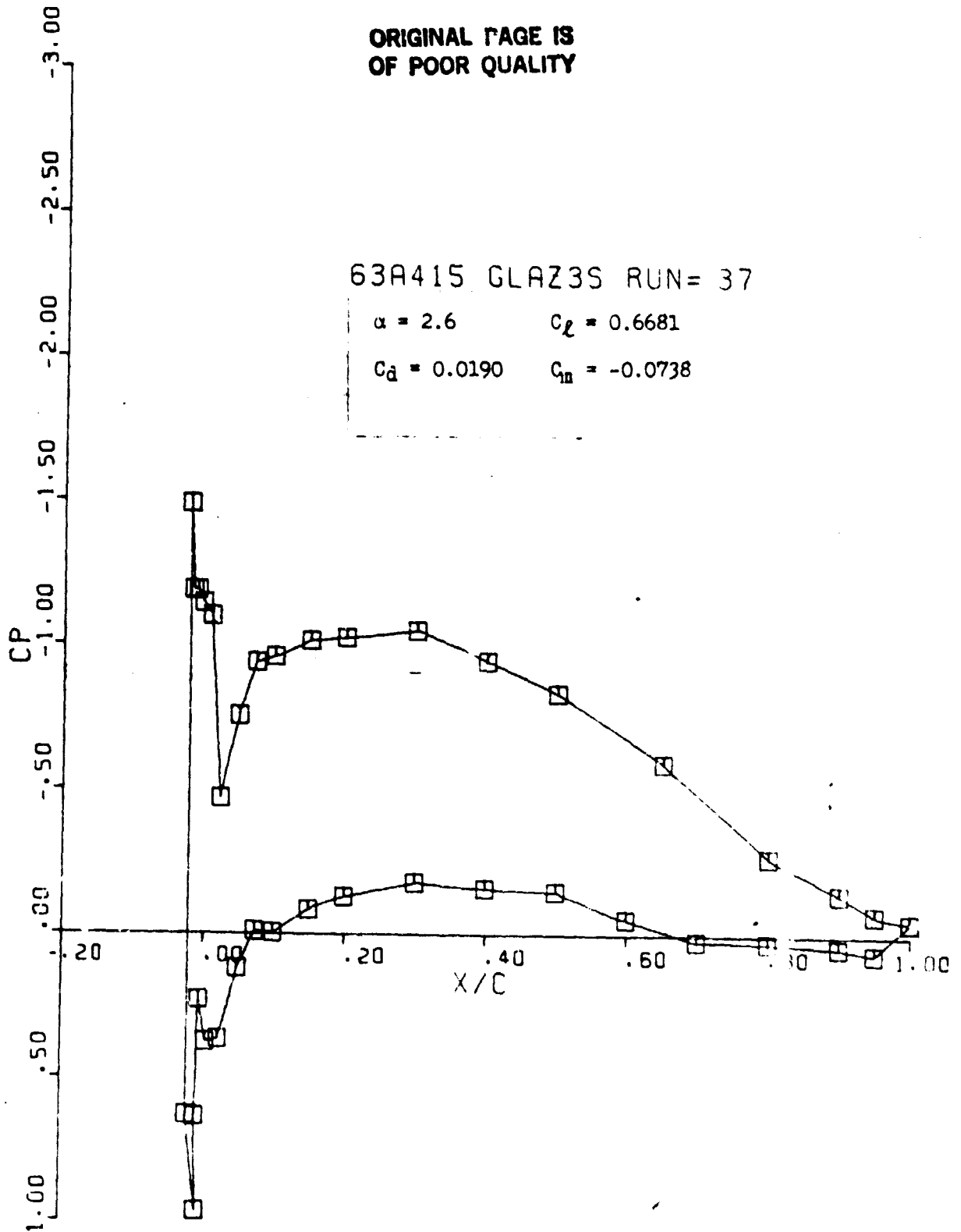
63A415 GLAZ3S RUN= 37

$\alpha = 2.6$

$C_L = 0.6681$

$C_d = 0.0190$

$C_{m1} = -0.0738$



ORIGINAL PAGE IS
OF POOR QUALITY

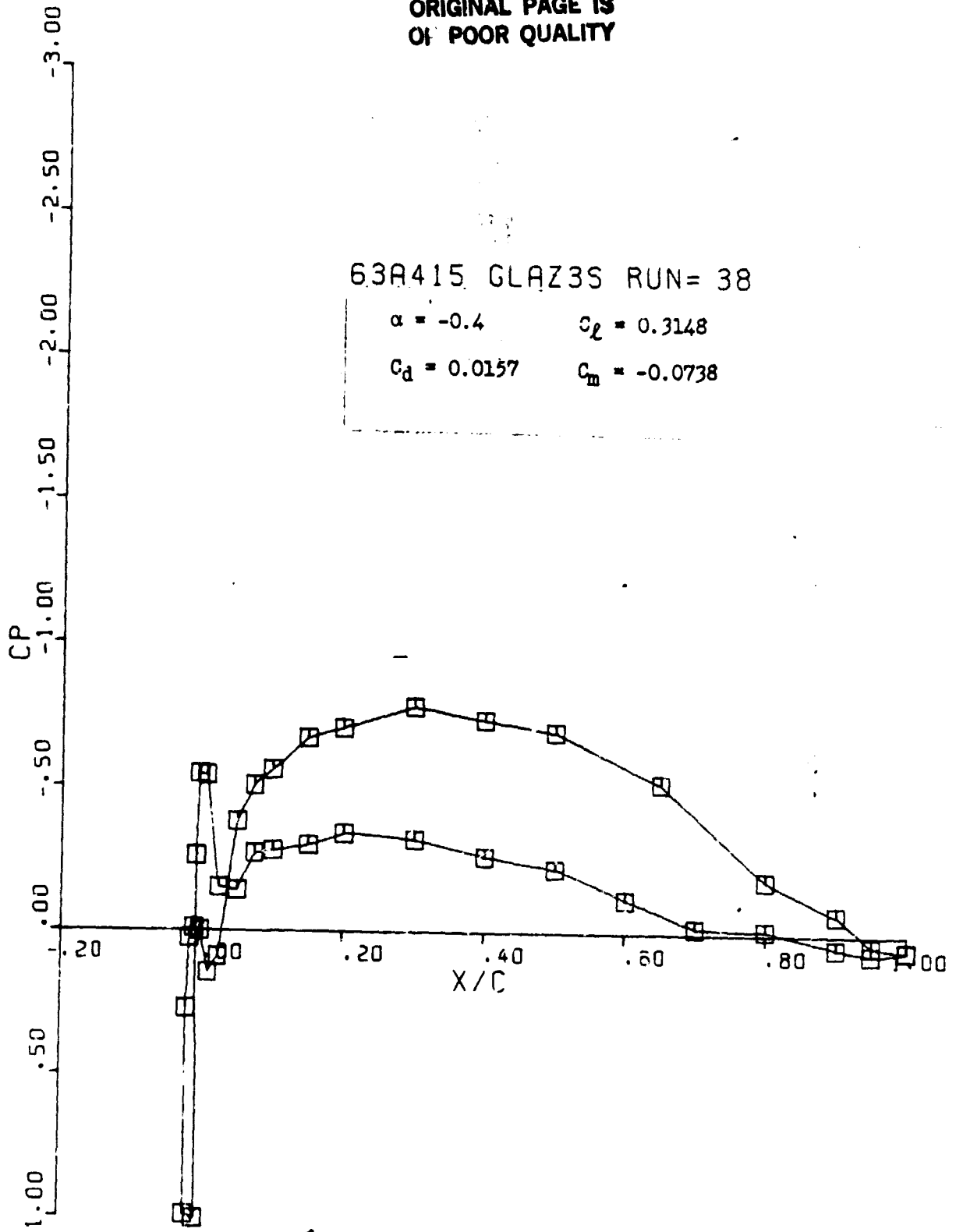
63A415 GLAZ3S RUN= 38

$\alpha = -0.4$

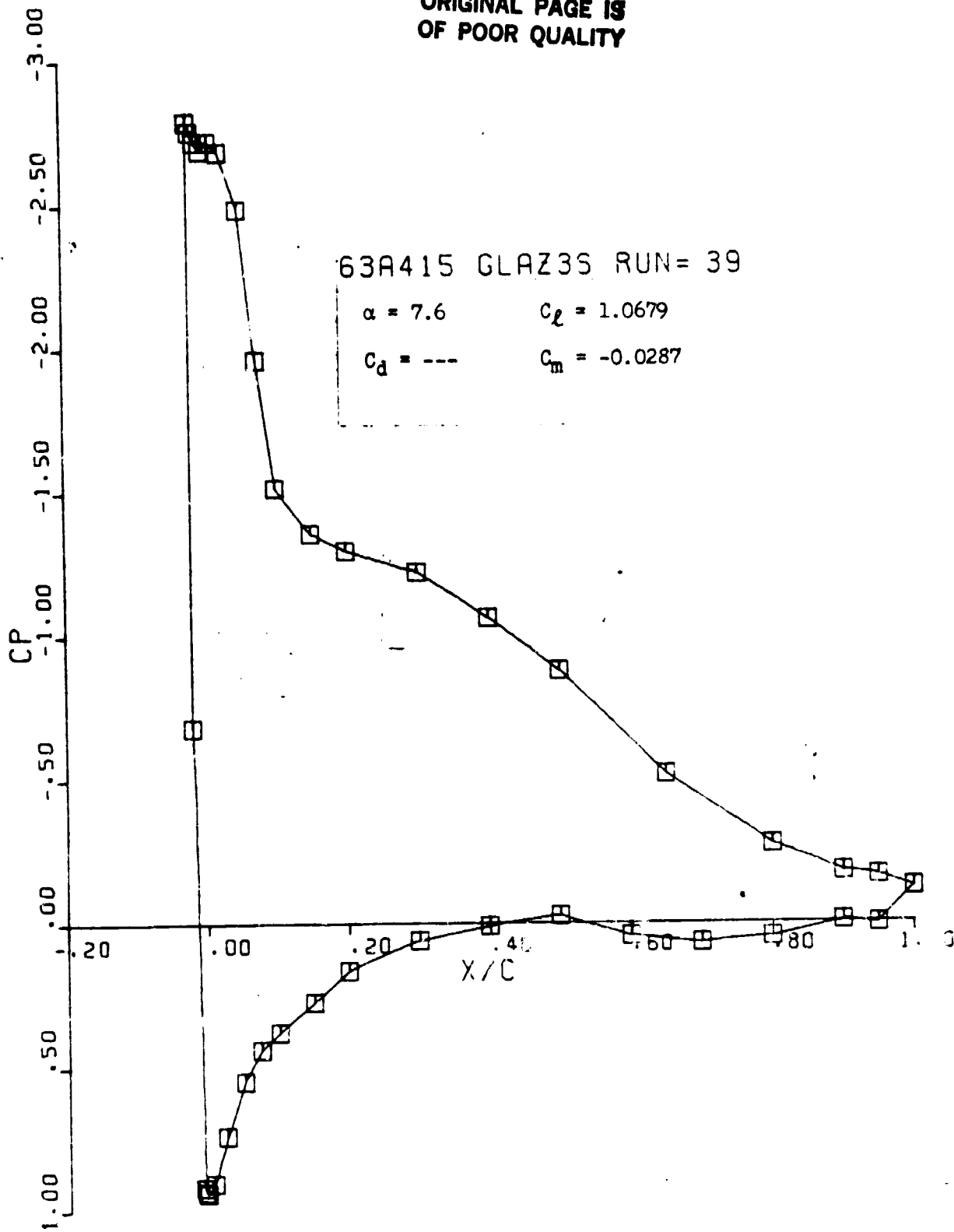
$C_l = 0.3148$

$C_d = 0.0157$

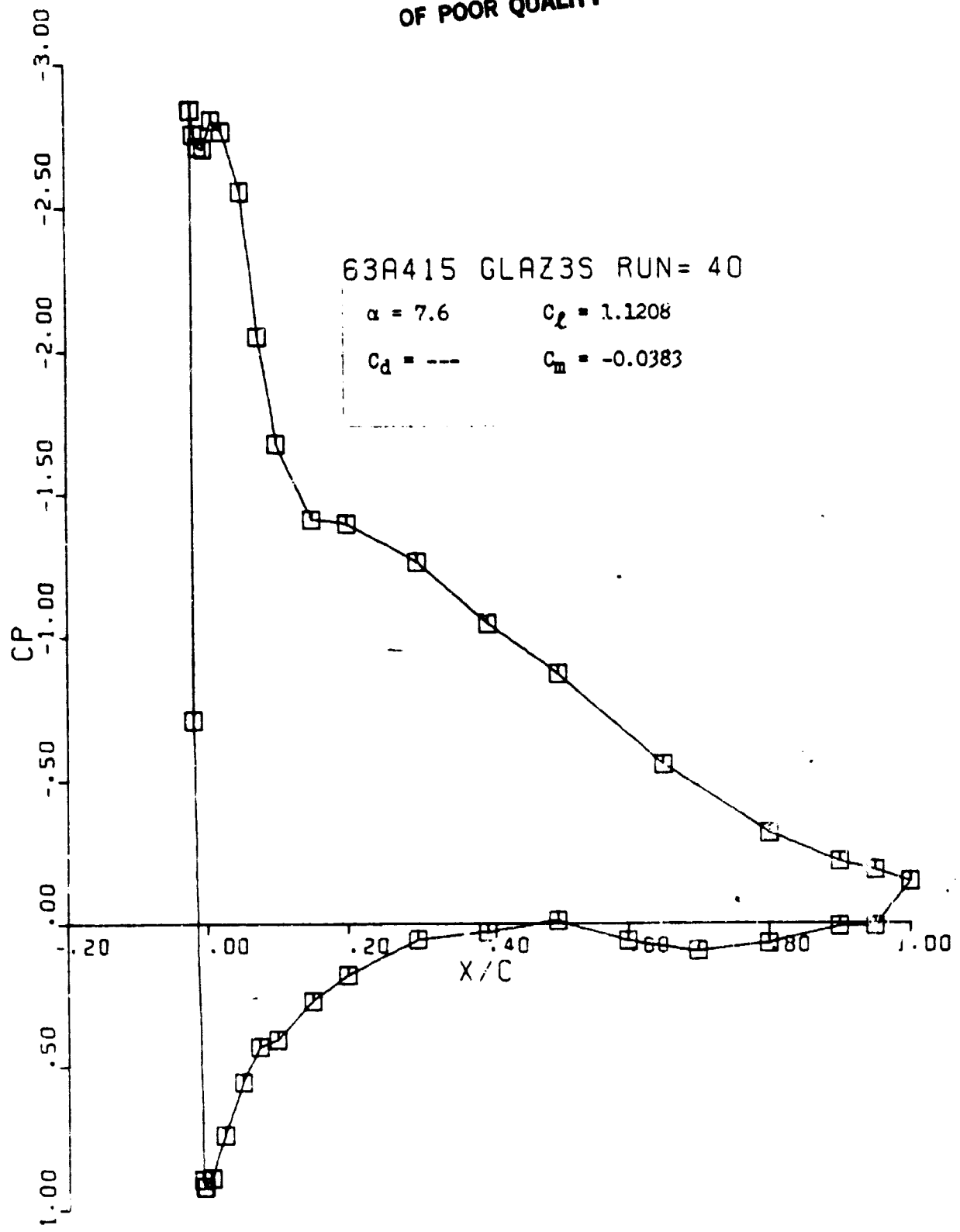
$C_m = -0.0738$



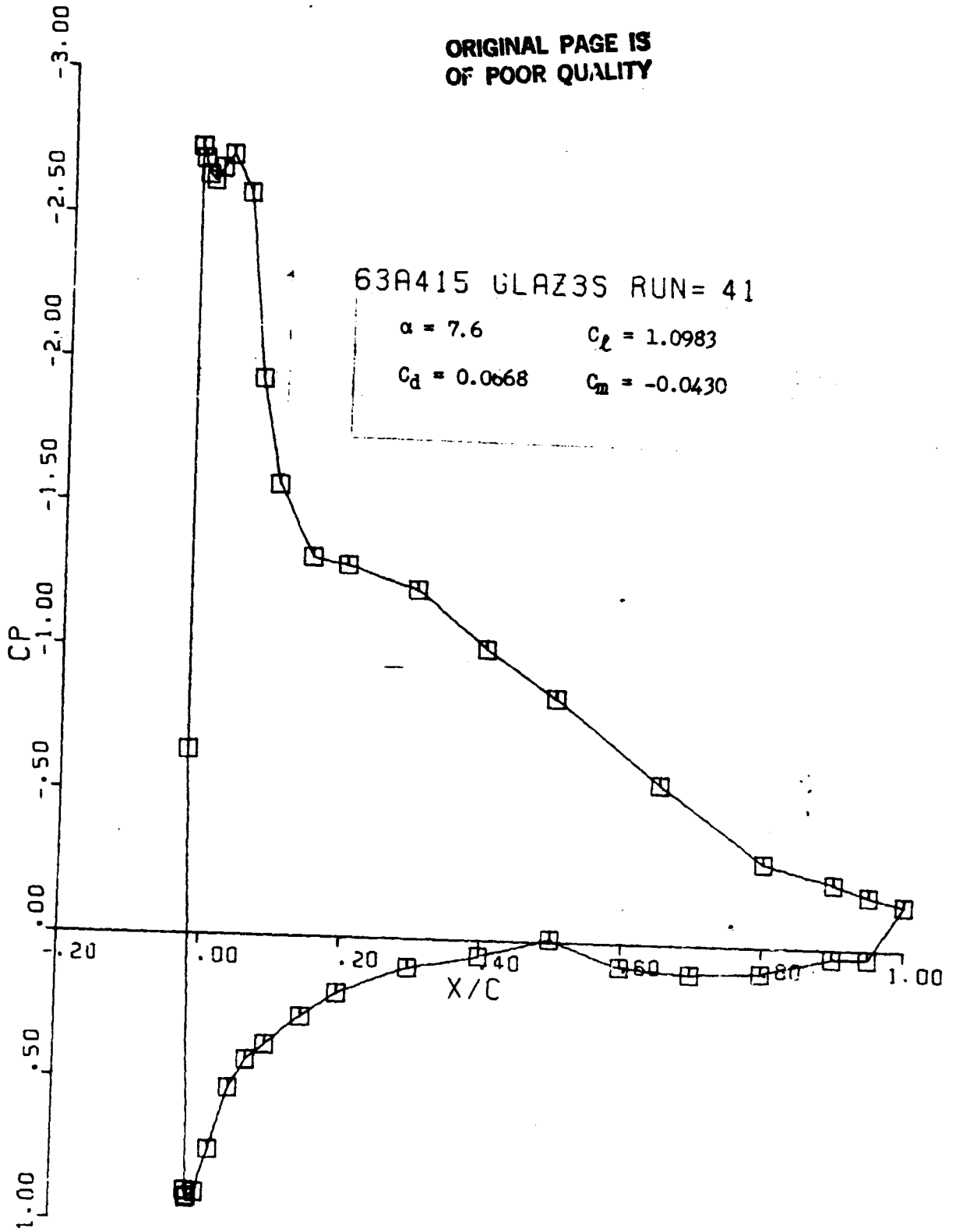
ORIGINAL PAGE IS
OF POOR QUALITY



ORIGINAL PAGE IS
OF POOR QUALITY

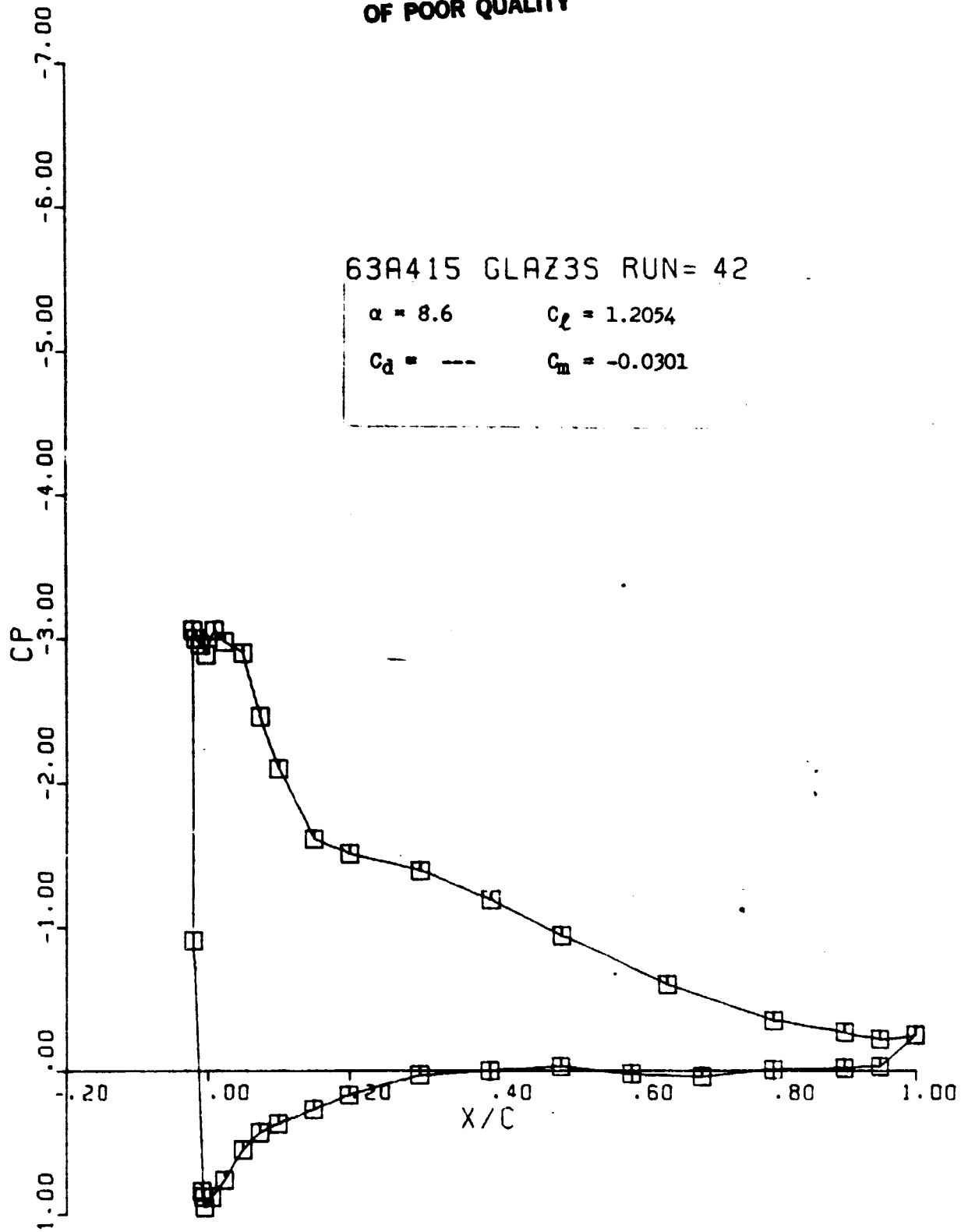


ORIGINAL PAGE IS
OF POOR QUALITY

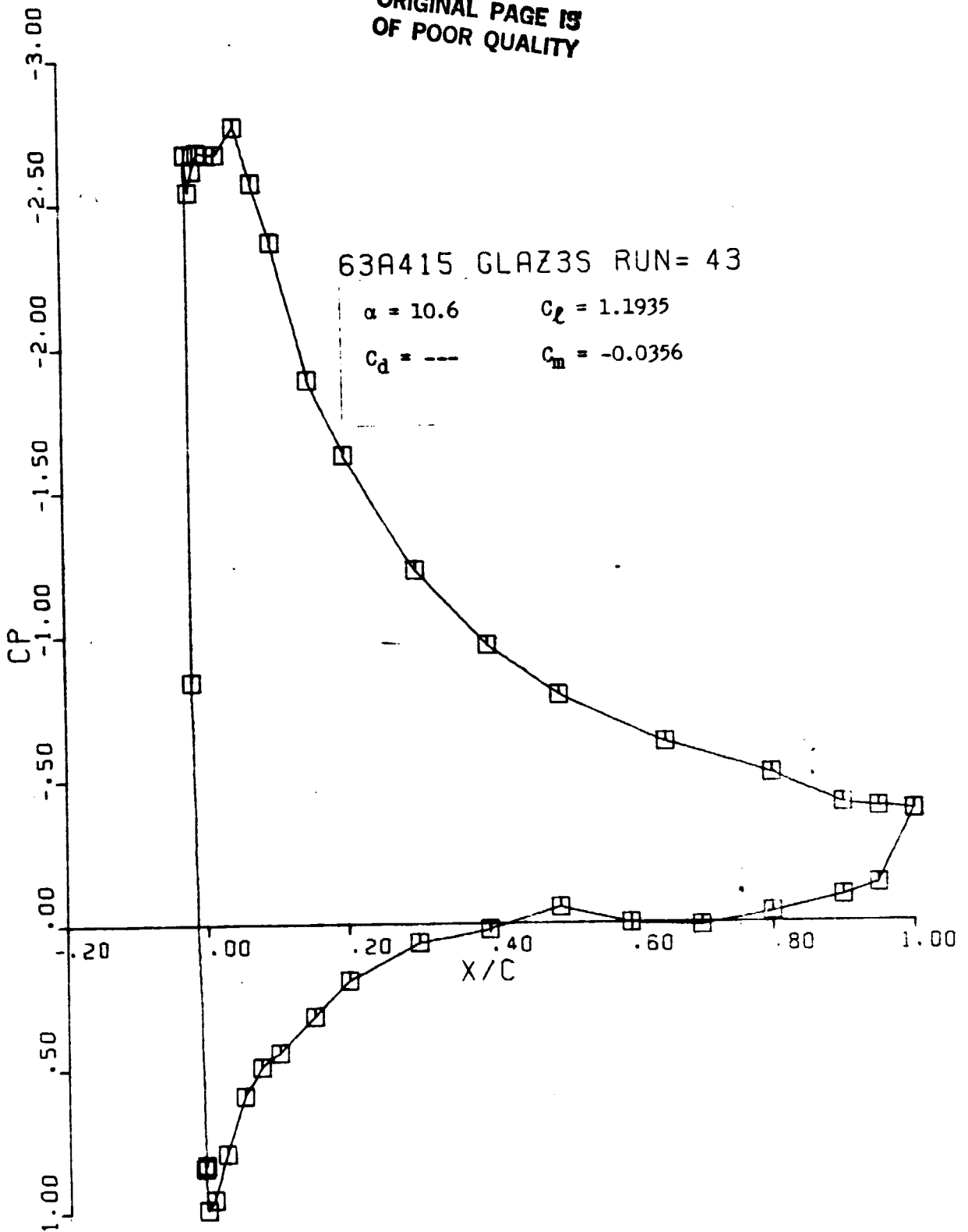


C-2

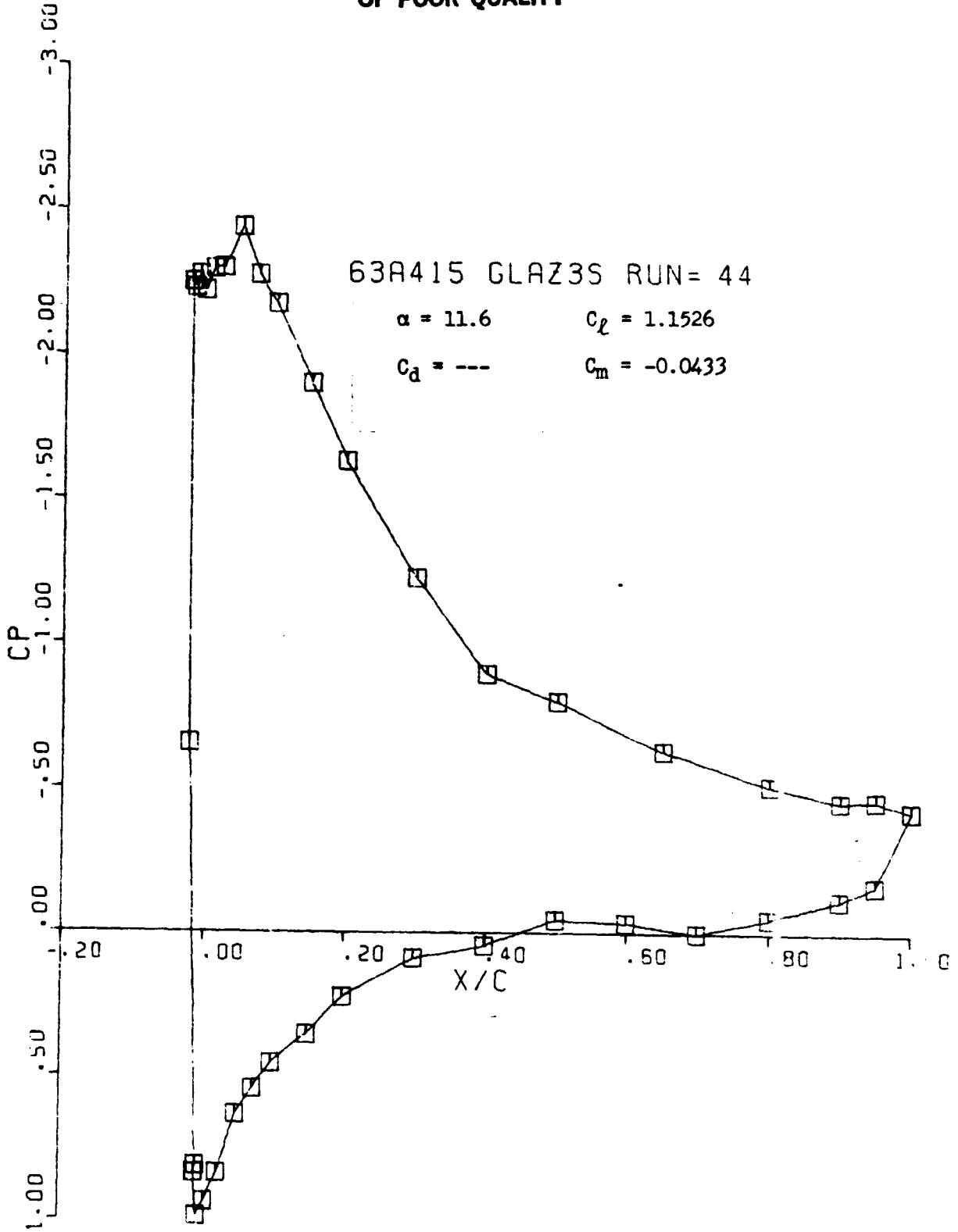
ORIGINAL PAGE 19
OF POOR QUALITY



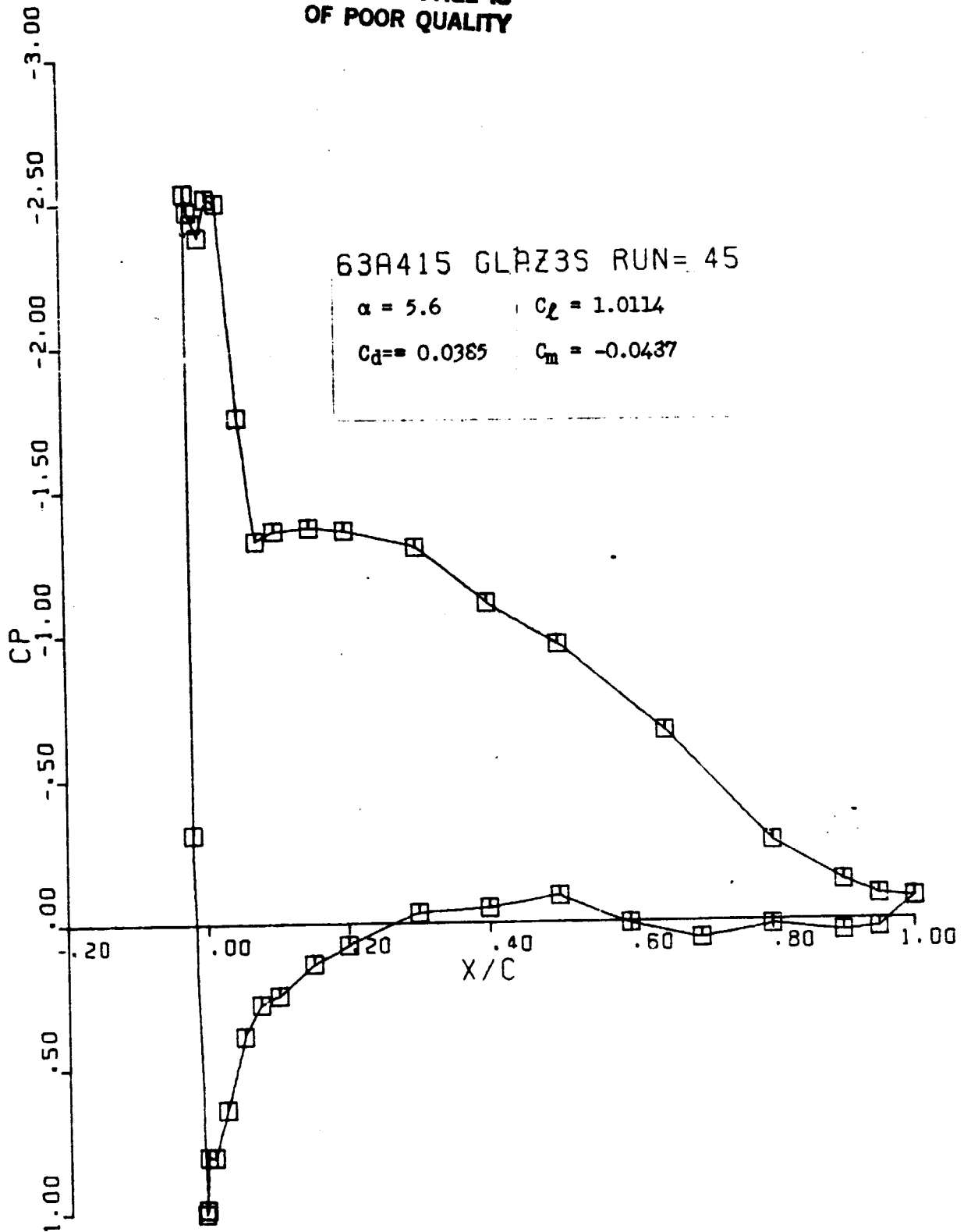
ORIGINAL PAGE IS
OF POOR QUALITY



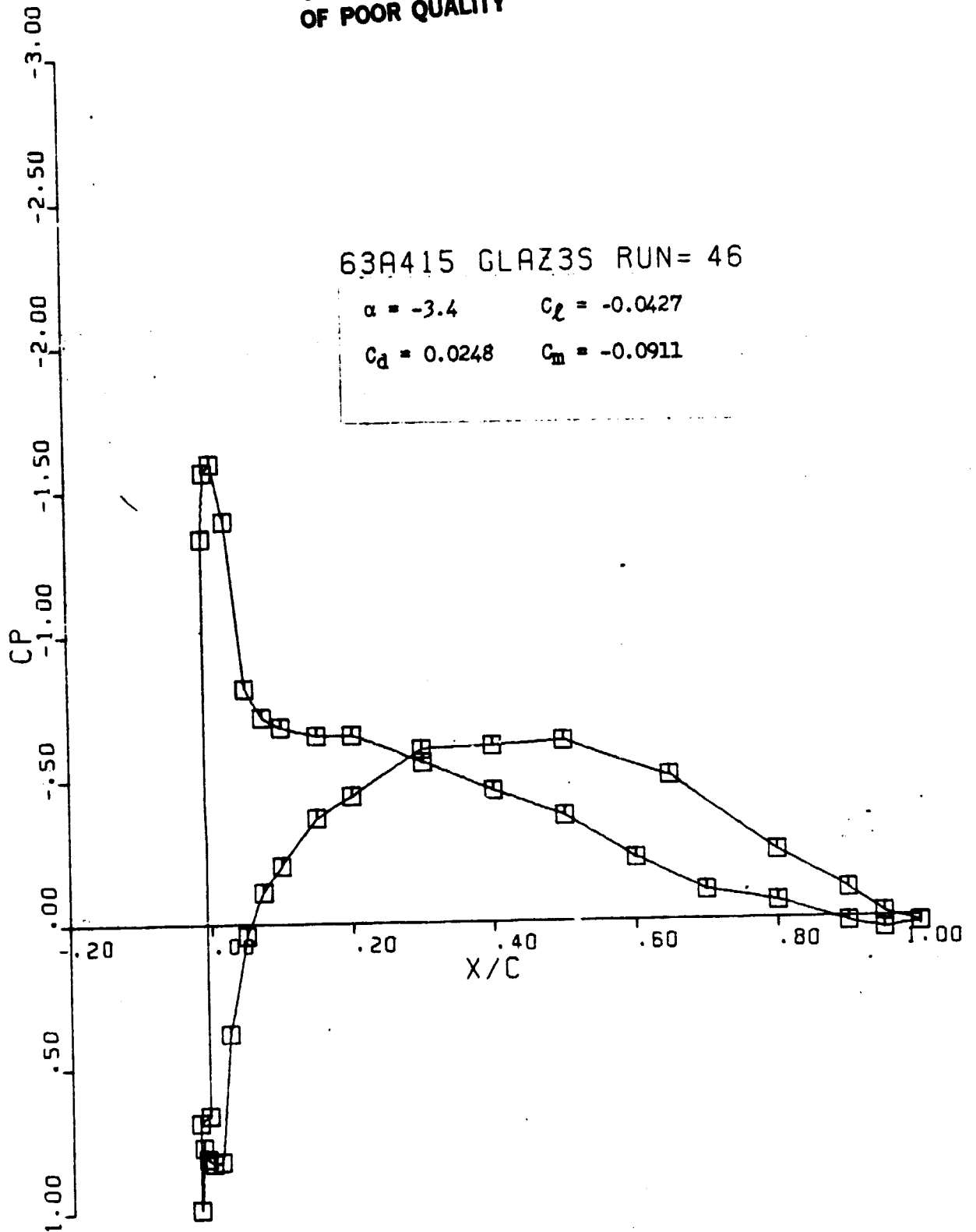
ORIGINAL PAGE IS
OF POOR QUALITY



ORIGINAL PAGE IS
OF POOR QUALITY



ORIGINAL PAGE IS
OF POOR QUALITY



ORIGINAL PAGE IS
OF POOR QUALITY

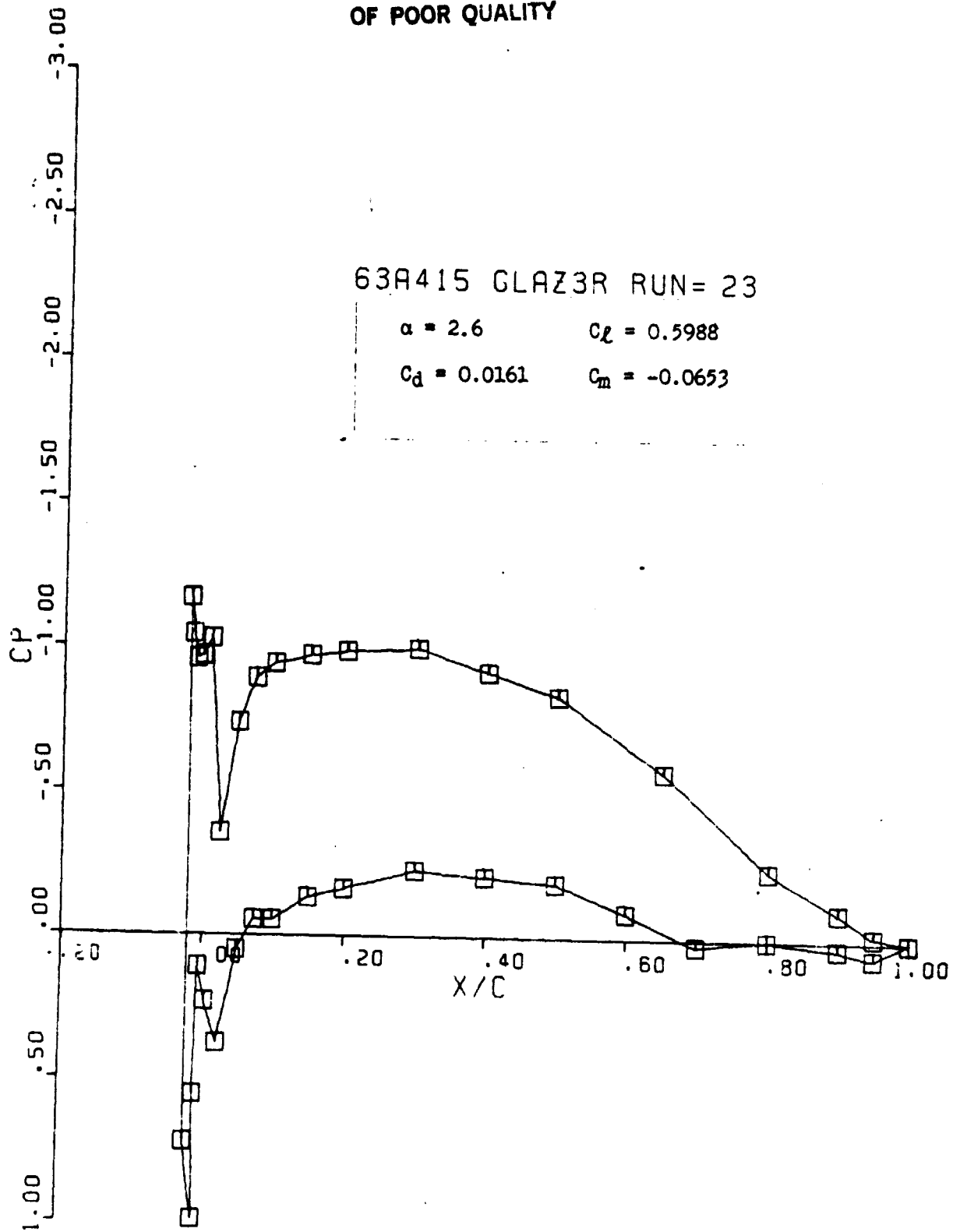
63A415 GLAZ3R RUN= 23

$\alpha = 2.6$

$C_L = 0.5988$

$C_d = 0.0161$

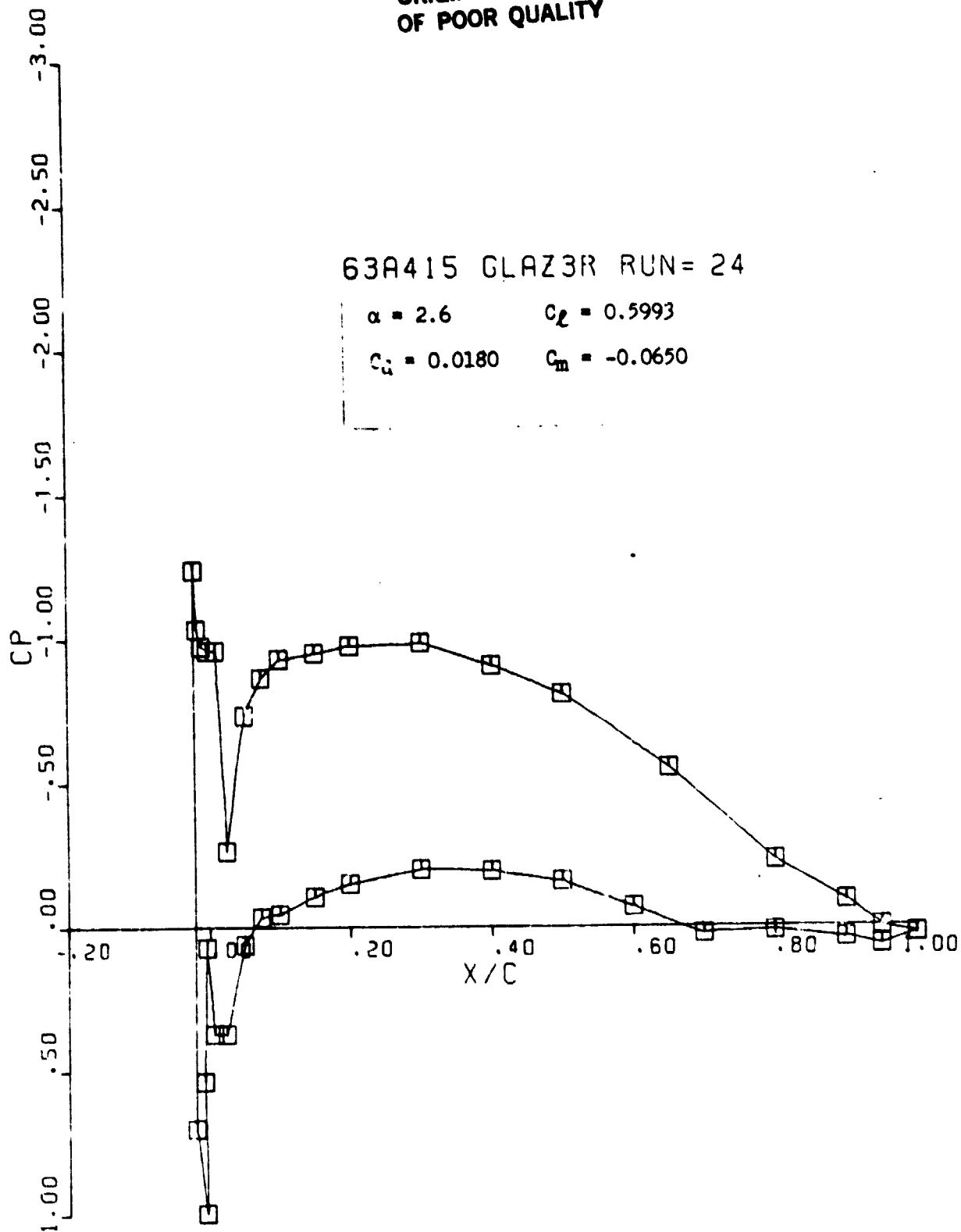
$C_m = -0.0653$



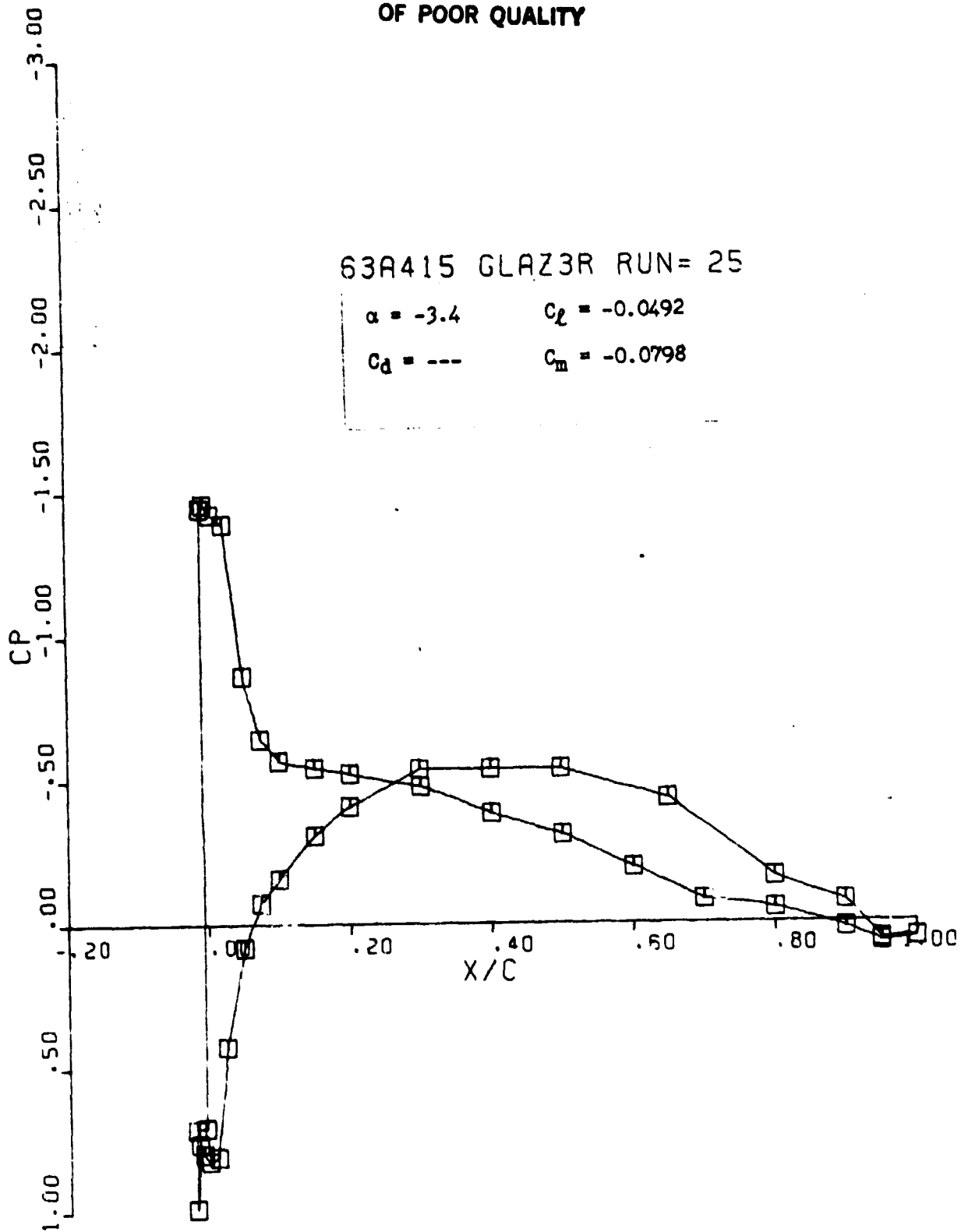
ORIGINAL PAGE IS
OF POOR QUALITY

63A415 GLAZ3R RUN= 24

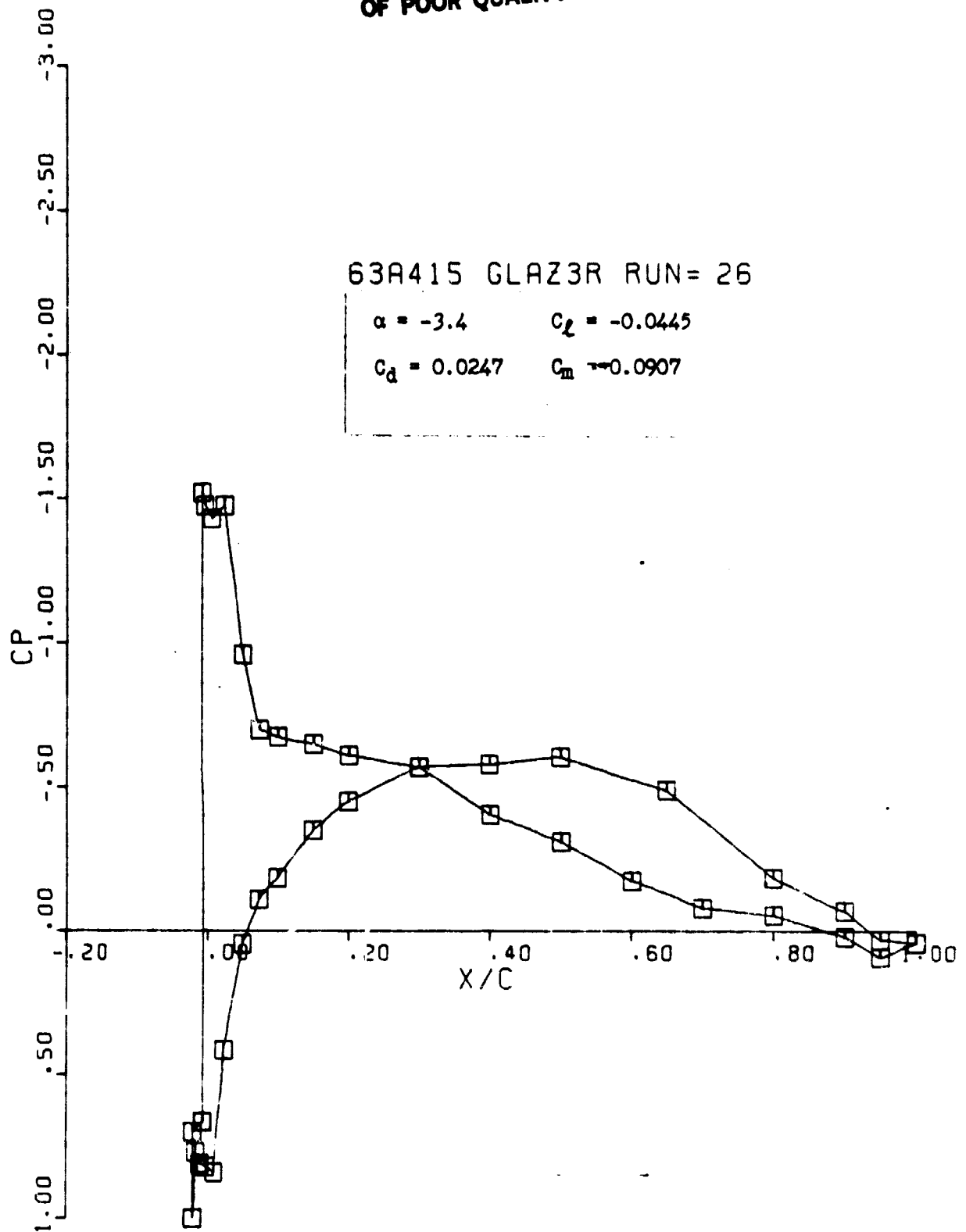
$\alpha = 2.6$ $C_L = 0.5993$
 $C_u = 0.0180$ $C_m = -0.0650$



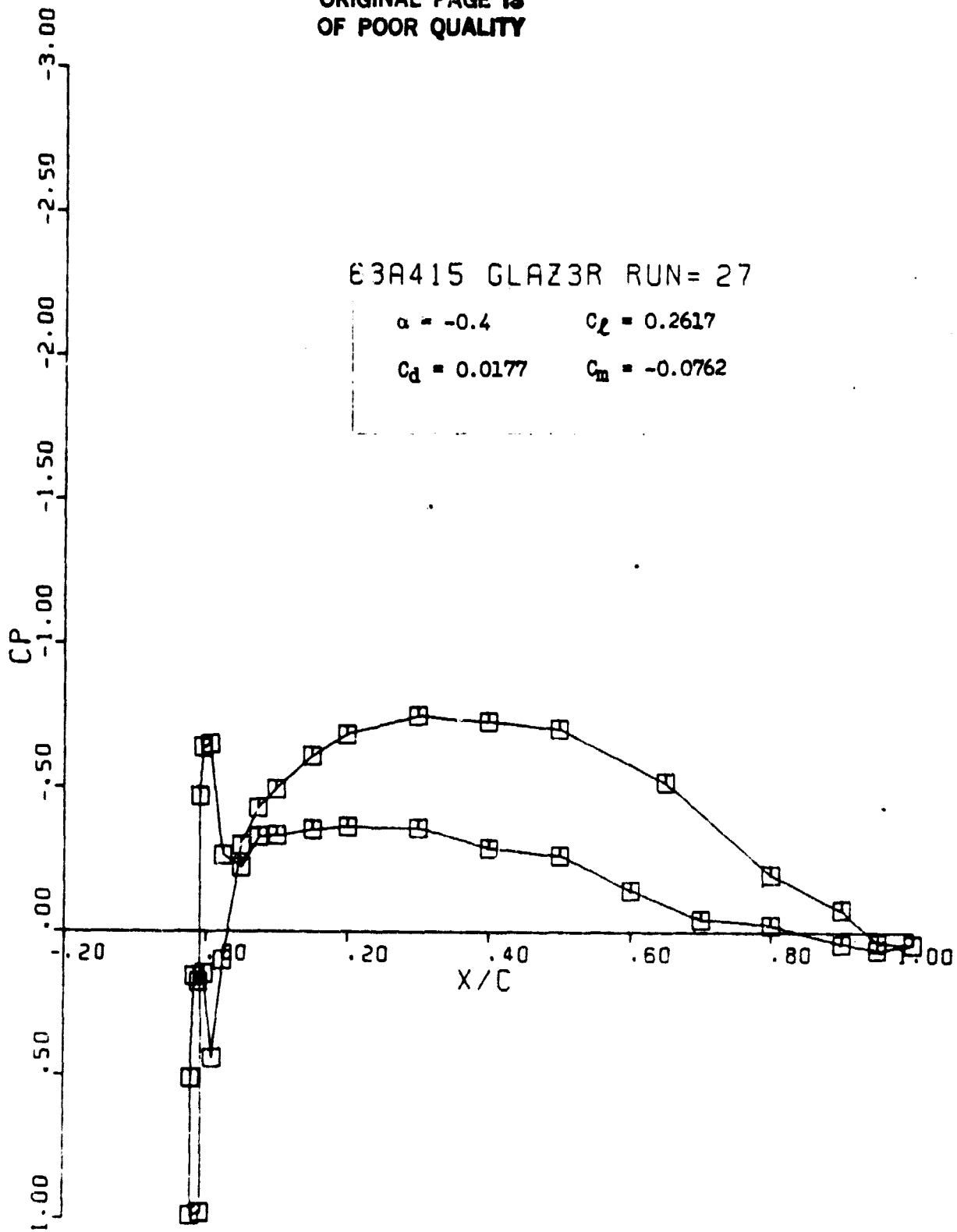
ORIGINAL PAGE IS
OF POOR QUALITY



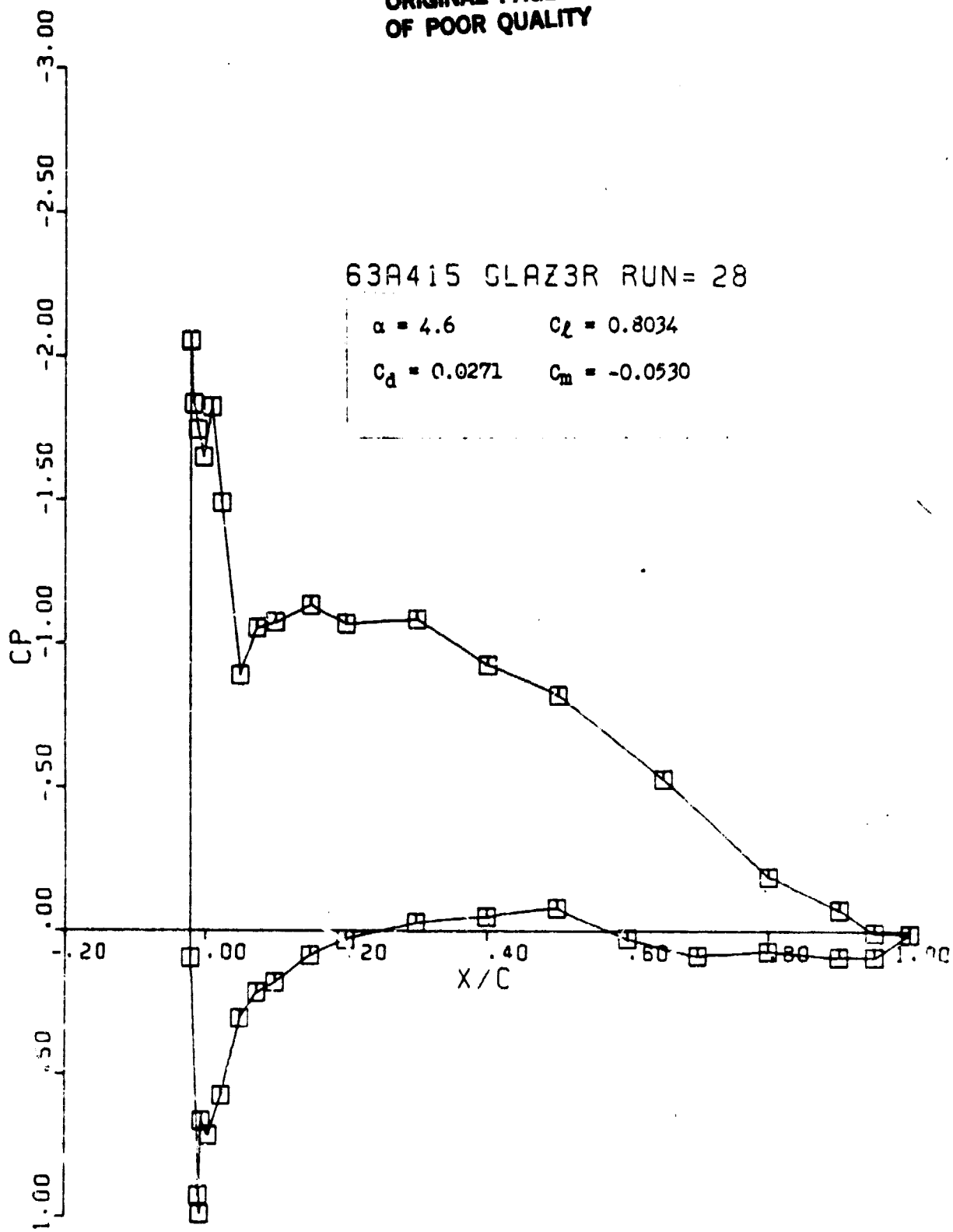
ORIGINAL PAGE IS
OF POOR QUALITY



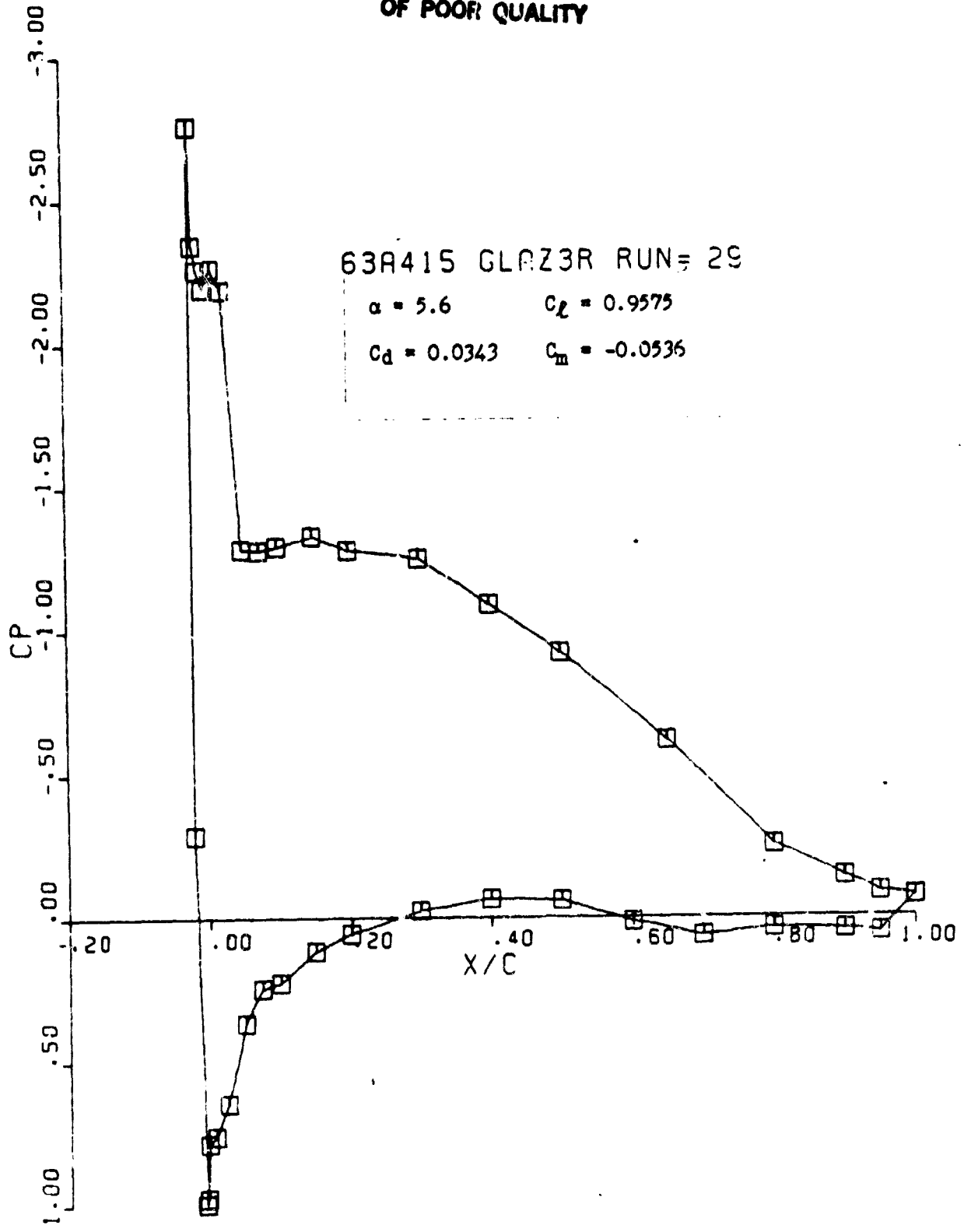
ORIGINAL PAGE IS
OF POOR QUALITY



ORIGINAL PAGE IS
OF POOR QUALITY



ORIGINAL PAGE IS
OF POOR QUALITY



ORIGINAL PAGE IS
OF POOR QUALITY

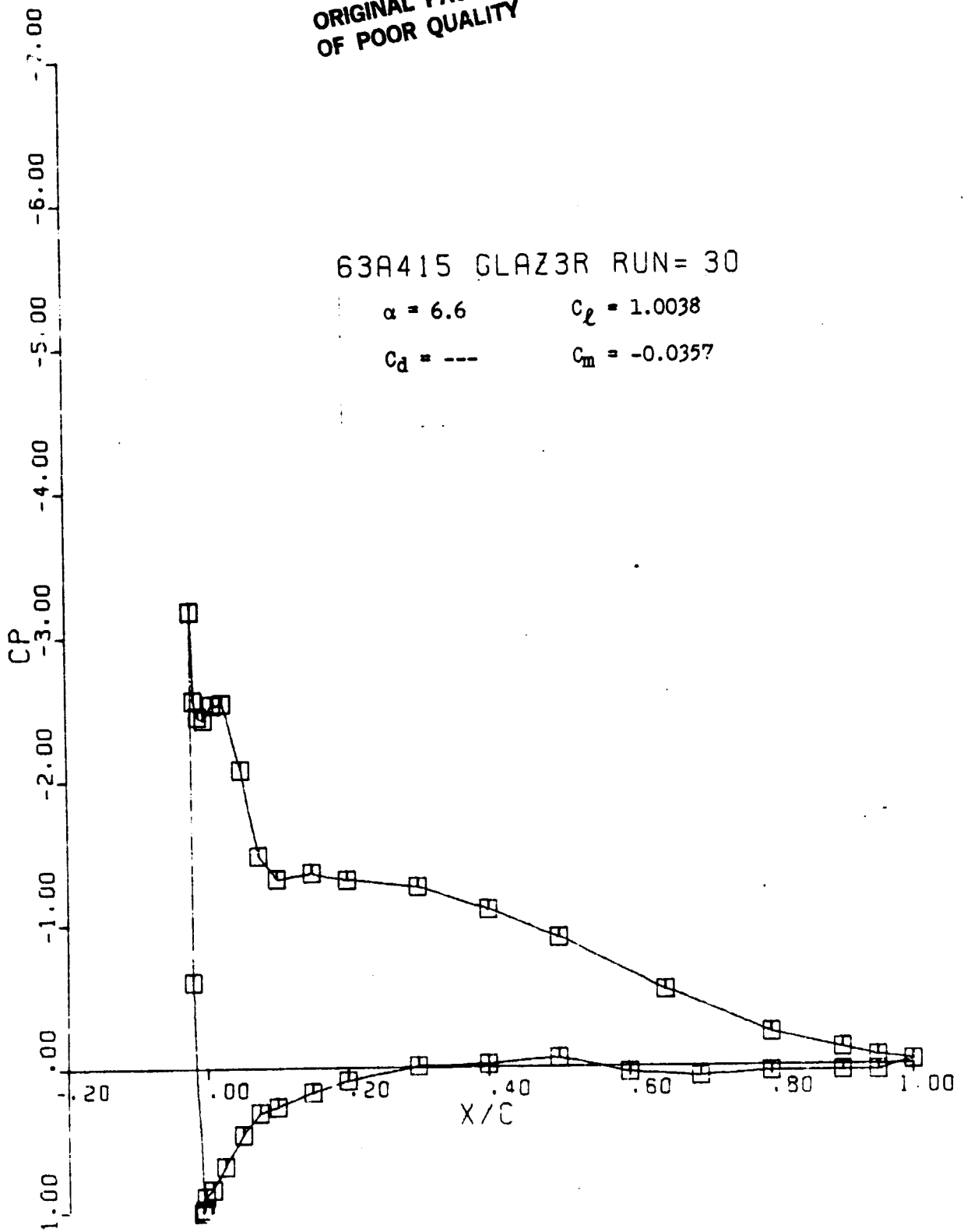
63A415 GLAZ3R RUN= 30

$\alpha = 6.6$

$C_l = 1.0038$

$C_d = \text{---}$

$C_m = -0.0357$



ORIGINAL PAGE IS
OF POOR QUALITY

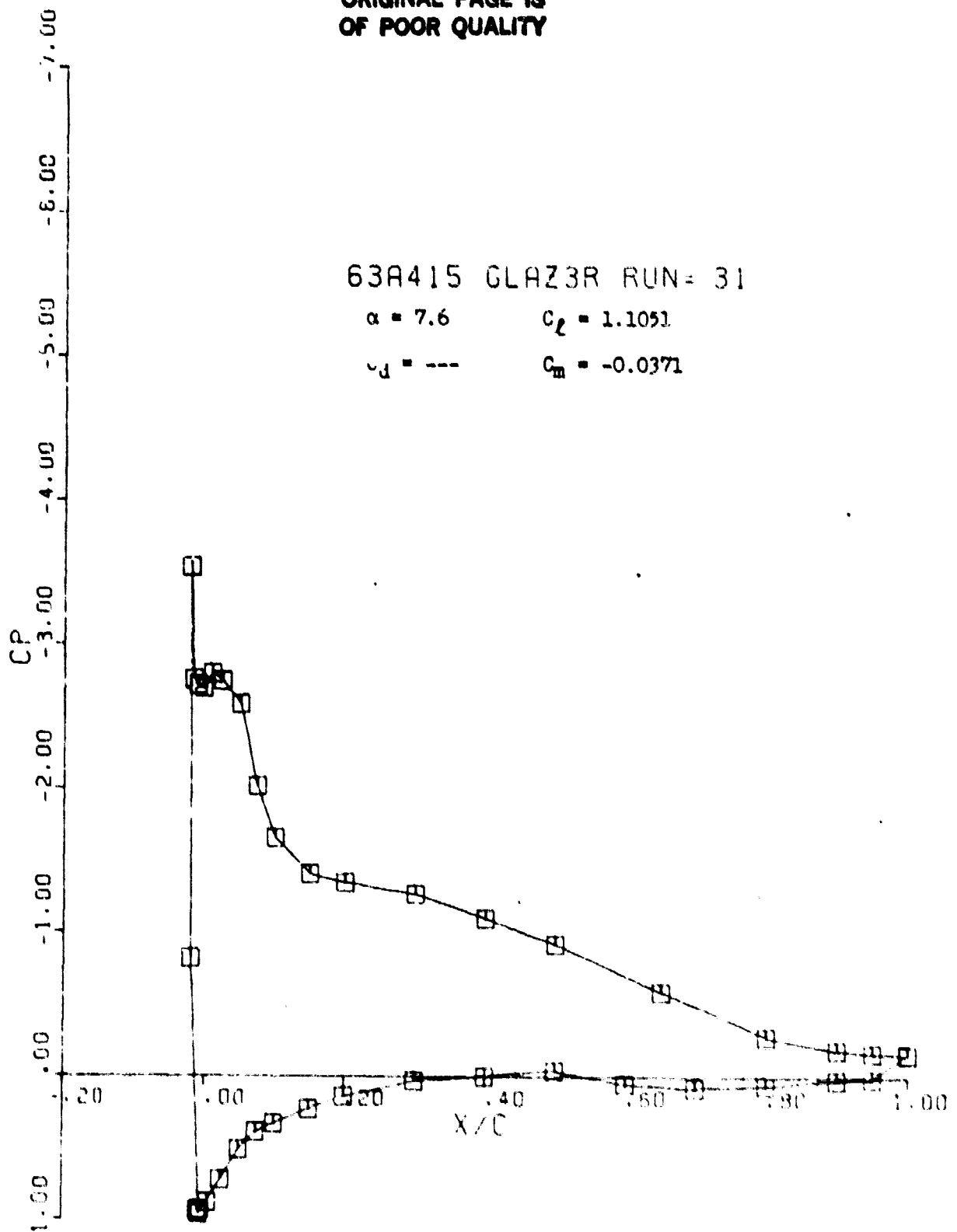
63A415 GLAZER RUN = 31

$\alpha = 7.6$

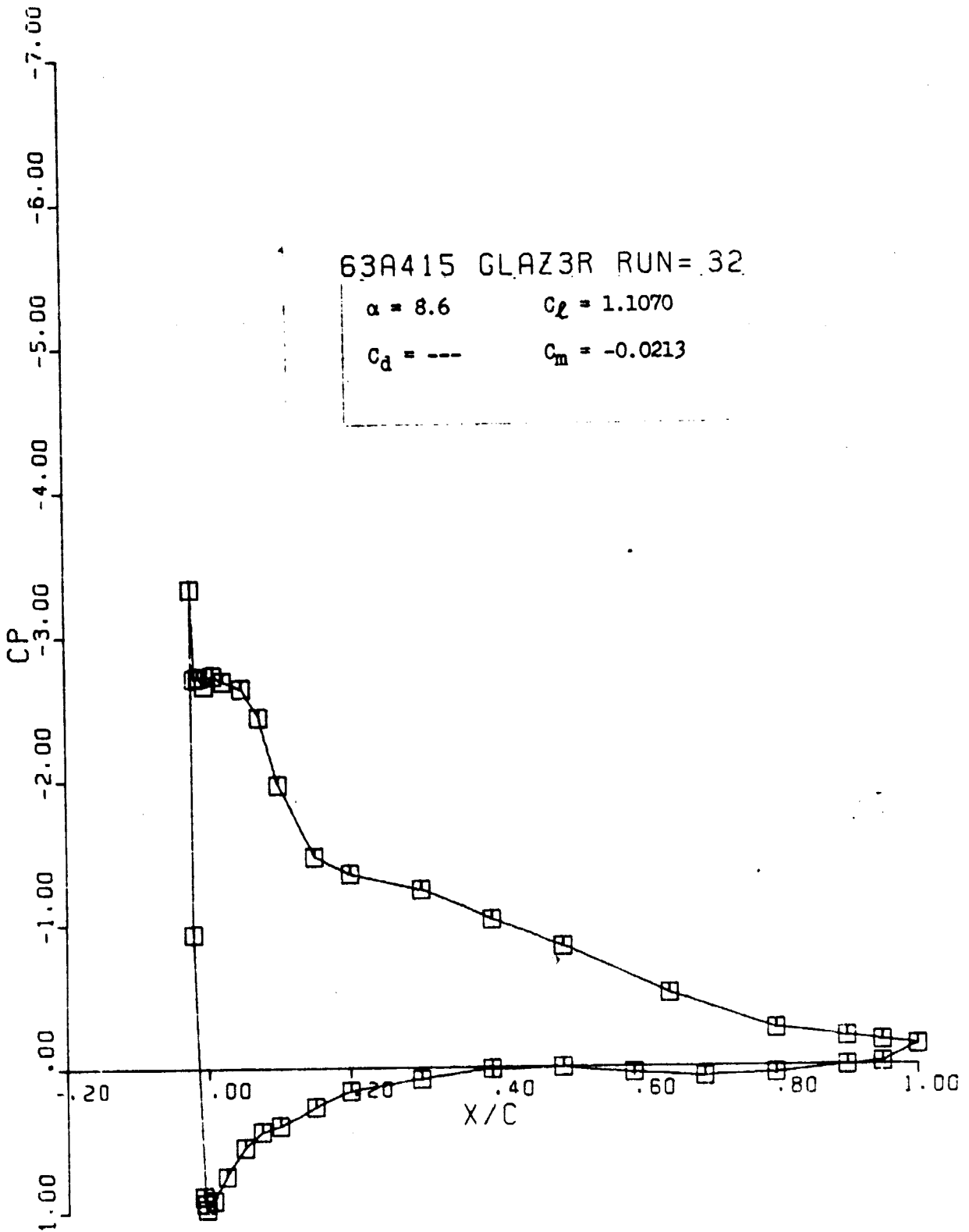
$C_L = 1.1051$

$C_D = \dots$

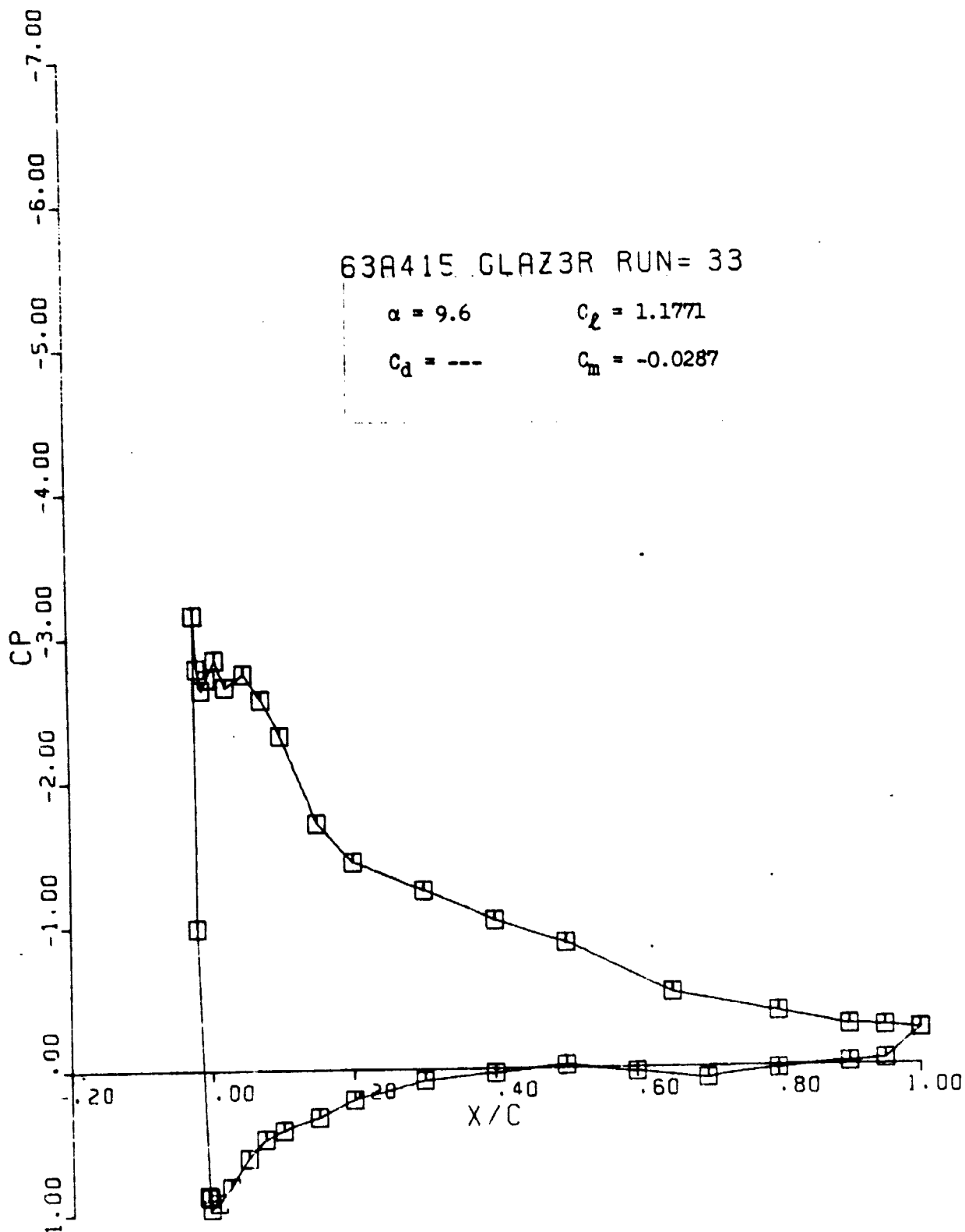
$C_M = -0.0371$



ORIGINAL PAGE IS
OF POOR QUALITY



ORIGINAL PAGE IS
OF POOR QUALITY



ORIGINAL PAGE IS
OF POOR QUALITY.

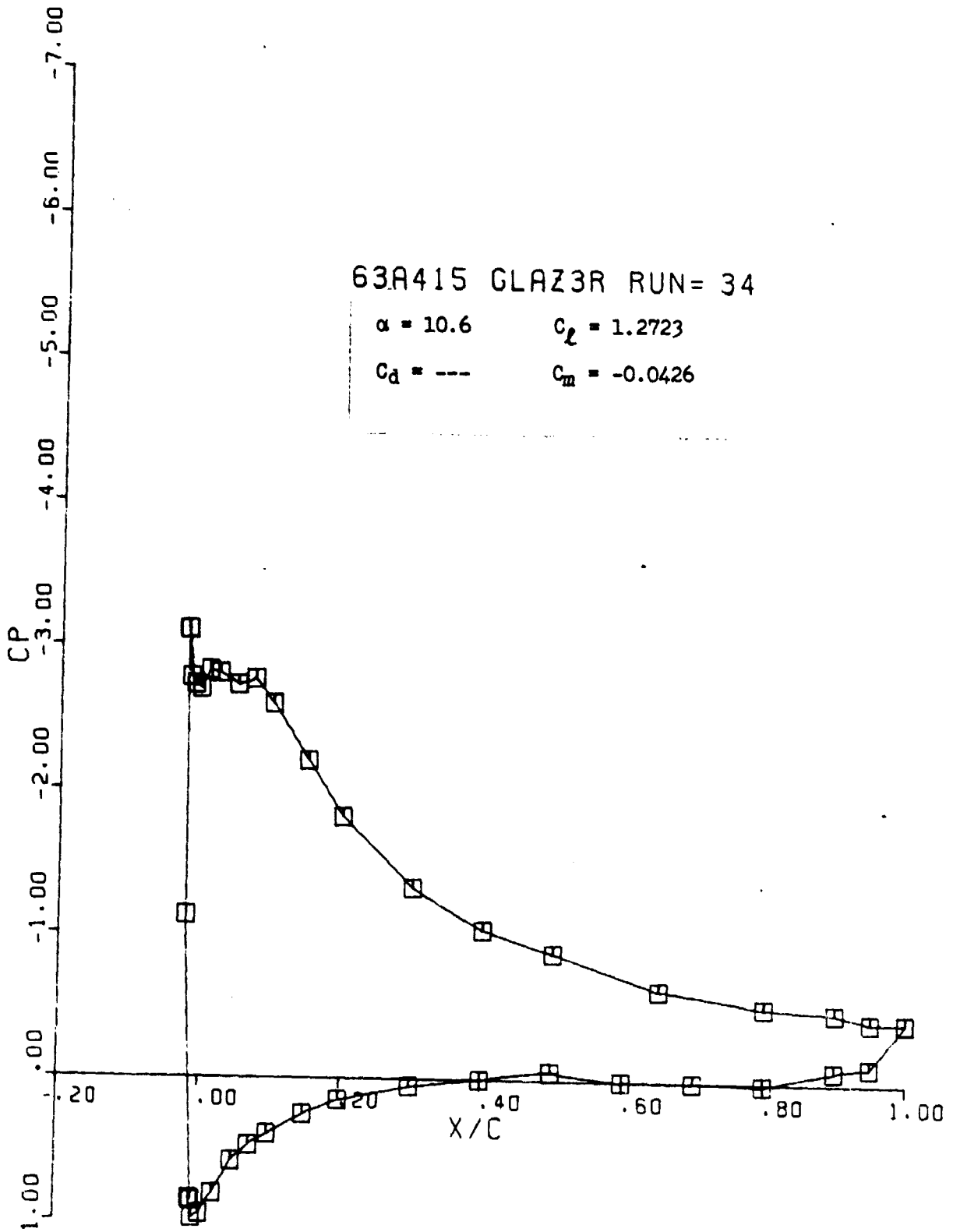
63A415 GLAZ3R RUN= 34

$\alpha = 10.6$

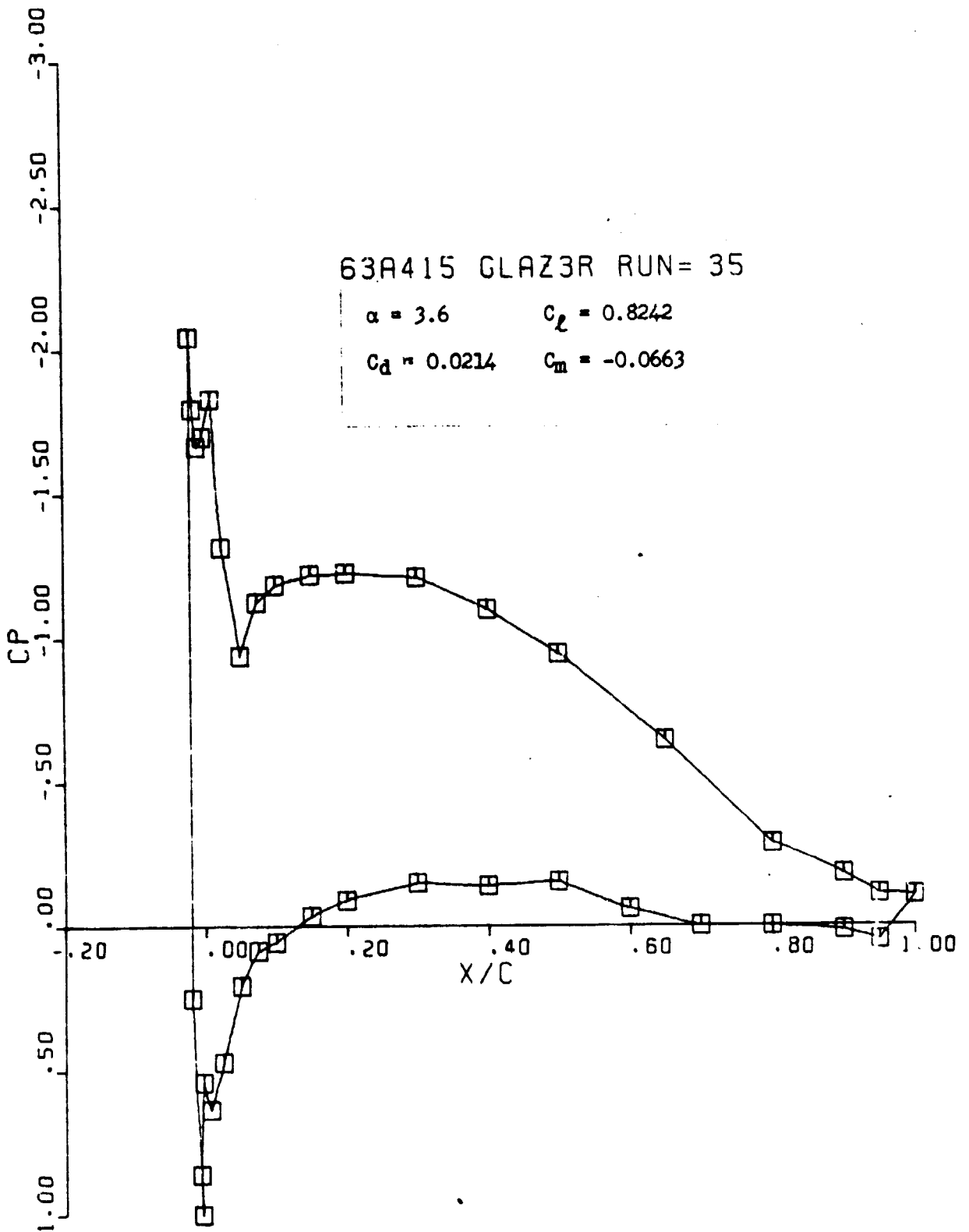
$C_L = 1.2723$

$C_d = \text{---}$

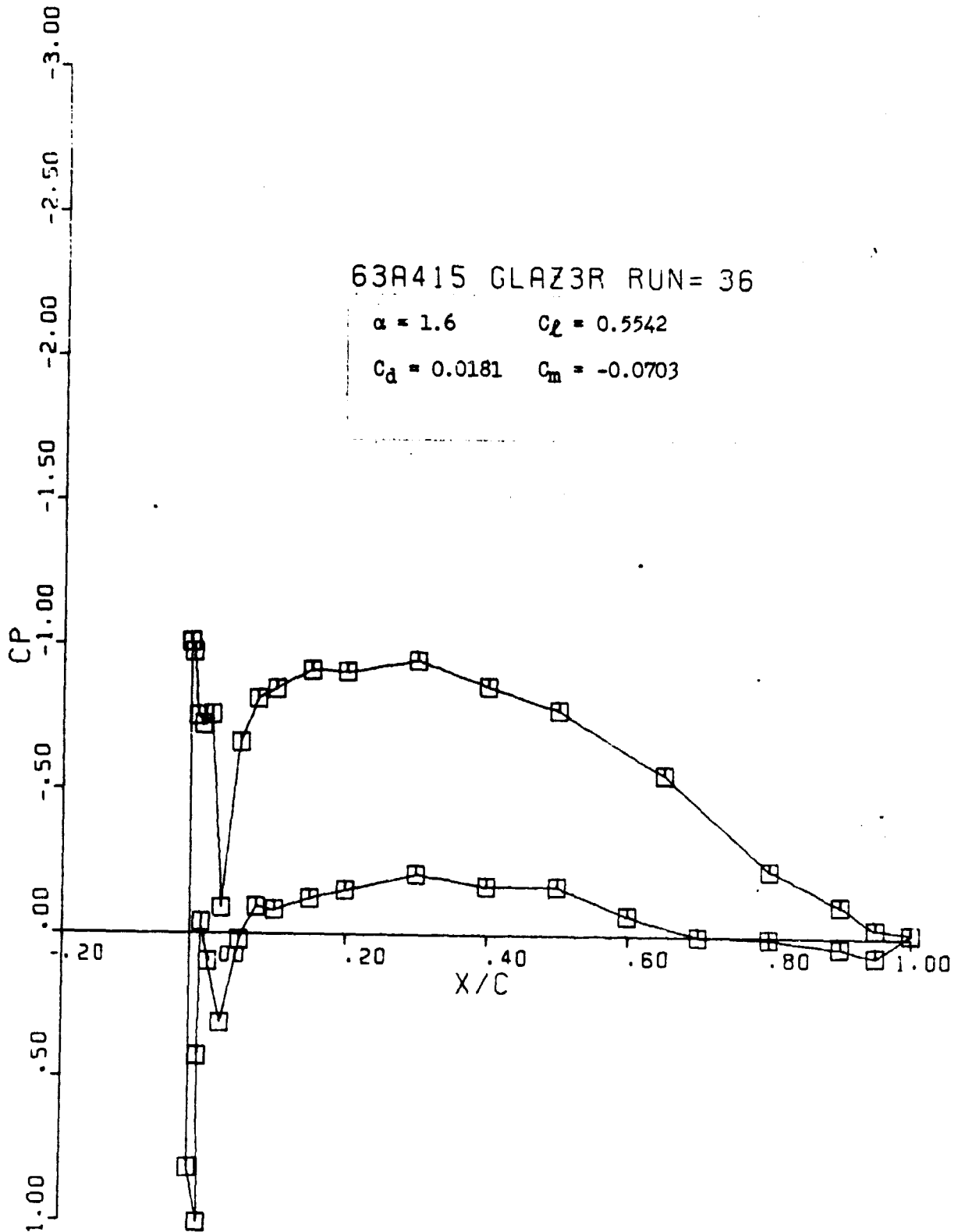
$C_m = -0.0426$



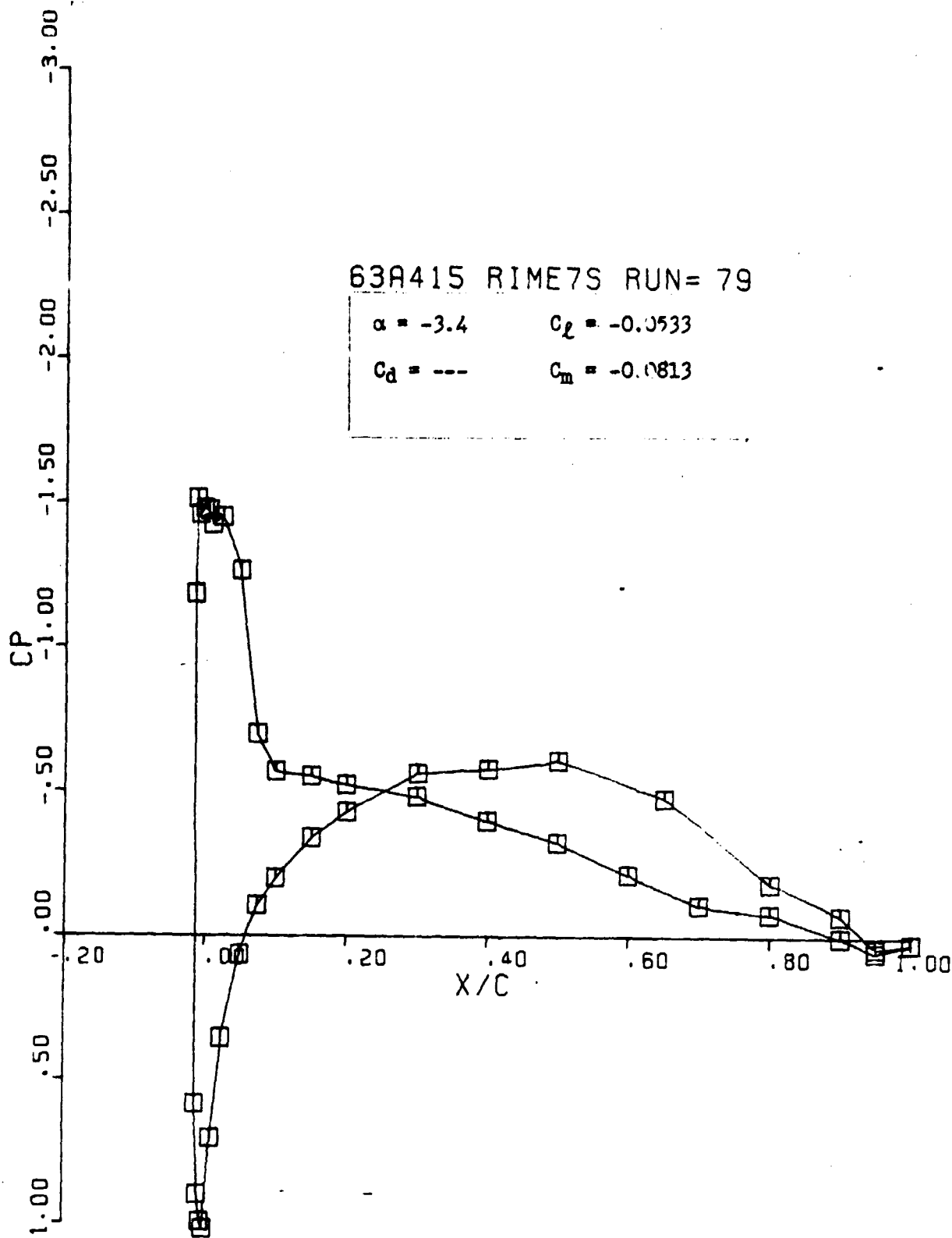
ORIGINAL PAGE IS
OF POOR QUALITY



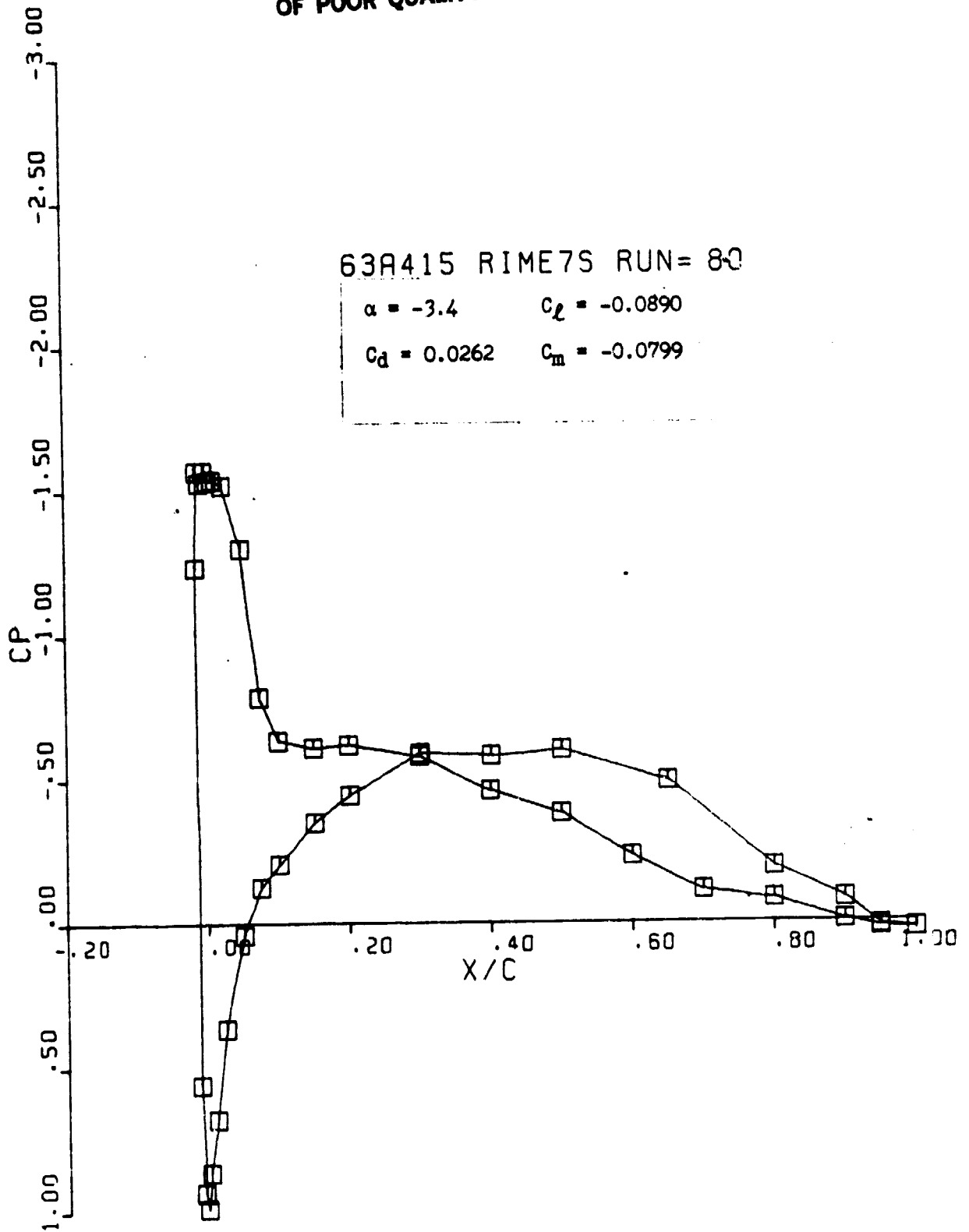
ORIGINAL PAGE IS
OF POOR QUALITY



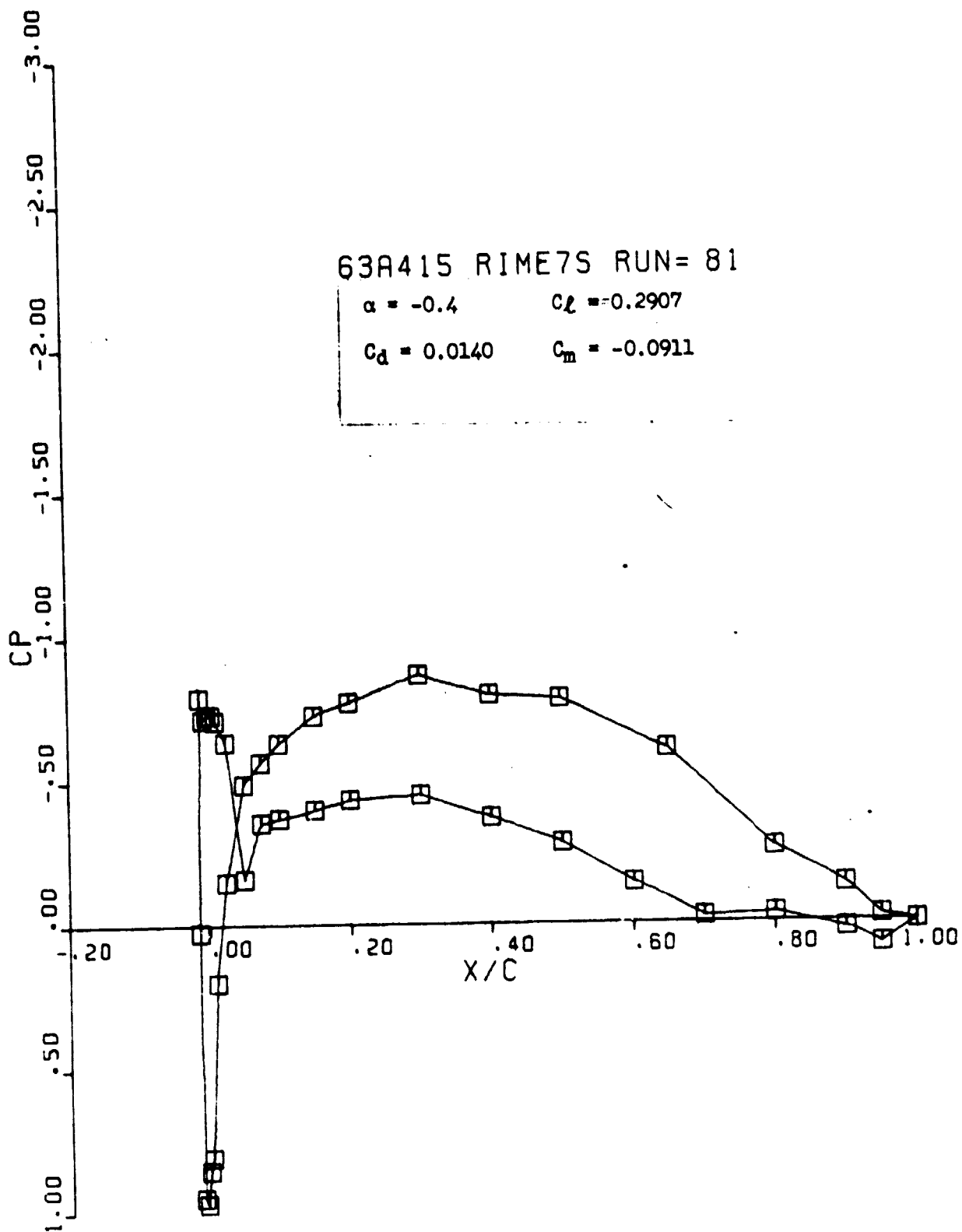
ORIGINAL PAGE IS
OF POOR QUALITY



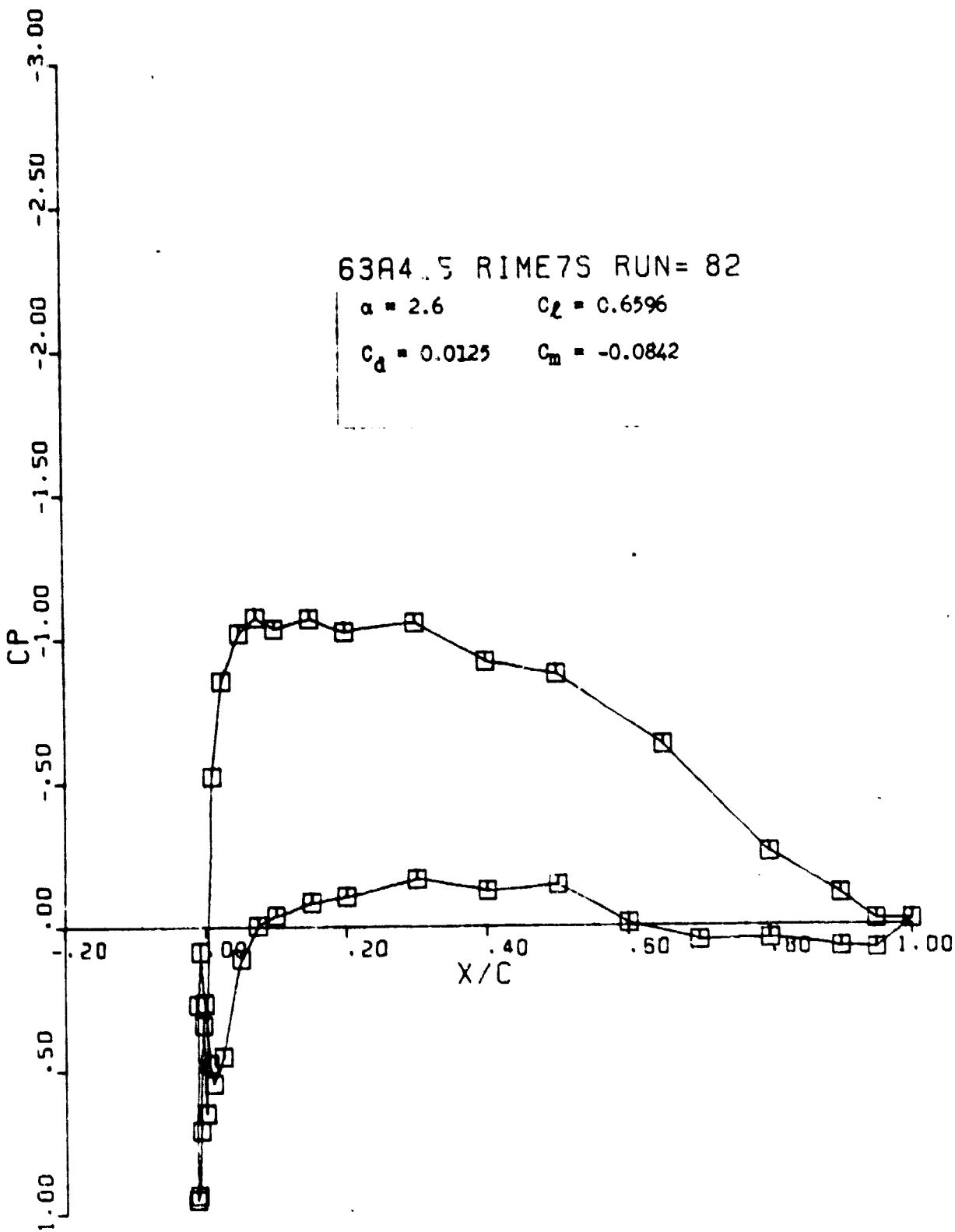
ORIGINAL PAGE IS
OF POOR QUALITY



ORIGINAL PAGE IS
OF POOR QUALITY



ORIGINAL PAGE IS
OF POOR QUALITY



ORIGINAL PAGE IS
OF POOR QUALITY

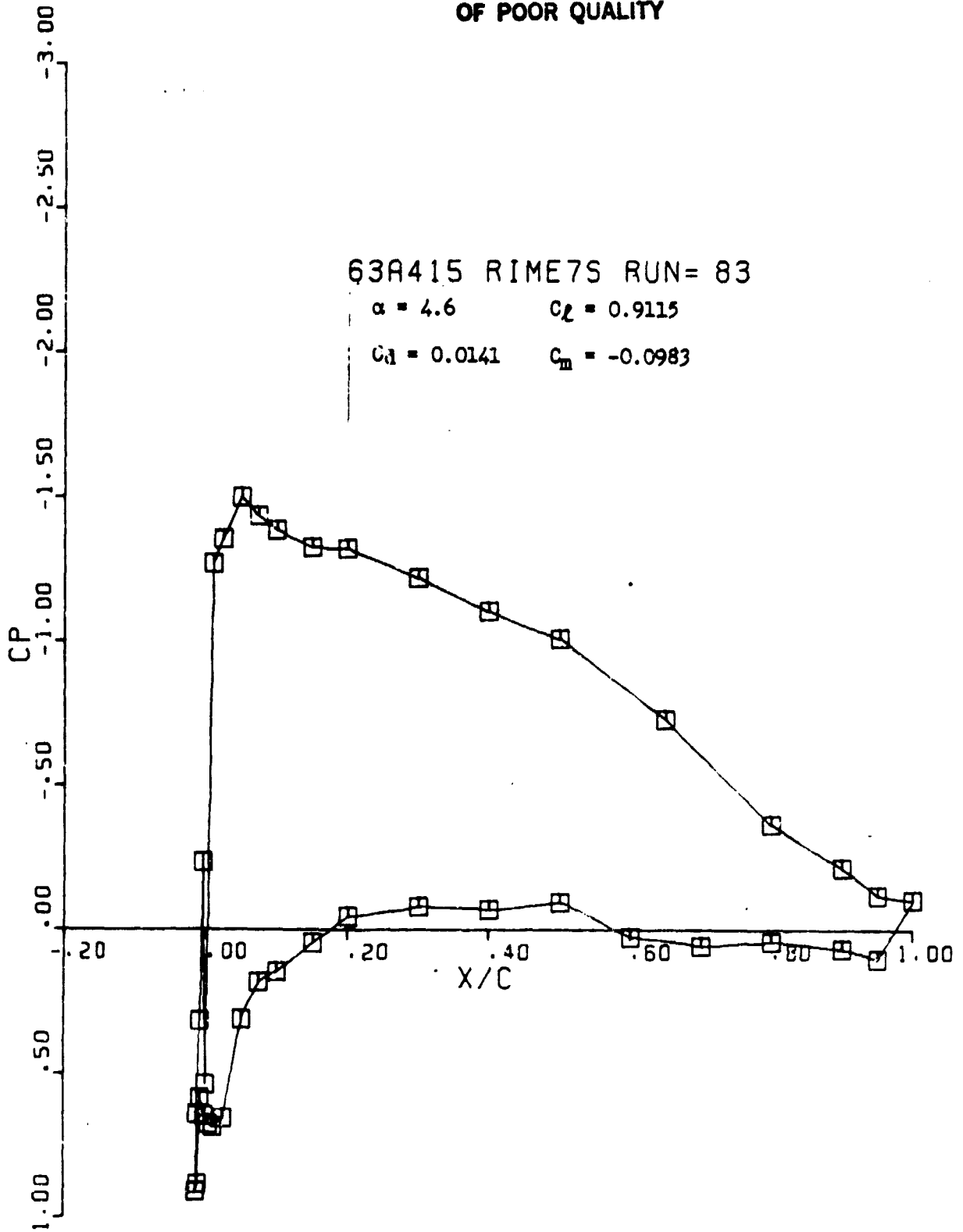
63A415 RIME7S RUN= 83

$\alpha = 4.6$

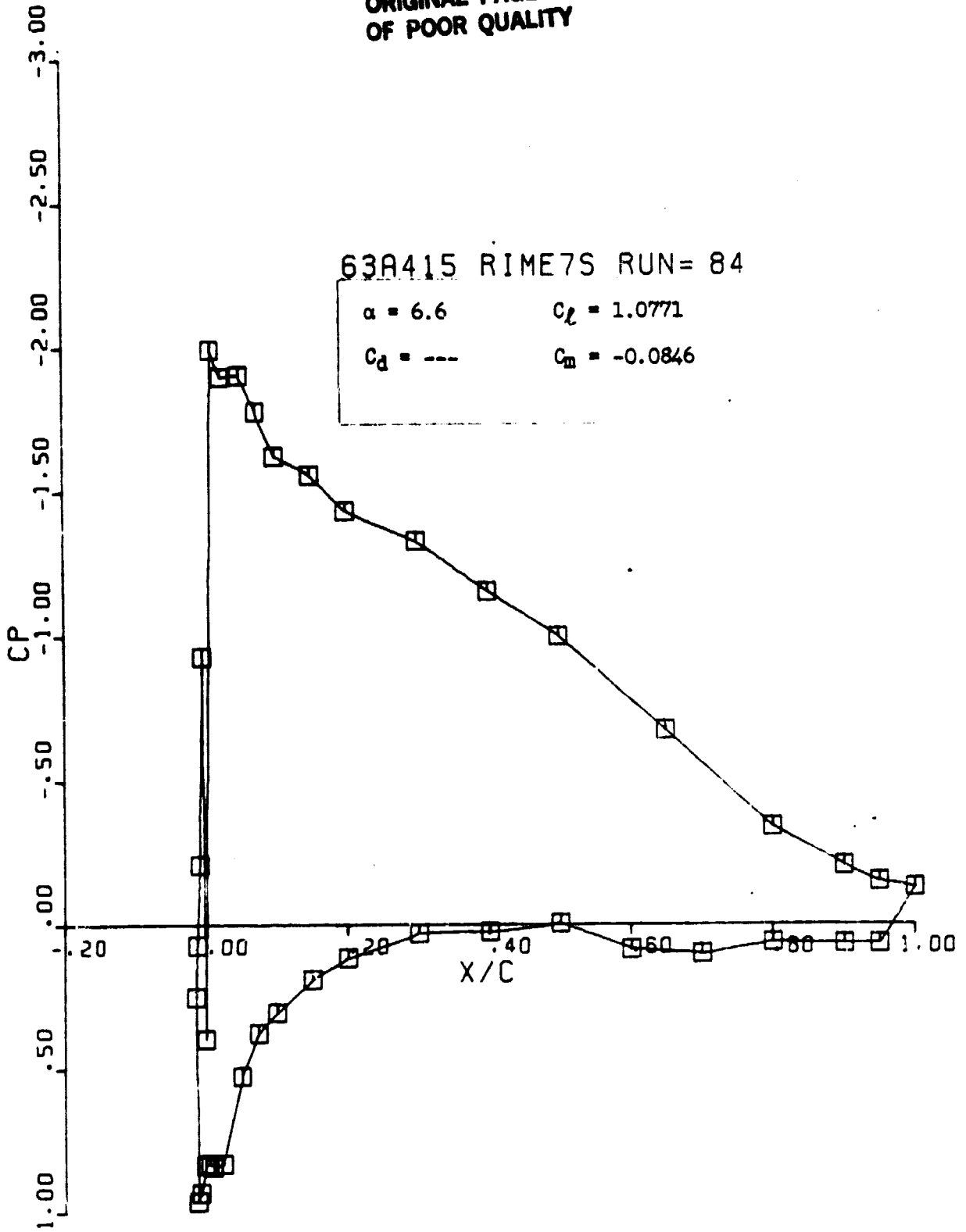
$C_L = 0.9115$

$C_D = 0.0141$

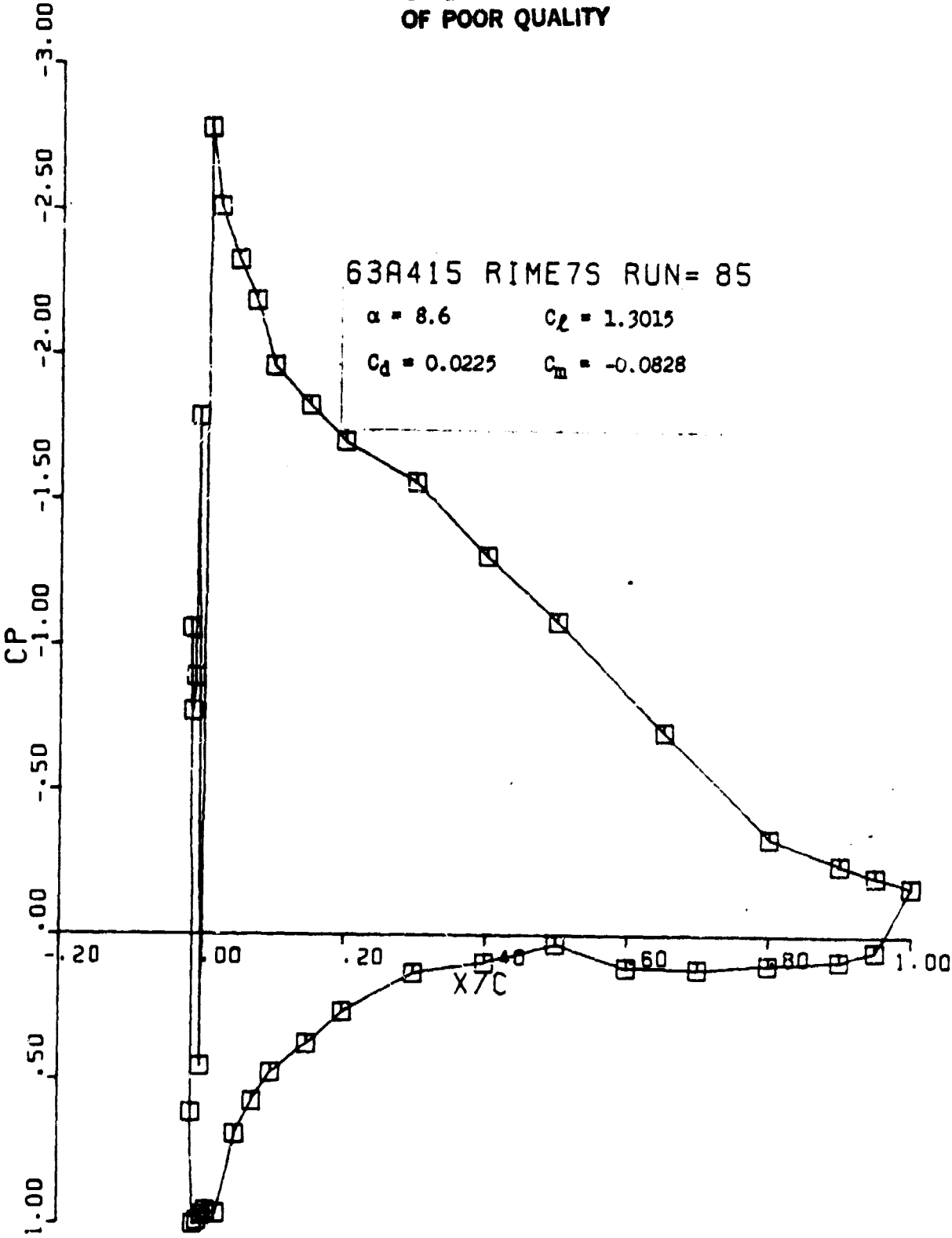
$C_M = -0.0983$



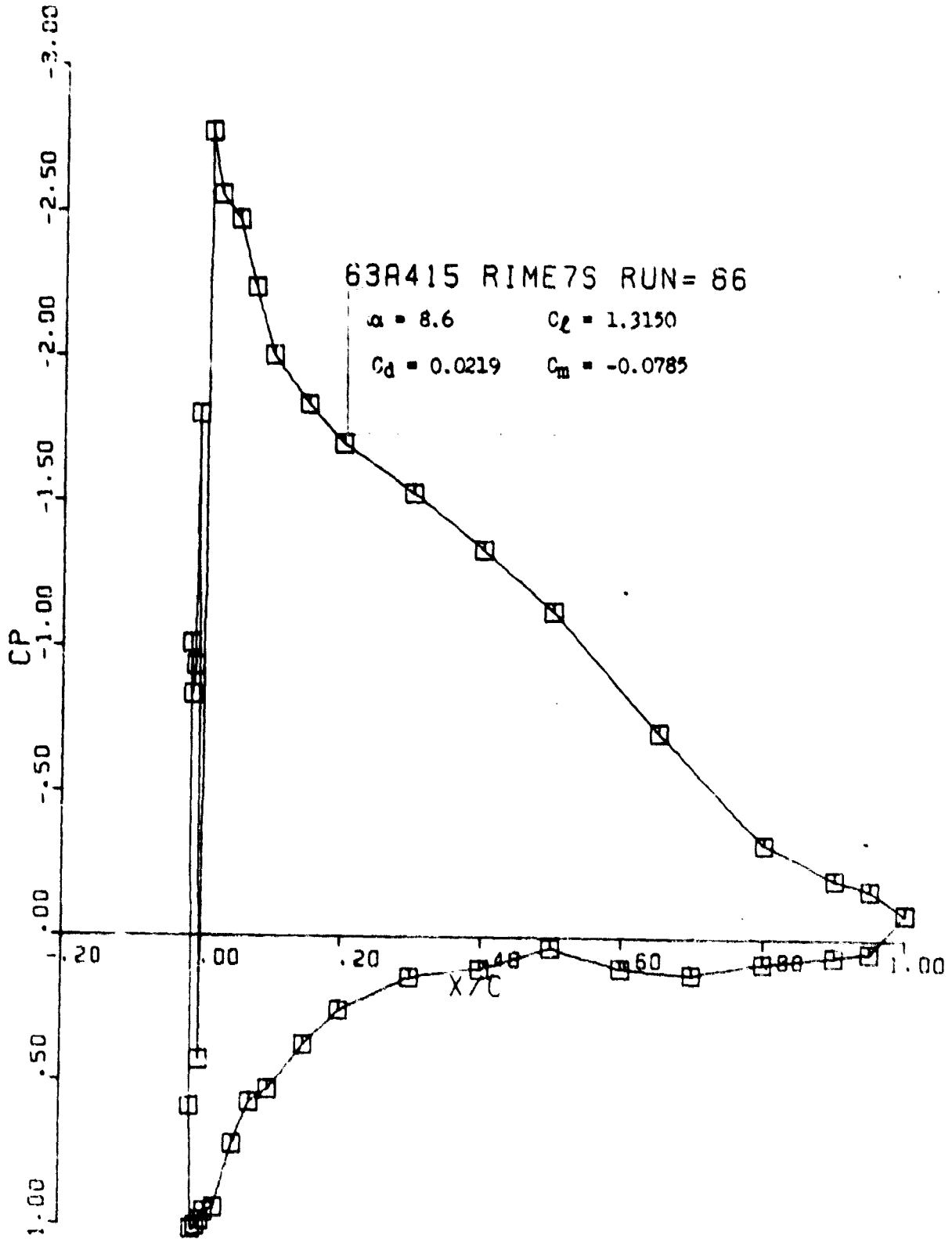
ORIGINAL PAGE IS
OF POOR QUALITY



ORIGINAL PAGE 13
OF POOR QUALITY



ORIGINAL PAGE IS
OF POOR QUALITY

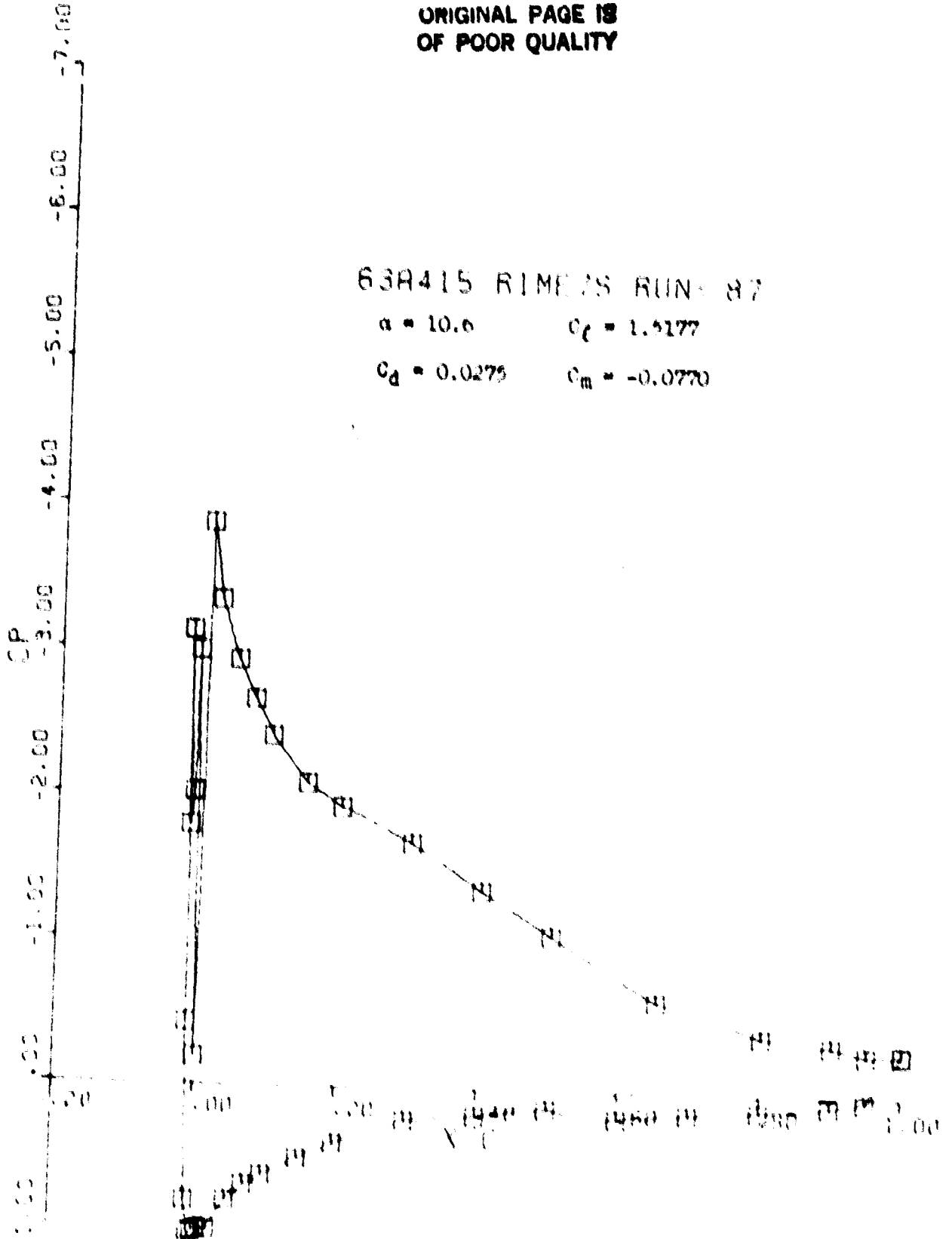


ORIGINAL PAGE IS
OF POOR QUALITY

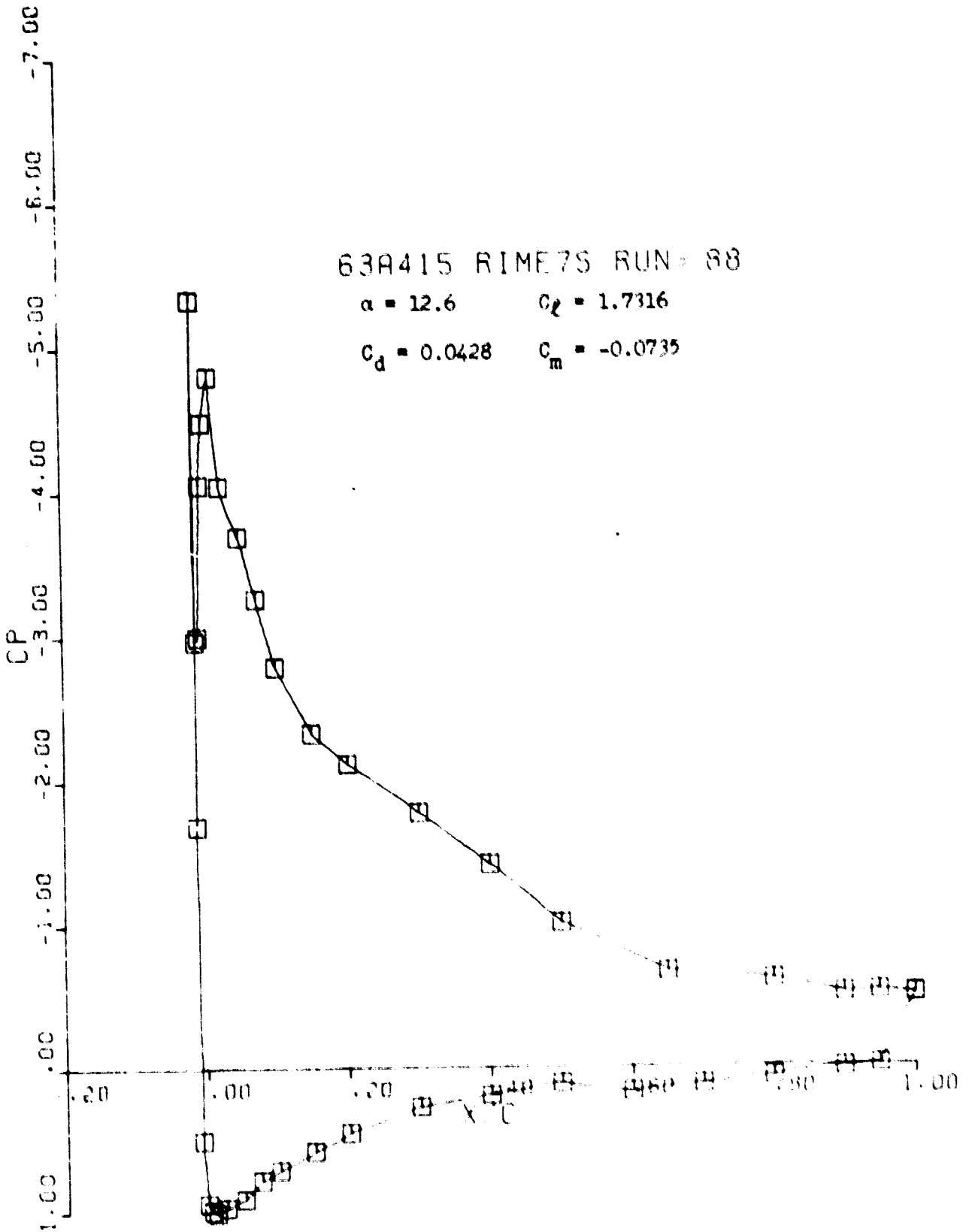
63R415 RIME 25 RUN 87

$\alpha = 10.6$ $C_L = 1.5177$

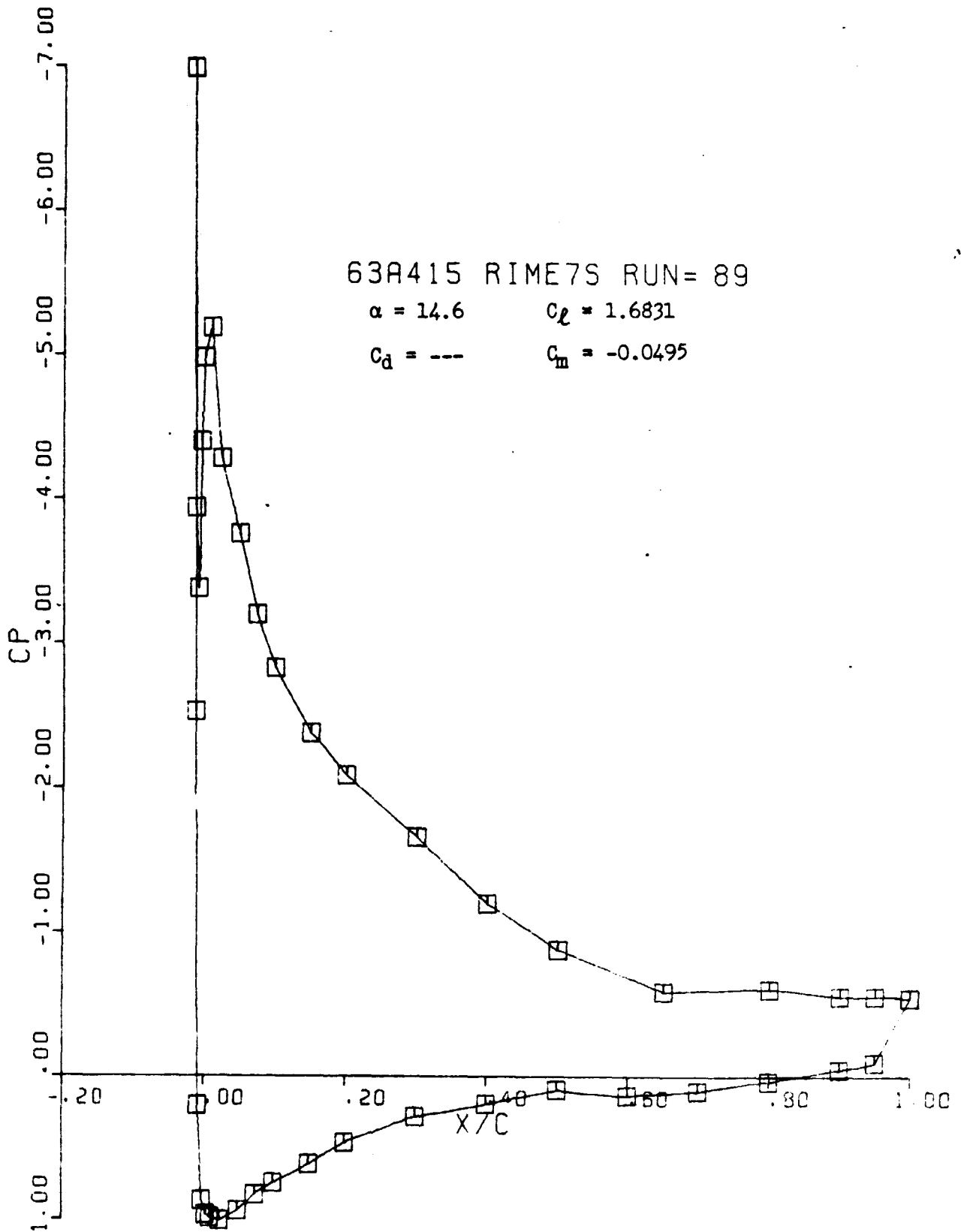
$C_d = 0.0275$ $C_m = -0.0770$



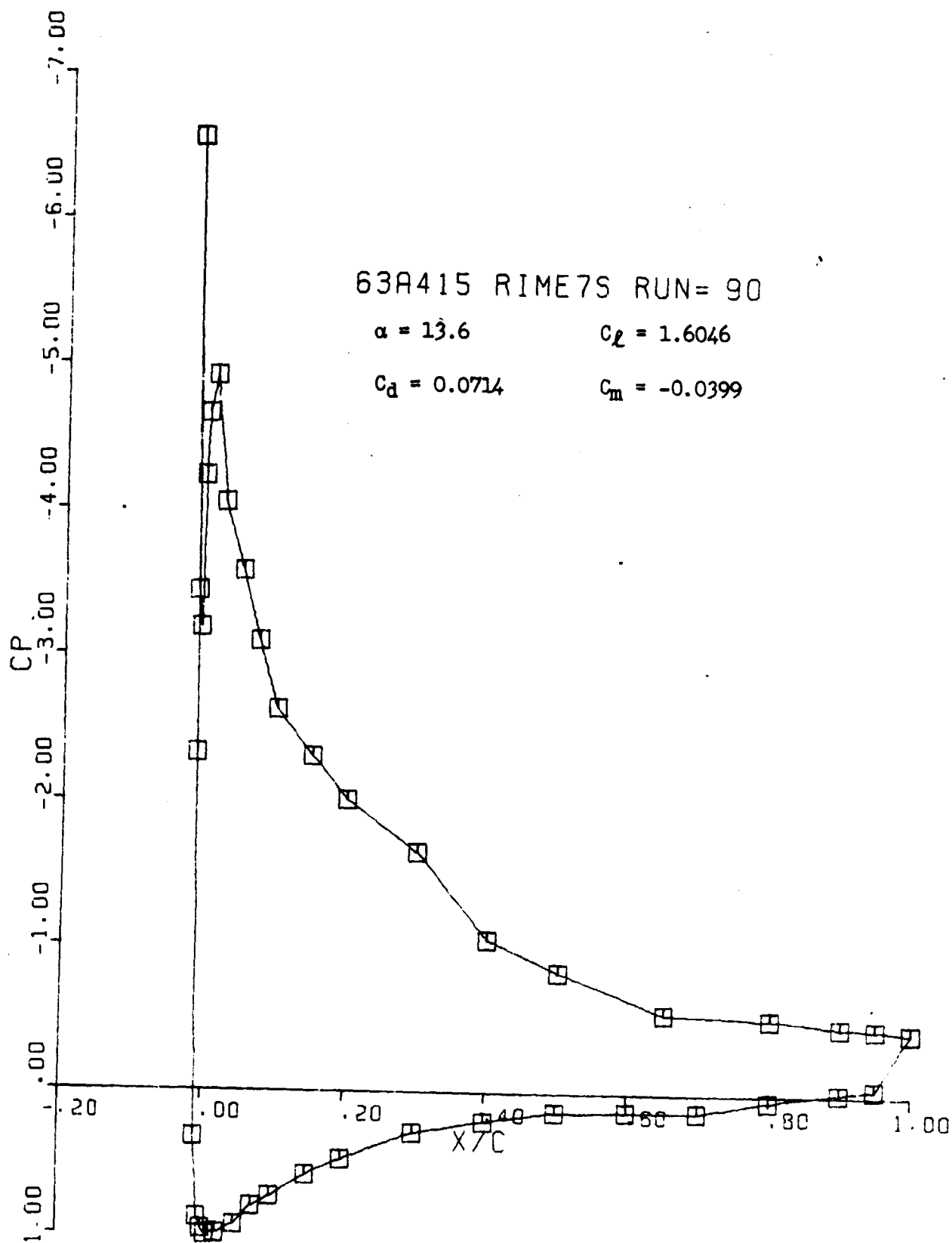
ORIGINAL PAGE IS
OF POOR QUALITY



ORIGINAL PAGE IS
OF POOR QUALITY



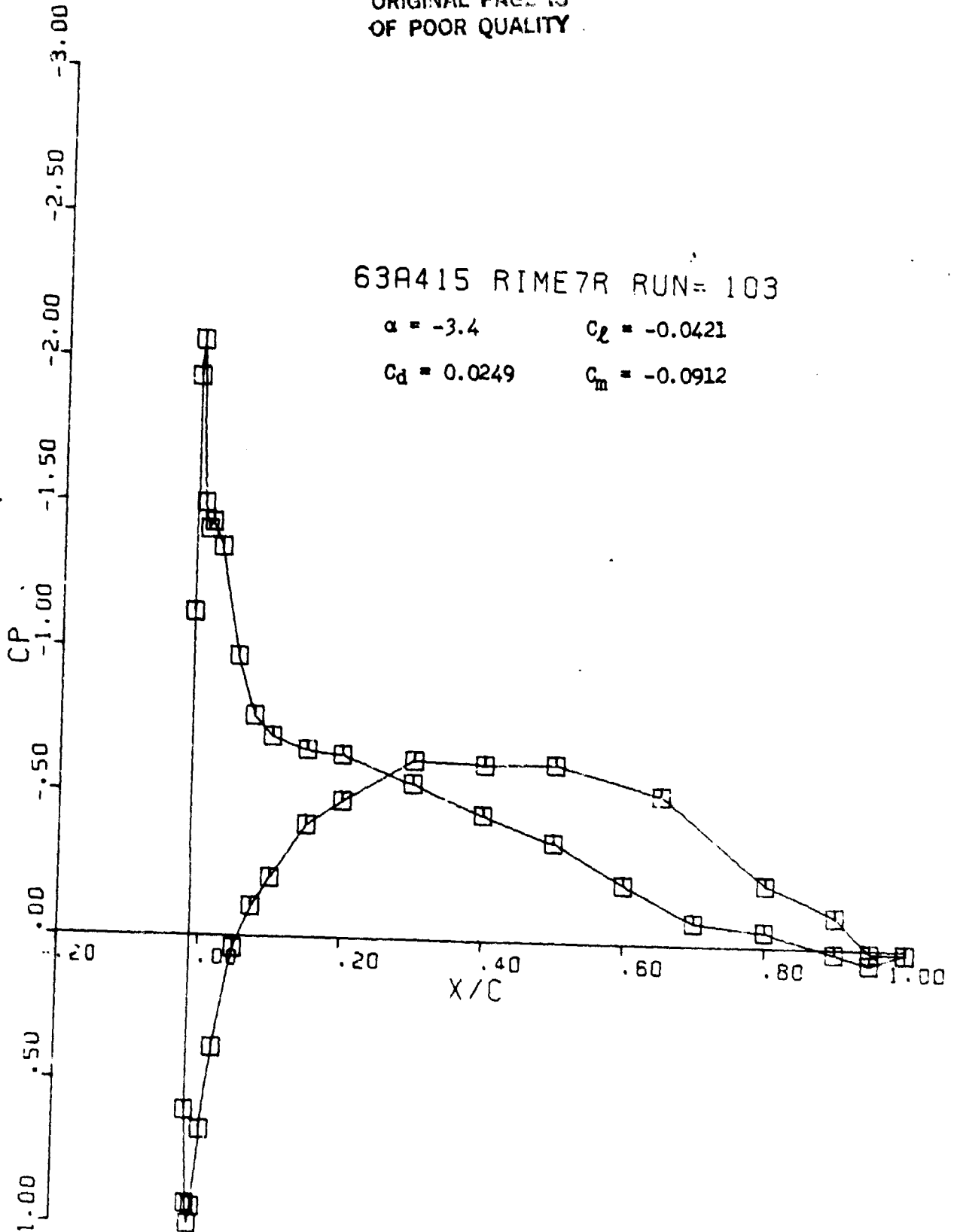
ORIGINAL PAGE IS
OF POOR QUALITY



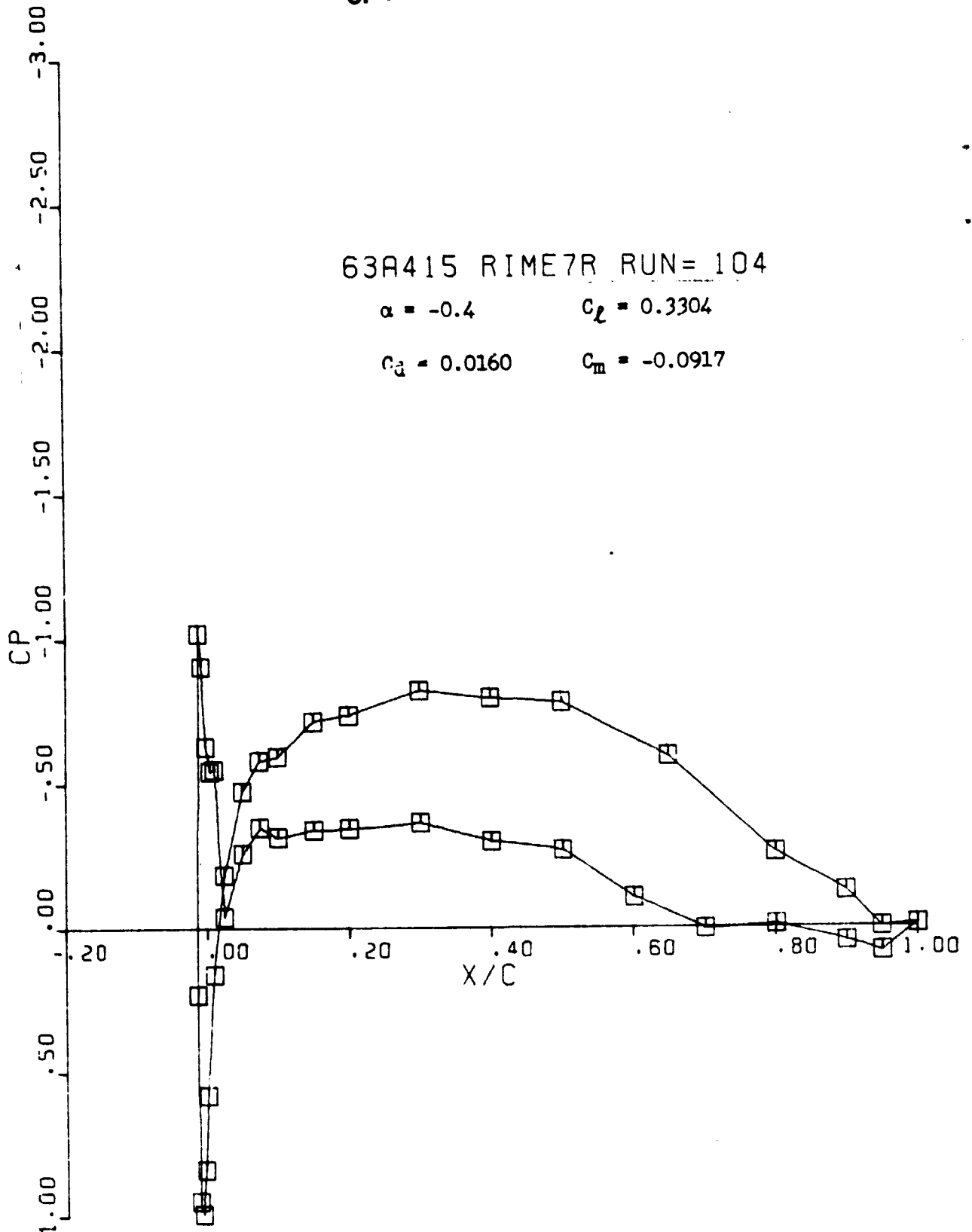
ORIGINAL PAGE IS
OF POOR QUALITY

63A415 RIME7R RUN= 103

$\alpha = -3.4$ $C_l = -0.0421$
 $C_d = 0.0249$ $C_m = -0.0912$



ORIGINAL PAGE IS
OF POOR QUALITY



ORIGINAL PAGE IS
OF POOR QUALITY

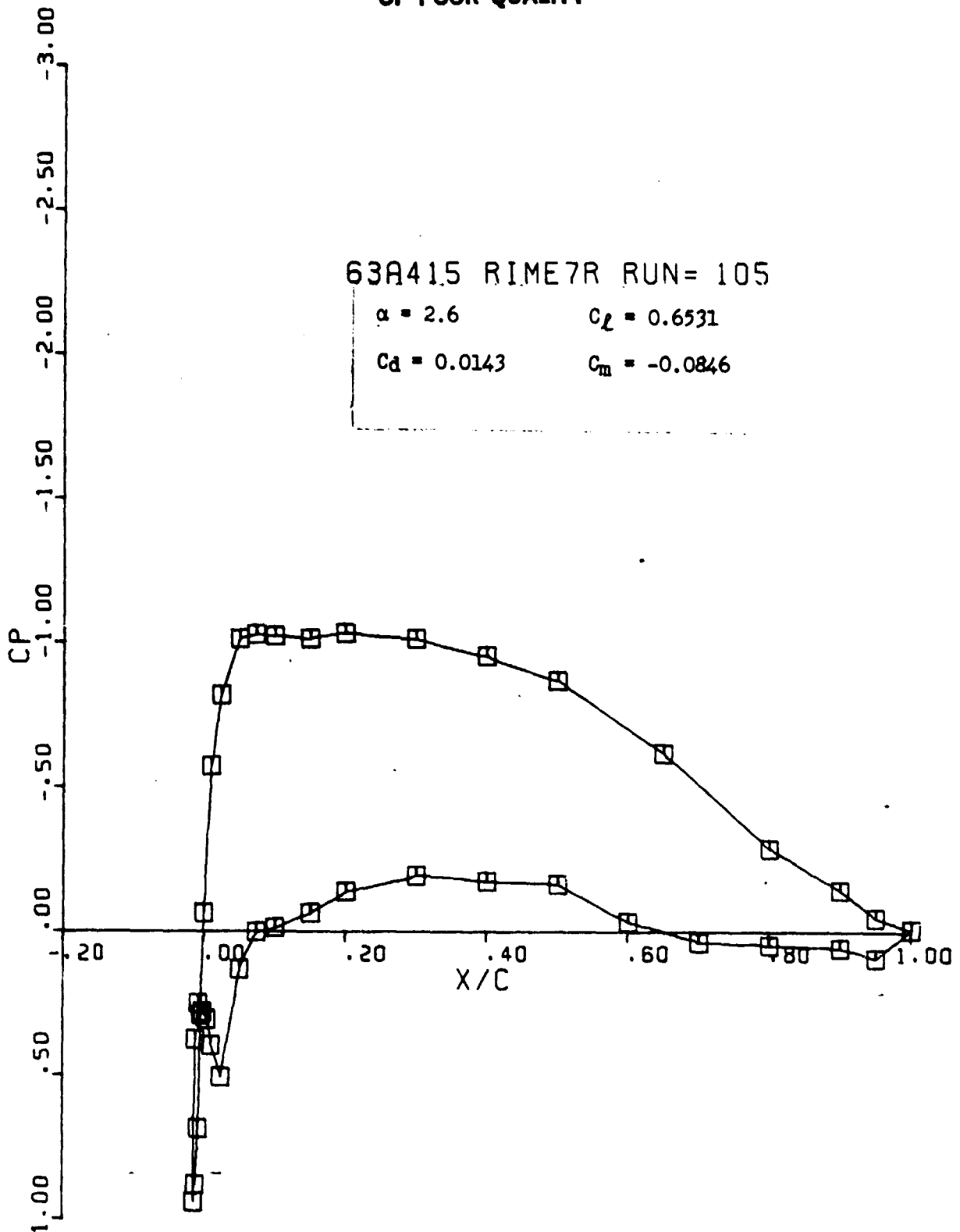
63A415 RIME7R RUN= 105

$\alpha = 2.6$

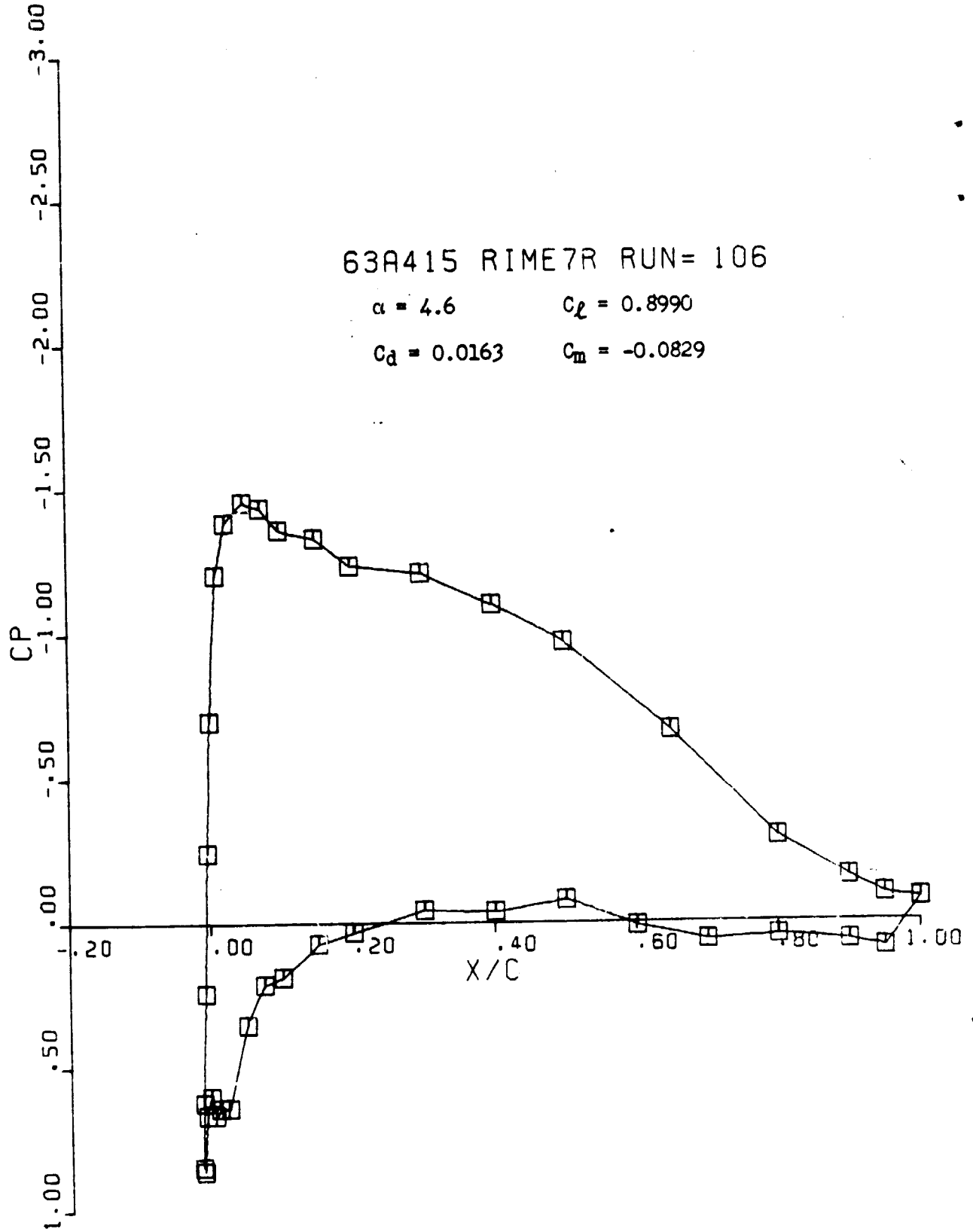
$C_l = 0.6531$

$C_d = 0.0143$

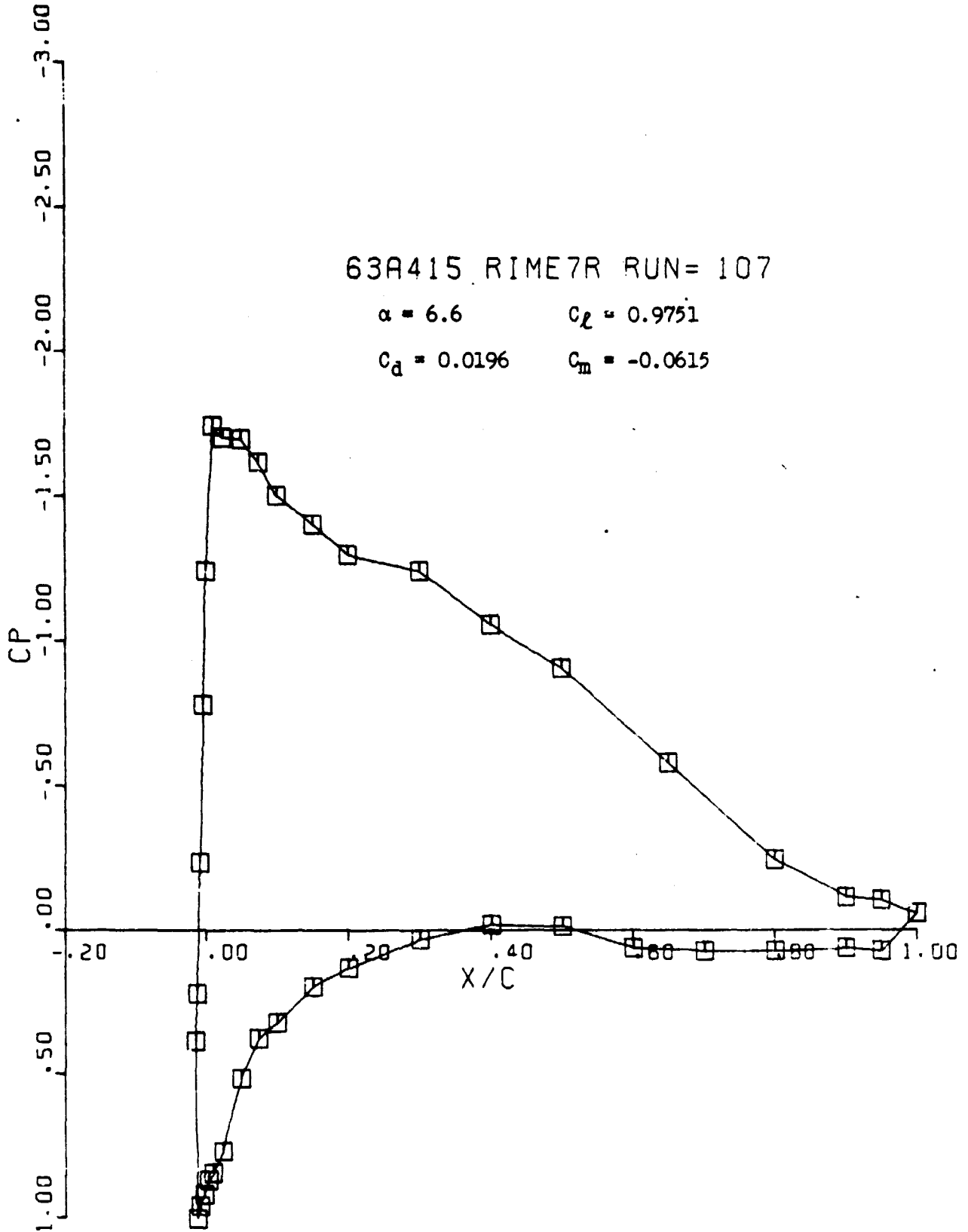
$C_m = -0.0846$



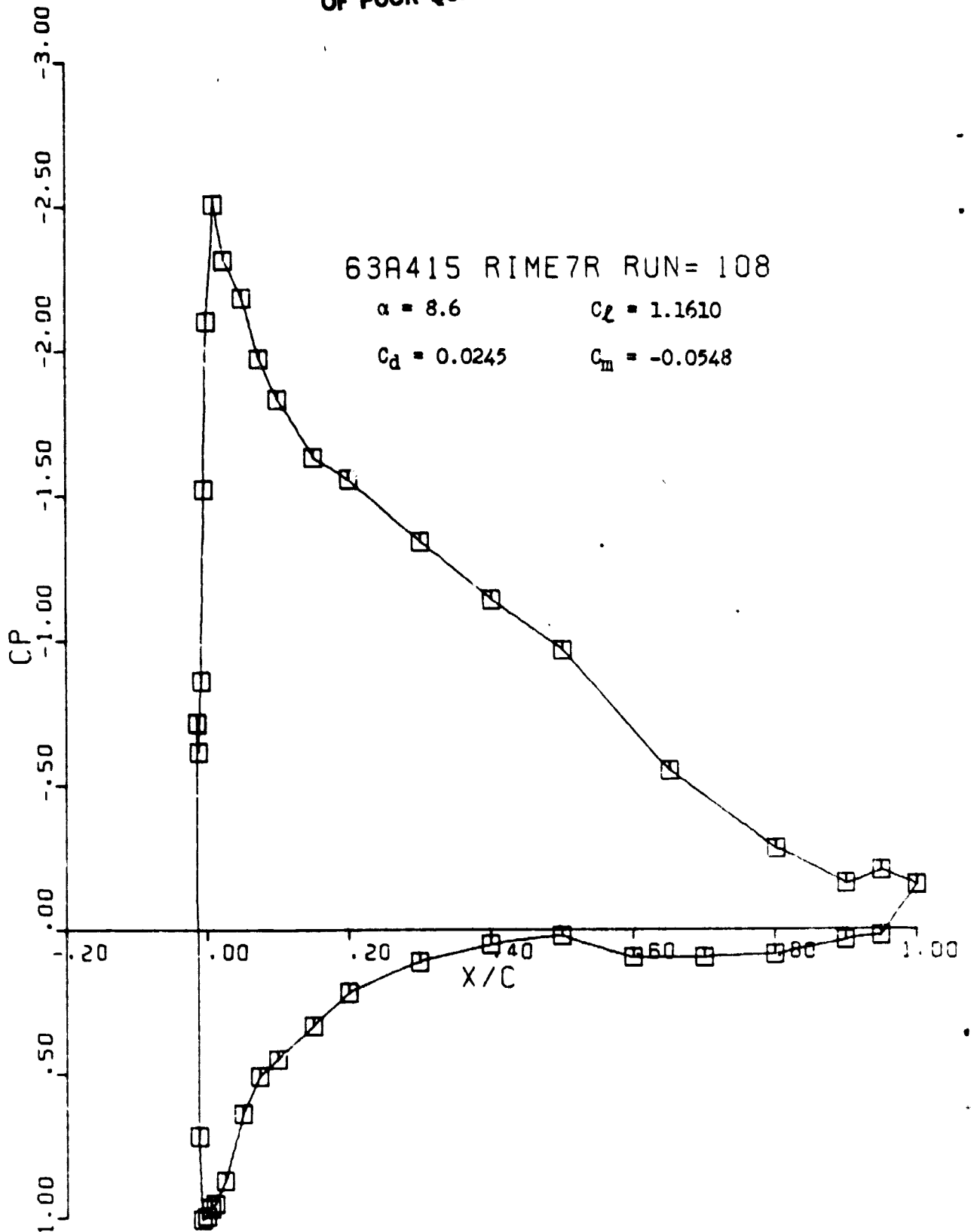
ORIGINAL PAGE IS
OF POOR QUALITY



ORIGINAL PAGE IS
OF POOR QUALITY



ORIGINAL PAGE IS
OF POOR QUALITY



ORIGINAL PAGE IS
OF POOR QUALITY

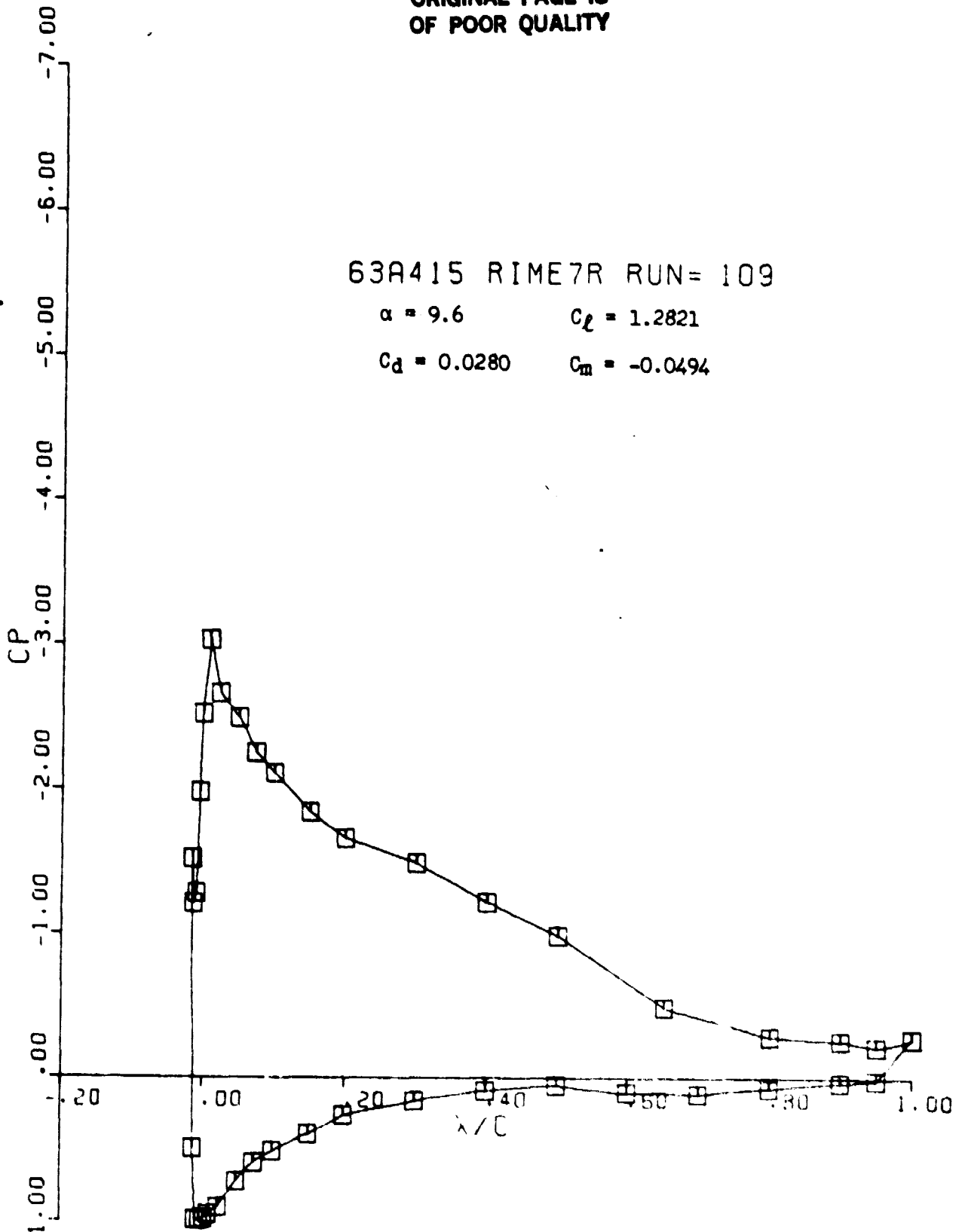
63A415 RIME7R RUN= 109

$\alpha = 9.6$

$C_l = 1.2821$

$C_d = 0.0280$

$C_m = -0.0494$



ORIGINAL PAGE IS
OF POOR QUALITY

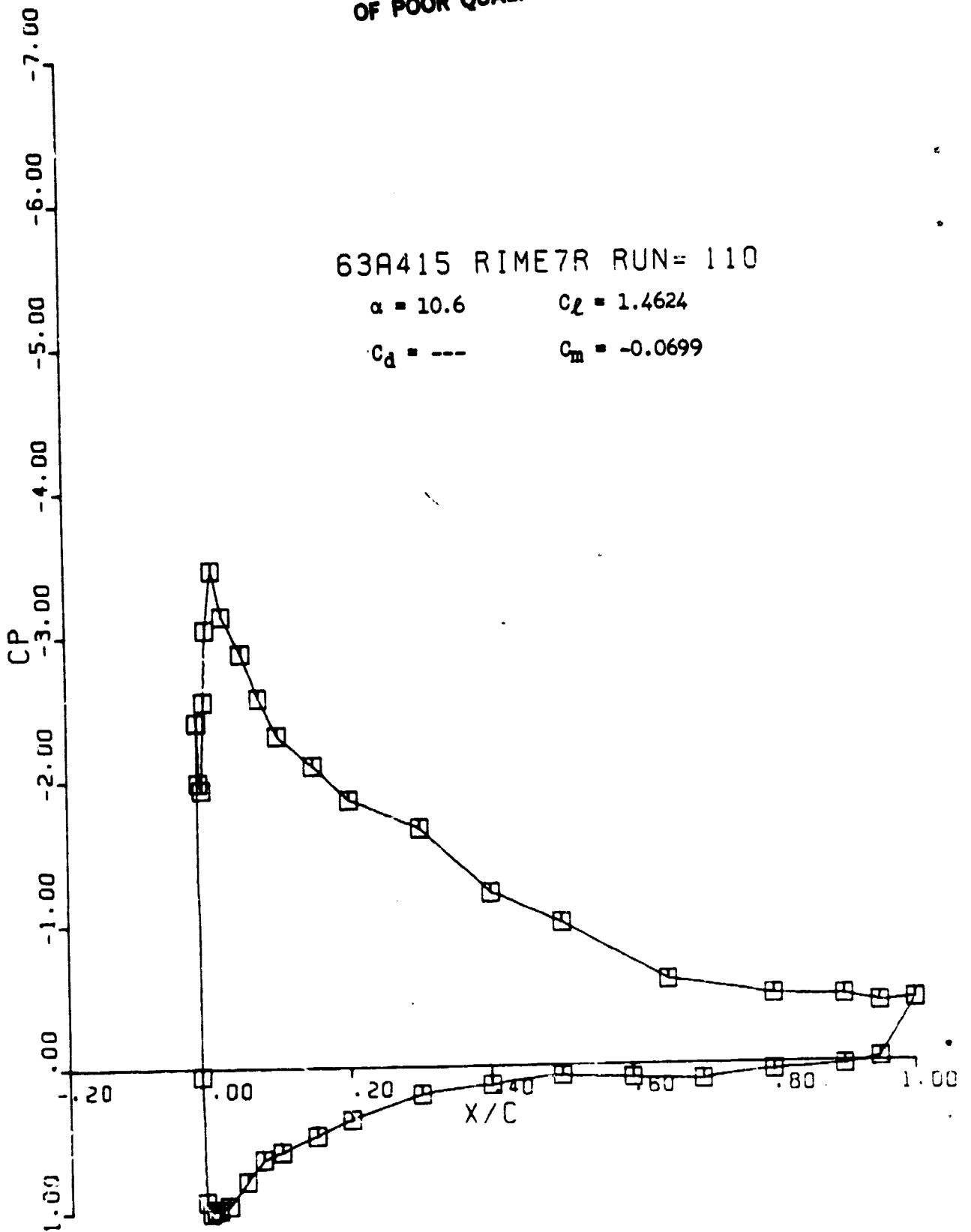
63A415 RIME7R RUN= 110

$\alpha = 10.6$

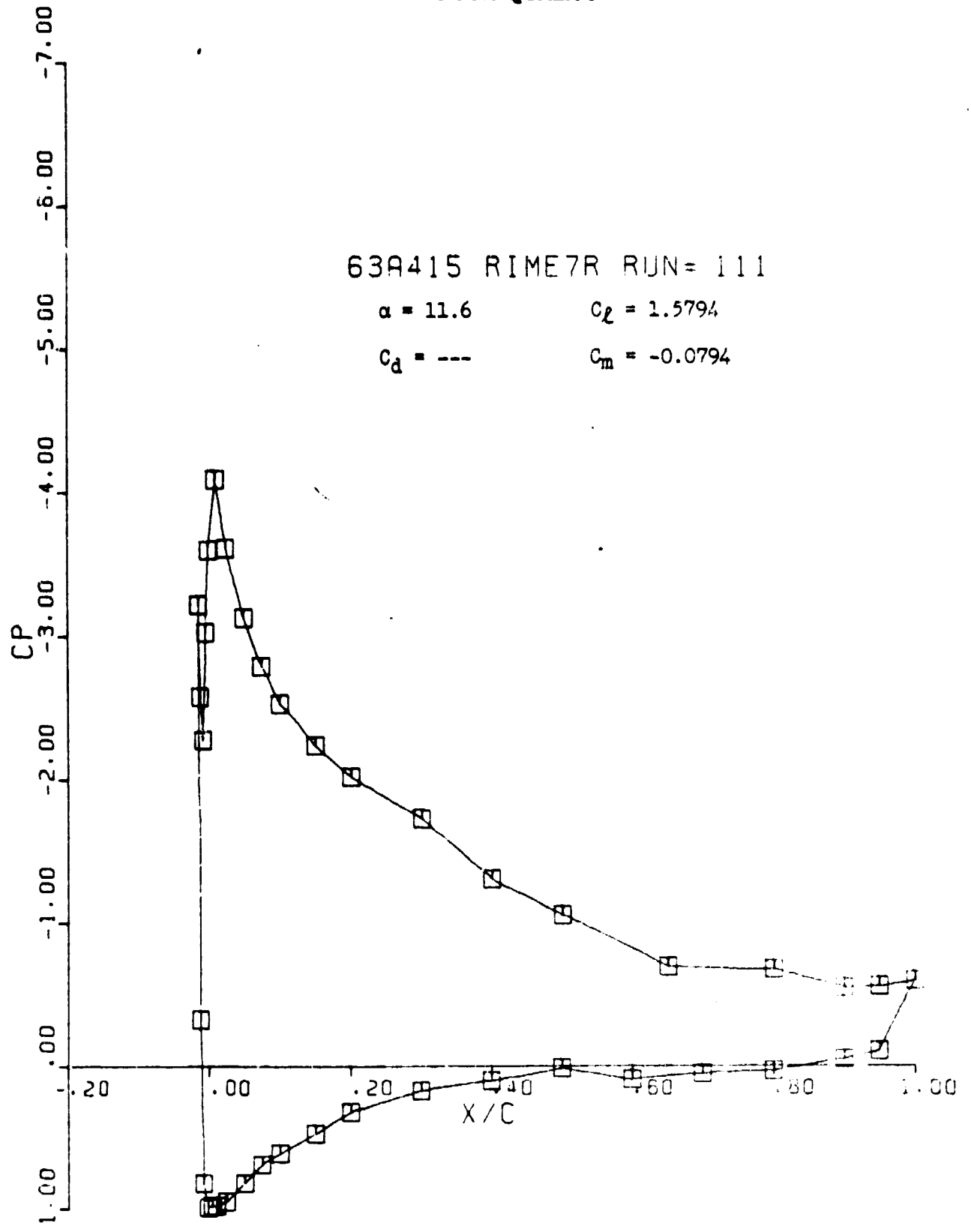
$C_L = 1.4624$

$C_d = \text{---}$

$C_m = -0.0699$



ORIGINAL PAGE IS
OF POOR QUALITY



ORIGINAL PAGE IS
OF POOR QUALITY

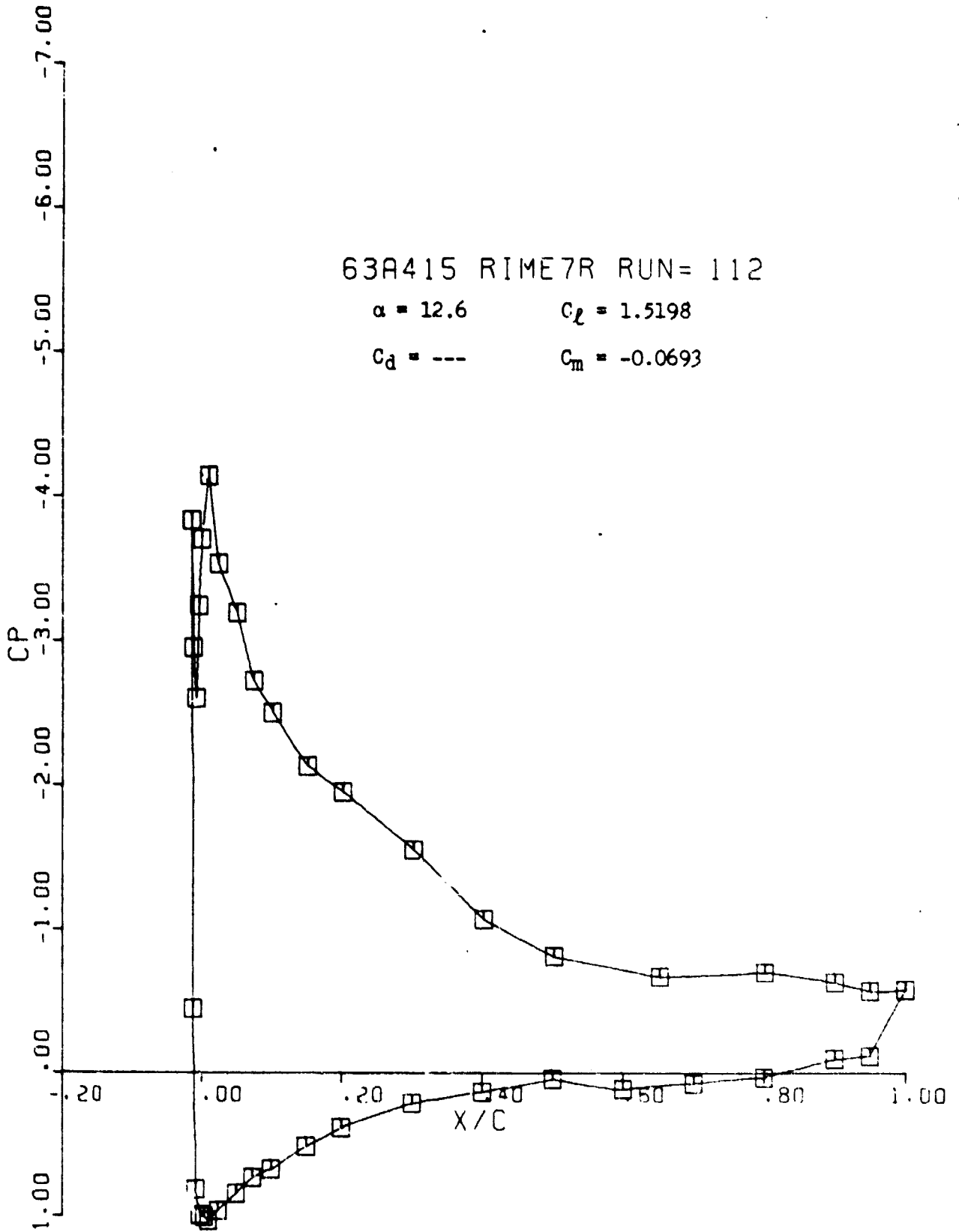
63A415 RIME7R RUN= 112

$\alpha = 12.6$

$C_l = 1.5198$

$C_d = \text{---}$

$C_m = -0.0693$



ORIGINAL PAGE IS
OF POOR QUALITY

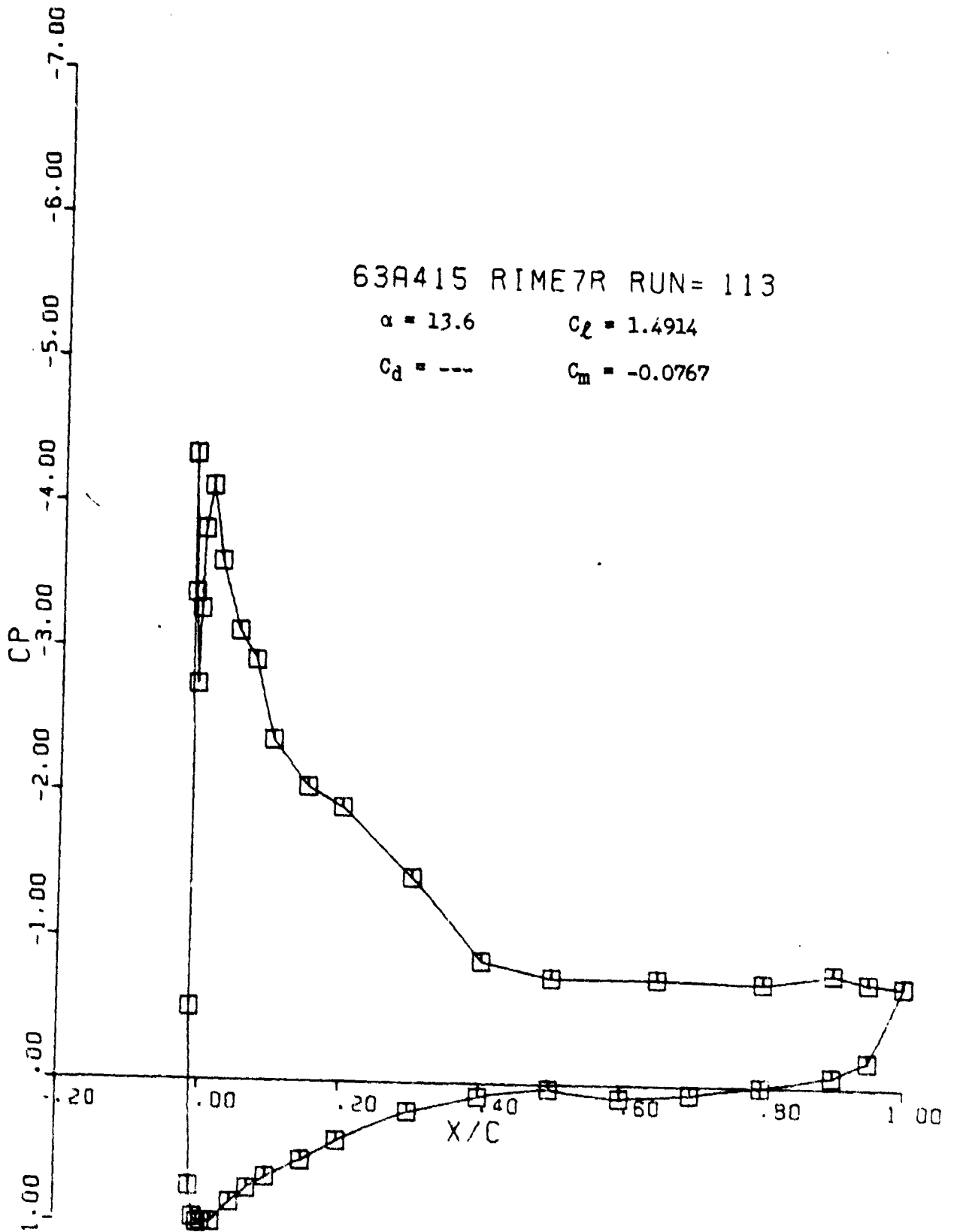
63A415 RIME7R RUN= 113

$\alpha = 13.6$

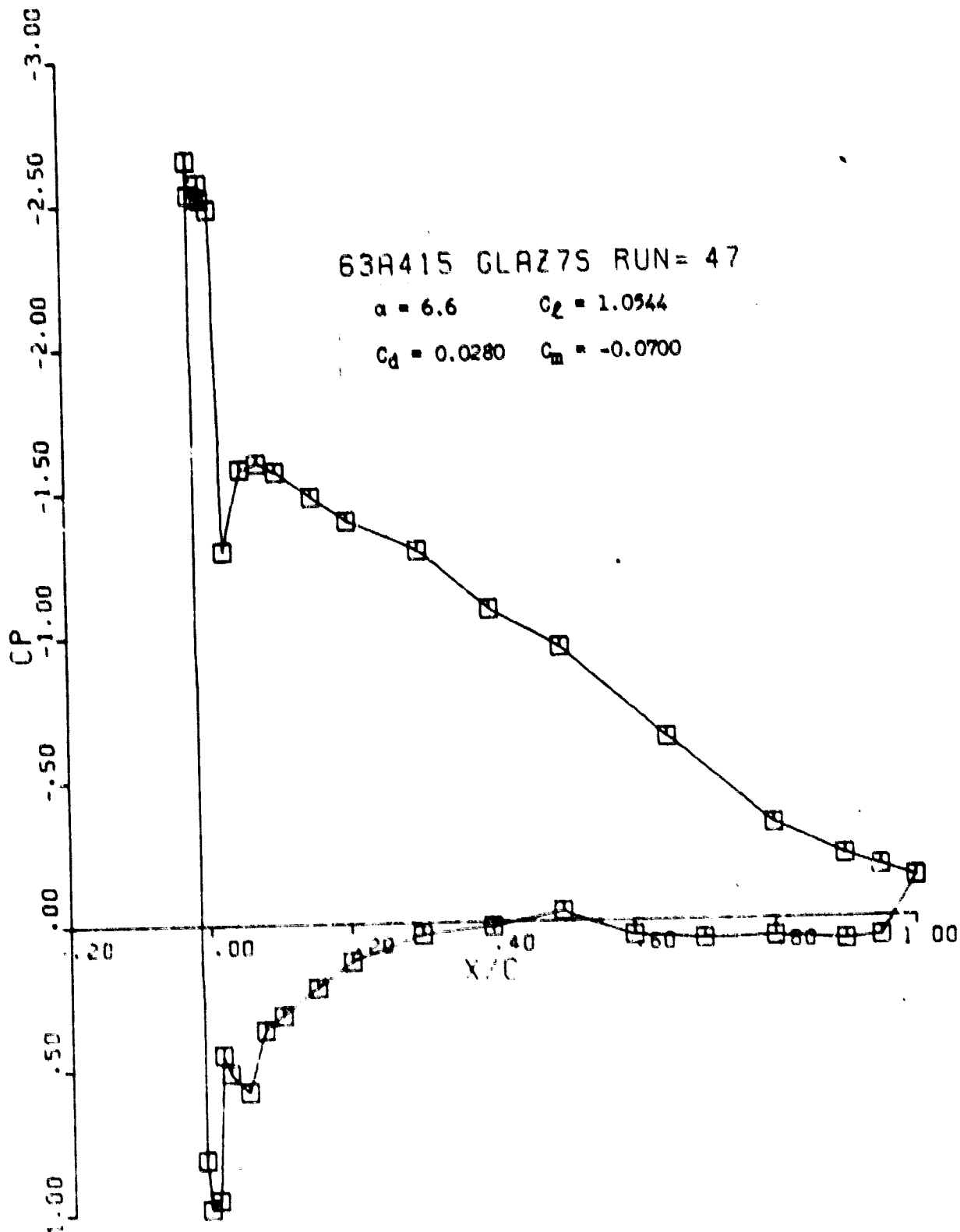
$C_l = 1.4914$

$C_d = \text{---}$

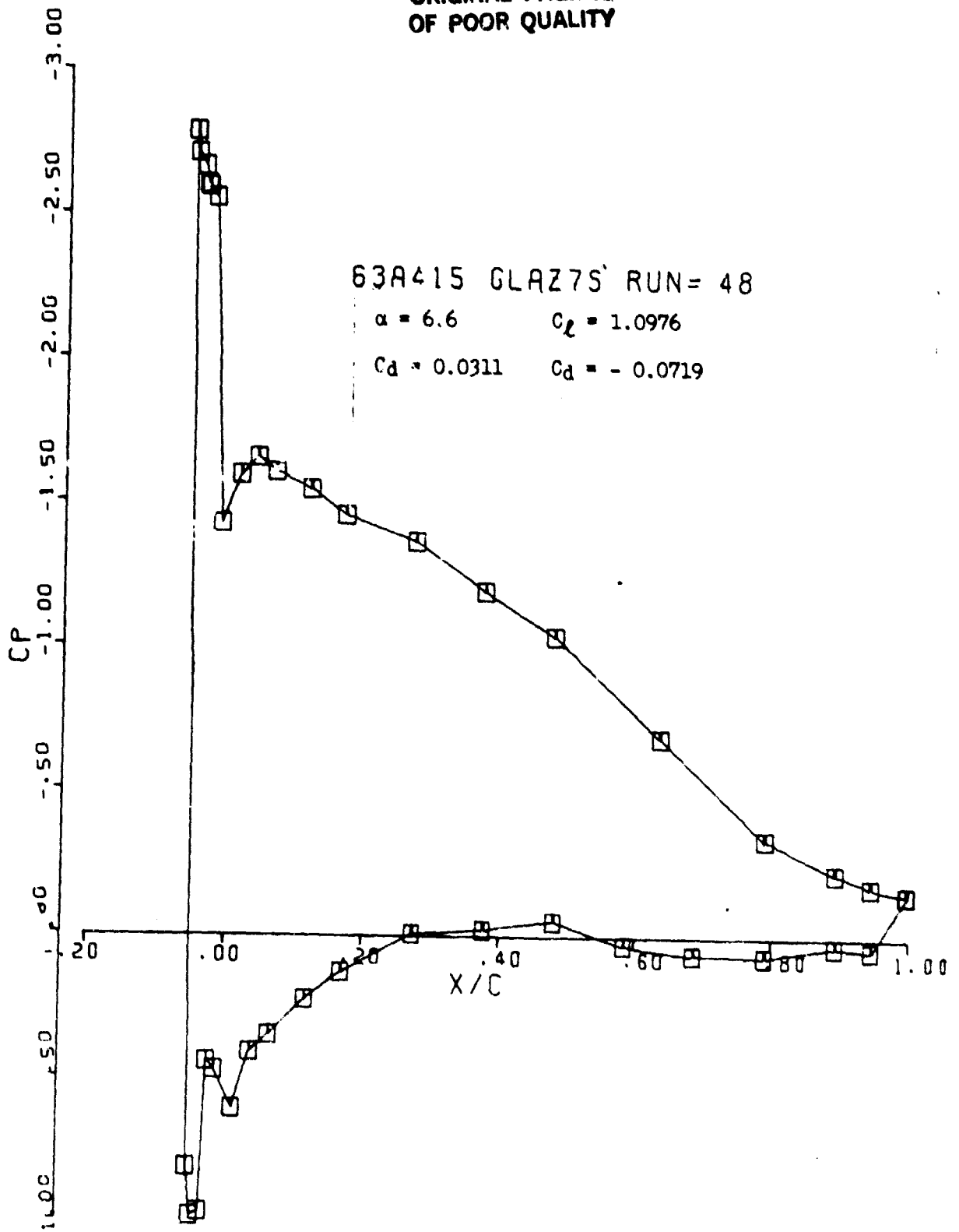
$C_m = -0.0767$



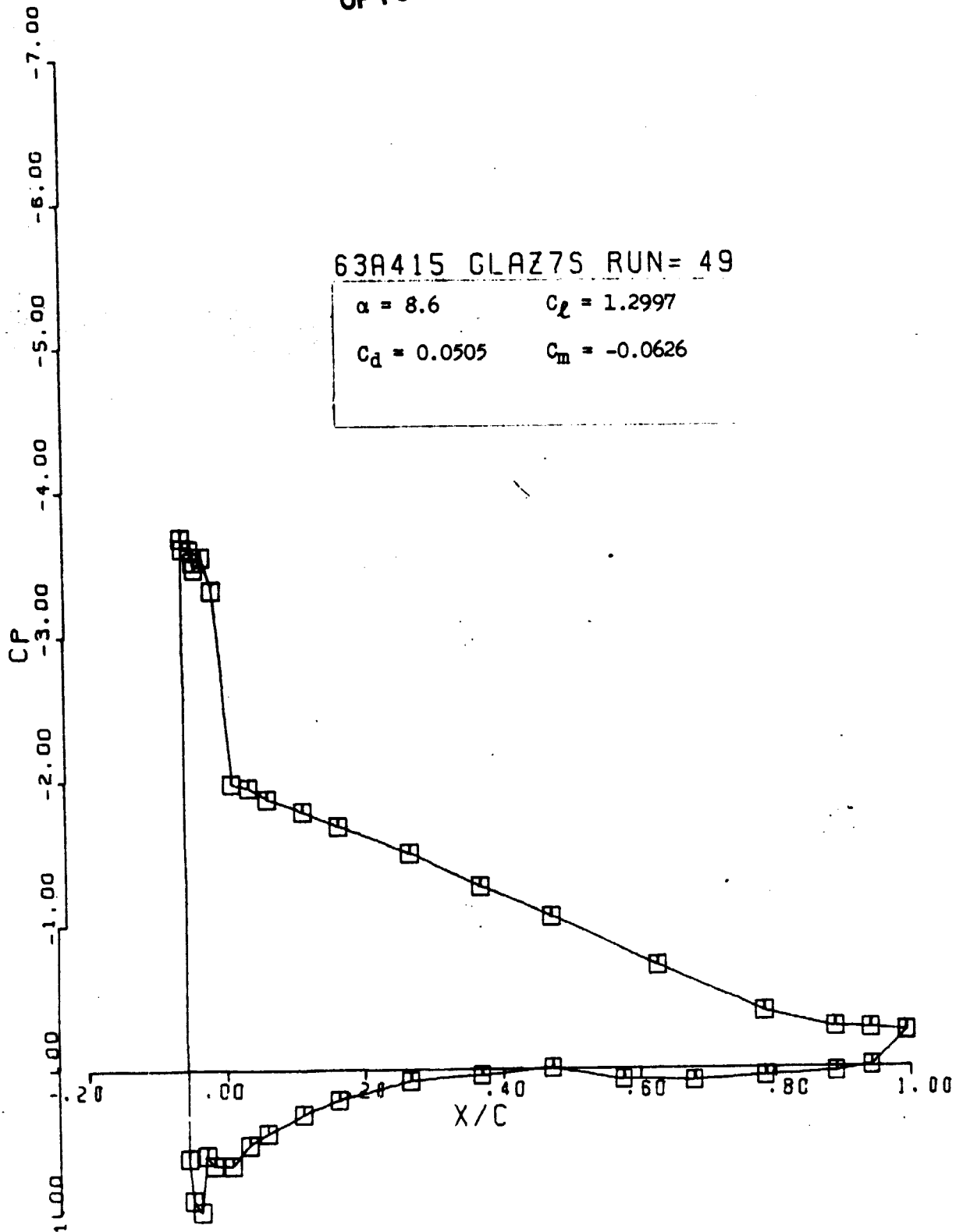
ORIGINAL PAGE IS
OF POOR QUALITY



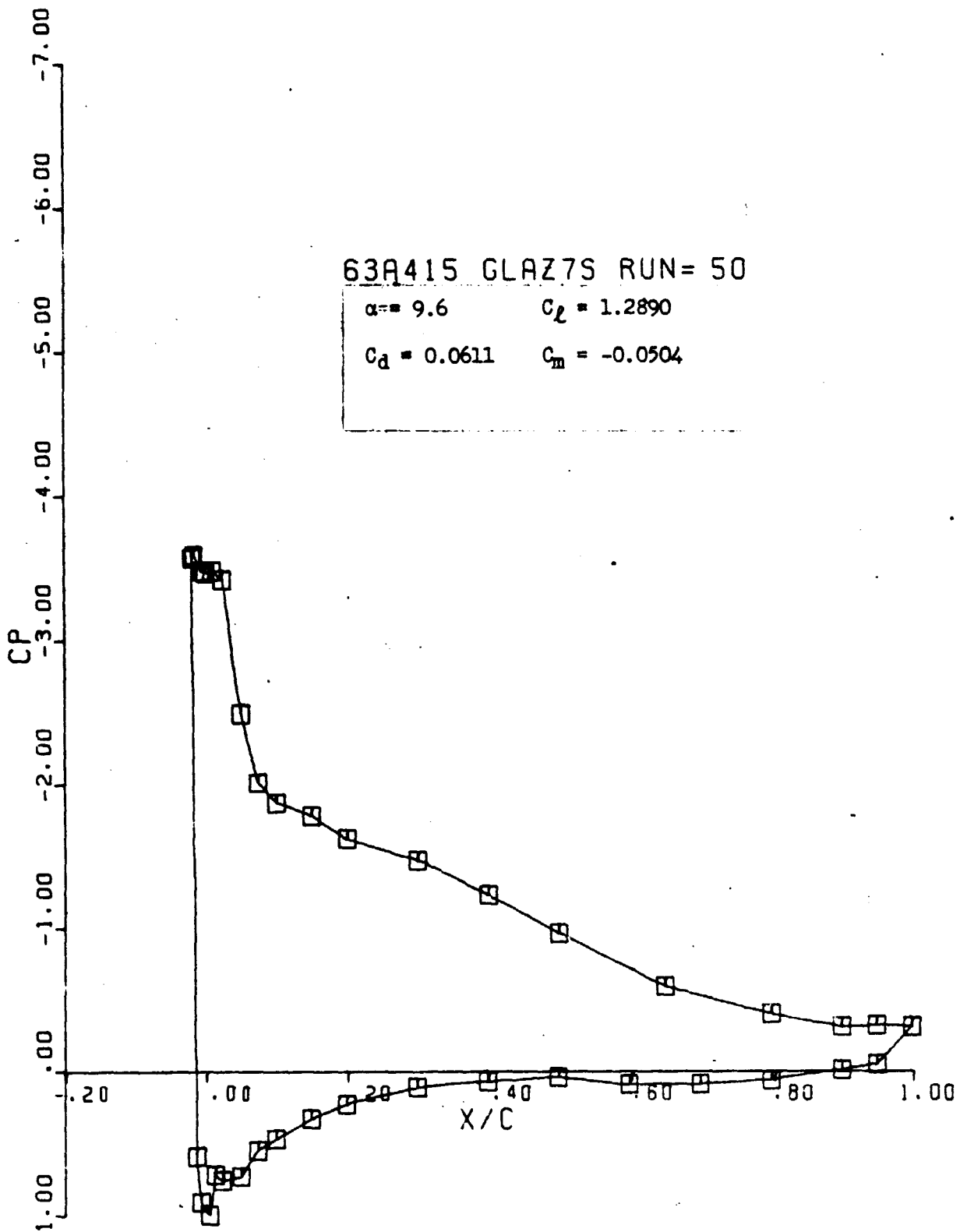
ORIGINAL PAGE IS
OF POOR QUALITY



ORIGINAL PAGE IS
OF POOR QUALITY



ORIGINAL PAGE IS
OF POOR QUALITY



ORIGINAL PAGE IS
OF POOR QUALITY

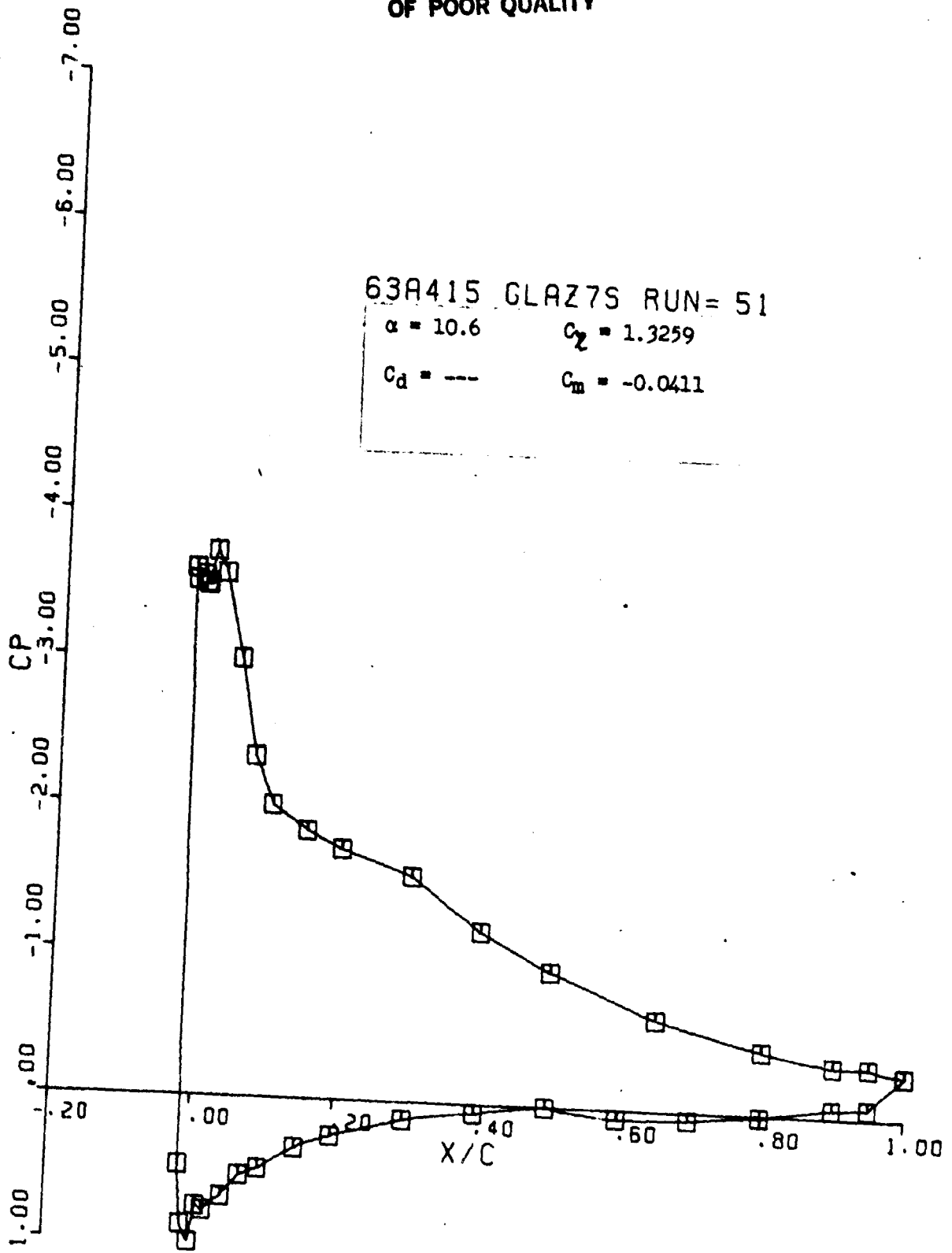
63A415 GLAZ7S RUN= 51

$\alpha = 10.6$

$C_2 = 1.3259$

$C_d = \text{---}$

$C_m = -0.0411$



ORIGINAL PAGE IS
OF POOR QUALITY

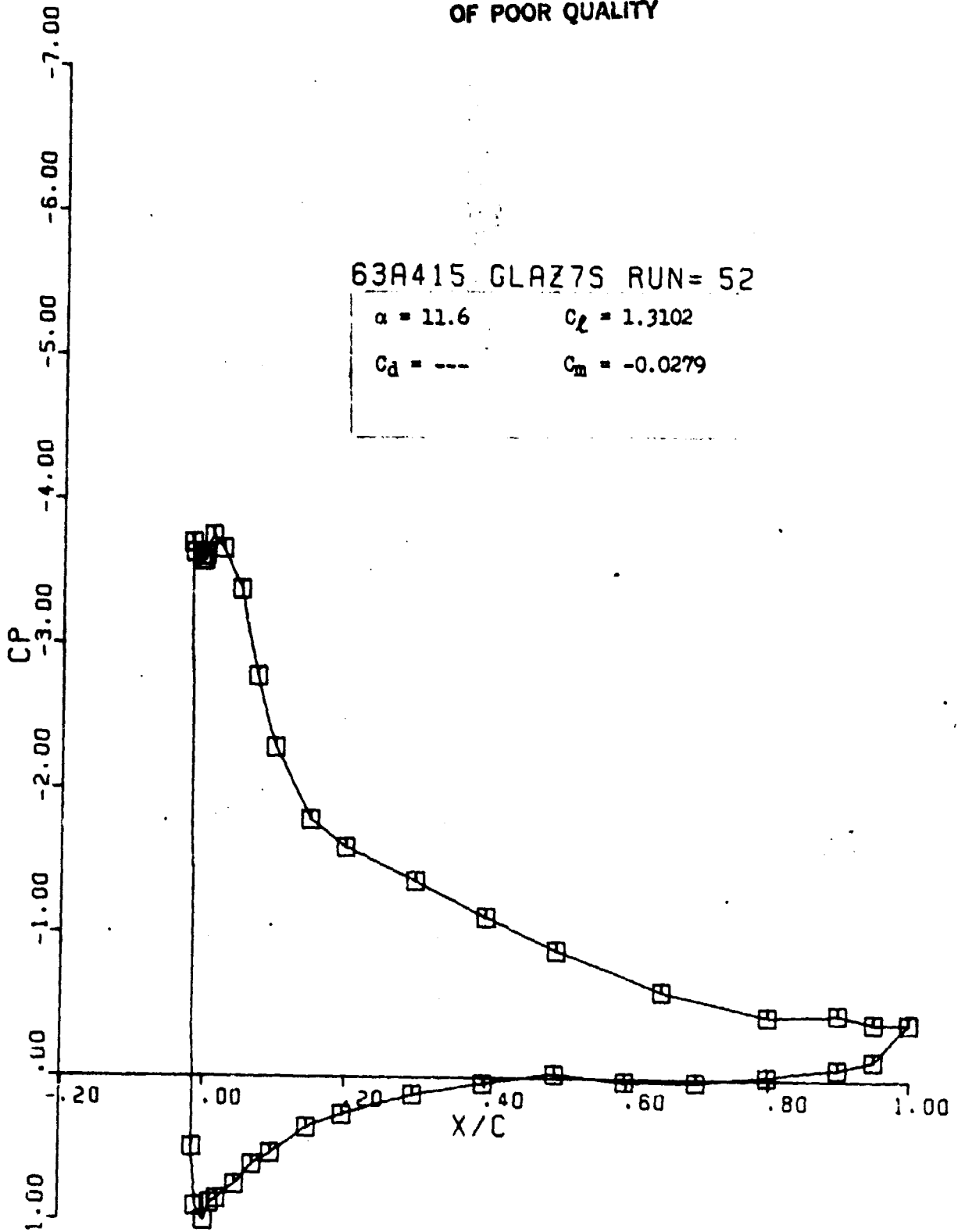
63A415 GLAZ7S RUN= 52

$\alpha = 11.6$

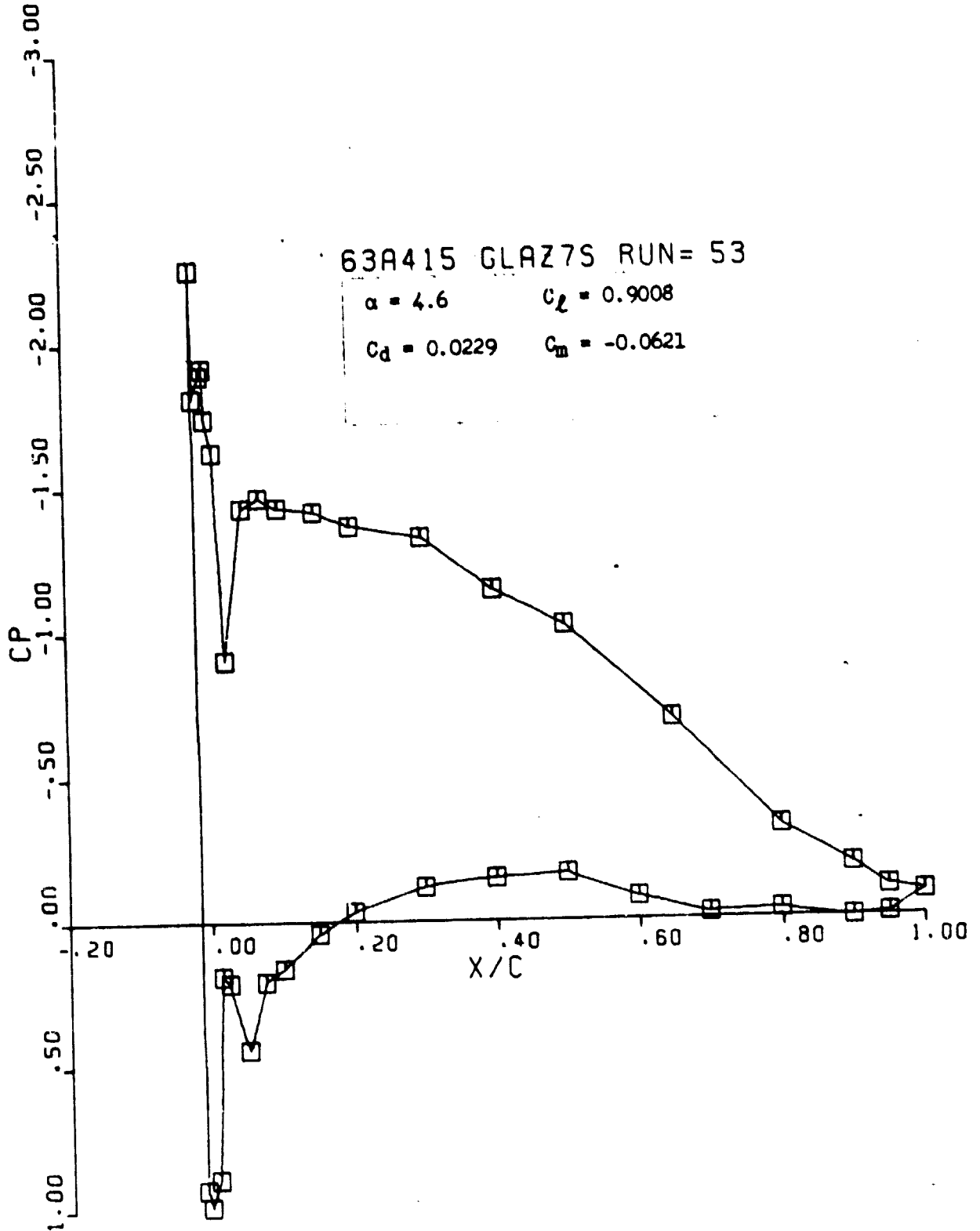
$C_L = 1.3102$

$C_d = \text{---}$

$C_m = -0.0279$



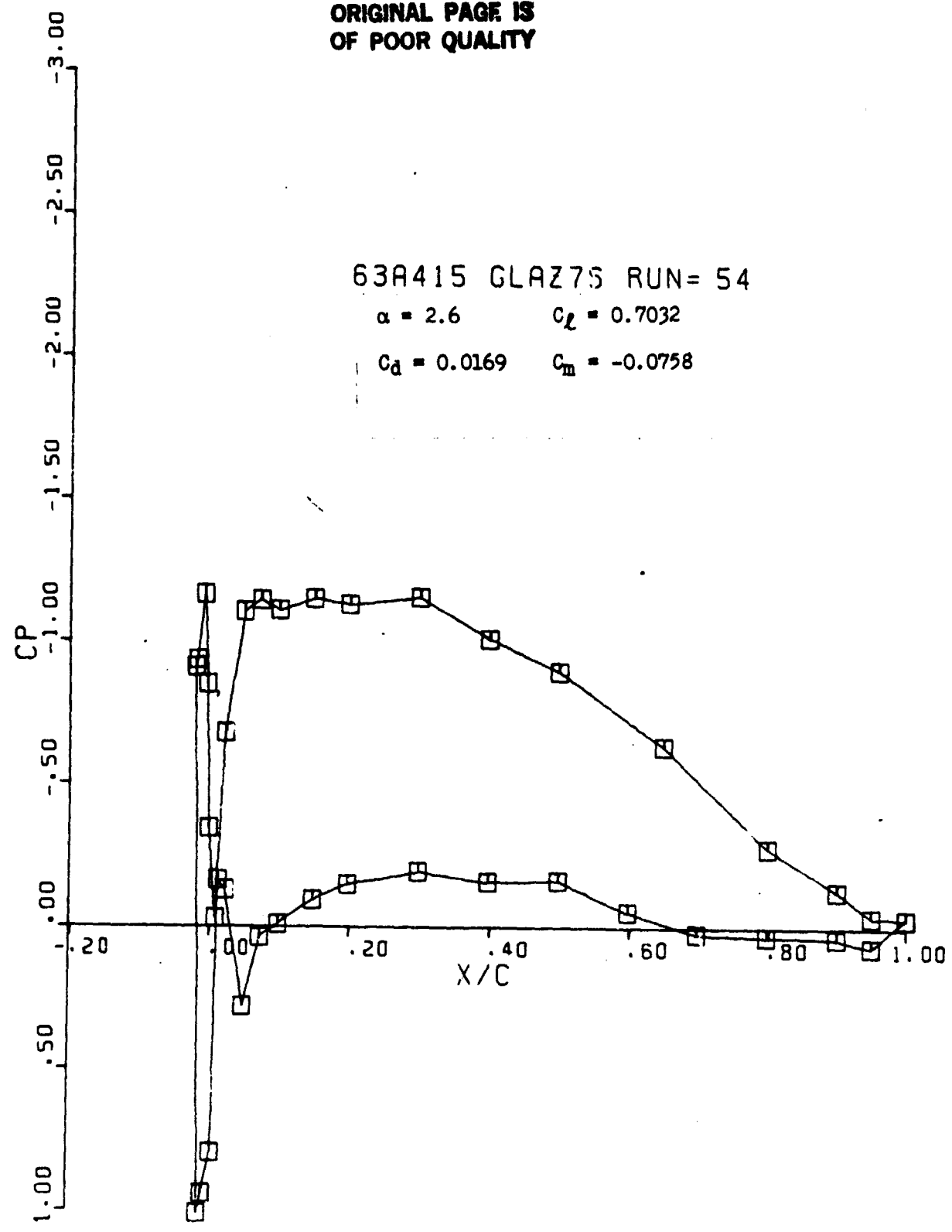
ORIGINAL PAGE IS
OF POOR QUALITY



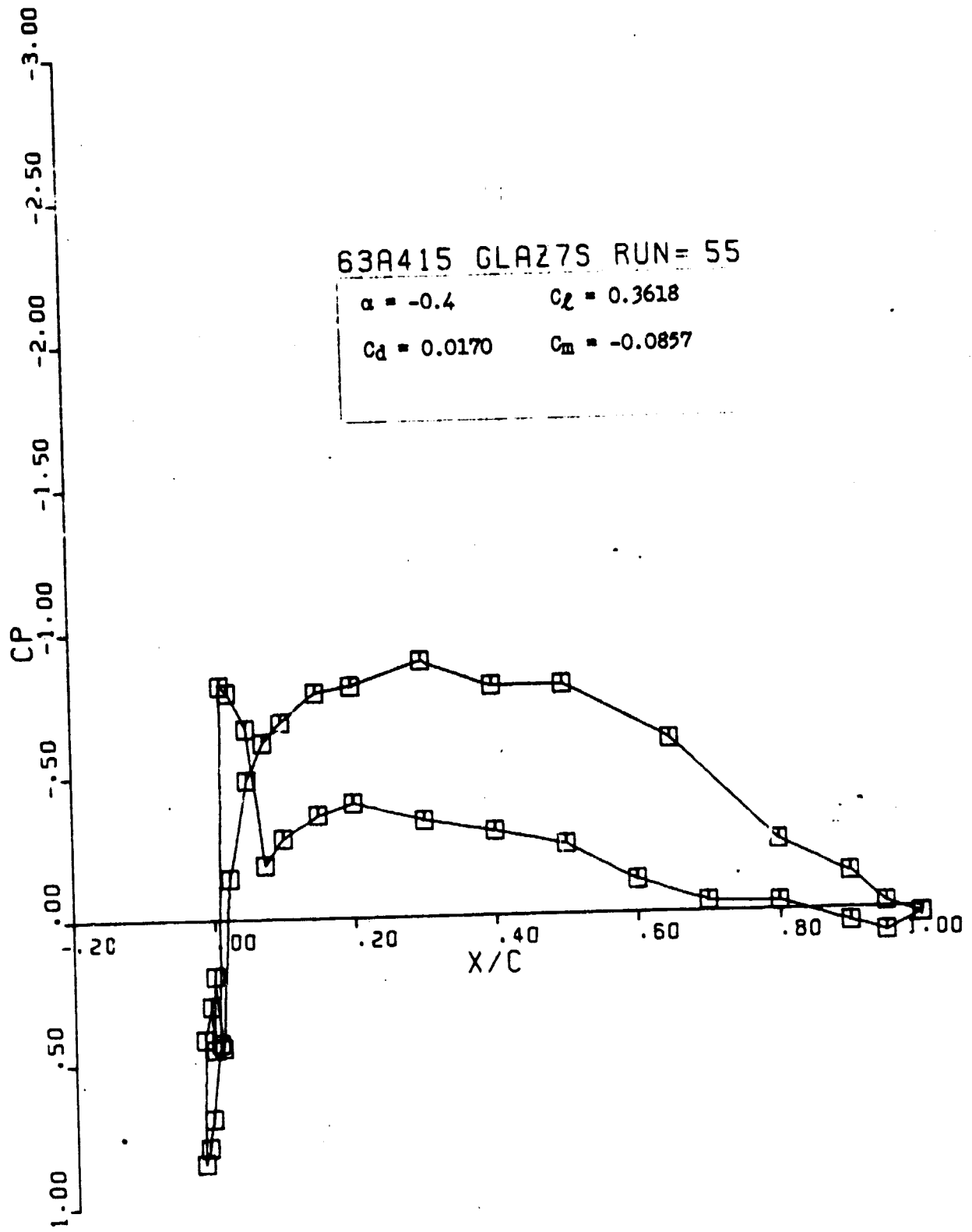
ORIGINAL PAGE IS
OF POOR QUALITY

63A415 GLAZ75 RUN= 54

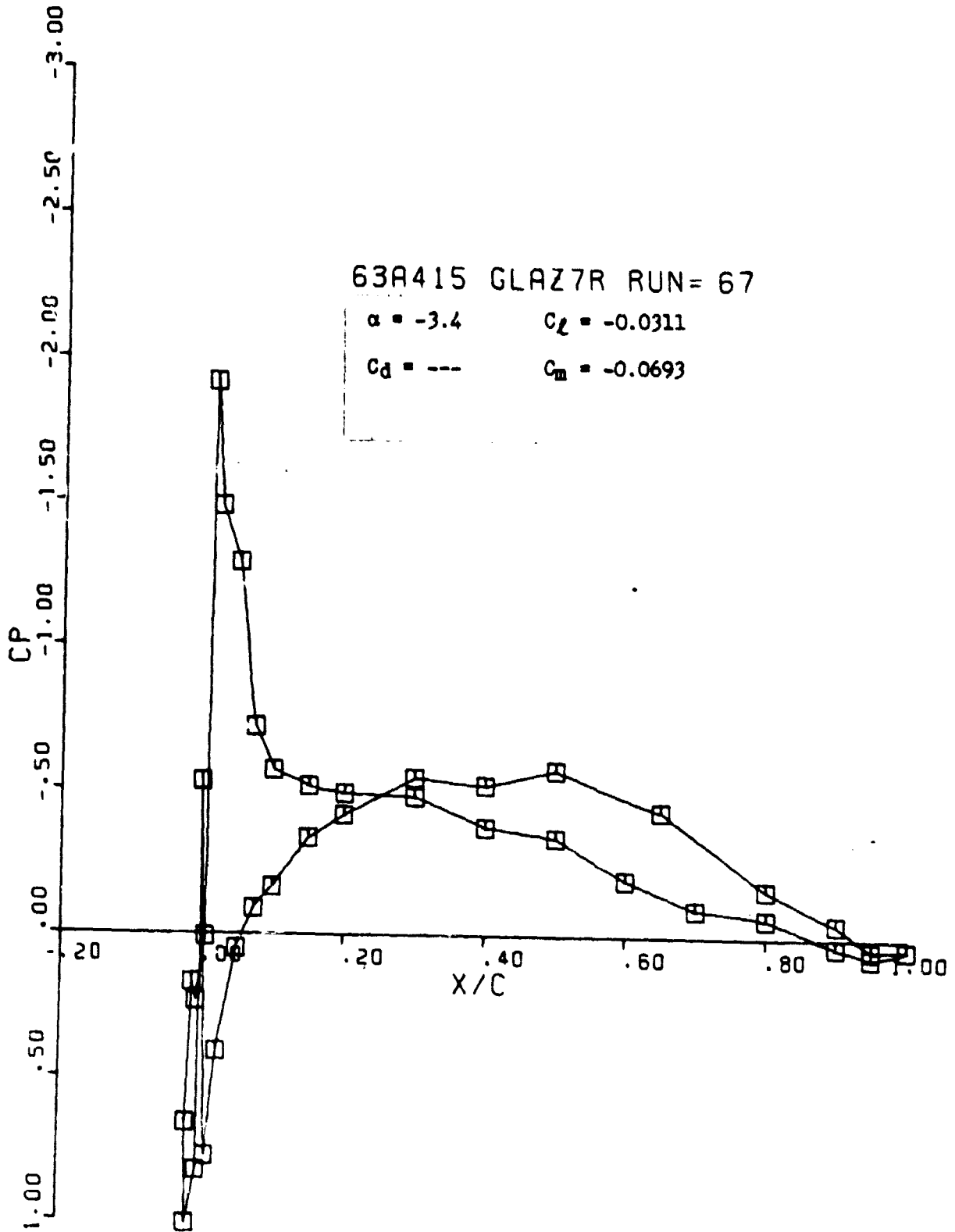
$\alpha = 2.6$ $C_L = 0.7032$
 $C_D = 0.0169$ $C_M = -0.0758$



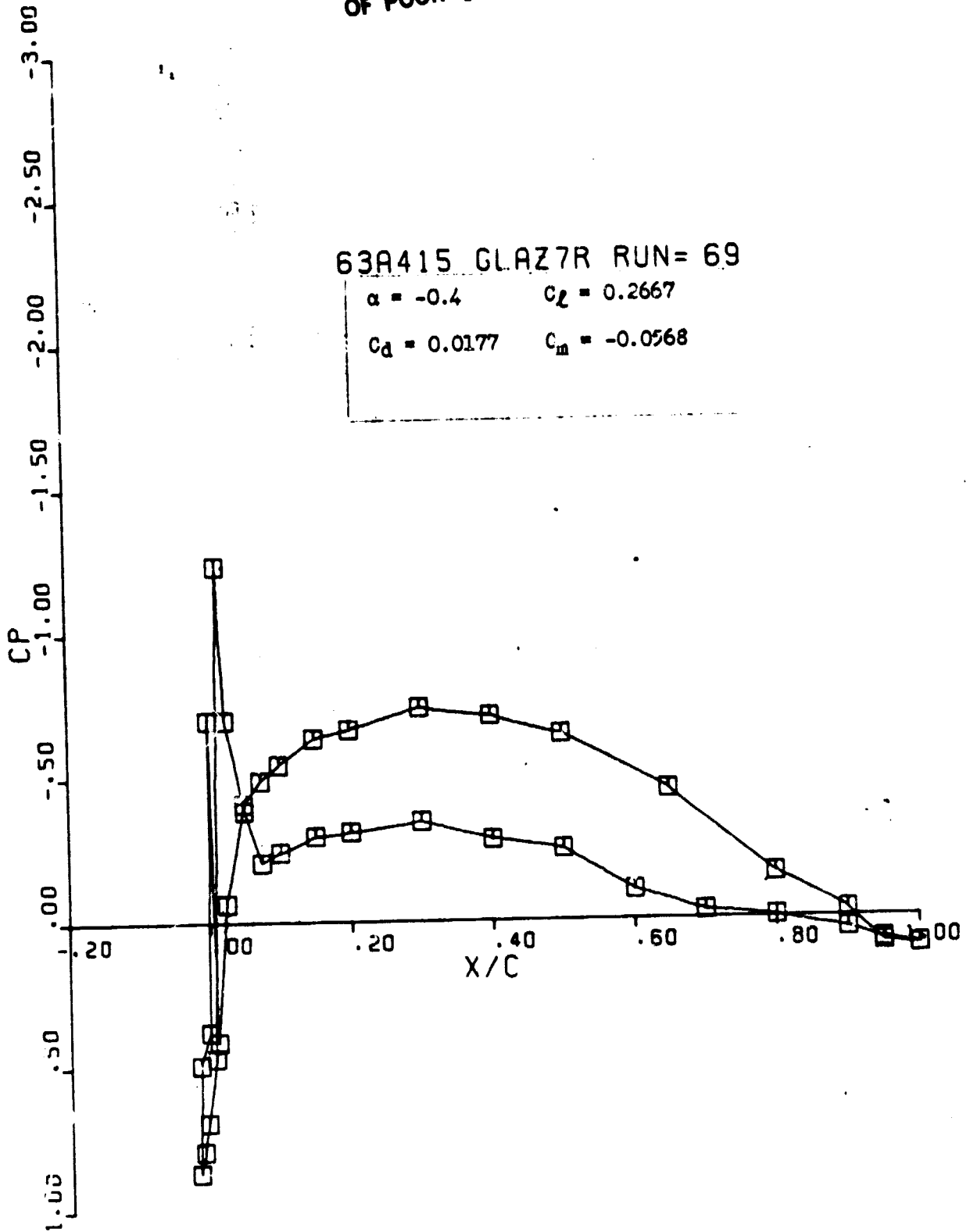
ORIGINAL PAGE IS
OF POOR QUALITY



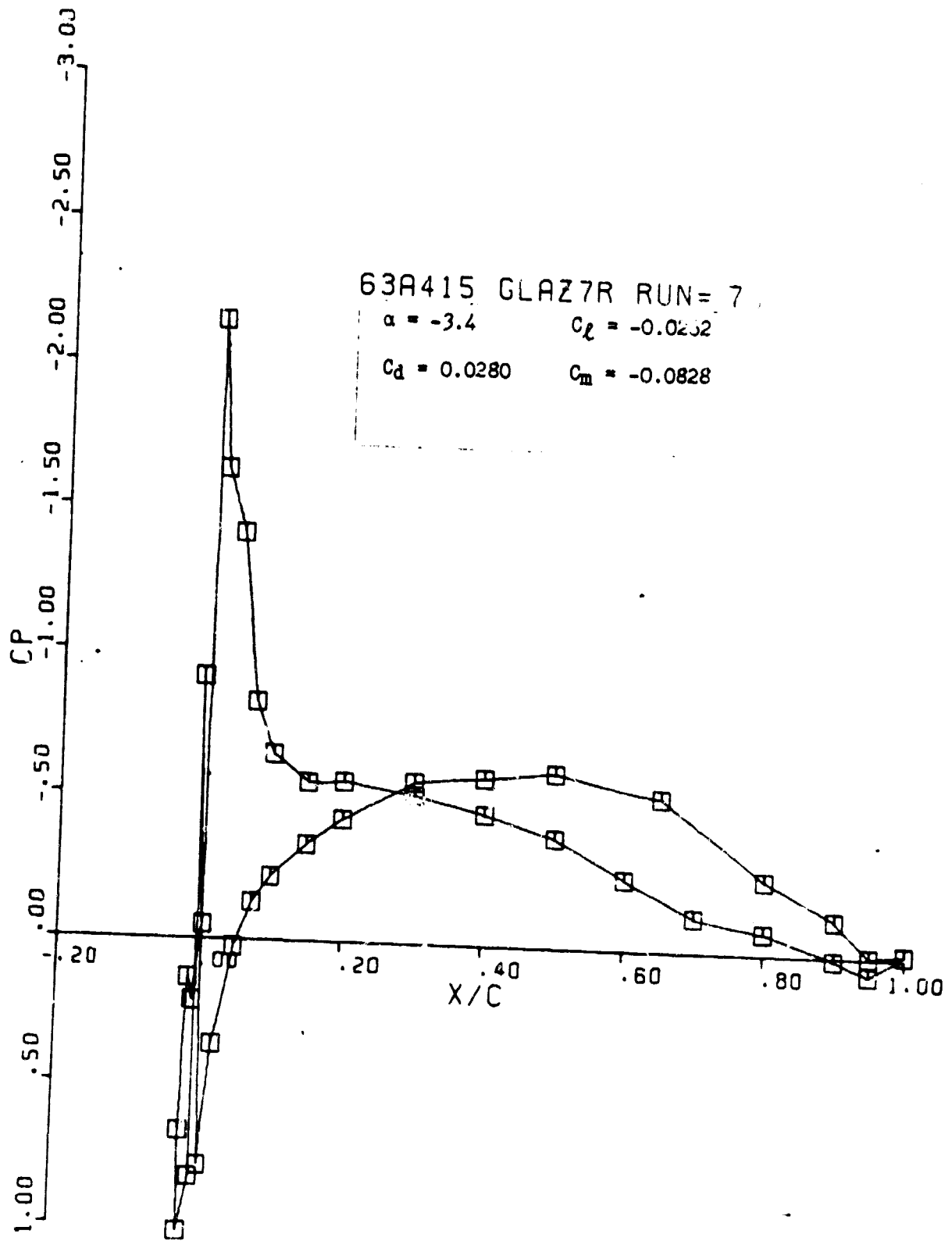
ORIGINAL PAGE IS
OF POOR QUALITY



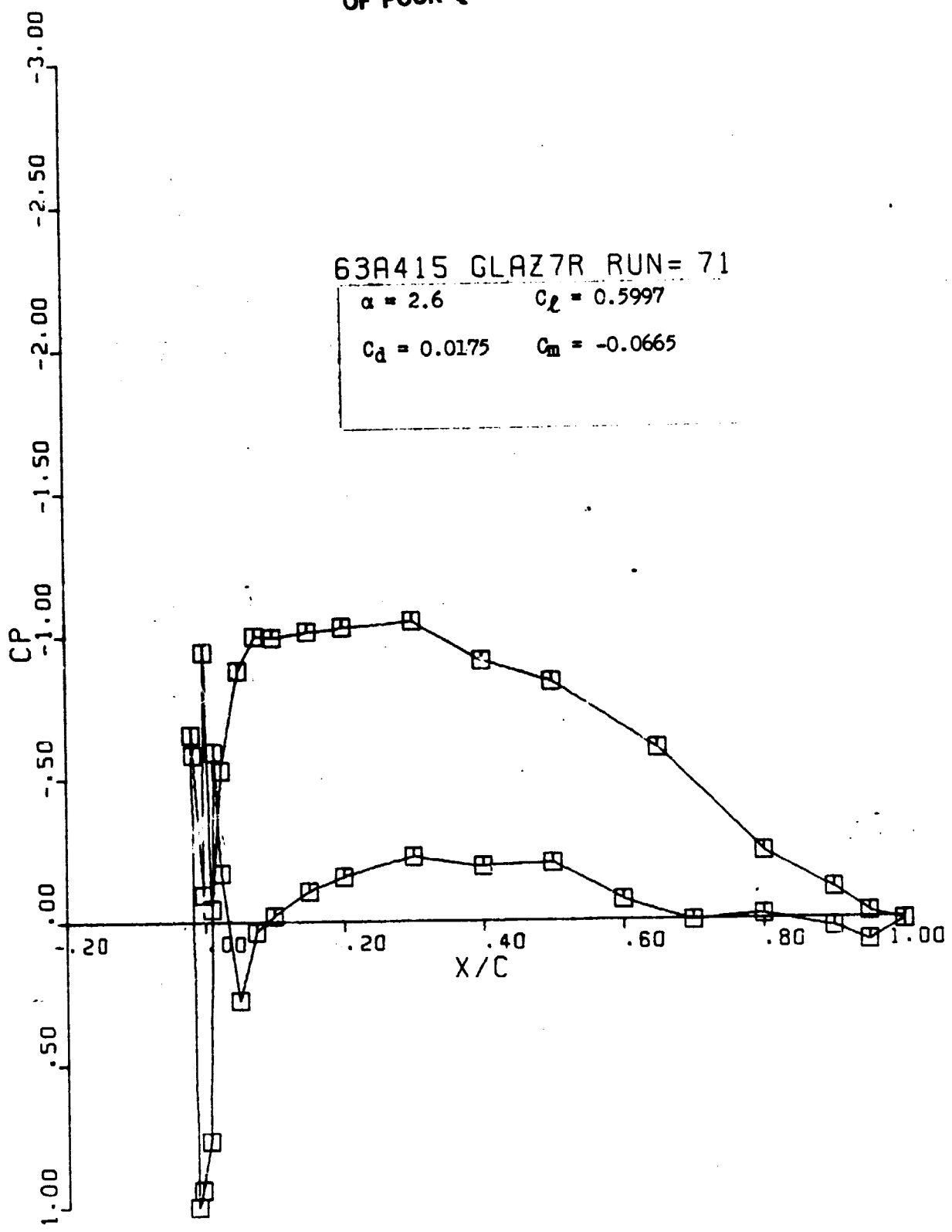
ORIGINAL PAGE IS
OF POOR QUALITY



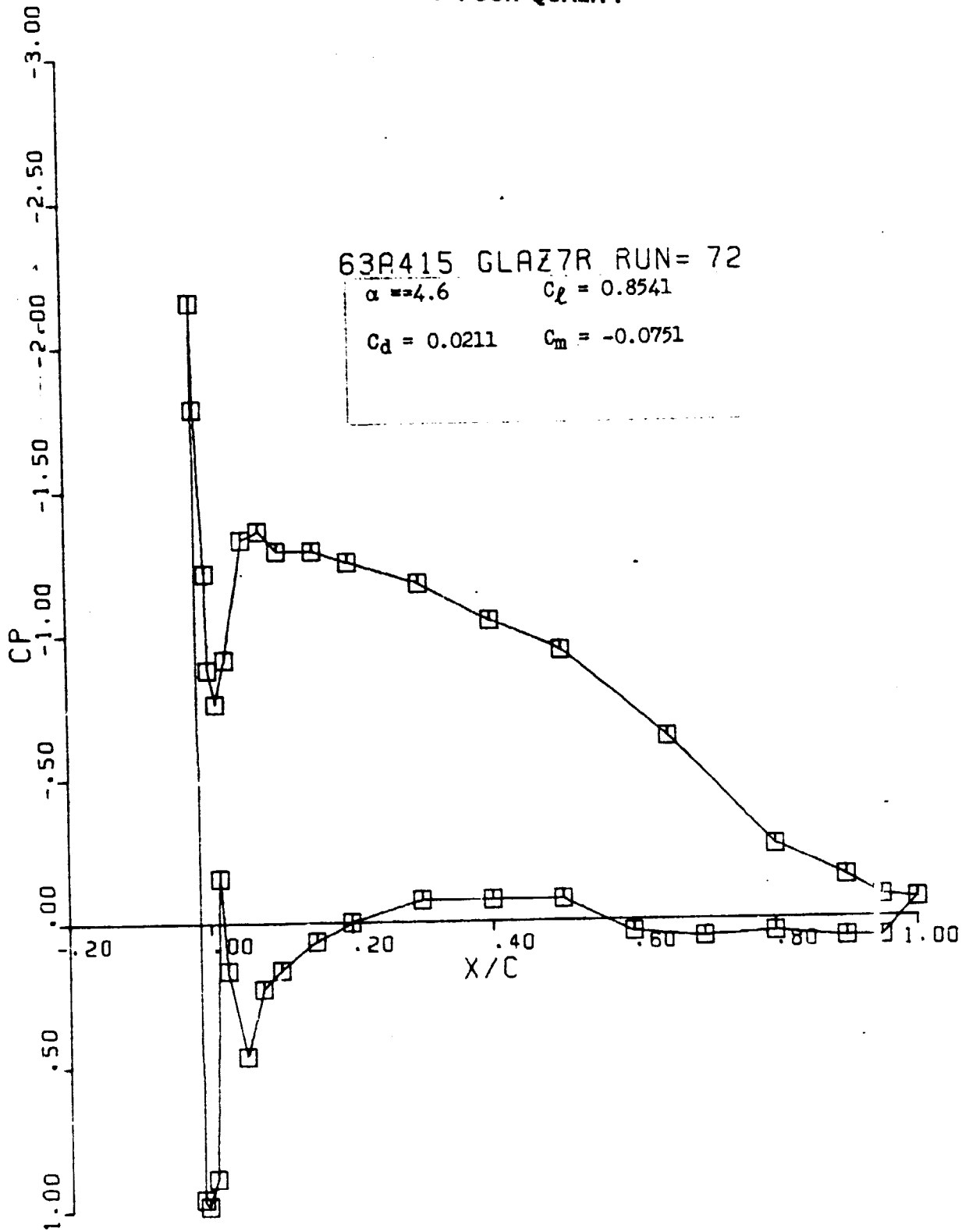
ORIGINAL PAGE IS
OF POOR QUALITY



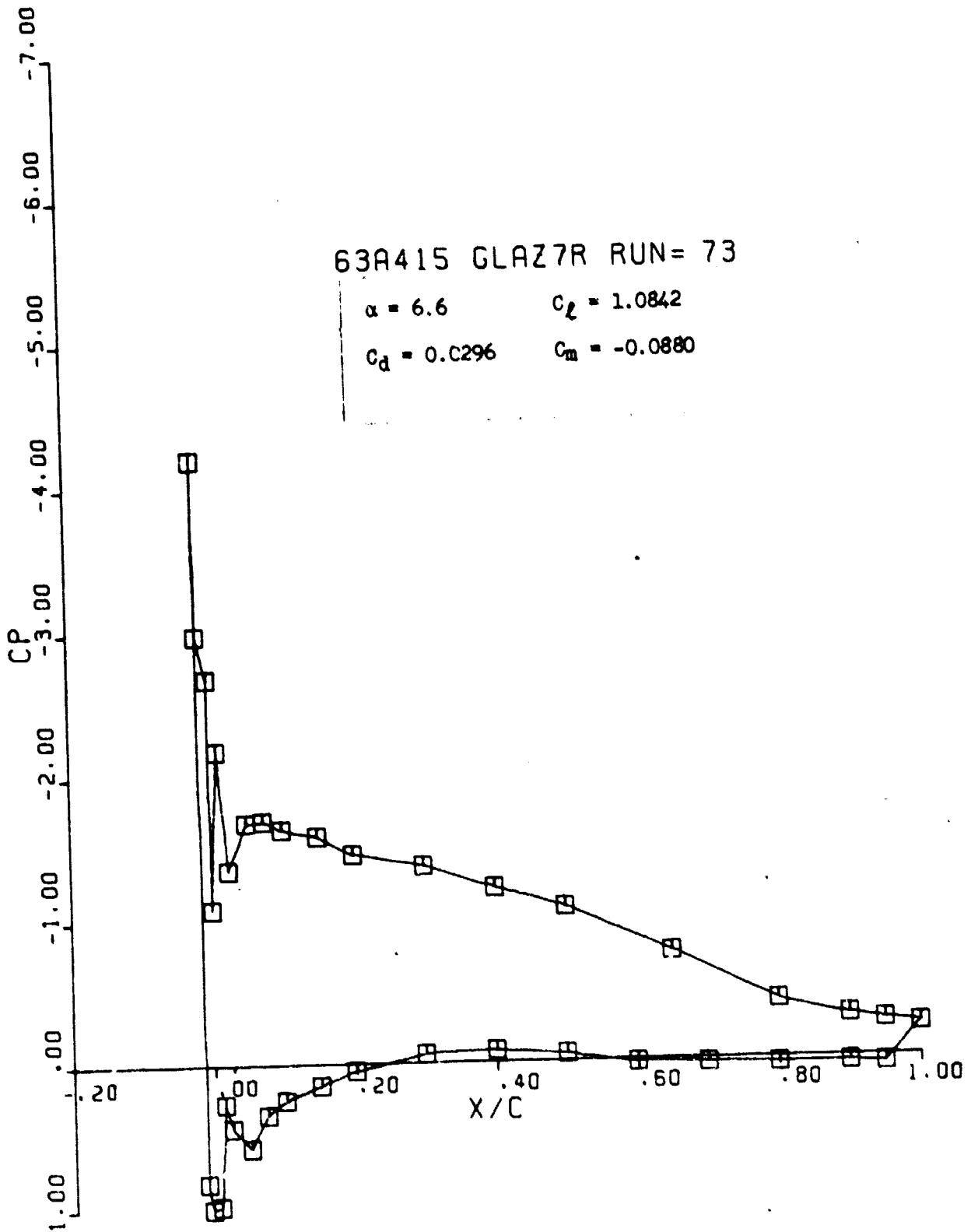
ORIGINAL PAGE IS
OF POOR QUALITY



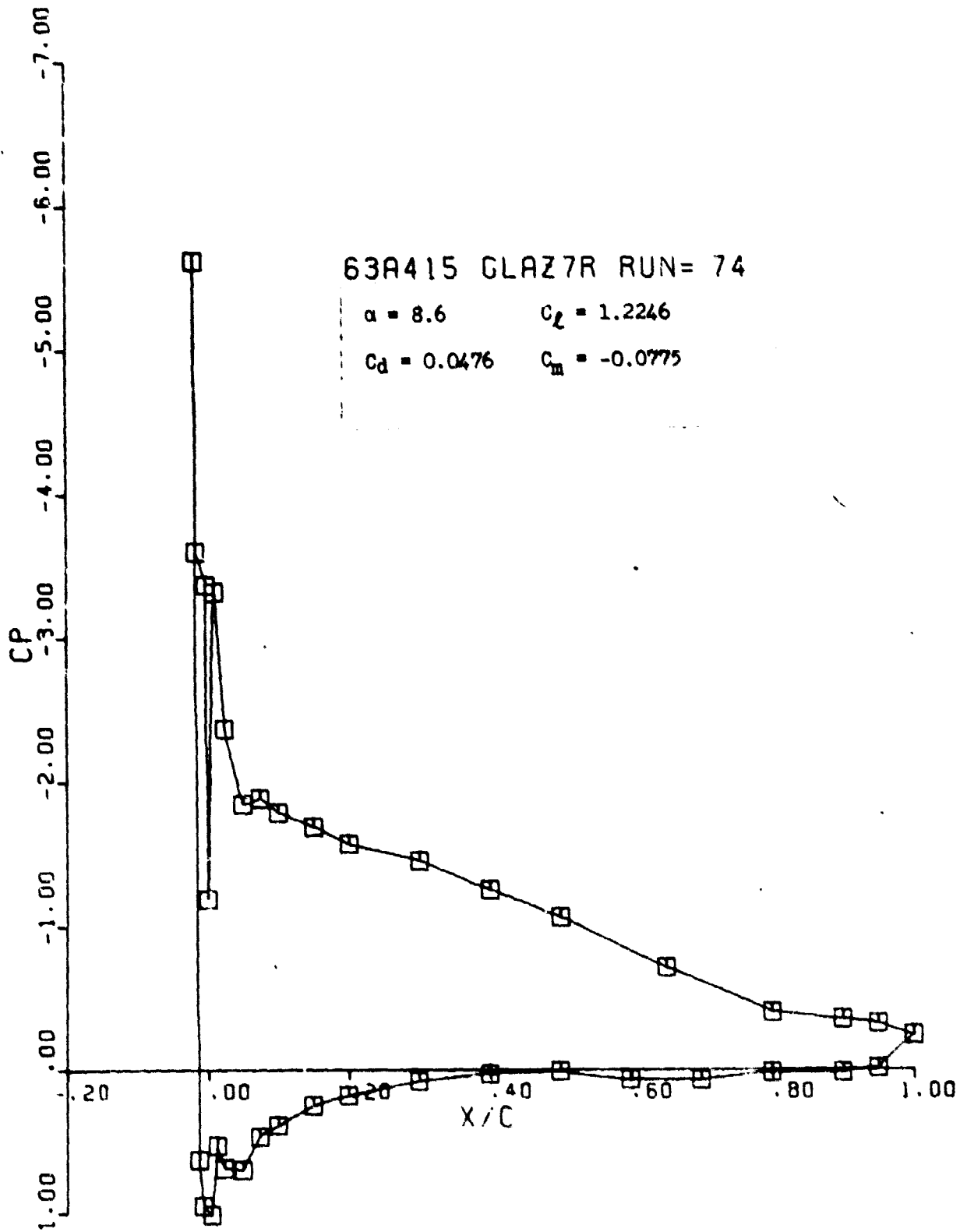
ORIGINAL PAGE IS
OF POOR QUALITY



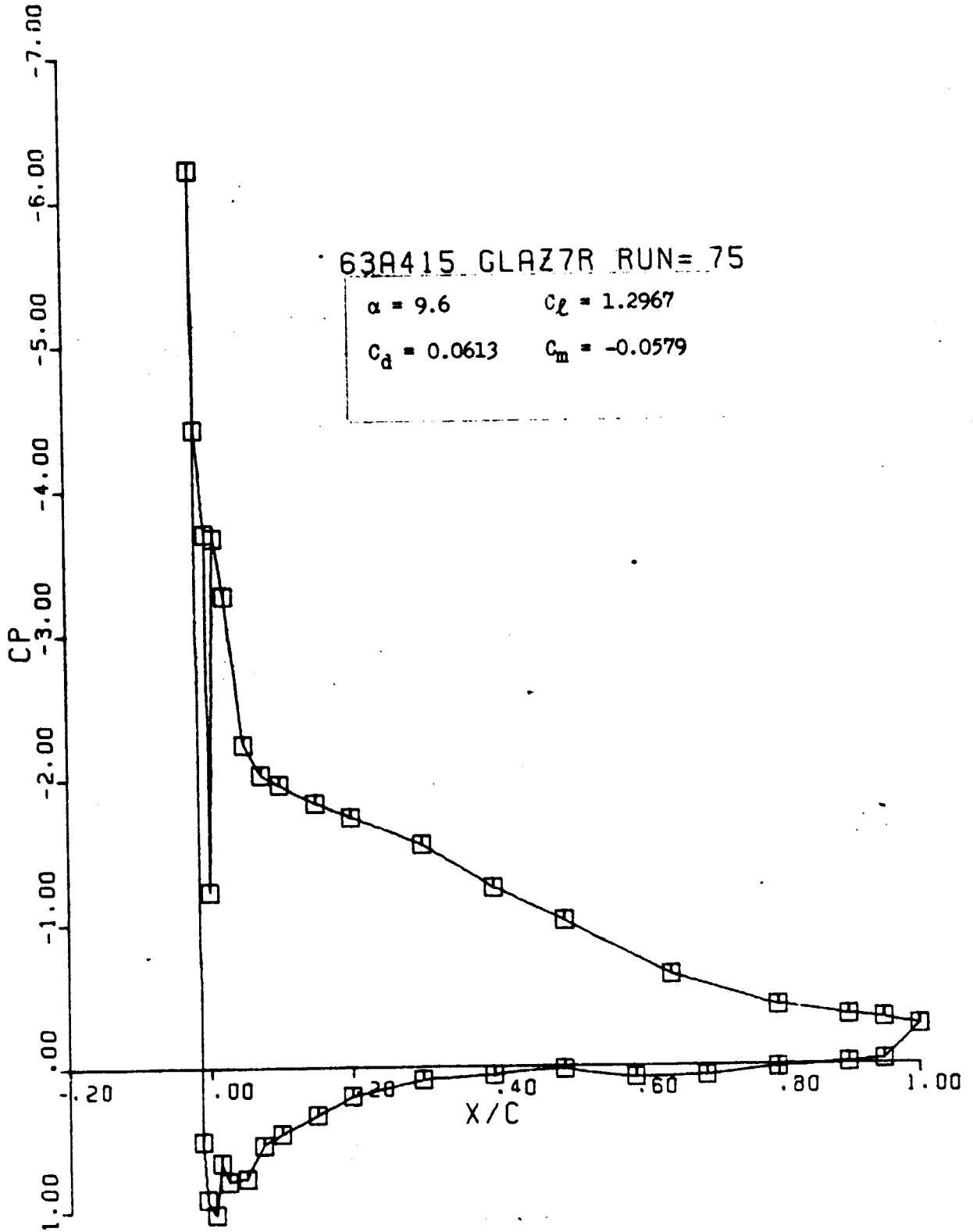
ORIGINAL PAGE IS
OF POOR QUALITY



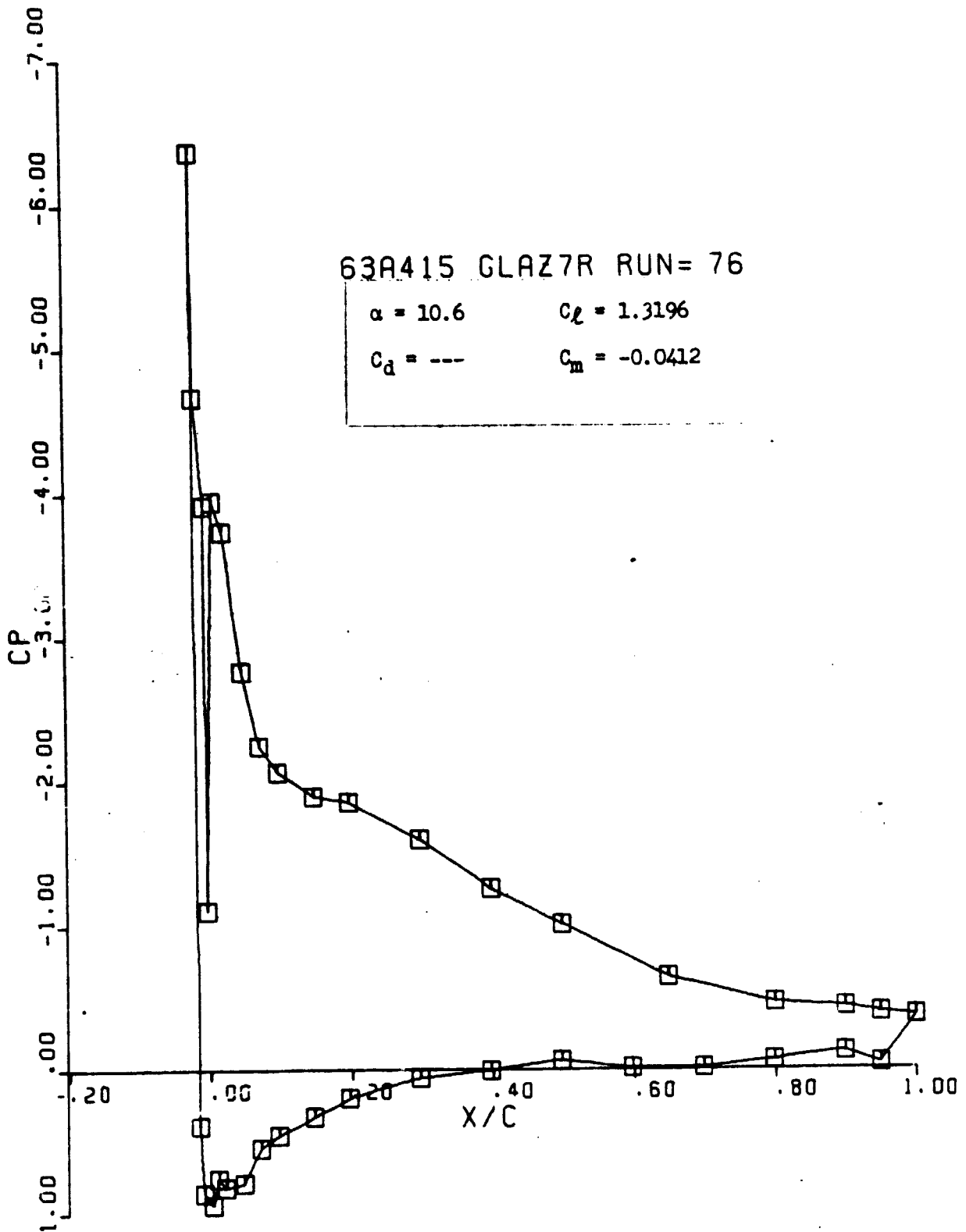
ORIGINAL PAGE IS
OF POOR QUALITY



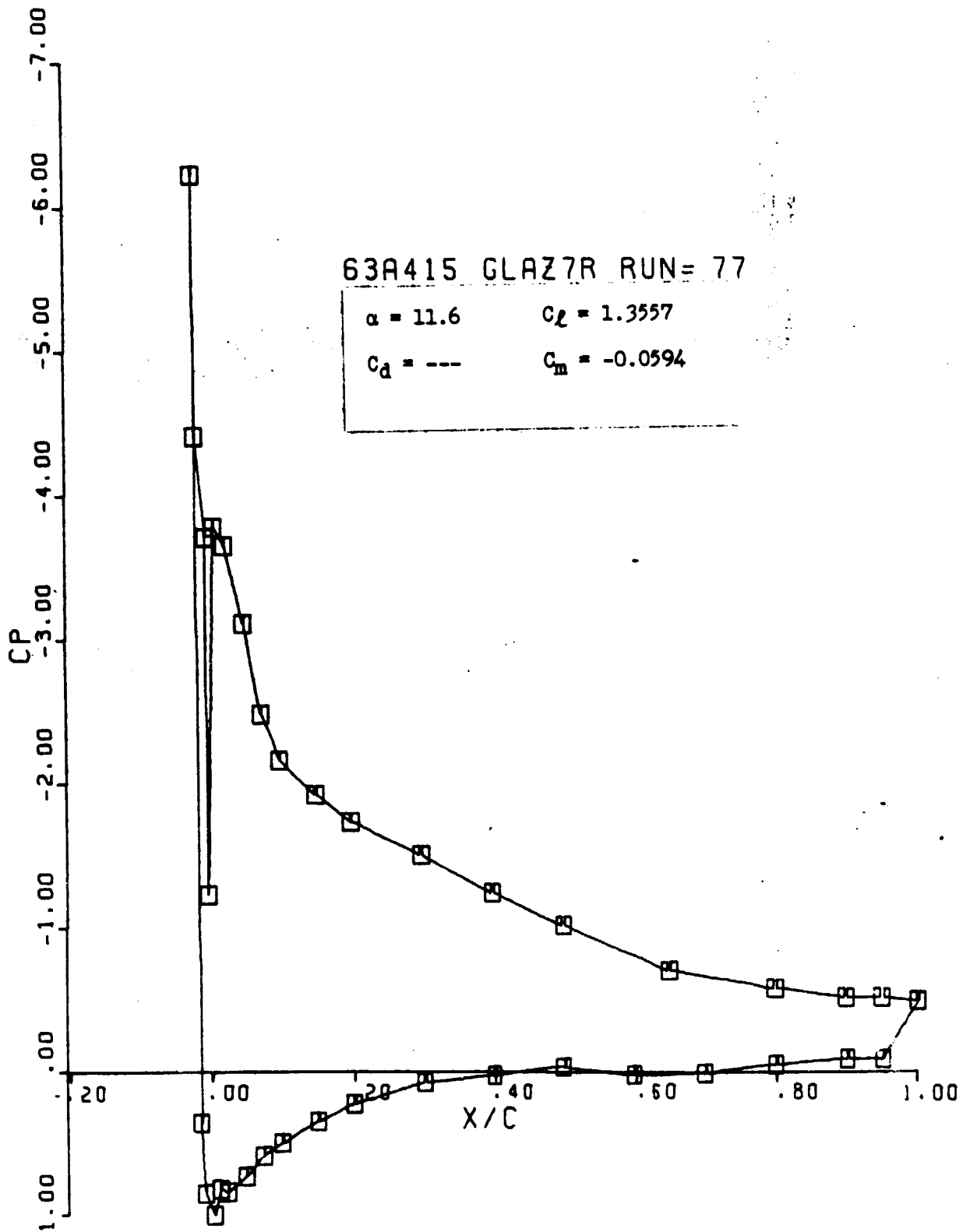
ORIGINAL PAGE IS
OF POOR QUALITY



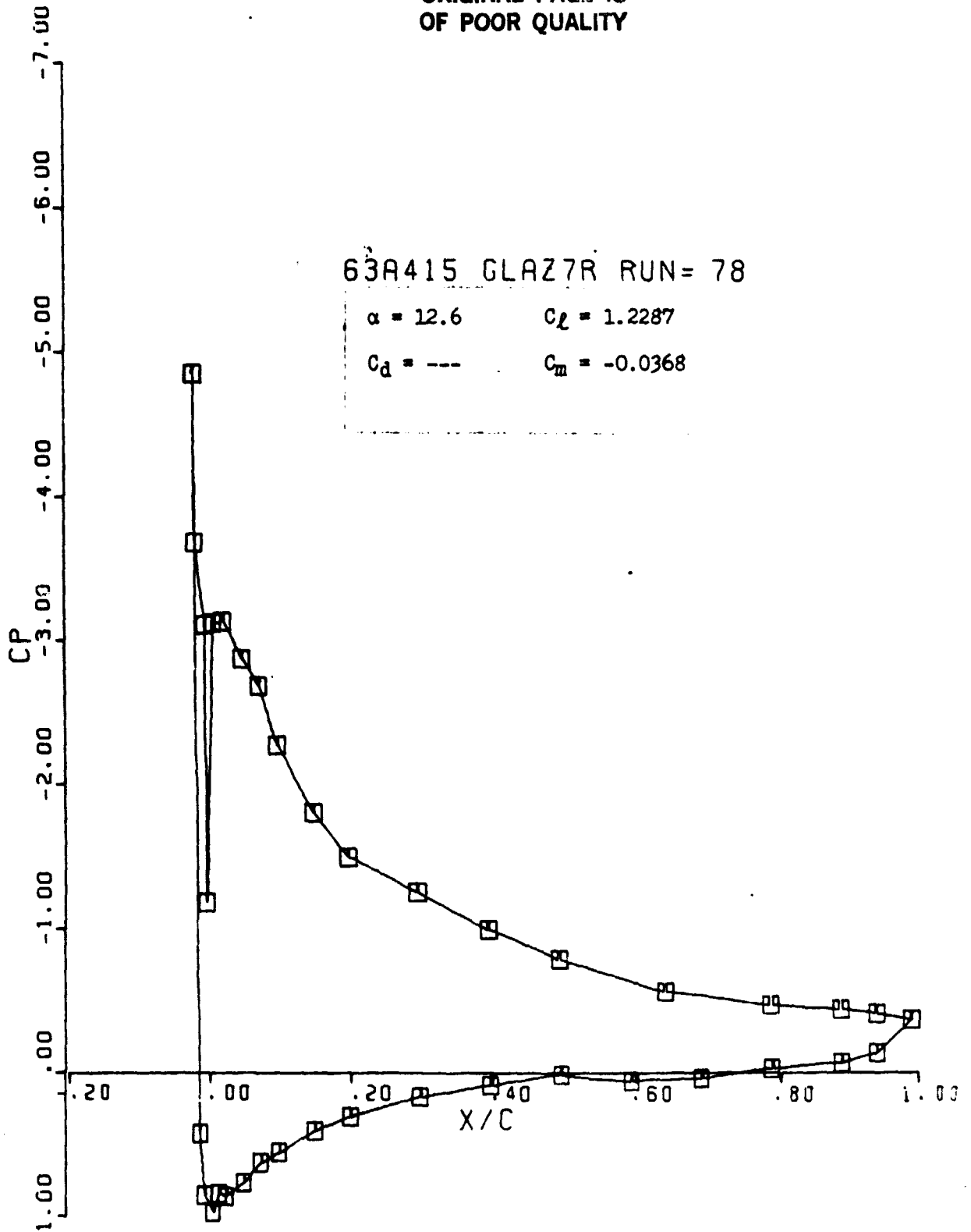
ORIGINAL PAGE IS
OF POOR QUALITY



ORIGINAL PAGE IS
OF POOR QUALITY



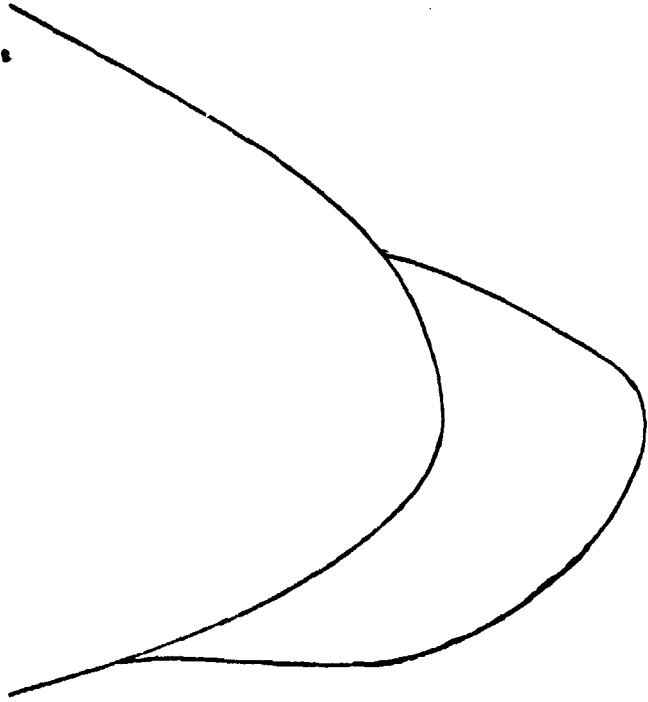
ORIGINAL PAGE IS
OF POOR QUALITY



REFERENCES

1. Bragg, M. B., Gregorek, G. M., and Shaw, R. J., "Wind Tunnel Investigation of Airfoil Performance Degradation Due to Icing", AIAA Paper No. 82-0582 presented at the 12th Aerodynamic Testing Conference, Williamsburg, Virginia, March 22-24, 1982.
2. Shaw, R. J., Sotos, R. G., and Solano, F. R., "An Experimental Study of Airfoil Icing Characteristics", NASA TM 82790, January 1982.
3. Freuler, R. J. and Hoffmann, M. J., "Experiences With An Airborne Digital Computer System for General Aviation Flight Testing", AIAA Paper No. 79-1834, presented at the AIAA Aircraft Systems and Technology Meeting, New York, New York, August 20-22, 1979.
4. Schlichting, H., Boundary-Layer Theory, Sixth Edition, McGraw-Hill, New York, 1968.
5. Abbott, Ira H. and Von Doenhoff, Albert E., "Theory of Wing Sections", Dover Publications, Inc., New York, 1959.

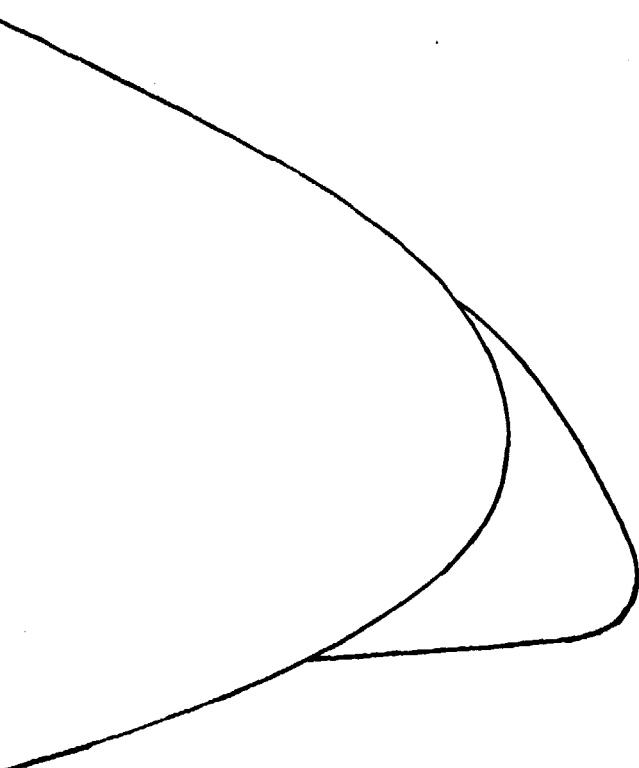
ORIGINAL PAGE IS
OF POOR QUALITY



x/c	z/c
.004455	.01982
-.00278	.01815
-.01204	.01426
-.01889	.00963
-.02454	.00278
-.02593	-.00389
-.02296	-.01019
-.01593	-.01315
-.00796	-.01407
.00093	-.01463

FIGURE 1A. R3 ICE SHAPE

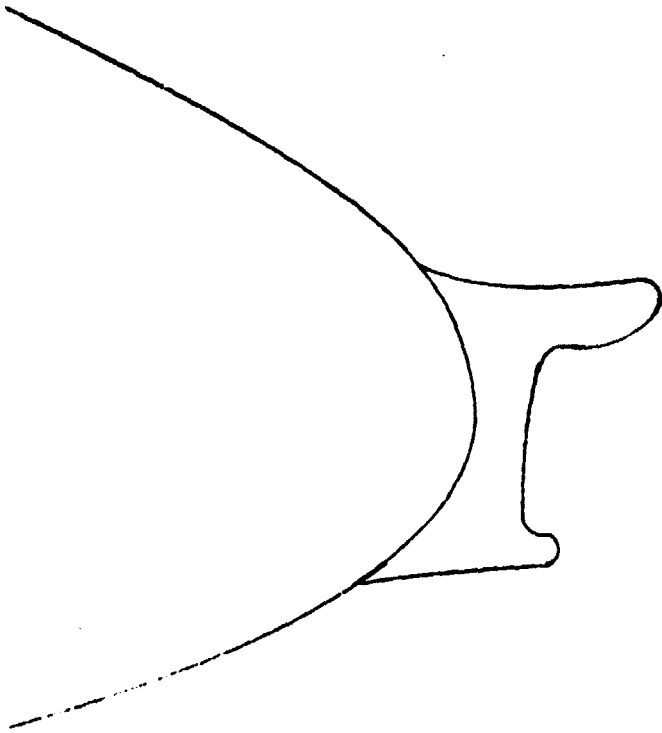
ORIGINAL PAGE IS
OF POOR QUALITY



X/C	Z/C
.00000	.01157
-.00417	.00630
-.00815	.00000
-.01157	-.00602
-.01315	-.01167
-.01130	-.01519
-.00778	-.01685
-.00139	-.01759
.00370	-.01815
.01000	-.01852

FIGURE 1B. R7 ICE SHAPE

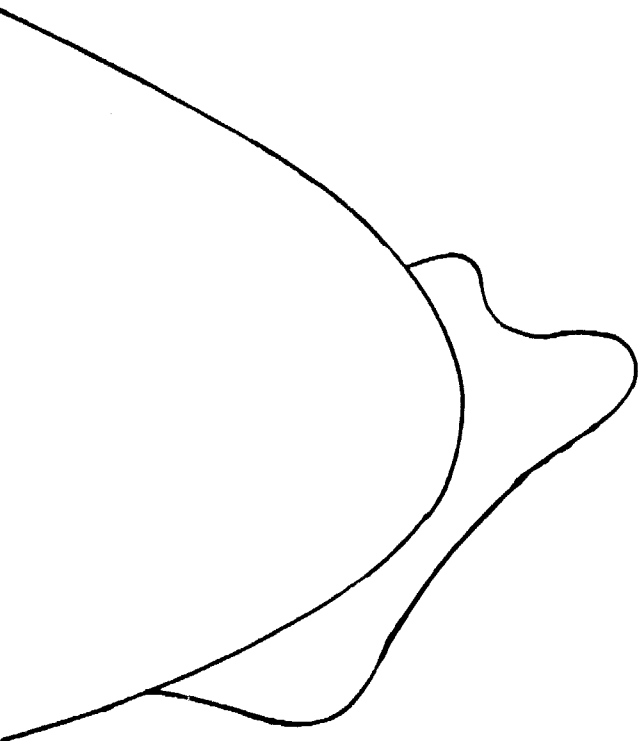
ORIGINAL PAGE IS
OF POOR QUALITY



X/C	Z/C
-.00232	.01435
-.01019	.01389
-.01667	.01407
-.01944	.01315
-.01907	.01019
-.00648	.00241
-.00556	-.00593
-.00889	-.01204
-.00389	-.01389
.00667	-.01482

FIGURE 1C. G3 ICE SHAPE

ORIGINAL PAGE IS
OF POOR QUALITY



X/C	Z/C
.00093	.01759
-.00278	.01620
-.00648	.00972
-.01667	.00778
-.01796	.00519
-.01157	-.00093
-.00509	-.00602
.00556	-.01759
.01435	-.02732
.02500	-.02593

FIGURE 1D. G7 ICE SHAPE

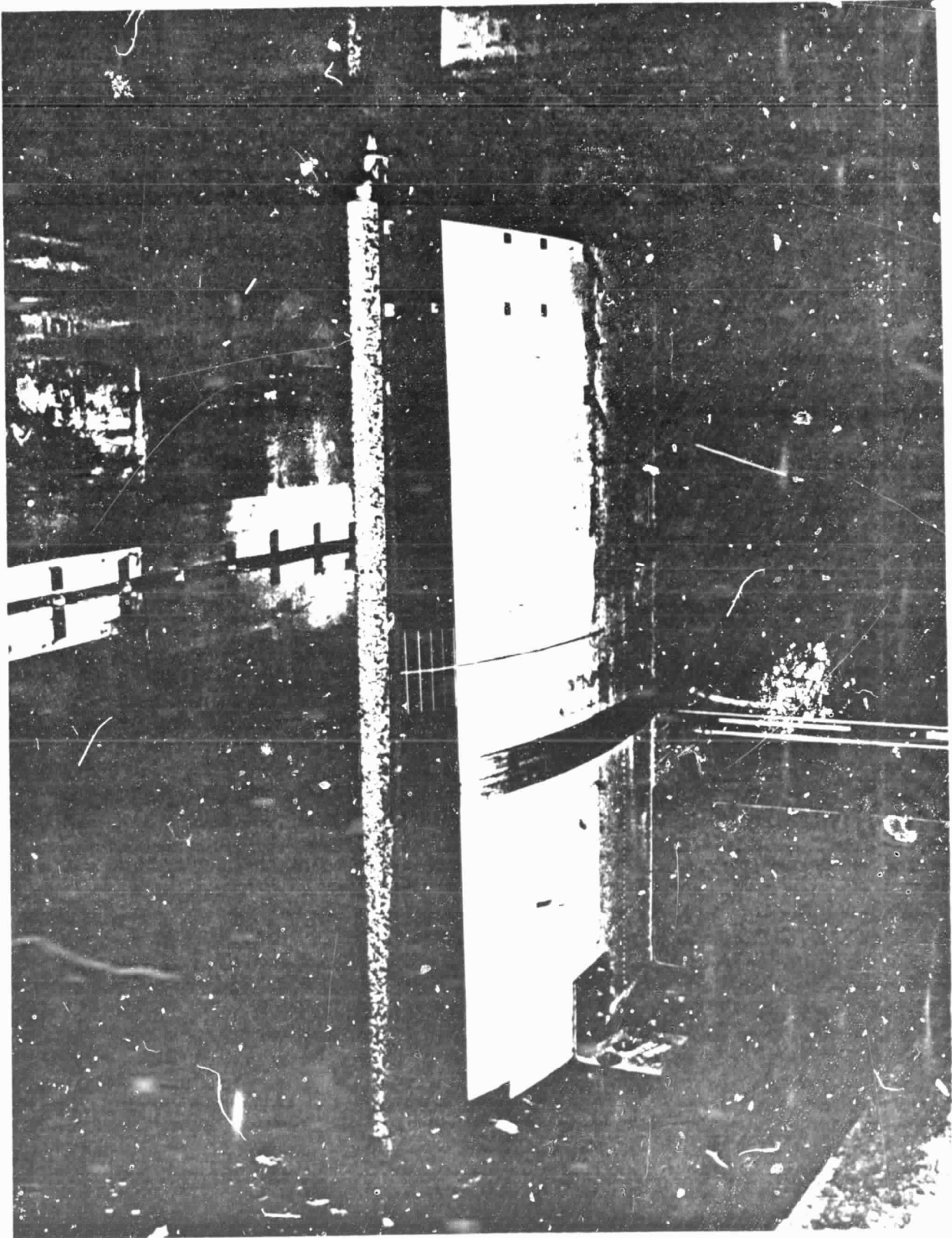


FIGURE 2. 63A415 WING IN LEWIS ICING RESEARCH TUNNEL

ORIGINAL PAGE IS
OF POOR QUALITY

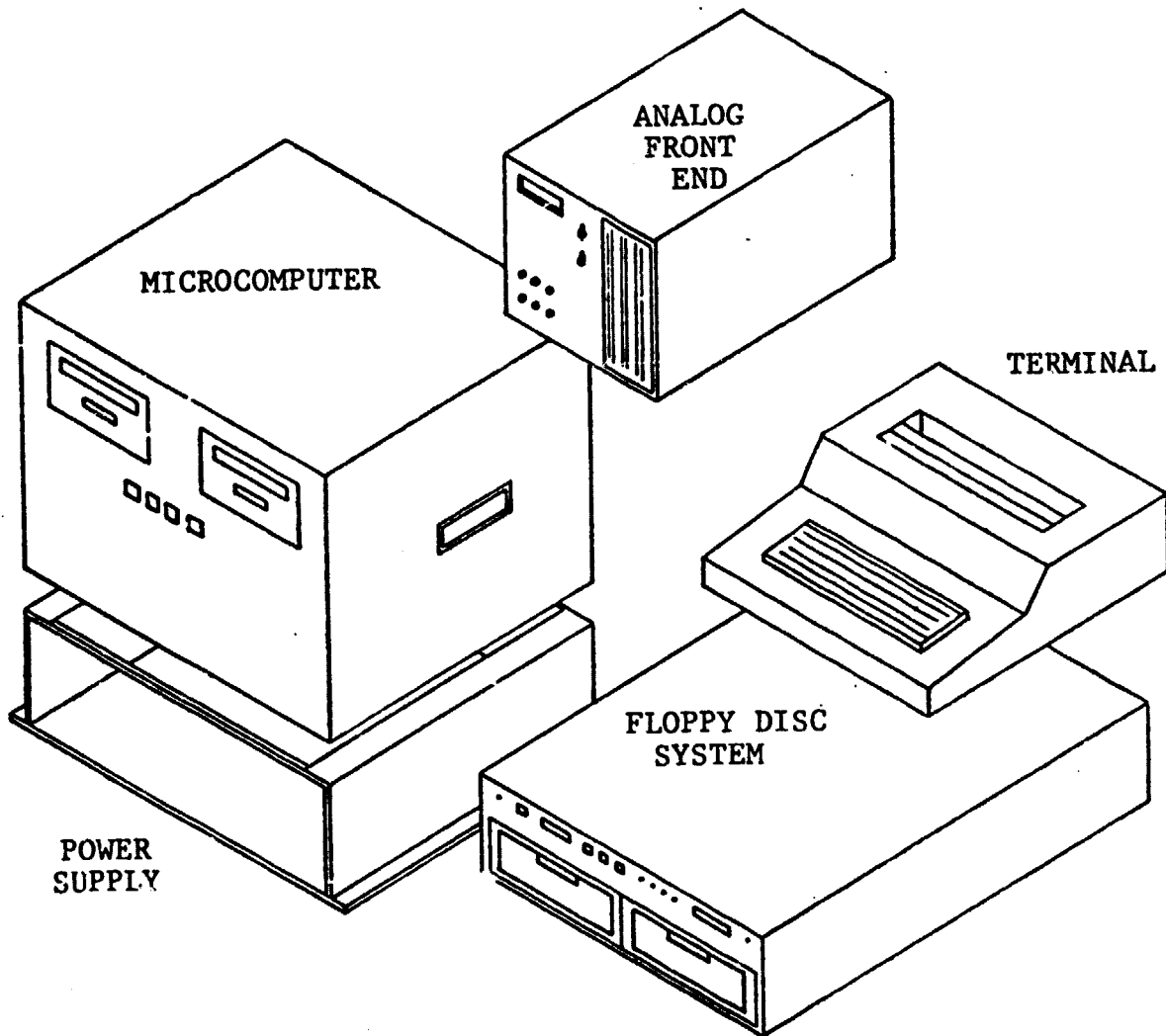


FIGURE 3. OSU DIGITAL DATA ACQUISITION AND REDUCTION SYSTEM

ORIGINAL PAGE IS
OF POOR QUALITY

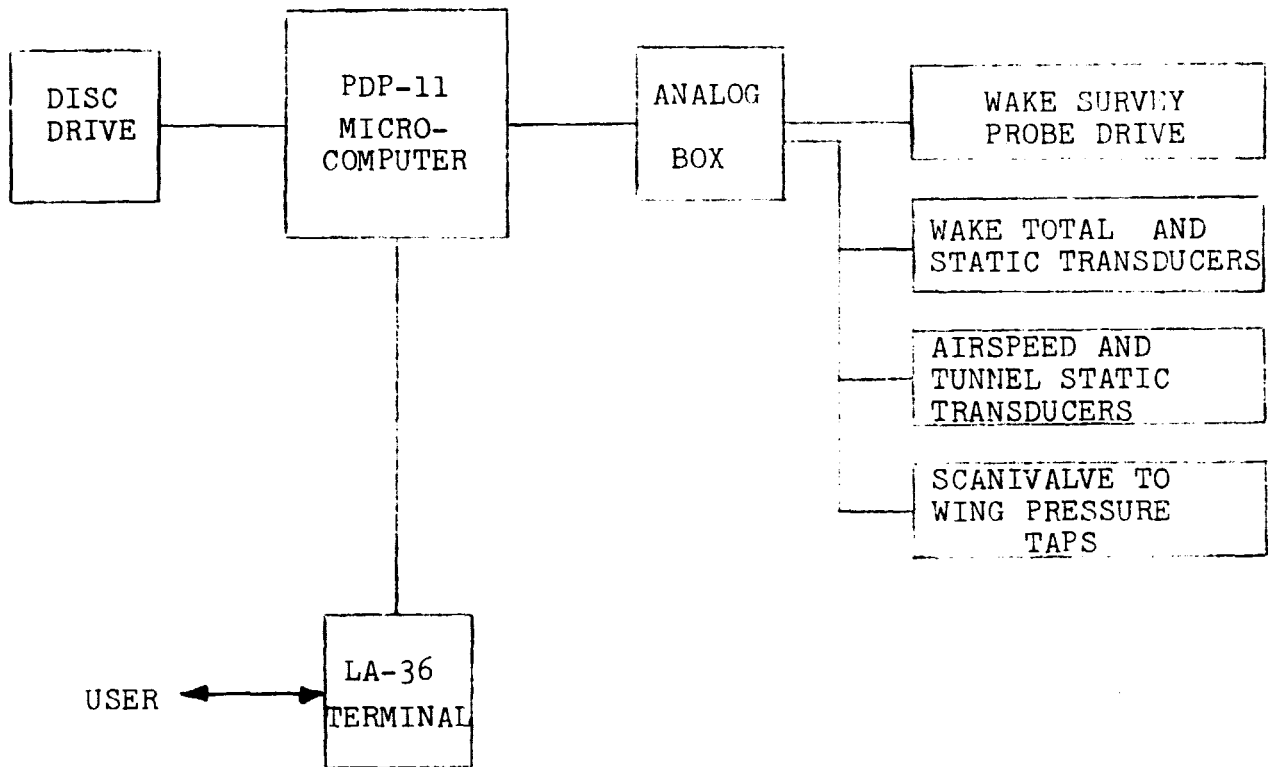


FIGURE 4. OSU ICING RESEARCH TUNNEL DATA ACQUISITION SYSTEM

ORIGINAL PAGE IS
OF POOR QUALITY

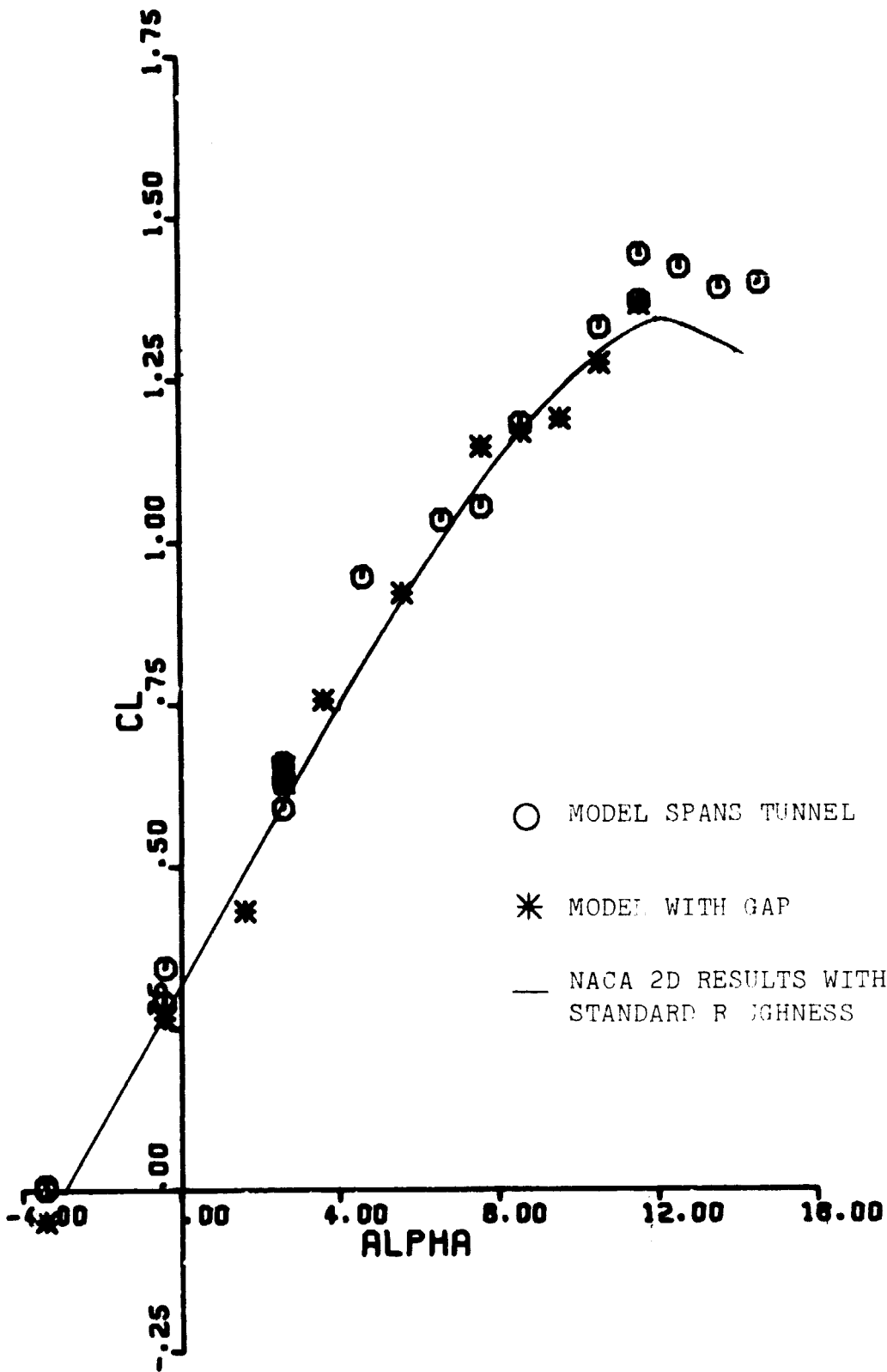


FIGURE 5. EFFECT OF MODEL SPAN ON LIFT

ORIGINAL PAGE IS
OF POOR QUALITY

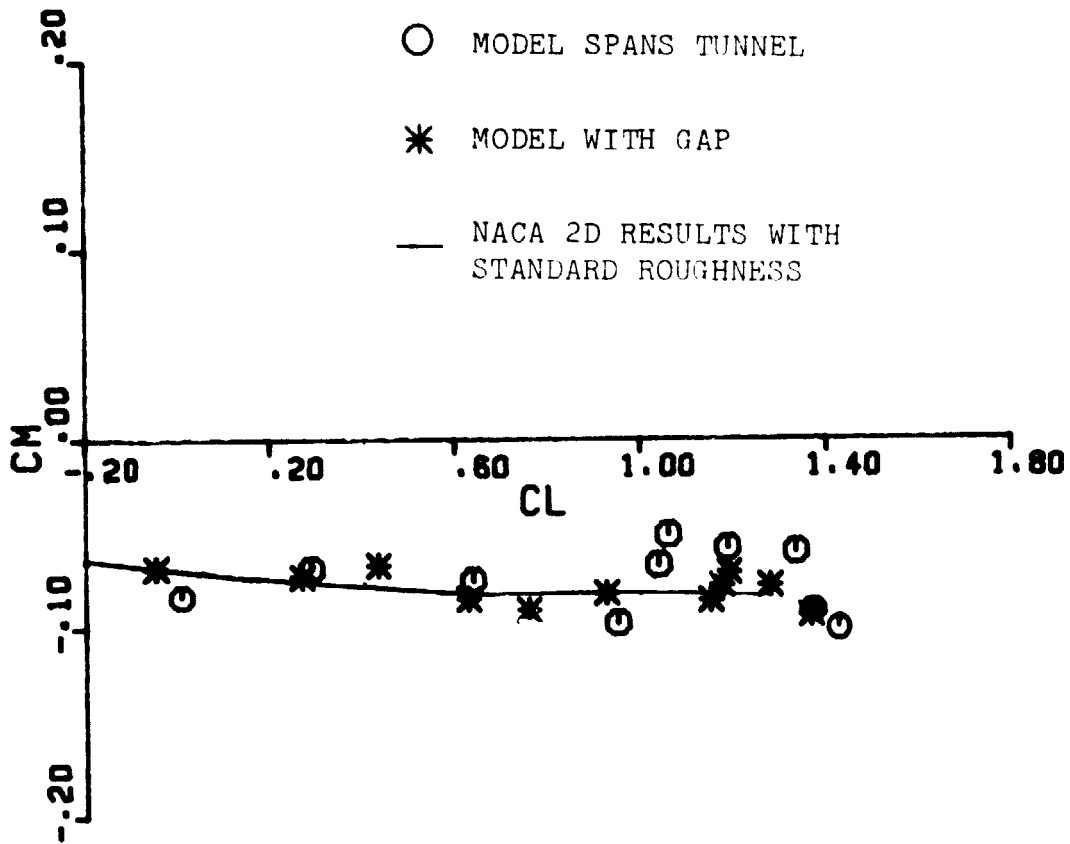


FIGURE 7. EFFECT OF MODEL SPAN ON PITCHING MOMENT